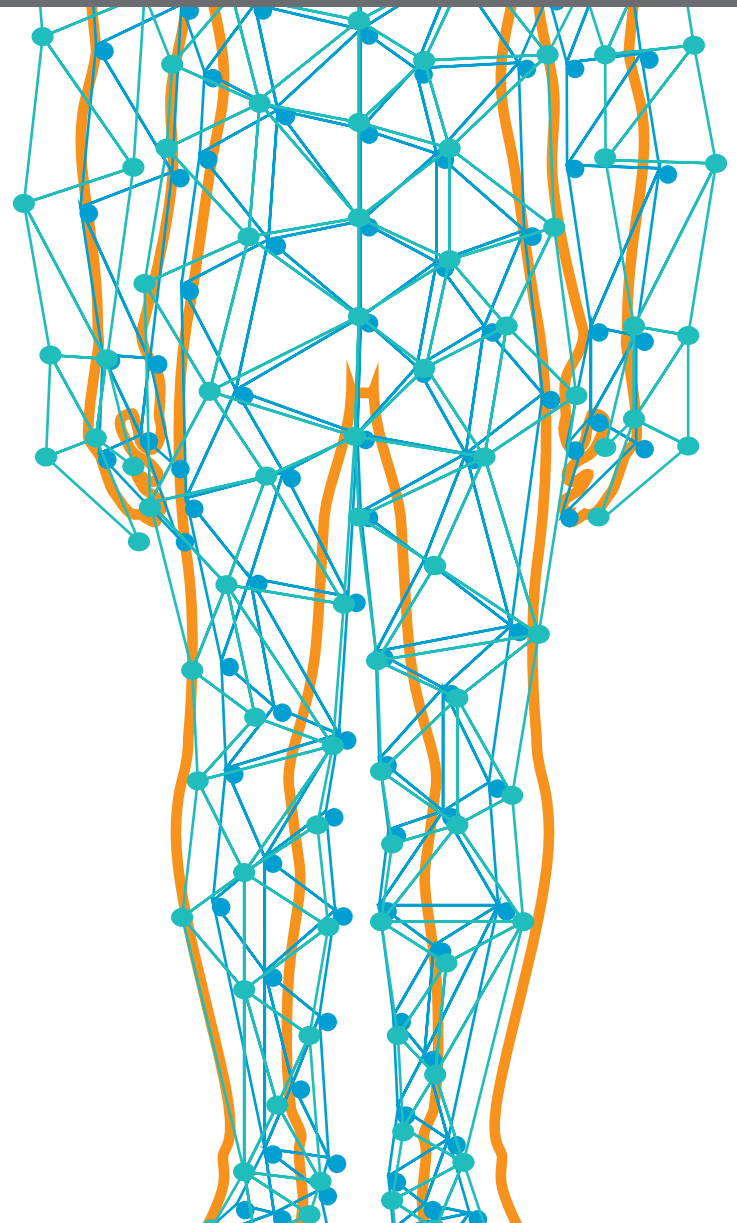
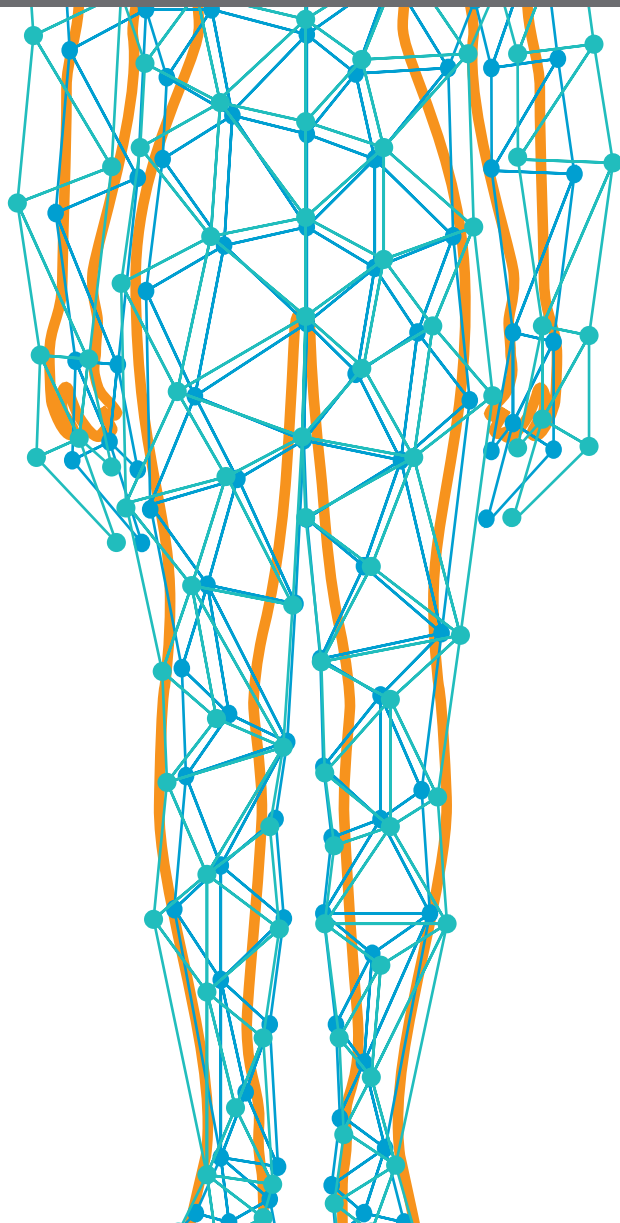




CORNEAL TRANSPLANTATION & EYE BANKING

EDITED BY: Vito Romano, Hannah Levis, Stefano Ferrari and Mohit Parekh
PUBLISHED IN: *Frontiers in Medicine*





frontiers

Frontiers eBook Copyright Statement

The copyright in the text of individual articles in this eBook is the property of their respective authors or their respective institutions or funders. The copyright in graphics and images within each article may be subject to copyright of other parties. In both cases this is subject to a license granted to Frontiers.

The compilation of articles constituting this eBook is the property of Frontiers.

Each article within this eBook, and the eBook itself, are published under the most recent version of the Creative Commons CC-BY licence.

The version current at the date of publication of this eBook is CC-BY 4.0. If the CC-BY licence is updated, the licence granted by Frontiers is automatically updated to the new version.

When exercising any right under the CC-BY licence, Frontiers must be attributed as the original publisher of the article or eBook, as applicable.

Authors have the responsibility of ensuring that any graphics or other materials which are the property of others may be included in the CC-BY licence, but this should be checked before relying on the CC-BY licence to reproduce those materials. Any copyright notices relating to those materials must be complied with.

Copyright and source acknowledgement notices may not be removed and must be displayed in any copy, derivative work or partial copy which includes the elements in question.

All copyright, and all rights therein, are protected by national and international copyright laws. The above represents a summary only. For further information please read Frontiers' Conditions for Website Use and Copyright Statement, and the applicable CC-BY licence.

ISSN 1664-8714

ISBN 978-2-88976-459-4

DOI 10.3389/978-2-88976-459-4

About Frontiers

Frontiers is more than just an open-access publisher of scholarly articles: it is a pioneering approach to the world of academia, radically improving the way scholarly research is managed. The grand vision of Frontiers is a world where all people have an equal opportunity to seek, share and generate knowledge. Frontiers provides immediate and permanent online open access to all its publications, but this alone is not enough to realize our grand goals.

Frontiers Journal Series

The Frontiers Journal Series is a multi-tier and interdisciplinary set of open-access, online journals, promising a paradigm shift from the current review, selection and dissemination processes in academic publishing. All Frontiers journals are driven by researchers for researchers; therefore, they constitute a service to the scholarly community. At the same time, the Frontiers Journal Series operates on a revolutionary invention, the tiered publishing system, initially addressing specific communities of scholars, and gradually climbing up to broader public understanding, thus serving the interests of the lay society, too.

Dedication to Quality

Each Frontiers article is a landmark of the highest quality, thanks to genuinely collaborative interactions between authors and review editors, who include some of the world's best academicians. Research must be certified by peers before entering a stream of knowledge that may eventually reach the public - and shape society; therefore, Frontiers only applies the most rigorous and unbiased reviews.

Frontiers revolutionizes research publishing by freely delivering the most outstanding research, evaluated with no bias from both the academic and social point of view. By applying the most advanced information technologies, Frontiers is catapulting scholarly publishing into a new generation.

What are Frontiers Research Topics?

Frontiers Research Topics are very popular trademarks of the Frontiers Journals Series: they are collections of at least ten articles, all centered on a particular subject. With their unique mix of varied contributions from Original Research to Review Articles, Frontiers Research Topics unify the most influential researchers, the latest key findings and historical advances in a hot research area! Find out more on how to host your own Frontiers Research Topic or contribute to one as an author by contacting the Frontiers Editorial Office: frontiersin.org/about/contact

CORNEAL TRANSPLANTATION & EYE BANKING

Topic Editors:

Vito Romano, University of Brescia, Italy

Hannah Levis, University of Liverpool, United Kingdom

Stefano Ferrari, Fondazione Banca degli Occhi del Veneto Onlus - FBOV, Italy

Mohit Parekh, University College London, United Kingdom

Citation: Romano, V., Levis, H., Ferrari, S., Parekh, M., eds. (2022). Corneal Transplantation & Eye Banking. Lausanne: Frontiers Media SA.
doi: 10.3389/978-2-88976-459-4

Table of Contents

- 04 Editorial: Corneal Transplantation and Eye Banking**
Vito Romano, Stefano Ferrari, Hannah J. Levis and Mohit Parekh
- 07 Proliferation Increasing Genetic Engineering in Human Corneal Endothelial Cells: A Literature Review**
Wout Arras, Hendrik Vercammen, Sorcha Ní Dhubhghaill, Carina Koppen and Bert Van den Bogerd
- 17 Long-Term Anatomical and Functional Survival of Boston Type 1 Keratoprosthesis in Congenital Aniridia**
Ariann Dyer, Alix De Faria, Gemma Julio, Juan Álvarez de Toledo, Rafael I. Barraquer and Maria Fideliz de la Paz
- 23 A New Pre-descemetic Corneal Ring (Neoring) in Deep Anterior Lamellar Keratoplasty for Moderate-Advanced Keratoconus: A Pilot 2-Year Long-Term Follow-Up Study**
Belén Alfonso-Bartolozzi, Carlos Lisa, Luis Fernández-Vega-Cueto, David Madrid-Costa and José F. Alfonso
- 31 Artificial Cornea: Past, Current, and Future Directions**
Gráinne Holland, Abhay Pandit, Laura Sánchez-Abella, Andrea Haiek, Iraida Loinaz, Damien Dupin, Maria Gonzalez, Eva Larra, Aritz Bidaguren, Neil Lagali, Elizabeth B. Moloney and Thomas Ritter
- 50 Ultrastructural Analysis of Rehydrated Human Donor Corneas After Air-Drying and Dissection by Femtosecond Laser**
Emilio Pedrotti, Erika Bonacci, Adriano Fasolo, Arianna De Rossi, Davide Camposampiero, Gary L. A. Jones, Paolo Bernardi, Flavia Merigo, Diego Ponzin, Giorgio Marchini and Andrea Sbarbati
- 59 The Effects of Donor-Recipient Age and Sex Compatibility in the Outcomes of Deep Anterior Lamellar Keratoplasties**
Hon Shing Ong, Nathalie Chiam, Hla Myint Htoon, Ashish Kumar, Anshu Arundhati and Jodhbir S. Mehta
- 69 Donor-Related Risk Factors for Graft Decompensation Following Descemet's Stripping Automated Endothelial Keratoplasty**
Sota Nishisako, Takefumi Yamaguchi, Masatoshi Hirayama, Kazunari Higa, Dai Aoki, Chiaki Sasaki, Hisashi Noma and Jun Shimazaki
- 79 Extracellular Vesicles Derived From Human Corneal Endothelial Cells Inhibit Proliferation of Human Corneal Endothelial Cells**
Mohit Parekh, Hefin Rhys, Tiago Ramos, Stefano Ferrari and Sajjad Ahmad
- 95 Impact of the COVID-19 Pandemic on Corneal Transplantation: A Report From the Italian Association of Eye Banks**
Rita Mencucci, Michela Cennamo, Diego Ponzin, Federico Genzano Besso, Giulio Pocobelli, Matilde Buzzi, Carlo Nucci and Francesco Aiello on behalf of Italian Society Eye Bank Group (SIBO)



OPEN ACCESS

EDITED AND REVIEWED BY

Jodhbir Mehta,
Singapore National Eye
Center, Singapore

*CORRESPONDENCE

Mohit Parekh
m.parekh@ucl.ac.uk

SPECIALTY SECTION

This article was submitted to
Ophthalmology,
a section of the journal
Frontiers in Medicine

RECEIVED 01 July 2022

ACCEPTED 06 July 2022

PUBLISHED 21 July 2022

CITATION

Romano V, Ferrari S, Levis HJ and
Parekh M (2022) Editorial: Corneal
transplantation and eye banking.
Front. Med. 9:983580.
doi: 10.3389/fmed.2022.983580

COPYRIGHT

© 2022 Romano, Ferrari, Levis and
Parekh. This is an open-access article
distributed under the terms of the
[Creative Commons Attribution License](#)
(CC BY). The use, distribution or
reproduction in other forums is
permitted, provided the original
author(s) and the copyright owner(s)
are credited and that the original
publication in this journal is cited, in
accordance with accepted academic
practice. No use, distribution or
reproduction is permitted which does
not comply with these terms.

Editorial: Corneal transplantation and eye banking

Vito Romano¹, Stefano Ferrari², Hannah J. Levis³ and
Mohit Parekh^{4*}

¹Department of Medical and Surgical Specialties, Radiological Specialties and Public Health, University of Brescia, Brescia, Italy, ²International Center for Ocular Physiopathology, Fondazione Banca degli Occhi del Veneto Onlus, Venice, Italy, ³Institute of Life Course and Medical Sciences, University of Liverpool, Liverpool, United Kingdom, ⁴Institute of Ophthalmology, University College London, London, United Kingdom

KEYWORDS

corneal transplant, cornea donor, eye bank, lamellar keratoplasty, cornea

Editorial on the Research Topic

Corneal Transplantation and Eye Banking

Cornea, the front transparent layer of the eye, is responsible for vision clarity. Disease or dysfunction in any layer of this multilayer tissue can lead to corneal blindness in addition to pain and discomfort. Corneal transplantation is the most popular choice of treatment where a healthy donor graft obtained from a cadaver is harvested, stored or processed in an eye bank and used to replace the diseased host tissue (1). However, human cadaveric corneal tissues have a worldwide shortage, so researchers are finding alternative solutions to treat corneal disorders (2). Improved surgical techniques, graft restoration procedures, cell and molecular based treatment options, and tissue alternatives have all contributed to the advancement in the field of corneal transplant and eye banking (3). In addition, since the pandemic impacted tissue procurement significantly, a huge waiting list was observed due to lack of tissues for elective surgeries (4, 5). However, with significant amount of work to improve the donation rate, the corneal transplantation has resumed and now fully functional with tissue donations being actively pursued.

The studies in this special issue on *Corneal transplantation and eye banking* highlighted recent advances. Novel and long-term clinical outcomes suggested that Boston type 1 KPro can be used for patients with aniridia associated keratopathy (AAK), however, it was suggested that glaucoma and restroprosthetic membrane formation must be considered before transplanting such device in these patients (Dyer et al.). Deep anterior lamellar keratoplasty (DALK) is routinely performed to replace the anterior cornea. Usually, the donor tissue is cut to a desired thickness and the diseased anterior stroma replaced. However, a recent long-term study evaluated a new polymethylmethacrylate (PMMA) ring (Neoring) and showed that this synthetic device can be used as a viable, effective, and safe option for pre-Descemet DALK to optimize

the post-operative results for moderate-severe keratoconus (Alfonso-Bartolozzi et al.). Gender mismatch in corneal transplantation (6, 7) has been one of the concerns that has not been widely studied. However, a study published in this special issue showed no significant influence of donor-recipient sex- or age-match on graft rejection and failure in eyes that had undergone DALK surgeries (Ong et al.). For endokeratoplasty, pseudophakic status and/or presence of preoperative endothelial folds have been indicated as significant donor risk factors for endothelial failure in non-FECD patients following DSAEK (Nishisako et al.). In addition, many studies have investigated the impact of COVID-19 pandemic on corneal transplantation. Techniques for optimal utilization (8, 9) and extended storage of human donor corneas became crucial during COVID. Therefore, new techniques like femtosecond laser (FSL) incision of rehydrated human donor corneas after air-drying has been evaluated for new and optimized use of donor tissues (Pedrotti et al.). In addition, an Italian study reported that vigorous work and continuous effort toward resuming keratoplasties to a near-normal standard despite the pandemic led to an increase in endokeratoplasties, thus suggesting that the corneal transplantation field is evolving rapidly (Mencucci et al.).

Corneal endothelium has been studied and reviewed extensively. However, due to lack of a standard cell/molecular based treatment approach, many new developments have been observed. Corneal endothelium is the inner monolayer of cells that is considered to be non-proliferative. Hence, it must be maintained as its loss due to disease or dysfunction could lead to corneal blindness. Apart from corneal transplantation, intracameral injection of cultured corneal endothelial cells (10), biomedical engineering of endothelial grafts, novel scaffolds (11) and many other options have been evaluated. An extensive review on diverse array of genes targeted to induce proliferation of corneal endothelial cells has also been compiled in this special issue (Arras et al.). In addition, extracellular vesicles (Parekh et al.) from corneal endothelial cells have shown to inhibit the proliferation of endothelial cells and the miRNAs

present in the extracellular vesicles, possibly the exosomes, must be evaluated to target the induction of proliferation by downregulating the causative gene. These studies may help understanding the pathology of corneal endothelial dysfunction and provide further insights in the development of future therapeutic treatment options.

In conclusion, genes modulating the proliferative capacity of endothelial cells, artificial and bio-mimetic corneas, extracellular vesicles, synthetic keratoprosthesis (Holland et al.) with or without the inclusion of biomolecules, advanced bioengineering, 3D corneal bioprinting, biomaterials, artificial corneas, etc. have shown to be promising in advancing the field of *Corneal transplantation and eye banking*.

Author contributions

VR, SF, HL, and MP: compiled, drafted, reviewed, and approved. All authors contributed to the article and approved the submitted version.

Conflict of interest

The authors declare that the research was conducted in the absence of any commercial or financial relationships that could be construed as a potential conflict of interest.

Publisher's note

All claims expressed in this article are solely those of the authors and do not necessarily represent those of their affiliated organizations, or those of the publisher, the editors and the reviewers. Any product that may be evaluated in this article, or claim that may be made by its manufacturer, is not guaranteed or endorsed by the publisher.

References

1. Parekh M, Salvalaio G, Ruzza A, Camposampiero D, Griffoni C, Zampini A, et al. Posterior lamellar graft preparation: a prospective review from an eye bank on current and future aspects. *J Ophthalmol.* (2013) 2013:769860. doi: 10.1155/2013/769860
2. Parekh M, Wongvisavavit R, Cubero Cortes ZM, Wojcik G, Romano V, Tabernero SS, et al. Alternatives to endokeratoplasty: an attempt towards reducing global demand of human donor corneas. *Regen Med.* (2022) 17:461–75. doi: 10.2217/rme-2021-0149
3. Català P, Thuret G, Skottman H, Mehta JS, Parekh M, Ní Dhubghaill S, et al. Approaches for corneal endothelium regenerative medicine. *Prog Retin Eye Res.* (2022) 87:100987. doi: 10.1016/j.preteyeres.2021.100987
4. Parekh M, Nathawat R, Parihar JKS, Jhanji V, Sharma N. Impact of COVID-19 restrictions on corneal tissue donation and utilization rate - time to bring reforms? *Indian J Ophthalmol.* (2021) 69:3782–4. doi: 10.4103/ijo.IJO_2714_21
5. Parekh M, Ferrari S, Romano V, Myerscough J, Jones G, Griffoni C, et al. Impact of COVID-19 on corneal donation and distribution. *Eur J Ophthalmol.* (2022) 32:NP269–70. doi: 10.1177/1120672120948746
6. Romano V, Parekh M, Virgili G, Coco G, Leon P, Islein K, et al. Gender matching did not affect 2-year rejection or failure rates following DSAEK for fuchs endothelial corneal dystrophy. *Am J Ophthalmol.* (2022) 235:204–10. doi: 10.1016/j.ajo.2021.09.029

7. Hopkinson CL, Romano V, Kaye RA, Steger B, Stewart RM, Tsagkatakis M, et al. The influence of donor and recipient gender incompatibility on corneal transplant rejection and failure. *Am J Transplant.* (2017) 17:210–7. doi: 10.1111/ajt.13926
8. Gadhvi KA, Coco G, Pagano L, Kaye SB, Ferrari S, Levis HJ, et al. Expanding the supply of donor grafts. *Cornea.* (2021) 40:e16–7. doi: 10.1097/ICO.0000000000002777
9. Parekh M, Ferrari S, Ruzza A, Leon P, Franch A, Camposampiero D, et al. Biobanking corneal tissues for emergency procedures during COVID-19 era. *Indian J Ophthalmol.* (2021) 69:167–8. doi: 10.4103/ijo.IJO_2615_20
10. Kinoshita S, Koizumi N, Ueno M, Okumura N, Imai K, Tanaka H, et al. Injection of cultured cells with a ROCK inhibitor for bullous keratopathy. *N Engl J Med.* (2018) 378:995–1003. doi: 10.1056/NEJMoa1712770
11. Parekh M, Romano V, Hassanin K, Testa V, Wongvisavavit R, Ferrari S, et al. Biomaterials for corneal endothelial cell culture and tissue engineering. *J Tissue Eng.* (2021) 12:2041731421990536. doi: 10.1177/2041731421990536



Proliferation Increasing Genetic Engineering in Human Corneal Endothelial Cells: A Literature Review

Wout Arras¹, Hendrik Vercammen¹, SORCHA NI Dhubhghaill^{1,2,3}, Carina Koppen^{1,2} and Bert Van den Bogerd^{1*}

¹ Antwerp Research Group for Ocular Science (ARGOS), Translational Neurosciences, Faculty of Medicine and Health Sciences, University of Antwerp, Wilrijk, Belgium, ² Department of Ophthalmology, Antwerp University Hospital, Edegem, Belgium, ³ Netherlands Institute for Innovative Ocular Surgery (NIIOS), Rotterdam, Netherlands

OPEN ACCESS

Edited by:

Hannah Levis,
University of Liverpool,
United Kingdom

Reviewed by:

Daniel Kampik,
University Hospital
Wuerzburg, Germany
Monika Valtink,
Technische Universität
Dresden, Germany

*Correspondence:

Bert Van den Bogerd
Bert.VandenBogerd@uantwerpen.be

Specialty section:

This article was submitted to
Ophthalmology,
a section of the journal
Frontiers in Medicine

Received: 30 March 2021

Accepted: 07 June 2021

Published: 29 June 2021

Citation:

Arras W, Vercammen H, Ni
Dhubhghaill S, Koppen C and Van
den Bogerd B (2021) Proliferation
Increasing Genetic Engineering in
Human Corneal Endothelial Cells: A
Literature Review.
Front. Med. 8:688223.
doi: 10.3389/fmed.2021.688223

The corneal endothelium is the inner layer of the cornea. Despite comprising only a monolayer of cells, dysfunction of this layer renders millions of people visually impaired worldwide. Currently, corneal endothelial transplantation is the only viable means of restoring vision for these patients. However, because the supply of corneal endothelial grafts does not meet the demand, many patients remain on waiting lists, or are not treated at all. Possible alternative treatment strategies include intracameral injection of human corneal endothelial cells (HCEncs), biomedical engineering of endothelial grafts and increasing the HCEnc density on grafts that would otherwise have been unsuitable for transplantation. Unfortunately, the limited proliferative capacity of HCEncs proves to be a major bottleneck to make these alternatives beneficial. To tackle this constraint, proliferation enhancing genetic engineering is being investigated. This review presents the diverse array of genes that have been targeted by different genetic engineering strategies to increase the proliferative capacity of HCEncs and their relevance for clinical and research applications. Together these proliferation-related genes form the basis to obtain a stable and safe supply of HCEncs that can tackle the corneal endothelial donor shortage.

Keywords: genetic engineering, cell therapy, cell proliferation, corneal endothelial cells, corneal endothelial transplant

INTRODUCTION

When light enters the eye, the first tissue it passes through is the cornea. This highly specialized transparent tissue is comprised of 5 anatomical layers; the epithelium, Bowman's layer, stroma, Descemet's membrane and finally its most posterior layer, the endothelium. This inner layer of the cornea acts as a leaky barrier that allows the exchange of nutrients and waste products between the corneal stroma and the aqueous humor, but also actively pumps excessive water out of the cornea to maintain a state of relative deturgescence (1). Throughout adulthood, the endothelial cell density (ECD) decreases by 0.3–0.6 % each year because these cells lack the proliferative capacity to compensate for their attrition (2, 3). Human corneal endothelial cells (HCEncs) are arrested in the G1-phase of the cell cycle due to cell-cell contact inhibition, reduced exposure to growth factors and inhibition of S-phase entry by TGF- β 2 in the aqueous humor (4).

When these cells are lost or damaged, they rely on a combination of migration and enlargement to preserve the function and integrity of the corneal endothelium (5). Traumatic and congenital pathologies, however, may push these compensatory mechanisms to their limit, causing the cornea to become edematous resulting in a loss of transparency. The current gold standard of treatment is to remove the dysfunctional cell layer and replace it with a corneal endothelial transplant. Due to the corneal donor shortage and lack of banking infrastructures globally, an estimated 12.7 million people are awaiting corneal transplantation worldwide, more than half of which is due to corneal endothelial dysfunction (6).

Over the past decades, different approaches to increase corneal endothelial graft availability have been investigated. Recently, the first results of a clinical trial using a lab-cultured suspension of HCEncs administered as an intracameral injection was reported in a cohort of patients with endothelial disease with positive results (7). While the effects of this treatment may be altered by the severity of disease at the level of the Descemet membrane (8), it is convincing evidence that such novel cell therapies can be effective (7, 9). Another approach comprises the biomedical engineering of corneal endothelial grafts in the laboratory. As a result, a plethora of corneal endothelial scaffolds have been proposed for use in patients, onto which HCEncs can be seeded (10, 11). Alternatively, instead of using scaffolds, donor grafts with low ECD counts could also be used for transplantation by increasing the amount of HCEncs on these grafts (12, 13).

Regardless of the approach, the bottleneck of all these strategies remains the limited amount of primary HCEncs that can only be obtained through standard cell and organ culturing methods. While primary HCEncs can be cultured *ex vivo*, they can only generate 20–30 population doublings (PD) under standard culturing conditions before becoming senescent (14, 15). The amount of PD that can be obtained is also largely dependent on donor age, as cultures originating from older donors proliferate slower and transform to a senescent phenotype faster (15, 16). In some cell cultures, HCEncs undergo endothelial-to-mesenchymal transition (EnMT), which can be recognized by the change from their typical hexagonal shape to an elongated morphology, loss of cell-cell contact inhibition and an altered extracellular matrix composition. EnMT also has a detrimental effect on the HCEnC barrier function, rendering them unusable for clinical applications (15). When further optimization of cell culture protocols reaches its limits, genetic engineering may be of benefit. The focus of this alternative approach is to increase the proliferative capacity of HCEncs without losing their essential characteristics. In general, these genetic engineering strategies are based on

viral/cellular oncogene introduction, RNA interference (RNAi) or the clustered regularly interspaced short palindromic repeats (CRISPR)/deactivated CRISPR-associated protein 9 (dCas9) activation system (Figure 1).

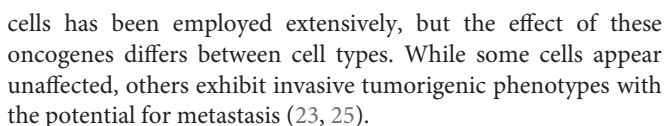
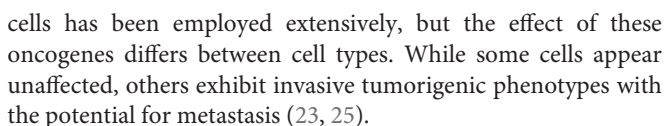
GENERAL OVERVIEW OF CELL CYCLE ENTRY

The cell cycle is a tightly regulated process with similar features across all eukaryotic cells. It is regulated by the sequential up- and downregulation of cell cycle related genes where cyclin-dependent kinases (CDKs) play a central role (17). Upon mitogenic activation of cells in G0 or early G1, a chain of events is initiated causing an upregulation of different cell cycle regulating factors including cyclins (18). Cyclins interact with their corresponding CDKs causing the latter enzymes to become activated and phosphorylate their downstream targets. By regulating CDK activities throughout the different phases of the cell cycle, cell cycle-related proteins can be activated in a sequential manner (19). Cyclin D can activate CDK 4 and 6, which induce phosphorylation of the retinoblastoma (Rb) family members (pRb, p107, and p130) (20). In quiescent cells (and in early G1), these proteins are bound to E2F transcription factors, preventing cell cycle progression (18). However, hyperphosphorylation of the Rb proteins diminishes their control over E2F, causing some of the E2F family members to start upregulating their (cell-cycle-associated) target genes (20) (Figure 2). The amounts of active E2F is further increased by a process of positive feedback, which eventually tips the cell over the restriction point. After this “point-of-no-return,” the cell is committed to the following phases of the cell cycle independent of the presence of mitogenic stimuli (18). However, cyclin-dependent kinase inhibitors (CKIs) are also present within the cell. They function as negative regulatory mechanisms that stabilize the G0-phase and induce G1 cell cycle arrest (18, 21). In this group of CKIs, the INK4 proteins and the CIP/KIP protein family can be distinguished based on their structure and specific target. The INK4 family targets specific CDKs (i.e., CDK 4 and 6) while the CIP/KIP family inhibits cyclin-CDK complexes (21). Additionally, p53 is an important suppressor of the cell cycle as it can induce cell cycle arrest, and even apoptosis, in response to the activation of oncogenes or DNA damage. To induce G1-phase arrest, p53 mainly relies on p21CIP1, which prevents the activation of E2F by inhibiting different cyclin-CDK complexes including cyclin D/CDK4 (22).

PROLIFERATION ENHANCEMENT THROUGH VIRAL ONCOGENE INTRODUCTION

Some viruses have the potential to stimulate the proliferation of mammalian cells by using oncogenes to increase the production of their own genetic material (23). The human viral oncogenes often stimulate proliferation through the inhibition of the tumor suppressor p53 and/or members of the Rb family (24). This capacity to increase the proliferation of a wide range of

Abbreviations: CDKs, cyclin-dependent kinases; CKIs, cyclin-dependent kinase inhibitors; CRISPR, clustered regularly interspaced short palindromic repeats; dCas9, deactivated CRISPR-associated protein 9; ECD, endothelial cell density; EnMT, endothelial-to-mesenchymal transition; HCEncs, human corneal endothelial cells; HPV-16, human papilloma virus type 16; TERT, human telomerase reverse transcriptase; PD, population doublings; Rb, retinoblastoma; RNAi, RNA interference; shRNA, short hairpin RNA; SOX2, sex-determining region Y-box 2; SV40, simian virus 40; TAZ, transcriptional co-activator with PDZ-binding domain; YAP, Yes-associated protein.



One of the first viral oncogenes used in HCEncs was a modified simian virus 40 (SV40) early gene region encoding the SV40 large T-antigen (26). This viral protein stimulates cell proliferation by inhibition of p53 and disruption of the Rb-E2F complex through binding with p53 and Rb, respectively. E2F is then free to induce gene transcription needed for cell cycle entry (23). In HCEncs, SV40 large T-antigen was found to increase the expression of CDK1, CDK2, and CDK4 but also cyclin A and D were upregulated. Conversely, western blotting indicated that the cell cycle inhibitors p27KIP1 and p21CIP1 decreased compared to primary HCEncs (27).

The expression of SV40 large T-antigen in HCEnCs resulted in an increased proliferation rate and extended survival of HCEnCs from both old and young donors (26–29). Primary HCEnC cultures with low proliferative capacity were found to grow rapidly after expression of the SV40 large T-antigen (29). The cells exhibited a cobblestone-like polygonal morphology at confluence, which differed only slightly from the flatter appearance of unmodified HCEnCs (26, 27). The proliferation rate of transformed HCEnCs decreased when nearing confluence as a result of contact inhibition. However, extended periods of confluence resulted in cell stratification, which is not a feature of the normal corneal endothelium (26). While expression of the SV40 large T-antigen is associated with aneuploidy, chromosomal aberrations in HCEnCs were not routinely assessed (30). However, in these instances where karyotyping was performed, most transformed HCEnCs were found to be diploid (28).

SV40 Large and Small T-Antigen

SV40 small T-antigen is another SV40-related oncogene, that increases cell proliferation through binding with the protein phosphatase 2A and inhibition of heterochromatin protein 1-binding protein 3 (31). While expression of SV40 small T-antigen alone is not enough to induce transformation, it contributes to SV40 large T-antigen-mediated cell transformation (23, 31).

Expression of both the SV40 large and small T-antigens in HCEncs resulted in similar outcomes as described for the SV40 large T-antigen alone. However, one culture (obtained from a 91-year-old female donor) recovered from crisis and proliferated indefinitely (>300 PD) while maintaining the characteristic hexagonal shape and size of HCEncs at confluence (32). Seeding this heterogeneous immortalized HCEnc line (named HCEC-12) onto the denuded Descemet's membrane of a donor cornea *in vitro*, was found to yield a functional endothelial monolayer without exceeding the boundaries of the trabecular meshwork. These cells also exhibited an active pumping capacity, which is a key characteristic of functional HCEncs (33).

Cells from the HCEC-12 cell line were adapted to serum-free growth conditions and subcloned into two homogeneous immortalized HCEnc lines designated HCEC-B4G12 and HCEC-H9C1. While the phenotype exhibited by the HCEC-B4G12 line resembles that of cultured primary HCEncs, it was suggested that the HCEC-H9C1 cell line represents transitional HCEncs due to its atypical phenotype (34). Nowadays, both immortalized cell lines are commonly used in HCEnc research, though not for clinical applications.

Human Papilloma Virus Type 16 E6/E7

In addition to SV40-related oncogenes, the E6 and E7 viral oncogenes of human papilloma virus type 16 (HPV-16) have also been used to increase proliferation of HCEncs (28, 35). The E6 oncoprotein increases cell proliferation by stimulating the degradation of p53 while E7 induces the ubiquitination of the Rb proteins (36, 37). Aside from promoting the degradation of p53 and the Rb proteins, E6 and E7 also interact with many other cellular factors to increase cell proliferation, which is reviewed elsewhere (38).

Stable expression of both E6 and E7 oncoproteins resulted in immortalization of the HCEncs while expression of E6 alone only extended their life span by 30 PD (14, 28, 35, 39). Similar to the SV40 large T-antigen expressing HCEncs, the HPV-16 E6/E7 immortalized cell lines exhibited a cobblestone-like polygonal morphology, were mostly diploid, but also displayed a tendency to form a multilayer when maintained at confluence (28, 35). ZO-1 and N-cadherin mRNA (two popular markers for HCEnc barrier function) were detected, but these results could not be corroborated with immunocytochemical staining of their respective protein and subsequent functional evaluation by means of an Ussing chamber indicated a reduced pump function (35, 39). Subcutaneous injection in nude mice did not result in the formation of solid tumors, indicating that these cells were not tumorigenic (35).

PROLIFERATION ENHANCEMENT THROUGH CELLULAR ONCOGENE INTRODUCTION

Human Telomerase Reverse Transcriptase

During cell division, the telomeres at the chromosomal ends of differentiated somatic cells shorten progressively as a result of features inherent to the DNA replication mechanism. Telomeres prevent the cell from recognizing these chromosomal ends as DNA damage. However, excessive cell division shortens the telomeres to such extent that they are no longer able to properly function, causing replicative senescence and apoptosis to occur (40). The replicative senescence that arises is a consequence of p53 activation, which (through p21CIP1) induces cell cycle arrest (41). Telomerase activity is associated with cells that exhibit a high proliferative capacity while it is absent in most differentiated somatic cells (42, 43). Human telomerase reverse transcriptase (TERT), the catalytic subunit of telomerase, can be introduced to prevent the shortening of telomeres. In addition, ectopic TERT expression was also found to enhance cellular proliferation in a cell-type dependent manner. Its effect ranges from inducing no increase of cell proliferation, to a limited life span extension or even immortalization (44–46).

In HCEncs, the introduction of TERT did not increase life span for most donors under standard cell culturing conditions (14, 47, 48). However, TERT was found to extend cell survival by approximately 18 PD when culture conditions were adapted to reduce oxidative stress (14). After transfection of the HCEncs from a 15-day old donor with TERT, a subpopulation of fast proliferating cells was found that could be cultured for about 36 PD. These TERT-transfected cells exhibited many HCEnc-associated characteristics including contact inhibition, presence of ZO-1 and N-cadherin on protein level and an intact Na⁺/K⁺-ATPase pump function. Furthermore, no aneuploidy or tumorigenicity was observed (47). Schmedt et al. introduced TERT into a uniform-appearing subpopulation of cells that was present within a culture of mostly senescent primary HCEncs. Before TERT was introduced, the life span of this subpopulation had already exceeded that of a normal HCEncs culture. The ectopic expression of TERT caused the cell doubling time to be preserved at higher passages. Extensive characterization of these TERT overexpressing cells did not indicate any adverse effect on HCEnc-associated characteristics and functionality (48).

The relatively low impact of TERT on the HCEnc phenotype combined with its telomere lengthening function make it a viable candidate to induce immortalization when combined with another oncogene. The introduction of TERT in combination with HPV 16 E6 or CDK4 resulted in the immortalization of HCEncs, while stable expression of CDK4 or HPV 16 E6 alone merely extended their life span. The TERT/CDK4 immortalized HCEnc line remained responsive to contact inhibition and a transcriptome analysis indicated relatively close resemblance to cultured HCEncs (14).

CDK4 and Cyclin D1

A variant of CDK4, together with the gene coding for cyclin D1 (CCND1), has also been introduced in HCEncs (35). In this

CDK4 variant, arginine on position 24 is replaced by cysteine (CDK4R24C) (49). While CDK4R24C has the same functional activity as CDK4, it is not inhibited by p16INK4A and can therefore stimulate cell cycle entry more effectively (50). The cells that stably expressed both CDK4R24C and cyclin D1 were found to have an increased proliferative capacity and cell survival was extended by about 15 PD (35). Their morphology and expression of ZO-1 and N-cadherin mRNA was similar to that of primary cells. Both proteins were also detected by immunofluorescent staining but ZO-1 was particularly prominent around the nucleus instead of being mainly focused at the cellular junctions. Na⁺/K⁺-ATPase driven pump function seemed to be intact, albeit more variable when compared to primary cells, which could indicate a reduced Na⁺/K⁺-ATPase or barrier function. Subcutaneous injection of the transduced cells in nude mice did not result in tumor formation (35).

E2F2

In contrast to the genetic modifications described above using cells in culture, increasing the ECD by stimulating the proliferation of HCEncs on their own Descemet's membrane has also been reported (12, 13). Since corneal transplants can be stored in warm organ culture for weeks prior to use (51), *ex vivo* grafts with a low ECD could still be used for transplantation if the ECD is increased. By using adenoviruses, the HCEncs on full-thickness corneal specimen were transduced with the gene coding for the E2F2 transcription factor (13). As a result, the ECD was found to increase, while the characteristic hexagonal shape and monolayer feature of the HCEncs were preserved. Since adenoviral-mediated gene introduction only conveys transient gene expression, the number of E2F2 overexpressing cells decreased after 2 weeks (13).

ZONAB

Another target to increase the proliferative capacity of HCEncs is the ZONAB/ZO-1 pathway. ZONAB is a Y-box transcription factor that binds to ZO-1 and the cell cycle regulating protein CDK4 (52, 53). As cells are progressing toward confluence, they are known to upregulate ZO-1 expression to form a network of tight junctions (53). However, as ZO-1 is a tight junction associated protein, this causes the amount of cytoplasmic ZONAB to increase at the expense of its nuclear counterpart. Correspondingly, CDK4 was found to be mainly expressed in the cytoplasm and reduced in the nucleus, at confluence (52, 53). ZONAB itself also negatively regulates the *ERBB2* gene, which encodes an oncogenic growth factor receptor (53, 54). However, experiments in a canine kidney cell line indicate that alterations of *ERBB2* expression do not influence cell proliferation rates. Therefore, it was suggested that the ZONAB/ZO-1 pathway is more likely to regulate cell cycle arrest through CDK4 (52). ZONAB was also found to have a direct effect on the upregulation of other cell cycle associated genes including the one coding for cyclin D1 (55).

Overexpression of ZONAB in HCEncs present on the Descemet's membrane of full-thickness corneal specimen increased the ECD significantly, while immunohistochemical staining for F-actin indicated the distinct hexagonal HCEnC

morphology. Also the effects of ZO-1 repression, by employing short hairpin RNA (shRNA) targeting ZO-1, have been assessed in HCEncs but will further be discussed below (12).

PROLIFERATION ENHANCEMENT THROUGH RNA INTERFERENCE

RNAi-based methods can also be used to enhance cellular proliferation, avoiding the need for introducing oncogenes. With RNAi, specific genes can be downregulated by targeted degradation of their mRNAs while hopefully avoiding unexpected downstream effects.

ZO-1

Previously, the ZONAB/ZO-1 pathway has been discussed together with the effect of ZONAB overexpression on HCEnC proliferation. In this respect, the downregulation of ZO-1 by employing ZO-1 shRNA has been used with the goal of increasing the proliferative capacity of HCEncs on a donor graft by exploiting the same pathway. Interestingly, ZO-1 shRNA only increased the amount of HCEncs significantly on full-thickness donor grafts with a relatively low ECD, independent of age, while this was not reported in the cells overexpressing ZONAB (12). As a result, it was concluded that the ZO-1 downregulated cells were still very sensitive to contact inhibition. Immunohistochemical staining for F-actin and ZO-1 did not indicate disruption of HCEnC barrier but only a reduced expression of ZO-1. The HCEncs exhibited their characteristic hexagonal to polygonal shape (12). BrdU staining of a ZO-1 siRNA treated contact inhibited monolayer comprised of cultured corneal scleral HCEncs also indicated an absence of induced proliferation (56). These results indicate that a downregulation of ZO-1 by RNAi is not sufficient to promote HCEnC proliferation in the presence of contact inhibition.

p53 and CKIs

Other negative regulatory mechanisms of the cell cycle have been targeted to increase the proliferation of HCEncs aside from the silencing of ZO-1. Targeting of p53 mRNA by stable expression of p53 shRNA was found to increase survival by about 12 PD while combination with TERT overexpression induced immortalization of HCEncs (14).

Downregulation of the CKI p27KIP1 in a confluent culture by p27KIP1 siRNA caused a 30% increase of ECD in young donors (<28 years) while no increase was observed in HCEncs originating from older donors (>60 years) (57). The p27KIP1 siRNA transfected cells showed a normal morphology and ZO-1 immunocytochemical staining. Both the use of p27KIP1 siRNA and antisense oligonucleotides was attempted. While both successfully decreased the expression of p27KIP1, p27KIP1 antisense oligonucleotides resulted in a lower survival rate. Therefore, p27KIP1 antisense oligonucleotide-based silencing was not pursued further (57). While p27KIP1 siRNA did not increase the ECD when using cells of older donors, the average amount of HCEncs between such donors was found to more than double when the expression of p21CIP1 and P16INK4 was simultaneously downregulated by electroporation with their

respective siRNA. However, due to extensive variations between the donors, this was not enough to establish a significant difference compared to the control (58).

p120 Catenin/Kaiso

Cell-cell junctions are important for the maintenance of contact inhibition and barrier function in the HCEC monolayer (12, 59). The effect of the tight junction associated ZO-1/ZONAB pathway has been discussed, but adherens junctions are also associated with a decreased proliferative capacity of HCECs (59). Adherens junctions consist of an extracellular side comprising cadherins that establish cell-cell interactions. On the cytoplasmic side, these cadherins interact with catenins to induce intracellular changes (60). One of these catenins, p120 catenin, both stabilizes E-cadherin and inhibits Kaiso, a transcriptional repressor (61, 62).

Downregulation of p120 catenin (*CTNND1*), by introducing p120 catenin siRNA, decreased the amount of p120 catenin at the cell junction in a contact inhibited monolayer of cultured peripheral HCECs (56). Counterintuitively, the amount of nuclear p120 catenin increased through nuclear translocation of this protein, allowing it to inhibit Kaiso (56, 63). This caused the surface area of the HCEC monolayer to double compared to the control, while maintaining a healthy ECD. This proliferative effect, elicited by p120 catenin/Kaiso signaling, can be partially explained by inhibition of the Hippo pathway (56). The Hippo pathway suppresses cellular proliferation by phosphorylation of transcriptional co-activators Yes-associated protein (YAP) and transcriptional coactivator with PDZ-binding motif (TAZ) (64). The p120 catenin siRNA was found to increase nuclear unphosphorylated YAP and TAZ, allowing them to interact with their (proliferation related) target genes (56). Ectopic expression of YAP in immortalized HCECs (B4G12 cell line) induced an overexpression of the previously mentioned cell cycle promoting cyclin D1, which has been identified as a target gene of YAP (65, 66). Cell cycle inhibitors p27KIP1 and p21CIP1 were found to be downregulated (65). It is important to note that the primary HCECs from these experiments were not dissociated into single cells by using EDTA-trypsin. Instead, they were isolated while leaving intercellular junctions intact. This was done because disruption of intercellular junctions with EDTA-trypsin, followed by p120 catenin siRNA treatment, negatively influenced proliferation (56).

The apparent relationship between the p120 catenin-mediated Kaiso inhibition and cell proliferation, led to investigating the effect of Kaiso knockdown. Treatment with Kaiso siRNA alone, did not influence nuclear Kaiso expression nor increased BrdU labeling (56). However, Kaiso siRNA was found to work synergistically with p120 catenin siRNA and their combination resulted in a significant expansion of the HCEC monolayer compared to p120 catenin siRNA alone (56, 63). By combining p120 catenin and Kaiso siRNA, one-quarter of a corneoscleral rim (< 1 mm diameter) could be expanded up to 6.8 ± 0.3 mm in diameter, which lies within the range of a transplantable graft. The hexagonal morphology of the cells was preserved and one week after withdrawal from siRNA treatments,

immunocytochemical staining indicated similar F-actin, ZO-1 and Na^+/K^+ -ATPase staining to the control (63).

Weekly p120 catenin and Kaiso siRNA treatment in modified embryonic stem cell medium instead of the supplemental hormonal epithelial medium that was used in the corresponding experiments described above, further increased the proliferative capacity of the HCECs. It allowed for the expansion of HCECs from one-eighth of the corneoscleral rim to make a graft of 11 ± 0.6 mm in diameter after 5 weeks (67).

PROLIFERATION ENHANCEMENT THROUGH CRISPR/DCAS9

The CRISPR/dCas9-system allows the overexpression of endogenous target genes by directing a fusion protein, comprising dCas9 and a transactivation domain, to specific gene promoters through coexpression with guide RNA. The guide RNA determines the target, while the transactivation domain facilitates gene expression (68). This technique has garnered a lot of research attention of late and could be used to increase cell proliferation by enhancing the expression of endogenous oncogenes.

Sex-Determining Region Y-box 2

Sex-determining region Y-box 2 (SOX2) is a transcription factor that belongs to the SOX family of proteins. The SOX family members are characterized by a specific DNA-binding motif, that allows them to bind to their target genes (69). SOX2 is indispensable for mammalian development, but has also been related to several of the hallmarks of cancer (70). However, it is probably best known as one of the four Yamanaka factors, that were used to convert somatic cells into pluripotent stem cells (i.e., cells able to differentiate into lineages of all three germ layers) (71).

CRISPR/dCas9-mediated overexpression of SOX2 significantly increased cell proliferation and viability in HCECs, while maintaining proper ZO-1 expression. Both CDK1 and cyclin D1 were upregulated and expression of the gene coding for p16INK4a was repressed. Interestingly, SOX2 upregulation also caused a repression of COL8A2 (72). Downregulation of the latter has been found to negatively influence HCEC functionality and proliferation (73). However, this is contradictory to the effects observed with SOX2 overexpression (72). A possible explanation is a difference in the extent of COL8A2 suppression, but it is also likely that other effects of SOX2 upregulation came into play. *In vivo* SOX2 overexpression in a cryoinjured rat corneal endothelium, indicated an increased proliferation and preservation of function by reducing corneal opacification compared to the control. The results suggest that activation of AKT-mediated inhibition of FOXO3a is involved in the increased proliferation elicited by SOX2 in HCECs (72). However, aside from its relation to AKT, SOX2 has been found to influence proliferation by interacting with many other proliferation regulation factors (74). Therefore, it is not yet clear which factors are responsible for the observed increase of proliferation in HCECs.

TABLE 1 | Genes of which the expression has been modified to increase proliferation in HCEncs. For each gene of which the expression was altered in HCEncs to enhance cell proliferation, the strategy that was used for genetic engineering and the method of modification is shown.

Gene(s)	Genetic engineering strategy	Modification method	References
SV40 early region (SV40 Large T antigen)	Gene introduction	Electroporation	(26)
		Adenovirus	(27, 29)
		Retrovirus	(28)
SV40 early region (SV40 Large and small T antigen)	Gene introduction	Electroporation	(32)
HPV 16 E6	Gene introduction	Retrovirus	(14)
HPV 16 E6/E7	Gene introduction	Retrovirus	(28, 35, 39)
TERT	Gene introduction	Retrovirus	(14, 48)
		Lipid-based transfection reagent	(47)
TERT + HPV 16 E6	Gene introduction	Retrovirus	(14)
p53	RNAi (siRNA)	Retrovirus	(14)
TERT + p53	Gene introduction + RNAi (siRNA)	Retrovirus	(14)
CDK4	Gene introduction	Retrovirus	(14)
TERT + CDK4	Gene introduction	Retrovirus	(14)
CDK4 (CDK4R24C) + CCND1	Gene introduction	Retrovirus	(35)
E2F2	Gene introduction	Adenovirus	(13)
ZONAB	Gene introduction	Lentivirus	(12)
ZO-1	RNAi (shRNA)	Lentivirus	(12)
	RNAi (siRNA)	Lipid-based transfection reagent	(56)
P27KIP1	RNAi (siRNA)	Lipid-based transfection reagent	(57)
P21CIP1 + p16INK4a	RNAi (siRNA)	Electroporation	(58)
CTNND1 (p120 catenin)	RNAi (siRNA)	Lipid-based transfection reagent	(56, 63)
Kaiso	RNAi (siRNA)	Lipid-based transfection reagent	(56)
CTNND1 (p120 catenin) + Kaiso	RNAi (siRNA)	Lipid-based transfection reagent	(56, 63)
YAP	Gene introduction	Lipid-based transfection reagent	(65)
SOX2	Crispr/dCas9-mediated upregulation	Lipid-based transfection reagent	(72)
SIRT1	Crispr/dCas9-mediated upregulation	Lipid-based transfection reagent	(86)
APst I fragment of simian adenovirus type 7	Gene introduction	Microinjection	(90)
Adenovirus type 5 E1a/E1b	Gene introduction	Microinjection	(90)
Adenovirus E1a + HRAS	Gene introduction	Microinjection	(90)

CDK, cyclin-dependent kinase; CRISPR, clustered regularly interspaced short palindromic repeats; dCas9, deactivated CRISPR-associated protein 9; HCEncs, human corneal endothelial cells; HPV-16, human papilloma virus type 16; TERT, telomerase reverse transcriptase; RNAi, RNA interference; SOX2, sex-determining region Y-box 2; SV40, simian virus 40; YAP, Yes-associated protein.

SIRT1

The nicotinamide adenine dinucleotide-dependent deacetylase, SIRT1, is a member of the sirtuin family and has a diverse array of targets inside the cell (75, 76). Its targets comprise both histone and non-histone proteins through which SIRT1 can act as an epigenetic regulator and alter the activity of its target proteins such as p53 (77), c-MYC (78), Rb family members (79), E2F1 (80), FOXO3a transcription factor (81) and more (82). Accordingly, SIRT1 is involved in several cellular processes including proliferation, telomere maintenance, DNA damage response, oxidative stress, apoptosis and energy metabolism (82). However, its effect on proliferation is context dependent since SIRT1 can both promote (83) and limit (84) proliferation of human primary cells. Others also reported no effect of SIRT1 overexpression on replicative lifespan (85).

In HCEncs, endogenous overexpression of SIRT1 resulted in a significant increase of BrdU staining and cell viability while the polygonal shape of the cells was preserved (86). Correspondingly, cyclin A2 and p16INK4a were upregulated and downregulated, respectively. The same authors also conducted an *in vivo* study on cryoinjured rat corneas in which they found that SIRT1 overexpression decreased corneal opacity and increased ECD (86).

DISCUSSION

Throughout the years, a variety of genetic engineering strategies have been employed to introduce proliferation related genes into HCEncs (Table 1). They have increased our understanding of HCEnC proliferation and aid in

the search for strategies to expand the amount of these cells for research or clinical purposes. However, comparing proliferation enhancing genes with one another is challenging, because the characteristics that are required will depend on the application. Also the lack of a general consensus about which phenotypical and functional characteristics define a healthy HCEnC monolayer and the diversity of metrics used to quantify proliferation, complicates this matter (87).

The ideal proliferation enhancing gene is difficult to define. To make donor grafts with a low ECD available for transplantation, a relatively small increase in proliferation may suffice. However, if the goal is to use these cells for intracameral injection or in combination with endothelial scaffolds, the ideal endpoint would be an off-the-shelf product. While this is not possible for many other transplantable tissues, the immune-privileged environment of the anterior chamber does not require systematic patient/donor matching for corneal endothelial transplantation. Although the current gene engineering strategies allow to only temporarily increase cell proliferation through transient ectopic gene expression, there remain to be concerns with regard to the safety of these methods. Unfortunately, studies concerning the safety of proliferative enhanced HCEnCs are sparse, making it difficult to predict the behavior of these cells *in vivo*.

REFERENCES

- Bonanno JA. Identity and regulation of ion transport mechanisms in the corneal endothelium. *Prog Retin Eye Res.* (2003) 22:69–94. doi: 10.1016/S1350-9462(02)00059-9
- Bourne WM, Nelson LIL, Hodge DO. Central corneal endothelial cell changes over a ten-year period. *Investig Ophthalmol Vis Sci.* (1997) 38:779–82.
- Abdellah MM, Ammar HG, Anbar M, Mostafa EM, Farouk MM, Sayed K, et al. Corneal endothelial cell density and morphology in healthy egyptian eyes. *J Ophthalmol.* (2019) 2019:6370241. doi: 10.1155/2019/6370241
- Joyce NC. Proliferative capacity of corneal endothelial cells. *Exp Eye Res.* (2012) 95:16–23. doi: 10.1016/j.exer.2011.08.014
- Joyce NC. Proliferative capacity of the corneal endothelium. *Prog Retin Eye Res.* (2003) 22:359–89. doi: 10.1016/S1350-9462(02)00065-4
- Gain P, Jullienne R, He Z, Aldossary M, Acquart S, Cognasse F, et al. Global survey of corneal transplantation and eye banking. *JAMA Ophthalmol.* (2016) 134:167–73. doi: 10.1001/jamaophthalmol.2015.4776
- Kinoshita S, Koizumi N, Ueno M, Okumura N, Imai K, Tanaka H, et al. Injection of cultured cells with a ROCK inhibitor for bullous keratopathy. *N Engl J Med.* (2018) 378:995–1003. doi: 10.1056/NEJMoa1712770
- Peh GSL, Ong HS, Adnan K, Ang H, Lwin CN, Seah X, et al. Functional evaluation of two corneal endothelial cell-based therapies: tissue-engineered construct and cell injection. *Sci Rep.* (2019) 9:6087. doi: 10.1038/s41598-019-42493-3
- Van den Bogerd B, Dhubhghaill SN, Zakaria N. Cultured cells and ROCK inhibitor for bullous keratopathy. *N Engl J Med.* (2018) 379:1184–1185. doi: 10.1056/NEJMc1805808
- Teichmann J, Valtink M, Nitschke M, Gramm S, Funk R, Engelmann K, et al. Tissue engineering of the corneal endothelium: a review of carrier materials. *J Funct Biomater.* (2013) 4:178–208. doi: 10.3390/jfb4040178
- Hoorick JV, Delaey J, Vercammen H, Erps JV, Thienpont H, Dubrueel P, et al. Designer descemet membranes containing PDLLA and functionalized gelatins as corneal endothelial scaffold. *Adv Healthc Mater.* (2020) 9:2000760. doi: 10.1002/adhm.202000760
- Kampik D, Basche M, Georgiadis A, Luhmann UF, Larkin DF, Smith AJ, et al. Modulation of contact inhibition by ZO-1/ZONAB gene transfer—a new strategy to increase the endothelial cell density of corneal grafts. *Investig Ophthalmol Vis Sci.* (2019) 60:3170–7. doi: 10.1167/iops.18-26260
- McAlister JC, Joyce NC, Harris DL, Ali RR, Larkin DFP. Induction of replication in human corneal endothelial cells by E2F2 transcription factor cDNA transfer. *Investig Ophthalmol Vis Sci.* (2005) 46:3597–603. doi: 10.1167/iops.04-0551
- Sheerin AN, Smith SK, Jennert-Burston K, Brook AJ, Allen MC, Ibrahim B, et al. Characterization of cellular senescence mechanisms in human corneal endothelial cells. *Aging Cell.* (2012) 11:234–40. doi: 10.1111/j.1474-9726.2011.00776.x
- Bartakova A, Alvarez-Delfin K, Weisman AD, Salero E, Raffa GA, Merkhofer RM, et al. Novel identity and functional markers for human corneal endothelial cells. *Investig Ophthalmol Vis Sci.* (2016) 57:2749–62. doi: 10.1167/iops.15-18826
- Miyata K, Drake J, Osakabe Y, Hosokawa Y, Hwang D, Soya K, et al. Effect of donor age on morphologic variation of cultured human corneal endothelial cells. *Cornea.* (2001) 20:59–63. doi: 10.1097/00003226-200101000-00012
- Bertoli C, Skotheim JM, De Bruin RAM. Control of cell cycle transcription during G1 and S phases. *Nat Rev Mol Cell Biol.* (2013) 14:518–28. doi: 10.1038/nrm3629
- Yao G. Modelling mammalian cellular quiescence. *Interface Focus.* (2014) 4:20130074. doi: 10.1098/rsfs.2013.0074
- Suryadinata R, Sadowski M, Sarcevic B. Control of cell cycle progression by phosphorylation of cyclin-dependent kinase (CDK) substrates. *Biosci Rep.* (2010) 30:243–55. doi: 10.1042/BSR20090171
- Harbour JW, Luo RX, Dei Santi A, Postigo AA, Dean DC. Cdk phosphorylation triggers sequential intramolecular interactions that progressively block Rb functions as cells move through G1. *Cell.* (1999) 98:859–69. doi: 10.1016/S0092-8674(00)81519-6
- Sherr CJ, Roberts JM. CDK inhibitors: Positive and negative regulators of G1-phase progression. *Genes Dev.* (1999) 13:1501–12. doi: 10.1101/gad.13.12.1501

AUTHOR CONTRIBUTIONS

WA searched the literature and wrote the manuscript. WA and BV conceptualized the manuscript and designed figures. BV provided scientific guidance. BV, HV, SN, and CK critically revised and commented the manuscript. All authors have read and approved the final manuscript.

FUNDING

This study was supported by the BOF Kleine Projecten grant (ID 43440) of the University of Antwerp.

22. Chen J. The Cell-Cycle Arrest and Apoptotic Functions of p53 in Tumor Initiation and Progression. *Cold Spring Harb Perspect Biol.* (2016) 6:a026104. doi: 10.1101/cshperspect.a026104
23. Ahuja D, Sáenz-Robles MT, Pipas JM. SV40 large T antigen targets multiple cellular pathways to elicit cellular transformation. *Oncogene.* (2005) 24:7729–7745. doi: 10.1038/sj.onc.1209046
24. Zheng ZM. Viral oncogenes, noncoding RNAs, and RNA splicing in human tumor viruses. *Int J Biol Sci.* (2010) 6:730–55. doi: 10.7150/ijbs.6.730
25. Liu X, Dakic A, Chen R, Disbrow GL, Zhang Y, Dai Y, et al. Cell-Restricted Immortalization by Human Papillomavirus Correlates with Telomerase Activation and Engagement of the hTERT Promoter by Myc. *J Virol.* (2008) 82:11568–76. doi: 10.1128/JVI.01318-08
26. Wilson SE, Lloyd SA, He YG, McCash CS. Extended life of human corneal endothelial cells transfected with the SV40 large T antigen. *Investig Ophthalmol Vis Sci.* (1993) 34:2112–23.
27. Schönthal AH, Hwang JJ, Stevenson D, Trousdale MD. Expression and activity of cell cycle-regulatory proteins in normal and transformed corneal endothelial cells. *Exp Eye Res.* (1999) 68:531–9. doi: 10.1006/exer.1998.0634
28. Wilson SE, Weng J, Blair S, He YG, Lloyd S. Expression of E6/E7 or SV40 large T antigen-coding oncogenes in human corneal endothelial cells indicates regulated high-proliferative capacity. *Investig Ophthalmol Vis Sci.* (1995) 36:32–40.
29. Feldman ST, Gjerset R, Gately D, Chien KR, Feramisco JR. Expression of SV40 virus large T antigen by recombinant adenoviruses activates proliferation of corneal endothelium in vitro. *J Clin Invest.* (1993) 91:1713–20. doi: 10.1172/JCI116381
30. Stewart N, Bacchetti S. Expression of SV40 large T antigen, but not small t antigen, is required for the induction of chromosomal aberrations in transformed human cells. *Virology.* (1991) 180:49–57. doi: 10.1016/0042-6822(91)90008-Y
31. Oshikawa K, Matsumoto M, Kodama M, Shimizu H, Nakayama KI. A fail-safe system to prevent oncogenesis by senescence is targeted by SV40 small T antigen. *Oncogene.* (2020) 39:2170–86. doi: 10.1038/s41388-019-1139-1
32. Bednarz J, Teifel M, Friedl P, Engelmann K. Immortalization of human corneal endothelial cells using electroporation protocol optimized for human corneal endothelial and human retinal pigment epithelial cells. *Acta Ophthalmol Scand.* (2000) 78:130–6. doi: 10.1034/j.1600-0420.2000.078002130.x
33. Aboalchamat B, Engelmann K, Böhnke M, Eggl P, Bednarz J. Morphological and functional analysis of immortalized human corneal endothelial cells after transplantation. *Exp Eye Res.* (1999) 69:547–53. doi: 10.1006/exer.1999.0736
34. Valtink M, Gruschwitz R, Funk RHW, Engelmann K. Two clonal cell lines of immortalized human corneal endothelial cells show either differentiated or precursor cell characteristics. *Cells Tissues Organs.* (2008) 187:286–94. doi: 10.1159/000113406
35. Yokoi T, Seko Y, Yokoi T, Makino H, Hatou S, Yamada M, et al. Establishment of Functioning Human Corneal Endothelial Cell Line with High Growth Potential. *PLoS ONE.* (2012) 7:1–8. doi: 10.1371/journal.pone.0029677
36. Scheffner M, Werness BA, Huibregtse JM, Levine AJ, Howley PM. The E6 oncoprotein encoded by human papillomavirus types 16 and 18 promotes the degradation of p53. *Cell.* (1990) 63:1129–36. doi: 10.1016/0092-8674(90)90409-8
37. Huh K, Zhou X, Hayakawa H, Cho J-Y, Libermann TA, Jin J, et al. Human papillomavirus type 16 E7 oncoprotein associates with the cullin 2 ubiquitin ligase complex, which contributes to degradation of the retinoblastoma tumor suppressor. *J Virol.* (2007) 81:9737–47. doi: 10.1128/JVI.00881-07
38. Yeo-Teh NSL, Ito Y, Jha S. High-risk human papillomaviral oncogenes E6 and E7 target key cellular pathways to achieve oncogenesis. *Int J Mol Sci.* (2018) 19:1706. doi: 10.3390/ijms19061706
39. Kim HJ, Ryu YH, Ahn J Il, Park JK, Kim JC. Characterization of immortalized human corneal endothelial cell line using HPV 16 E6/E7 on lyophilized human amniotic membrane. *Korean J Ophthalmol.* (2006) 20:47–54. doi: 10.3341/kjo.2006.20.1.47
40. Muraki K, Nyhan K, Han L, Murnane JP. Mechanisms of telomere loss and their consequences for chromosome instability. *Front Oncol.* (2012) 2:135. doi: 10.3389/fonc.2012.00135
41. Herbig U, Jobling WA, Chen BPC, Chen DJ, Sedivy JM. Telomere shortening triggers senescence of human cells through a pathway involving ATM, p53, and p21CIP1, but Not p16INK4a. *Mol Cell.* (2004) 14:501–13. doi: 10.1016/S1097-2765(04)00256-4
42. Belair CD, Yeager TR, Lopez PM, Reznikoff CA. Telomerase activity: a biomarker of cell proliferation, not malignant transformation. *Natl Acad Sci.* (1998) 94:13677–82. doi: 10.1073/pnas.94.25.13677
43. Wright WE, Piatyszek MA, Rainey WE, Byrd W, Shay JW. Telomerase activity in human germline and embryonic tissues and cells. *Dev Genet.* (1996) 18:173–9. doi: 10.1002/(SICI)1520-6408
44. Di Donna S, Mamchaoui K, Cooper RN, Seigneurin-Venin S, Tremblay J, Butler-Browne GS, et al. Telomerase can extend the proliferative capacity of human myoblasts, but does not lead to their immortalization. *Mol Cancer Res.* (2003) 1:643–53.
45. Bodnar AG, Ouellette M, Frolkis M, Holt SE, Chiu CP, Morin GB, et al. Extension of life-span by introduction of telomerase into normal human cells. *Science.* (1998) 279:349–52. doi: 10.1126/science.279.5349.349
46. Evans RJ, Wyllie FS, Wynford-Thomas D, Kipling D, Jones CJ. A P53-dependent, telomere-independent proliferative life span barrier in human astrocytes consistent with the molecular genetics of glioma development. *Cancer Res.* (2003) 63:4854–61.
47. Liu Z, Zhuang J, Li C, Wan P, Li N, Zhou Q, et al. Long-term cultivation of human corneal endothelial cells by telomerase expression. *Exp Eye Res.* (2012) 100:40–51. doi: 10.1016/j.exer.2012.04.013
48. Schmedt T, Chen Y, Nguyen TT, Li S, Bonanno JA, Jurkunas U V. Telomerase immortalization of human corneal endothelial cells yields functional hexagonal monolayers. *PLoS ONE.* (2012) 7:e51427. doi: 10.1371/journal.pone.0051427
49. Wölfel T, Hauer M, Schneider J, Serrano M, Wölfel C, Klehmann-Hieb E, et al. A p16INK4a-insensitive CDK4 mutant targeted by cytolytic T lymphocytes in a human melanoma. *Science.* (1995) 269:1281–4. doi: 10.1126/science.7652577
50. Shapiro GI, Edwards CD, Ewen ME, Rollins BJ. p16INK4A Participates in a G1 Arrest checkpoint in response to DNA damage. *Mol Cell Biol.* (1998) 18:378–87. doi: 10.1128/MCB.18.1.378
51. Pels E, Rijnveld WJ. Organ culture preservation for corneal tissue. *Eye Bank.* (2009) 43:31–46. doi: 10.1159/000223837
52. Balda MS, Garrett MD, Matter K. The ZO-1-associated Y-box factor ZONAB regulates epithelial cell proliferation and cell density. *J Cell Biol.* (2003) 160:423–32. doi: 10.1083/jcb.200210020
53. Balda MS. The tight junction protein ZO-1 and an interacting transcription factor regulate ErbB-2 expression. *EMBO J.* (2000) 19:2024–33. doi: 10.1093/emboj/19.9.2024
54. Moasser MM. The oncogene HER2: Its signaling and transforming functions and its role in human cancer pathogenesis. *Oncogene.* (2007) 26:6469–87. doi: 10.1038/sj.onc.1210477
55. Sourisseau T, Georgiadis A, Tsapara A, Ali RR, Pestell R, Matter K, et al. Regulation of PCNA and Cyclin D1 Expression and epithelial morphogenesis by the ZO-1-regulated transcription factor ZONAB/DbpA. *Mol Cell Biol.* (2006) 26:2387–98. doi: 10.1128/MCB.26.6.2387-2398.2006
56. Zhu YT, Chen HC, Chen SY, Tseng SCG. Nuclear p120 catenin unlocks mitotic block of contactinhibited human corneal endothelial monolayers without disrupting adherent junctions. *J Cell Sci.* (2012) 125:3636–48. doi: 10.1242/jcs.103267
57. Kikuchi M, Zhu C, Senoo T, Obara Y, Joyce NC. p27kip1 siRNA induces proliferation in corneal endothelial cells from young but not older donors. *Investig Ophthalmol Vis Sci.* (2006) 47:4803–9. doi: 10.1167/iovs.06-0521
58. Joyce NC, Harris DL. Decreasing expression of the G1-phase inhibitors, p21Cip1 and p16ink4a, promotes division of corneal endothelial cells from older donors. *Mol Vis.* (2010) 16:897–906.
59. Zhu YT, Hayashida Y, Kheirkhah A, He H, Chen SY, Tseng SCG. Characterization and comparison of intercellular adherent junctions expressed by human corneal endothelial cells *in vivo* and *in vitro*. *Investig Ophthalmol Vis Sci.* (2008) 49:3879–86. doi: 10.1167/iovs.08-1693
60. Harris TJC, Tepass U. Adherens junctions: from molecules to morphogenesis. *Nat Rev Mol Cell Biol.* (2010) 11:502–14. doi: 10.1038/nrm2927
61. Ireton RC, Davis MA, Van Hengel J, Mariner DJ, Barnes K, Thoreson MA, et al. A novel role for p120 catenin in E-cadherin function. *J Cell Biol.* (2002) 159:465–76. doi: 10.1083/jcb.200205115

62. Kelly KE, Spring CM, Otchere AA, Daniel JM. NLS-dependent nuclear localization of p120ctn is necessary to relieve Kaiso-mediated transcriptional repression. *J Cell Sci.* (2004) 117:2675–86. doi: 10.1242/jcs.01101
63. Zhu YT, Han B, Li F, Chen SY, Tighe S, Zhang S, et al. Knockdown of both p120 catenin and kaiso promotes expansion of human corneal endothelial monolayers via rhoa-rock-noncanonical BMP-NFκB pathway. *Investig Ophthalmol Vis Sci.* (2014) 55:1509–18. doi: 10.1167/iows.13-13633
64. Zheng Y, Pan D. The Hippo signaling pathway in development and disease. *Dev Cell.* (2019) 50:264–82. doi: 10.1016/j.devcel.2019.06.003
65. Hsueh YJ, Chen HC, Wu SE, Wang TK, Chen JK, Ma DHK. Lysophosphatidic acid induces YAP-promoted proliferation of human corneal endothelial cells via PI3K and ROCK pathways. *Mol Ther Methods Clin Dev.* (2015) 2:15014. doi: 10.1038/mtm.2015.14
66. Mizuno T, Murakami H, Fujii M, Ishiguro F, Tanaka I, Kondo Y, et al. YAP induces malignant mesothelioma cell proliferation by upregulating transcription of cell cycle-promoting genes. *Oncogene.* (2012) 31:5117–22. doi: 10.1038/onc.2012.5
67. Zhu YT, Li F, Han B, Tighe S, Zhang S, Chen SY, et al. Activation of RhoA-ROCK-BMP signaling reprograms adult human corneal endothelial cells. *J Cell Biol.* (2014) 206:799–811. doi: 10.1083/jcb.2014.04032
68. Perez-Pinera P, Kocak DD, Vockley CM, Adler AF, Kabadi AM, Polstein LR, et al. RNA-guided gene activation by CRISPR-Cas9-based transcription factors. *Nat Methods.* (2013) 10:973–6. doi: 10.1038/nmeth.2600
69. Bowles J, Schepers G, Koopman P. Phylogeny of the SOX family of developmental transcription factors based on sequence and structural indicators. *Dev Biol.* (2000) 227:239–55. doi: 10.1006/dbio.2000.9883
70. Novak D, Hüser L, Elton JJ, Umansky V, Altevogt P. SOX₂ in development and cancer biology. *Semin Cancer Biol.* (2019) 67:74–82. doi: 10.1016/j.semcancer.2019.08.007
71. Takahashi K, Yamanaka S. Induction of pluripotent stem cells from mouse embryonic and adult fibroblast cultures by defined factors. *Cell.* (2006) 126:663–76. doi: 10.1016/j.cell.2006.07.024
72. Chang YK, Hwang JS, Chung TY, Shin YJ. SOX2 activation using CRISPR/dCas9 promotes wound healing in corneal endothelial cells. *Stem Cells.* (2018) 36:1851–62. doi: 10.1002/stem.2915
73. Hwang JS, Ma DJ, Choi J, Shin YJ. COL8A2 regulates the fate of corneal endothelial cells. *Invest Ophthalmol Vis Sci.* (2020) 61:26. doi: 10.1167/iows.61.11.26
74. Weina K, Utikal J. SOX2 and cancer: current research and its implications in the clinic. *Clin Transl Med.* (2014) 3:19. doi: 10.1186/2001-1326-3-19
75. Frye RA. Phylogenetic classification of prokaryotic and eukaryotic Sir2-like proteins. *Biochem Biophys Res Commun.* (2000) 273:793–798. doi: 10.1006/bbrc.2000.3000
76. Landry J, Sutton A, Tafrov ST, Heller RC, Stebbins J, Pillus L, et al. The silencing protein SIR2 and its homologs are NAD-dependent protein deacetylases. *Proc Natl Acad Sci U.S.A.* (2000) 97:5807–11. doi: 10.1073/pnas.110148297
77. Vaziri H, Dessain SK, Eaton EN, Imai S-I, Frye RA, Pandita TK, et al. hSIR2/SIRT1 Functions as an NAD-Dependent p53 Deacetylase. *Cell.* (2001) 107:149–59. doi: 10.1016/S0092-8674(01)00527-X
78. Yuan J, Minter-Dykhouse K, Lou Z. A c-Myc-SIRT1 feedback loop regulates cell growth and transformation. *J Cell Biol.* (2009) 185:203–11. doi: 10.1083/jcb.200809167
79. Wong S, Weber JD. Deacetylation of the retinoblastoma tumour suppressor protein by SIRT1. *Biochem J.* (2007) 407:451–60. doi: 10.1042/BJ20070151
80. Wang C, Chen L, Hou X, Li Z, Kabra N, Ma Y, et al. Interactions between E2F1 and SirT1 regulate apoptotic response to DNA damage. *Nat Cell Biol.* (2006) 8:1025–31. doi: 10.1038/ncb1468
81. Motta MC, Divecha N, Lemieux M, Kamel C, Chen D, Gu W, et al. Mammalian SIRT1 represses forkhead transcription factors. *Cell.* (2004) 116:551–63. doi: 10.1016/S0092-8674(04)00126-6
82. Yuan H, Su L, Chen W. The emerging and diverse roles of sirtuins in cancer: a clinical perspective. *Onco Targets Ther.* (2013) 6:1399–416. doi: 10.2147/OTT.S37750
83. Yuan HF, Zhai C, Yan XL, Zhao DD, Wang JX, Zeng Q, et al. SIRT1 is required for long-term growth of human mesenchymal stem cells. *J Mol Med.* (2012) 90:389–400. doi: 10.1007/s00109-011-0825-4
84. Blander G, Bhimavarapu A, Mammone T, Maes D, Elliston K, Reich C, et al. SIRT1 promotes differentiation of normal human keratinocytes. *J Invest Dermatol.* (2009) 129:41–9. doi: 10.1038/jid.2008.179
85. Michishita E, Park JY, Burneskis JM, Barrett JC, Horikawa I. Evolutionarily conserved and nonconserved cellular localizations and functions of human SIRT proteins. *Mol Biol Cell.* (2005) 16:4623–35. doi: 10.1091/mbc.e05-01-0033
86. Joo HJ, Ma DJ, Hwang JS, Shin YJ. Sirt1 activation using CRISPR/dCas9 promotes regeneration of human corneal endothelial cells through inhibiting senescence. *Antioxidants.* (2020) 9:1–8. doi: 10.3390/antiox911085
87. Van den Bogerd B, Zakaria N, Adam B, Matthyssen S, Koppen C, Dhubbghaill SN. Corneal endothelial cells over the past decade: Are we missing the mark(er)? *Transl Vis Sci Technol.* (2019) 8: doi: 10.1167/tvst.8.6.13
88. Thuret G, Courrier E, Poinard S, Gain P, Baud'Huin M, Martinache I, et al. One threat, different answers: the impact of COVID-19 pandemic on cornea donation and donor selection across Europe. *Br J Ophthalmol.* (2020) 0:1–7. doi: 10.1136/bjophthalmol-2020-317938
89. Ang M, Moriyama A, Colby K, Sutton G, Liang L, Sharma N, et al. Corneal transplantation in the aftermath of the COVID-19 pandemic: an international perspective. *Br J Ophthalmol.* (2020) 104:1477–1481. doi: 10.1136/bjophthalmol-2020-317013
90. Zavizion BA, Pistov MY, Bergerson SM, Miroshnichenko OL, Trakht IN. Transformation of human corneal endothelial cells by micro-injection of oncogenes. *Biulleten'eksperimental'noi Biol i meditsiny.* (1990) 109:395–98. doi: 10.1007/BF00840058

Conflict of Interest: The authors declare that the research was conducted in the absence of any commercial or financial relationships that could be construed as a potential conflict of interest.

Copyright © 2021 Arras, Vercammen, Ni Dhubbghaill, Koppen and Van den Bogerd. This is an open-access article distributed under the terms of the Creative Commons Attribution License (CC BY). The use, distribution or reproduction in other forums is permitted, provided the original author(s) and the copyright owner(s) are credited and that the original publication in this journal is cited, in accordance with accepted academic practice. No use, distribution or reproduction is permitted which does not comply with these terms.



Long-Term Anatomical and Functional Survival of Boston Type 1 Keratoprosthesis in Congenital Aniridia

Ariann Dyer^{1,2†}, Alix De Faria^{1,2*†}, Gemma Julio^{1,2}, Juan Álvarez de Toledo^{1,2}, Rafael I. Barraquer^{1,2,3} and Maria Fideliz de la Paz^{1,2‡}

¹ Centro de Oftalmología Barraquer, Barcelona, Spain, ² Institut Universitari Barraquer, Universitat Autònoma de Barcelona, Barcelona, Spain, ³ Department of Medicine, Universitat Internacional de Catalunya, Barcelona, Spain

OPEN ACCESS

Edited by:

Stefano Ferrari,
Fondazione Banca degli Occhi del
Veneto Onlus - FBOV, Italy

Reviewed by:

Carina Koppen,
University of Antwerp, Belgium
Yoav Nahum,
Rabin Medical Center, Israel

*Correspondence:

Alix De Faria
defariaalix@gmail.com

[†]These authors have contributed
equally to this work and share first
authorship

[‡]Senior author

Specialty section:

This article was submitted to
Ophthalmology,
a section of the journal
Frontiers in Medicine

Received: 28 July 2021

Accepted: 30 August 2021

Published: 30 September 2021

Citation:

Dyer A, De Faria A, Julio G, Álvarez de
Toledo J, Barraquer RI and de la
Paz MF (2021) Long-Term Anatomical
and Functional Survival of Boston
Type 1 Keratoprosthesis in Congenital
Aniridia. *Front. Med.* 8:749063.
doi: 10.3389/fmed.2021.749063

Purpose: To analyze the long-term anatomical survival, functional survival, and complications of Boston type 1 keratoprosthesis (KPro) in the eyes with congenital aniridia-associated keratopathy (AAK).

Methods: A retrospective review of 12 eyes with congenital aniridia that underwent a Boston type 1 KPro surgery was conducted. A Kaplan–Meier analysis was performed. Anatomical and functional success criteria were KPro retention and a best corrected visual acuity (BCVA) ≤ 1.3 LogMAR (≥ 0.05 decimal) at the end of a follow-up period. Postoperative complications were recorded.

Results: The mean preoperative BCVA was 2.1 ± 0.9 (range: 3.8–1) LogMAR, and glaucoma was a comorbidity in all the cases. Five years after the surgery, the overall retention rate was 10/12 (83.3%), and 50% had functional success. Only three (25%) of the 12 cases did not achieve a BCVA ≤ 1.3 LogMAR. The cumulative probability of anatomical success was 92, 79, and 79% after 1, 5, and 10 years, respectively. The cumulative probability of functional success was 57 and 46% after 1 and 5 years, respectively. The mean anatomical and functional survival time was 10 ± 1.3 (95% IC = 7.5–12.3 years) and 3.8 ± 0.9 years (95% IC = 1.8–5.8 years), respectively. The most common postoperative complication was retroprosthetic membrane (RPM) formation in 8/16 cases (66%). The mean number of complications per case was 2.4 ± 1.8 (0–6).

Conclusions: The Boston type 1 KPro is a viable option for patients with AAK with good anatomical and functional long-term results. Glaucoma is an important preoperative condition that affects functional results. Retroprosthetic membrane formation seems to have a higher incidence in this condition.

Keywords: aniridia, Boston type-1 keratoprosthesis, extrusion, retroprosthetic membrane, aniridia associated keratopathy

INTRODUCTION

Congenital aniridia is a rare condition that affects 1/64,000 to 96,000 live births and has a major impact on vision and, therefore, quality of life (1). Classic aniridia is a panocular phenotypically heterogeneous condition (1, 2) that includes the partial or total absence of an iris, which may be associated with cataracts, foveal

and optic nerve hypoplasia, aniridia-associated keratopathy (AAK), and nystagmus (3). It is also associated with mutations in the PAX6 gene. Mutations in other genes contribute to other aniridia-like phenotypes with aniridia-related comorbidities (3–5).

Besides glaucoma, AAK is the most common cause of progressive vision loss, and it can present as early as the first decade of life; however, the median age of diagnosis is 33 years old (4). Aniridia-associated keratopathy is characterized by limbal stem cell deficiency, which causes progressive vascular pannus, corneal conjunctivalization, recurrent epithelial erosions, and subepithelial fibrosis, eventually leading to corneal opacification (2). Because of limbal cell deficiency, penetrating keratoplasty (PK) is usually unsuccessful in the long term, and keratolimbal allografts with or without subsequent PK may be a better alternative; however, aggressive long-term systemic immunosuppression is required (2, 6).

Reported evidence proposes a primary or secondary Boston type 1 keratoprosthesis (KPro) to treat debilitating conditions that carry poor prognoses with PK (2). Traditionally, patients with a KPro have been stratified into three broad categories according to their preoperative diagnoses: (i) recurrent immunologic rejection (including aniridia), (ii) chemical injury, and (iii) autoimmune disease. The first category has a better prognosis when a KPro is implanted. Additionally, a KPro is considered as a treatment option only after several graft failures (7, 8).

The objective of this study was to analyze the long-term anatomical and functional survival and complications of the Boston type 1 KPro in 12 eyes with congenital aniridia. In the last KPro study group meeting (2020), it was suggested that patients with aniridia should be categorized as a separate group rather than be included in the recurrent immunologic rejection category, as previously suggested by other authors (1). This is due to the higher incidence of complications in AAK than most disorders included in this category (1). It is for this reason that this study was conducted.

MATERIALS AND METHODS

This original article includes a retrospective review of 12 eyes (10 patients) with congenital aniridia that underwent Boston type 1 KPro surgeries at the Centro de Oftalmología Barraquer, Barcelona, Spain.

The subjects provided written informed consent for the surgery and to participate in clinical research projects at the Centro de Oftalmología Barraquer, Barcelona, Spain. Institutional review board approval was obtained for the retrospective review of the clinical records of the patients, and this study adhered to the tenets of the Declaration of Helsinki.

The surgical technique used for the implantation of the Boston type 1 KPro has been described widely (9). In summary, an 8.5- to 9-mm corneal donor button was trephined, and a 3-mm opening was created at its center with a punch. The optical stem of the KPro was placed through the central hole, the back plate was located in place, and then a titanium locking ring was fixed into

a groove in the optical stem. Finally, the cornea was sutured as in a standard PK. If an eye was pseudophakic, the intraocular lens (IOL) was left in place; if it was phakic, the lens was removed, making the eye aphakic.

Postoperative treatment includes the use of a permanent Proclear® (CooperVision Inc, Scottsville, NY, United States) soft contact lens that is 16-mm diameter, and an 8.8-mm base curve placed at the end of the surgery, along with wide-spectrum topical antibiotics (ciprofloxacin 3 mg/ml TID for 1 week and vancomycin 14 mg/ml BID to be continued for life), prednisolone acetate 1% (three to five times per day) with slow taper for 1 month, and anti-glaucomatous treatment as deemed necessary. A fornix rinse with povidone-iodine was performed every month in all the patients after the 1st month of the surgery.

A retrospective review of the medical records of all patients with congenital aniridia who underwent Boston type 1 KPro implantations from December 2010 to October 2019 was conducted at the Centro de Oftalmología Barraquer. Three experienced surgeons (AT, RIB, and MdP) implanted the Boston type 1 KPro in all the studied eyes.

Gender, age at surgery, visual acuity (VA), aniridia-related comorbidities, anatomical retention period, follow-up time, and postoperative complications were recorded and analyzed. The pre- and postoperative best corrected visual acuity (BCVA) of all the patients were measured and recorded on a decimal scale and then converted into a LogMAR scale for statistical analysis.

The main outcomes were graft retention and the BCVA. Secondary outcomes were postoperative complications.

A Kaplan–Meier survival analysis was performed. Anatomic success was defined as prosthesis retention during the follow-up period. Extrusion was considered as the exposure of the back plate due to corneal melting that needs surgical resolution such as a lamellar patch or KPro exchange.

Functional success was defined as BCVA ≤ 1.3 LogMAR (≥ 0.05 decimal) at the end of the follow-up period. The mean time of functional success was the estimated mean time with a maintained BCVA ≤ 1.3 LogMAR (≥ 0.05 decimal).

The follow-up period represents the time between the KPro surgery and the last recorded appointment with no signs of extrusion, or the interval of time between the KPro surgery and the first extrusion, which is when it was diagnosed. The follow-up period for the functional survival analysis was the time with a maintained BCVA ≤ 1.3 LogMAR.

RESULTS

Demographic Data

The 12 eyes of 10 patients were studied. There were three (30%) male and seven (70%) female patients. Nine (90%) of the patients were Caucasian, and one (10%) was African. The mean age at surgery was 37.1 years (range: 5–63 years). The mean follow-up time was 58.7 ± 41.4 months (range: 9–142 months).

Table 1 shows a list of individual demographic and clinical preoperative characteristics. The Boston type 1 KPro was a primary indication in seven eyes (58%), and the secondary Boston type 1 KPro was performed in five eyes (42%), which had undergone previous PKs that, in some cases, had multiple failed

TABLE 1 | Demographics and clinical preoperative features in each case.

Eye code	Age range	Gender	Preoperative BCVA (LogMar)	Previous surgeries	Comorbid conditions	Additional procedure
1	35	F	2.1	LA, PK, CE+IOL, S	N, OSD,G, FH,CC	
2	37	F	1.3	CE+IOL,S	N, OSD,G, FH,CC	IOLR
3	72	M	3.2	CE	N, OSD, G,CC	
4	5	F	1.3	CE,S	OSD,G, FH,CC	V
5	6	F	2.3	CE,S	OSD,G, FH,CC	V
6	35	F	1.7	CE+IOL,GS	OSD,G	
7	63	F	1	LA, PK,CE+IOL,GS, SIOL	N, OSD,G, FH	
8	13	M	3.8	PK, CE+IOL,GS	N, OSD,G, CC	
9	33	F	3.2	LA, CE+IOL, GS	N, OSD,G, CC	
10	51	M	2.1	PK, CE+IOL	N, OSD,G, FH,CC	
11	38	F	1.6	LA, CE+IOL, GS, E	N, OSD,G, CC	
12	57	F	1.5	LA, PK,CE+IOL	OSD,G, CC	

CC, congenital cataract; CE + intraocular lens (IOL), cataract extraction with IOL; CE, cataract extraction; E, epitheliectomy; F, female; FH, foveal hypoplasia; G, glaucoma; GS, glaucoma surgery; IOLR, IOL removal; M, male; N, nystagmus; LA, limbal allograft; OSD, ocular surface disease; PK, penetrating keratoplasty; RD, retinal detachment; S, strabismus; SIOL, suture of the IOL; V, vitrectomy.

attempts. Five of the eyes (42%) had previously undergone ocular surface stem-cell treatments (limbal allografts) without success.

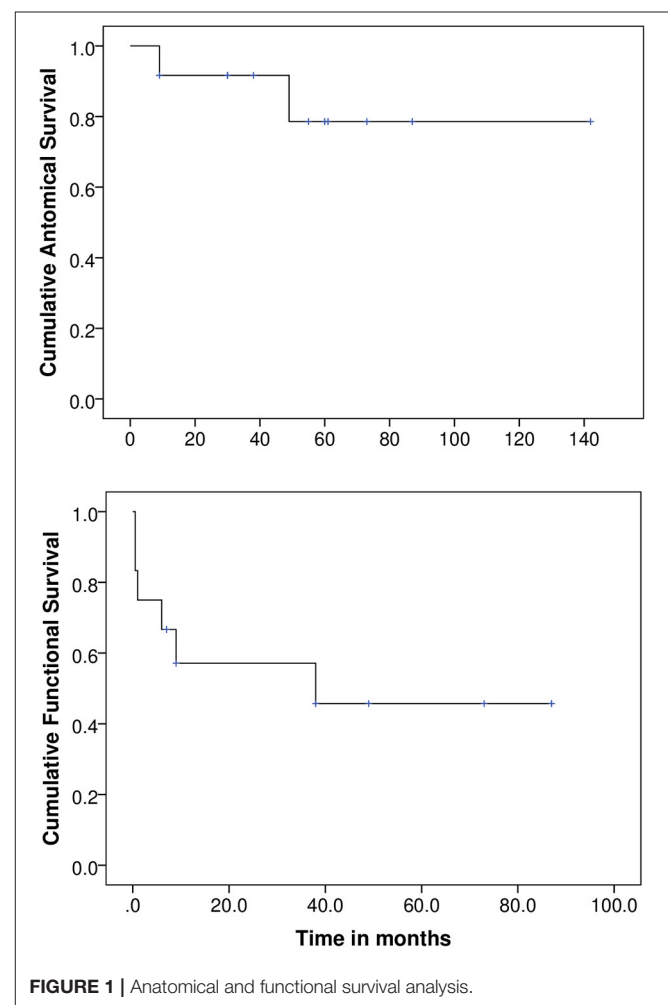
Most of the patients had poor preoperative visual acuities. The mean preoperative BCVA was 2.1 ± 0.9 LogMAR (range: 3.8–1 LogMAR). Aniridia-related comorbidities, such as nystagmus, were present in eight of the 12 cases (67%) and foveal hypoplasia was in six of the 12 cases (50%). All of the cases had both ocular surface diseases and glaucoma. Previously operated congenital cataracts were reported in 10 of the 12 cases (83%), and none of our patients suffered retinal detachments before the Boston type 1 KPro surgery.

Anatomical Results

The overall retention rate of the Boston type 1 KPro 5 years after the surgery was 83.3% (10/12). The mean follow-up for the anatomical survival analysis was 53.6 ± 36.6 months (range: 9–142 months). The cumulative success rate by the Kaplan–Meier analysis was 92, 79, and 79% after 1, 5, and 10 years, respectively. **Figure 1** illustrates these results. The mean anatomical survival time was 119 ± 15 months (95% CI = 90–148 months). Failures appeared in both eyes of the same patient. One of the failures underwent the first extrusion 9 months after the surgery. After that, several tectonic surgeries had to be performed because of continuous extrusions (see **Table 2** for individual details). The second eye had its first extrusion after 49 months of follow-up and required a transmucosal Boston type 1 KPro procedure, as described by Camacho et al. (10), because of repeated extrusions that were not solved with tectonic grafts. The functional success was achieved in both cases before the first extrusion and both eyes maintained BCVA <1.3 LogMAR (≥ 0.05 decimal) during 15 and 55 months respectively after secondary rescue procedures, although visual acuity was progressively decreasing in one case.

Functional Results

The overall rate of functional success 5 years after surgery was 50% (6/12). The eyes maintained a

**FIGURE 1** | Anatomical and functional survival analysis.

BCVA ≤ 1.3 LogMAR (≥ 0.05 decimal) throughout the entire follow-up period and improved their final BCVA with a mean difference of 0.7 ± 0.5

TABLE 2 | Individual data of postoperative complications and procedures.

Eye code	Postoperative complication	PostKPro ocular procedures
1	GEm, RPMm	YM, YC, LTK, GDD, KProE
2	GEm, RPMm	YM, LTK, GDD,
3	SU, UIOP	TT
4	RPMm	YM
5	RPM, E	PPV
6	-	-
7	RPMm, RD	YM, PPV
8	RD	PPV
9	MK, RPM	YM
10	-	YC
11	RPM, RD	YM, PPV
12	SU, RPM, RD	PPV

GE, graft extrusion; MK, microbial keratitis; SU, sterile ulceration; WD, wound dehiscence; RPM, retroprosthetic membrane; RD, retinal detachment, UIOP, uncontrolled IOP; E, endophthalmitis; YM, yttrium-aluminum-garnet (YAG) membranotomy; YC, YAG capsulotomy; LTK, lamellar tectonic keratoplasty; GDD, glaucoma drainage devices; KProE, Boston type 1 keratoprosthesis (KPro) exchange; TT, temporal tarsorrhaphy; PPV, pars plana vitrectomy; m, multiple.

LogMAR (range:0.2–1.7 LogMAR), compared with their preoperative BCVA.

The mean follow-up for the functional survival analysis was 26.5 ± 30.2 months (range:0.5–87 months). **Figure 1** illustrates the cumulative probability of success by the Kaplan–Meier analysis, which was 57 and 46% at 1 and 5 years, respectively. The mean functional survival time was 46 months (95% CI: 22–69 months).

Of the six functional failures, three eyes did achieve a BCVA ≤ 1.3 LogMAR after the KPro surgery during a period of 6, 9, and 38 months, with a maximum improvement of 2.15, 0.6, and 0.25 LogMAR, respectively, compared with the preoperative BCVA. However, other complications, such as uncontrolled intraocular pressure (IOP) (in one case) and retinal detachments with macular involvement (in two cases), compromised the VA, resulting in functional failure.

Only three cases (25%) never achieved a BCVA ≤ 1.3 LogMAR, even though two of these eyes did improve their VA (**Figure 2** illustrates the BCVA changes in each case studied). Out of these three eyes, two started with very low VA (hand movement or light perception) due to aniridia-related comorbidities. The other eye suffered postoperative endophthalmitis that led to phthisis bulbi.

Postoperative Complications

The most common postoperative complications encountered were prosthesis extrusion (2/12–17%, explained in anatomical results) and retroprosthetic membrane (RPM) formation (8/12–66%). In five of the cases (40%), the complication occurred before 2 years, and in three (25%) after 2 years. The recurrence of RPM was the most frequent complication in each case, occurring up to three times in the same eye. Each case that required it was resolved by membranotomy with the yttrium-aluminum-garnet (YAG) laser (Lumenis Selecta®

Duet™, Salt Lake City, UT, United States). Other complications found were retinal detachment (33%), microbial keratitis (8%), sterile ulceration (8%), and endophthalmitis (8%). The mean number of complications per case was 2.4 ± 1.8 (range: 0–6).

Table 2 illustrates postoperative individual complications and procedures after Boston type 1 KPro in aniridia.

DISCUSSION

Aniridia-associated keratopathy is a major threat to vision in patients with aniridia, and it occurs in up to 90% of cases (1, 2, 11). This is the result of limbal stem cell deficiency, which leads to progressive corneal scarring and eventual blindness (1). This condition is very challenging to manage, and conventional PK has been proven to be ineffective because it fails to address the underlying cause; (2) PK with keratolimbal allografts requires serious systemic immunosuppression because of its higher than usual rate of immunological rejection (11). A keratoprosthetic implantation has become a treatment option in the past decade for severe conditions that have low probabilities of success, and the Boston type 1 KPro is the one that is most commonly used, even as a primary indication (1, 2).

All the cases in this study had poor preoperative visual acuities (BCVA ≥ 1 LogMAR, 0.09 decimal scale), as seen in previous studies on patients with aniridia (1, 2, 6, 11). We found that the rate of preoperative glaucoma (100%) was slightly higher than that described in publications (around 80%) (1, 2). The long follow-up period of this cohort, compared with published studies evaluating the clinical outcomes of patients with the congenital aniridia spectrum after implantation with the Boston type 1 KPro, strengthens the reliability of our results.

The KPro overall retention rate of 83.3% is lower than that found by Rixen et al., Akpek et al., and Bakhtiari et al. (100%), but is similar to that found by Hassanaly et al. (77%) and Shah et al. (87%) (1, 2, 5, 6, 11). This could possibly be attributed to the longer follow-up period, with one of the extrusions occurring after 49 months (4 years). This is longer than the median follow-up time published by some authors (2, 6, 11). Another reason could be our strict definition of extrusion; no other authors clarified what they considered an extrusion and, in one case, anatomical success was considered even after the KPro had to be changed (5). The probability of retention of the Boston type 1 KPro in our study population was 92, 79, and 79% after 1, 5, and 10 years, respectively.

The failures appeared to be due to corneal melting in both eyes of the same patient (9 months and 49 months after surgery). This could be due to an ocular surface/immunological personal predisposition. Several tectonic surgeries had to be performed in the first extruded KPro, and the second one required a transmucosal Boston type 1 KPro exchange after many failed tectonic grafts. This surgical technique may be considered an alternative in patients with ocular surface/immunological diseases (10). Other treatment options include a Boston type 2 KPro, osteo-odonto keratoprosthesis (OOKP), and osteo-keratoprosthesis (OKP); however, these are usually indicated in eyes with advanced-stage ocular surface diseases (12, 13).

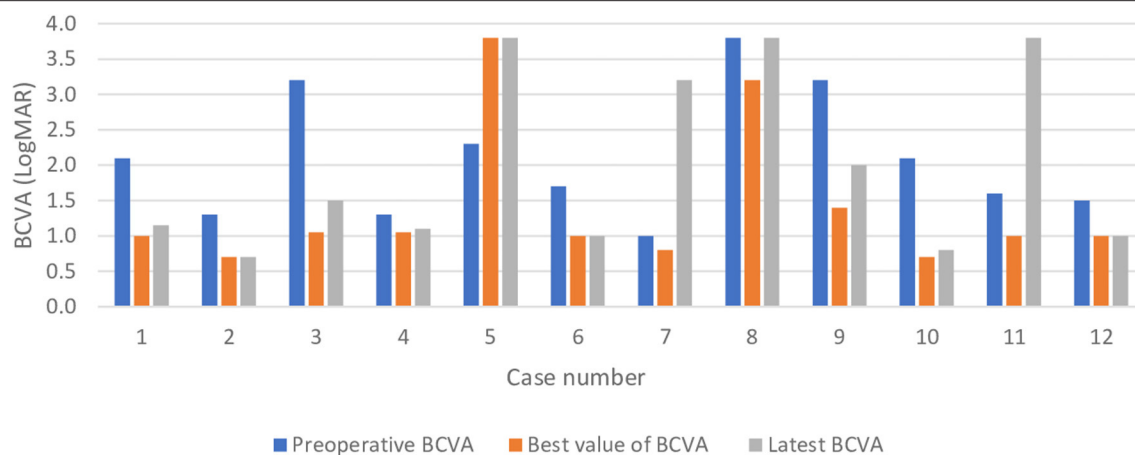


FIGURE 2 | Best corrected visual acuity changes in the sample.

There are limited outcome data on the Boston type 2 KPro in the literature (12), and fewer regarding type-2 implants or OOKP in patients with aniridia (12, 13). This could be because patients with aniridia usually have acceptable tear functions and good lid appositions, making the Boston type 1 KPro a more suitable option.

All but one case improved their VA after the surgery, which is similar to other published studies (5, 6, 11). Nevertheless, 50% of the cases achieved ambulatory vision ($VA > 0.025$ decimal) (14) and functional success ($BCVA \leq 1.3$ LogMAR) at the end of the follow-up period, with this value being the limit for legal blindness as defined by the WHO. These patients had vision good enough to see large objects at close range and the ability to move around in a familiar environment. These results are comparable with the 43.5% obtained by Shah et al. after 4.5 years of follow-up (1).

The probability of maintained VA over legal blindness limits in our study population was 57 and 46% at 1 and 5 years, respectively, to our knowledge, this is the first time a Kaplan–Meier survival analysis has been performed. In accordance with other authors, we attribute the limitation of achieving greater visual acuity in these patients to preexisting aniridia-related comorbidities such as foveal hypoplasia, nystagmus, and optic nerve hypoplasia (1, 2, 6). Moreover, the factors that tapered the VA in our cohort were retinal detachment (33%) with macular involvement and a high prevalence of preoperative glaucoma (100%) and its progression. Nearly all publication considered glaucoma as a major cause of visual loss that could have impacted the visual outcome results (1, 2, 5, 6, 11). Retinal detachment was also described by Akpek et al. as the cause of visual impairment in one of 16 cases and by Hassanaly in 31% of cases (2, 11). Our current surgical technique includes a planned pars plana vitrectomy (PPV) to reduce the risk of postoperative retinal detachment.

Retroprosthetic membrane formation (66%) was the most common complication in our study. Rudnisky et al. found a comparable rate (66.7%) in aniridia cases (15). This was

significantly higher than the RPM formation in all Boston type 1 patients, including other categories (31.7%) (15). They were able to demonstrate that aniridia increased the hazard of RPM formation by 3.13 (95% confidence interval 1.1–8.89). Since 2013, the Centro de Oftalmología Barraquer has only been using titanium backplates, as they seem to be associated with less RPM formation than polymethyl methacrylate (PMMA) (16).

The frequency of complications and the high need for postoperative procedures in our study group add evidence that there might be a physiopathologic process in these patients that makes them unique compared with non-aniridic cases (1). This could be due to aniridia fibrosis syndrome (5). This suggests that aniridia should be considered a separate category in the stratification by the preoperative diagnoses of KPro patients rather than be included in the recurrent immunologic rejection category (7). Because of the high rate of complications, we recommend not to implant bilateral Boston type 1 KPro simultaneously.

A limitation of this study is its retrospective design and limited sample size due to the low incidence of the disease. A quality-of-life questionnaire could have added valuable data to the study. However, this study provides valuable information to the existing literature, especially related to the long follow-up time.

Based on our results, we conclude that the Boston type 1 KPro is a viable option for the treatment of AAK, with good long-term results both anatomically and functionally. Uncontrolled glaucoma is an important condition that affects functional results. Aniridia may be considered a separate category in Boston type 1 KPro stratification, but this needs to be validated by future studies.

DATA AVAILABILITY STATEMENT

The original contributions presented in the study are included in the article/supplementary material, further inquiries can be directed to the corresponding author/s.

ETHICS STATEMENT

Ethical review and approval was not required for the study on human participants in accordance with the local legislation and institutional requirements. Written informed consent to participate in this study was provided by the participants' legal guardian/next of kin.

AUTHOR CONTRIBUTIONS

AD and ADF: research design, data acquisition, research execution, data analysis, interpretation, and

manuscript preparation. GJ: data analysis, interpretation, and manuscript preparation. RB: data analysis and interpretation. JA: data analysis and interpretation. MP: research design, data analysis, and interpretation. All authors contributed to the article and approved the submitted version.

ACKNOWLEDGMENTS

We thank Raquel Larena for processing the data of the manuscript.

REFERENCES

- Shah KJ, Cheung AY, Holland EJ. Intermediate-term and long-term outcomes with the boston type 1 keratoprosthesis in Aniridia. *Cornea*. (2018) 37:11–4. doi: 10.1097/ICO.0000000000001412
- Hassanali SI, Talajic JC, Harissi-Dagher M. Outcomes following Boston Type 1 Keratoprosthesis implantation in aniridia patients at the University of Montreal. *Am J Ophthalmol*. (2014) 158:1–8. doi: 10.1016/j.ajo.2014.05.009
- Samant M, Chauhan BK, Lathrop KL, Nischal KK. Congenital aniridia: etiology, manifestations and management. *Expert Rev Ophthalmol*. (2016) 11:135–44. doi: 10.1586/17469899.2016.1152182
- Yazdanpanah G, Bohm KJ, Hassan OM, Karas FI, Elhusseiny AM, Nonpassopon M, et al. Management of congenital aniridia-associated keratopathy: long-term outcomes from a tertiary referral center. *Am J Ophthalmol*. (2020) 210:8–18. doi: 10.1016/j.ajo.2019.11.003
- Bakhtiar P, Chan C, Welder JD, De La Cruz J, Holland EJ, Djalilian AR. Surgical and visual outcomes of the type I Boston Keratoprosthesis for the management of aniridic fibrosis syndrome in congenital aniridia. *Am J Ophthalmol*. (2012) 153:967–71.e2. doi: 10.1016/j.ajo.2011.10.027
- Rixen JJ, Cohen AW, Kitzmann AS, Wagoner MD, Goins KM. Treatment of aniridia with boston type I keratoprosthesis. *Cornea*. (2013) 32:947–50. doi: 10.1097/ICO.0b013e318281724a
- Belin MW, Güell JL, Grabner G. Suggested guidelines for reporting keratoprosthesis results: consensus opinion of the cornea society, Asia Cornea Society, EuCornea, PanCornea, and the KPRO study group. *Cornea*. (2016) 35:143–4. doi: 10.1097/ICO.0000000000000703
- Kang KB, Karas FI, Rai R, Hallak JA, Kang JJ, de la Cruz J, et al. Five year outcomes of Boston type I keratoprosthesis as primary versus secondary penetrating corneal procedure in a matched case control study. *PLoS ONE*. (2018) 13:1–12. doi: 10.1371/journal.pone.0192381
- de la Paz MF, Salvador-Culla B, Charoenrook V, Temprano J, Álvarez de Toledo J, Grabner G, et al. Osteo-odonto-, Tibial bone and Boston keratoprosthesis in clinically comparable cases of chemical injury and autoimmune disease. *Ocul Surf*. (2019) 17:476–83. doi: 10.1016/j.jtos.2019.04.006
- Camacho L, Soldevila A, Fideliz de la Paz M. Transmucosal Boston keratoprosthesis type I in a patient with advanced ocular cicatricial pemphigoid. *Cornea*. (2020) 39:1563–5. doi: 10.1097/ICO.0000000000002413
- Akpek EK, Harissi-Dagher M, Petrarca R, Butrus SI, Pineda R, Aquavella J V, et al. Outcomes of Boston keratoprosthesis in aniridia: a retrospective multicenter study. *Am J Ophthalmol*. (2007) 144:227–32. doi: 10.1016/j.ajo.2007.04.036
- Lee R, Khoueir Z, Tsikata E, Chodosh J, Dohlman CH, Chen TC. Long-term visual outcomes and complications of Boston keratoprosthesis type II implantation. *Ophthalmology*. (2017) 124:27–35. doi: 10.1016/j.ophtha.2016.07.011
- Iyer G, Srinivasan B, Agarwal S, Talela D, Rishi E, Rishi P, et al. Keratoprosthesis: current global scenario and a broad Indian perspective. *Indian J Ophthalmol*. (2018) 66:620–9. doi: 10.4103/ijo.IJO_22_18
- Chang YC, Hu DN, Wu WC. Effect of oral 13-cis-retinoic acid treatment on postoperative clinical outcome of eyes with proliferative vitreoretinopathy. *Am J Ophthalmol*. (2008) 146:440–7. doi: 10.1016/j.ajo.2008.05.002
- Rudnisky CJ, Belin MW, Todani A, Al-Arfaj K, Ament JD, Zerby BJ, et al. Risk factors for the development of retroprosthetic membranes with Boston keratoprosthesis type I: multicenter study results. *Ophthalmology*. (2012) 119:951–5. doi: 10.1016/j.ophtha.2011.11.030
- Todani A, Ciolino JB, Ament JD, Colby KA, Pineda R, Belin MW, et al. Titanium back plate for a PMMA keratoprosthesis: clinical outcomes. *Graefes Arch Clin Exp Ophthalmol*. (2011) 249:1515–8. doi: 10.1007/s00417-011-1684-y

Conflict of Interest: The authors declare that the research was conducted in the absence of any commercial or financial relationships that could be construed as a potential conflict of interest.

Publisher's Note: All claims expressed in this article are solely those of the authors and do not necessarily represent those of their affiliated organizations, or those of the publisher, the editors and the reviewers. Any product that may be evaluated in this article, or claim that may be made by its manufacturer, is not guaranteed or endorsed by the publisher.

Copyright © 2021 Dyer, De Faria, Julio, Álvarez de Toledo, Barraquer and de la Paz. This is an open-access article distributed under the terms of the Creative Commons Attribution License (CC BY). The use, distribution or reproduction in other forums is permitted, provided the original author(s) and the copyright owner(s) are credited and that the original publication in this journal is cited, in accordance with accepted academic practice. No use, distribution or reproduction is permitted which does not comply with these terms.



A New Pre-descemetic Corneal Ring (Neoring) in Deep Anterior Lamellar Keratoplasty for Moderate-Advanced Keratoconus: A Pilot 2-Year Long-Term Follow-Up Study

Belén Alfonso-Bartolozzi¹, Carlos Lisa¹, Luis Fernández-Vega-Cueto^{1*}, David Madrid-Costa² and José F. Alfonso¹

¹ Fernández-Vega Ophthalmological Institute, Universidad de Oviedo, Oviedo, Spain, ² Faculty of Optics and Optometry, Universidad Complutense de Madrid, Madrid, Spain

OPEN ACCESS

Edited by:

Hannah Levis,
University of Liverpool,
United Kingdom

Reviewed by:

Kunal Gadhvi,
Royal Liverpool University Hospital,
United Kingdom
Francesco Aiello,
University of Rome Tor Vergata, Italy

*Correspondence:

Luis Fernández-Vega-Cueto
lfvc@fernandez-vega.com

Specialty section:

This article was submitted to
Ophthalmology,
a section of the journal
Frontiers in Medicine

Received: 06 September 2021

Accepted: 04 October 2021

Published: 04 November 2021

Citation:

Alfonso-Bartolozzi B, Lisa C, Fernández-Vega-Cueto L, Madrid-Costa D and Alfonso JF (2021) A New Pre-descemetic Corneal Ring (Neoring) in Deep Anterior Lamellar Keratoplasty for Moderate-Advanced Keratoconus: A Pilot 2-Year Long-Term Follow-Up Study. *Front. Med.* 8:771365. doi: 10.3389/fmed.2021.771365

Purpose: To assess the outcomes of implanting a new polymethylmethacrylate (PMMA) ring (Neoring; AJL Ophthalmic) in pre-descemet deep anterior lamellar keratoplasty (PD-DALK) procedure for moderate-advanced keratoconus.

Methods: This prospective study included 10 eyes of 10 patients with moderate-advanced keratoconus who underwent PD-DALK with Neoring implantation. Neoring was implanted in a pre-descemetic pocket. The post-operative examination included refraction, corrected distance visual acuity (CDVA), corneal tomography, and endothelial cell density (ECD). The root mean squares (RMSs) for coma-like aberrations and spherical aberration were evaluated for a pupil size of 4.5 mm. The junctional graft (Tg) and host (Th) thicknesses were measured. The post-operative follow-up was 24 months.

Results: Post-operative CDVA was 0.82 ± 0.14 (decimal scale), 100% of the eyes achieved a CDVA of 0.7 (decimal scale). The refractive cylinder was -2.86 ± 1.65 2-years after surgery. No eyes had a post-operative refractive cylinder ≥ 5.00 D and in five eyes (50%), it was ≤ 2.50 D. At the last visit, the mean keratometry was 45.64 ± 1.96 D, the RMS for coma-like aberrations was $0.30 \pm 0.15 \mu\text{m}$ and spherical aberration was 0.22 ± 0.09 . The mean ECD remains without changes over the follow-up ($P = 0.07$). At the last visit, Tg and Th were 679.9 ± 39.0 and $634.8 \pm 41.2 \mu\text{m}$, respectively. The thickness of the complex (host-Neoring) was $740.6 \pm 35.6 \mu\text{m}$. In all cases, this thickness was thicker than Tg.

Conclusion: The results of this study suggest that PD-DALK along Neoring implantation is a viable, effective, and safe option to optimize the post-operative results for moderate-severe keratoconus.

Keywords: corneal transplant, deep anterior lamellar keratoplasty (DALK), visual outcomes, refractive outcomes, keratoconus

INTRODUCTION

Deep anterior lamellar keratoplasty (DALK) is a surgical procedure in which a corneal donor, free from endothelium and Descemet's membrane (DM), is transplanted in patients affected by a corneal disease, in which the endothelium is healthy and can be preserved. DALK may be classified into two types according to the technique used: with and without DM exposure, known as Descemet-DALK (D-DALK), and pre-descemet DALK (PD-DALK), respectively. Overall, DALK has significant advantages over penetrating keratoplasty (PKP), including reduced risk of endophthalmitis, no immune reaction, and minor loss of endothelial cell density (ECD), among others (1). However, DALK is not free of potential intra- and post-operative complications. Some of these complications are related to the corneal transplantation itself (complications associated with the graft-host interface, graft epithelial problems, graft or host cornea vascularization, suture-related complications, stromal rejection, post-operative refractive errors) (1–6). Others are more technique-dependent (D-DALK seems to provide a faster visual recovery than PD-DALK; however, D-DALK is associated with a higher risk of intraoperative complications) (7, 8).

The ocular disease leading to corneal transplantation might also influence the DALK-related complications (6, 9–11). Advanced keratoconus is the most common indication for corneal transplantation in many countries (12, 13). The most common intraoperative complication is the DM rupture (14), being mainly associated with the D-DALK technique (2, 7, 8, 15). Complications related to the graft-host interface and the irregularity of the recipient corneal bed may make it difficult to achieve an optimal visual restoration in patients with severe keratoconus (16, 17).

We designed a new ring made of polymethylmethacrylate (PMMA), named Neoring (AJL Ophthalmic, Spain), to overcome the potential complications of DALK in advanced keratoconus. First, the Neoring is conceived for the PD-DALK technique owing to the fact that it is implanted in a PD pocket created through the trephination periphery. As previously pointed out, the most common intraoperative complication (rupture DM) is mainly associated with D-DALK. Second, the Neoring implantation aims to regularize the graft-host interface and recipient corneal bed. Notably, that corneal graft conforms, in part, to the recipient bed. Hence, the Neoring implantation might lead to a better corneal morphology restoration, consequently, improve the visual and refractive outcomes after surgery.

In the current prospective study, 10 eyes of 10 patients who underwent PD-DALK with Neoring implantation for advanced keratoconus were case per case analyzed over a follow-up of at least 24 months.

PATIENTS AND METHODS

This is a prospective case series study that included patients with moderate-advanced keratoconus, who underwent PD-DALK surgery with Neoring implantation at the Fernández-Vega Ophthalmological Institute in Oviedo, Spain. This study was

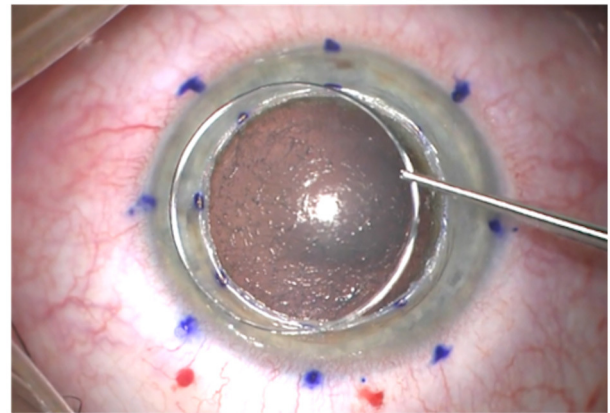


FIGURE 1 | Image of Neoring before implantation.

conducted in compliance with the tenets of the Declaration of Helsinki. The study was approved by the Ethics Committee of the “Principado de Asturias” (Oviedo, Spain). After receiving a complete description of the nature of the study and the possible consequences of surgery, all patients provided informed consent.

Inclusion criteria were the presence of keratoconus, poor or unsatisfactory corrected distance visual acuity (CDVA) with spectacle ($\leq 20/40$), intolerance to contact lens, mean keratometry ≥ 50 D, corneal thickness in the area of the central 3 mm ≤ 450 μ m, and axial length ≥ 23.50 mm. Exclusion criteria were an active ocular disease (other than keratoconus) and a history of ocular disorders with a potential impact on the variables under study (cataract, macular degeneration, glaucoma, retinal detachment, neuro-ophthalmic diseases, or ocular inflammation).

All DALK surgeries were performed by the same surgeon (JFA) using Anwar's technique (18). Neoring (AJL Ophthalmic, Spain) was implanted in all cases. This ring is made of PMMA with a circular cross-section, a thickness of 0.21 mm, and it is available with three diameters (8, 8.5, and 9 mm). Neoring is conceived to be implanted in a pre-descemet pocket created in the periphery of the trephination performed at the host cornea. The diameter of the Neoring must be 0.5 mm larger than the trephination diameter performed at the host cornea to achieve a correct ring fitting in the pre-descemet pocket (**Figure 1**).

Briefly, the more significant steps of the surgical procedure were as follows: a partial trephination of the host cornea was performed with a diameter of 8 mm. The donor graft was cut 0.25 mm larger than the size used for the recipient corneal trephination. A manual layer-by-layer stromal dissection was performed, starting at the trephination edge down to the deepest stromal layer adjacent to DM. A thin stromal layer was left behind (between 50 and 70 μ m at the central zone). A pre-descemet pocket was created to 0.25 mm outside the trephination of the recipient cornea. Subsequently, a Neoring of 8.5 mm of diameter was implanted in the pre-descemet pocket. The ring was provisionally fixated to the recipient cornea with two 8-0 silk sutures at 12 and 6 o'clock. Then, the donor button free

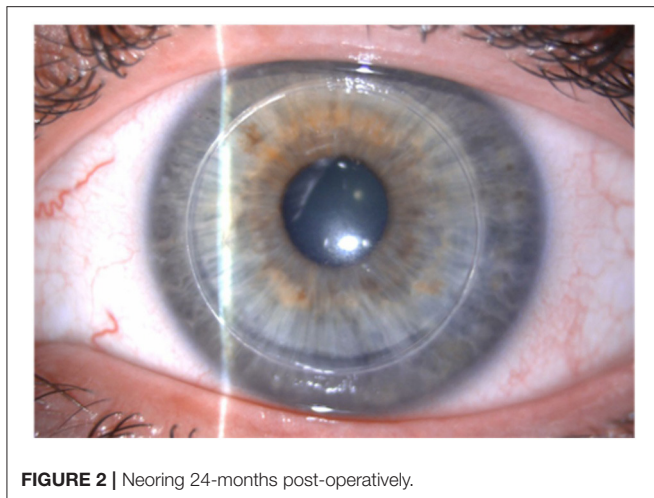


FIGURE 2 | Neoring 24-months post-operatively.

from DM and endothelium was transferred to the recipient bed and sutured to the host cornea with four interrupted 10-0 nylon sutures (from 90% of the donor button depth and going the suture needle over Neoring to ensure that it is placed at pre-descemetic level). Finally, the silk sutures for the ring fixation were removed, and the 16 interrupted 10-0 nylon sutures were completed.

Post-operatively, selective suture removal started at 6 months after DALK, and it was completed at 15 months. The post-operative treatment consisted of a regimen of 1% dexamethasone and ciprofloxacin 0.3% drops four times a day for 1 week. Antibiotic drops were then discontinued, and dexamethasone was progressively tapered down over the next 3 months. Subsequently, we maintained dexamethasone in a regimen of one drop per day for a year. Furthermore, Plasma Rich in Growth Factors (PRGF) eye drops were added topically four times daily for at least 3 months.

Post-operative follow-up visits were scheduled 1-, 7-days, and 1 month after surgery and then every 3 months until 24 months (**Figure 2**). The post-operative examination included Manifest refraction, CDVA, slit lamp examination, corneal tomography (Sirius, CSO, Italy), ECD (SP 3000P, Topcon Europa), and corneal thickness (CCT) (Casia II- OCT, Tomey, Japan). Furthermore, at the last follow-up visit (24 months), the root mean square (RMS) for coma-like aberrations [computed for the Zernike terms $Z(3, 1)$ and $Z(3, -1)$] and spherical aberration [Zernike coefficient $Z(4, 0)$] of the total cornea and the posterior corneal surface were evaluated for a pupil size of 4.5 mm. Finally, at the last visit, we used Casia II-OCT to measure the junctional graft thickness (Tg) and junctional host thickness (Th) and calculate the absolute value of the difference between Tg and Th (Tg-Th) according to the study of Zhao et al. (16). The corneal thickness of the complex host + Neoring was also measured.

Statistical analysis was carried out using Statistical Product and Service Solutions (SPSS) software for Windows (version 15.0, SPSS, Inc.). Pre-operative and post-operative data were

TABLE 1 | Pre-operative data of the patients.

	Mean \pm SD	Range (Min, Max)
Age (years)	36.90 \pm 2.28	(34, 40)
Refraction sphere (D)	-7.80 \pm 3.79	(-14.00, -3.00)
Refraction cylinder (D)	-8.40 \pm 4.12	(-16.00, -4.00)
CDVA (Snellen Scale)	0.44 \pm 0.07	(0.30, 0.50)
Axial length (mm)	25.45 \pm 1.41	(23.51, 26.94)
Minimum keratometry (D)	51.85 \pm 3.41	(48.12, 57.56)
Maximum keratometry (D)	59.55 \pm 5.20	(53.18, 66.75)
Mean keratometry (D)	55.70 \pm 3.98	(50.65, 61.50)
Corneal thickness (μ m)	390 \pm 52	(299, 444)
ECD (cells/mm ²)	2,450 \pm 543	(1,674, 3,522)

D, diopters; CDVA, corrected distance visual acuity; ECD, endothelial cell density; SD, standard deviation.

compared using the Friedman test. A $P < 0.05$ was considered statistically significant. Data are reported as the mean \pm SD.

RESULTS

The study included 10 eyes of 10 patients with a mean age of 36.90 ± 2.28 years (range 34–40 years). All patients completed the follow-up period of 2 years and attended all the follow-up visits. **Table 1** summarizes the pre-operative data of the patients. All the surgeries were uneventful, with no intra or post-operative complications. No cases required conversion to PKP.

Table 2 shows the pre-operative and post-operative clinical outcomes. All visual and refractive parameters significantly improved after DALK. CDVA was progressively improving visit by visit in all eyes until 24 months of follow-up. **Figure 3** shows the changes in CDVA for each case studied over the whole follow-up. At the last visit, 100% of the eyes achieved a CDVA of 0.7 (decimal scale) and 50% of the eyes achieved a CDVA of 0.8 (decimal scale) or better. The safety index (ratio between the post-operative CDVA and the pre-operative CDVA) was 1.87.

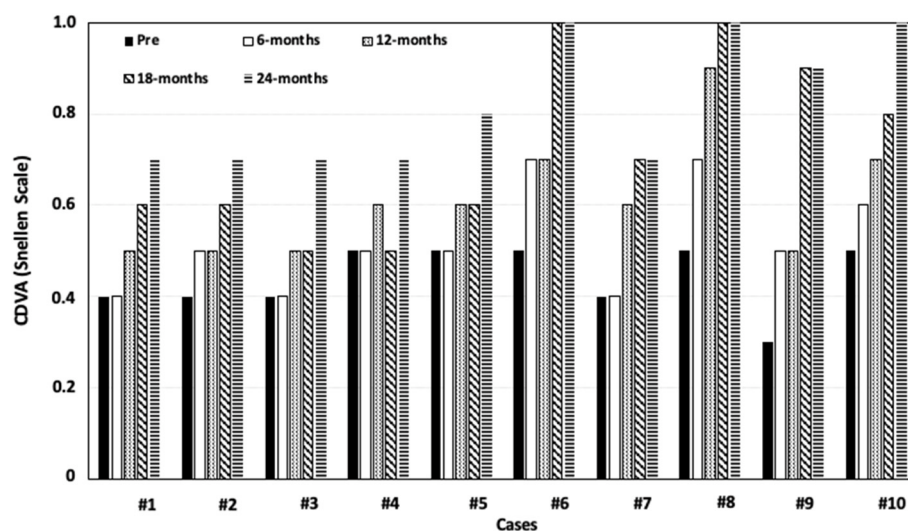
The spherical component of the refraction dropped from a pre-operative -7.80 ± 3.79 D to a 24-month post-operative value of -3.39 ± 2.58 D ($P = 0.0001$). At the last visit, only four eyes had a spherical refractive error ≥ 4.00 D. In these cases, the axial length was longer than 25 mm (**Figure 4**). The refractive cylinder changed from -8.40 ± 4.12 D pre-operatively to -2.86 ± 1.65 D 2 years after surgery ($P < 0.001$). At the last visit, no eyes had a post-operative refractive cylinder ≥ 5 D, and in five eyes (50%), it was ≤ 2.50 D. Both, the maximum and minimum K reading values, declined significantly after surgery. At the last visit, the mean keratometry was 45.64 ± 1.94 D (ranging from 43.47 to 49.57 D).

Regarding corneal aberrometry, the 24-month post-operative RMSs for coma-like and spherical aberrations of the posterior corneal surface were 0.12 ± 0.09 and $0.08 \pm 0.18 \mu$ m, respectively. In turn, the RMS for coma-like aberrations of the total cornea was $0.30 \pm 0.15 \mu$ m and the spherical aberration was $0.22 \pm 0.09 \mu$ m.

TABLE 2 | Pre-operative and post-operative clinical outcomes.

	Pre-operative	6-month*	12-month	18-month**	24-month
Refraction sphere (D) Range	-7.80 ± 3.79 (-14.00 to -3.00)	$1.90 \pm 3.90^{\#}$ (-9.00 to $+4.00$)	-1.75 ± 2.20 (-5.00 to $+1.00$)	$-3.03 \pm 2.42^{\#}$ (-7.00 to 0.00)	-3.39 ± 2.58 (-8.00 to -0.50)
Refraction cylinder (D) Range	-8.40 ± 4.12 (-16.00 to -4.00)	$-3.40 \pm 1.71^{\#}$ (-6.00 to -0.50)	-3.65 ± 1.80 (-6.00 to -1.50)	$-2.75 \pm 2.01^{\#}$ (-5.50 to -0.25)	-2.86 ± 1.65 (-5.00 to -1.00)
CDVA (Snellen scale) Range	0.44 ± 0.07 (0.30 to 0.50)	$0.52 \pm 0.11^{\#}$ (0.40 to 0.70)	$0.61 \pm 0.13^{\#}$ (0.50 to 0.90)	$0.72 \pm 0.19^{\#}$ (0.50 to 1.0)	$0.82 \pm 0.14^{\#}$ (0.70 to 1.0)
Keratometric cylinder (D) Range	7.70 ± 3.73 (2.25 to 14.49)	$4.09 \pm 2.92^{\#}$ (0.49 to 8.39)	3.56 ± 1.44 (2.08 to 5.59)	3.12 ± 1.43 (1.04 to 4.82)	3.19 ± 1.26 (1.04 to 4.87)
Minimum keratometry (D) Range	51.85 ± 3.41 (48.12 to 57.56)	$42.19 \pm 4.00^{\#}$ (35.62 to 48.78)	43.14 ± 2.88 (38.66 to 47.91)	43.88 ± 2.36 (39.83 to 47.21)	44.05 ± 1.89 (42.13 to 47.21)
Maximum keratometry (D) Range	59.55 ± 5.20 (53.18 to 66.75)	$46.27 \pm 3.13^{\#}$ (42.41 to 51.34)	46.70 ± 2.01 (44.18 to 50.88)	47.00 ± 2.40 (44.23 to 52.03)	47.22 ± 2.19 (44.80 to 51.92)
Mean keratometry (D) Range	55.70 ± 3.98 (50.65 to 61.50)	$44.23 \pm 3.28^{\#}$ (39.02 to 50.06)	44.92 ± 2.37 (41.46 to 49.40)	45.44 ± 2.27 (42.01 to 49.62)	45.64 ± 1.94 (43.47 to 49.57)
Corneal thickness (μm) Range	389.50 ± 51.58 (294 to 444)	$541.70 \pm 34.60^{\#}$ (502 to 595)	550.50 ± 30.17 (501 to 589)	554.56 ± 21.89 (510 to 580)	566.56 ± 30.65 (520 to 620)
ECD (cells/ mm^2) Range	$2,450 \pm 543$ (1,674 to 3,522)	$2,396 \pm 399$ (1,874 to 3,157)	$2,498 \pm 277$ (2,162 to 3,101)	$2,591 \pm 444$ (2,065 to 3,210)	$2,584 \pm 283$ (2,185 to 3,104)

*Starting of sutures removal (16 interrupted 10-0 nylon sutures in place); **3 months after completed sutures removal; [#]Statistically significant differences with the previous follow-up visit; D, diopters; CDVA, Corrected Distance Visual Acuity; ECD, endothelial cell density.

**FIGURE 3 |** Variation in corrected distance visual acuity (CDVA) over the whole follow-up for each case.

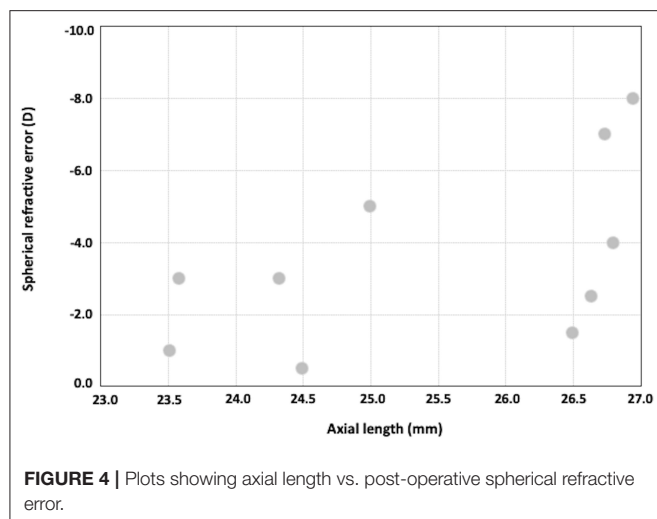
There were no significant changes in the mean ECD at any timepoint ($P = 0.07$). The mean CCT increased from $389.4 \pm 51.58 \mu\text{m}$ pre-operatively to $541.7 \pm 34.6 \mu\text{m}$ at 6 months post-operatively ($P = 0.0006$), and then it remains unchanged over the follow-up ($566.56 \pm 30.65 \mu\text{m}$ at the last visit).

At the last visit, Tg and Th were 679.9 ± 39.0 and $634.8 \pm 41.2 \mu\text{m}$, respectively. Consequently, the (Tg-Th) was $45.1 \pm 24.02 \mu\text{m}$. The thickness of the complex host + Neuring was $740.6 \pm 35.6 \mu\text{m}$, and in all cases, this thickness was thicker than Tg (Figure 5).

DISCUSSIONS

Advanced keratoconus is a corneal disease that causes severe visual impairment and is a leading indication for corneal transplantation (12, 13). Notably, keratoconus, even in its most advanced stages, affects young people; consequently, achieving a good visual quality that lasts for a lifetime must be the main aim.

DALK in keratoconus aims to improve visual quality through the restoration of corneal morphology. The graft-host matching is a key factor to achieve optimal visual and refractive outcomes



(16). The thickness of the corneal bed is also a factor that limits the visual acuity restoration after DALK, a recipient thickness of more than 80 μm reduces the post-operative visual acuity (17). In turn, the posterior corneal surface is also affected by keratoconus (19). It should be kept in mind that the graft conforms, at least in part, to the recipient DM, which remains intact after DALK. Therefore, the changes and the irregularities induced by keratoconus in the posterior corneal surface could contribute to worsening the optical quality of the corneal graft.

This pilot study evaluated the clinical outcomes of implanting a new PMMA ring (Neoring) in a pre-descemetica pocket in the PD-DALK procedure. PD-DALK for keratoconus may provide comparable CDVA outcomes to D-DALK (2, 7, 8, 20, 21), as long as, as noted above, the recipient bed thickness is thinner than 80 μm (17). Consequently, in our study, the stromal layer left behind was thinner than 70 μm at the central zone in all cases. Furthermore, the Neoring implantation aimed to achieve a better corneal morphology restoration by increasing the thickness of the retained peripheral recipient cornea and regularizing the recipient corneal bed.

The results showed satisfactory visual acuity. At the last visit, the CDVA was 0.82 ± 0.14 (decimal scale) (range from 0.7 to 1.0), 100% of the eyes achieved a CDVA of 0.7 (decimal scale), and 50% of the eyes achieved a CDVA of 0.8 (decimal scale) or better. Furthermore, it is important to note that three of the five eyes with a CDVA of 0.7 (decimal scale) had an axial length longer than 26.5 mm and a posterior staphyloma that reached the macular area. Hence, it seems that likely these cases obtained their maximum potential visual acuity. The safety index ratio was 1.87. Our visual results were better than those previously reported in the more advanced keratoconus. In the study of Feizi et al. (11), the CDVA was 0.19 and 0.20 logMAR (around 0.6 in decimal scale) for stage III and IV, respectively. Javadi et al. (22), in turn, reported a CDVA of 0.16 and 0.18 logMAR (about 0.7 decimal scale) for moderate and severe keratoconus using D-DALK. This study reported significantly worse CDVA for severe keratoconus with the PD-DALK technique (0.29 logMAR; around 0.5 in

decimal scale). We should be cautious with these comparisons because although our cases were prospectively analyzed, this is a pilot study including 10 eyes. However, it seems plausible that the Neoring implantation might benefit visual acuity restoration, as will be argued below.

Regarding refractive outcomes, at the last visit, only four eyes had a spherical refractive error ≥ 4 D. In these cases, the axial length was longer than 25 mm (Figure 4). Furthermore, the mean keratometry at the last visit was 45.64 ± 1.94 D. These results indicate that the post-operative sphere refraction was mainly associated with the elongation of the posterior segment, and not with a significant steepness of the corneal graft. The refractive cylinder changed from -8.40 ± 4.12 D pre-operatively to -2.86 ± 1.65 D 2 years after surgery ($P < 0.001$). The average reported refractive cylinder after DALK for keratoconus may vary among studies between 2.50 and 5.00 D (2, 23, 24). For the moderate and severe keratoconus, the reported post-DALK astigmatism is around 3.50 D but may reach up to 10.00 D (11). In the present study, at the last visit, no eyes had a post-operative refractive cylinder ≥ 5.00 D and in five eyes (50%), it was ≤ 2.50 D.

According to the visual and refractive outcomes found in this pilot study, it seems that PD-DALK along Neoring implantation might represent a viable option to optimize the post-operative results in moderate-severe keratoconus. We have reasons to accept the assumption that Neoring implantation influenced these results. First, it should be noted that the donor graft conforms, at least in part, to the morphology of the recipient intact bed. Therefore, it would imply that the more irregular the recipient bed, the worse regain the corneal refractive regularity. Advanced keratoconus has steeper corneas, and the posterior cornea is more irregular. Hence, it should be expected that an action to regularize the recipient bed might improve the post-operative visual and refractive outcomes. We hypothesized that a healing process mediated by activated keratocytes might occur around Neoring. In a similar way to what happens after intracorneal ring segment implantation (25). This wound-healing process might apply a pushing force on the periphery, which might lead to a flattening of the recipient corneal bed. Consequently, and considering that the recipient corneal radii of curvature are a factor influencing the post-operative graft radii of curvature (26), it might result in a less steep keratometry of the corneal graft. The post-operative mean keratometry in our study was 45.64 ± 1.94 D with no cases exceeded 50 D. In contrast, the post-operative mean keratometry reported by Feizi et al. (11) in stages III and IV were around 1.0 and 1.5 D steeper, respectively, and some cases had a Km up to 53.50 and 56.50 D, respectively.

Furthermore, Neoring implantation might mitigate the irregularities of the recipient bed induced by advanced keratoconus, and as a consequence, the total corneal aberrations. The 24-month post-operative RMSs for coma-like and spherical aberrations of the posterior corneal surface were 0.12 ± 0.09 and $0.08 \pm 0.18 \mu\text{m}$, respectively. In turn, the RMS for coma-like aberrations of the total cornea was $0.30 \pm 0.15 \mu\text{m}$ and the spherical aberration was $0.22 \pm 0.09 \mu\text{m}$. We cannot compare it with the pre-operative values. However, considering that posterior corneal aberrations increase in advanced keratoconus, it should be expected that the posterior coma-like and

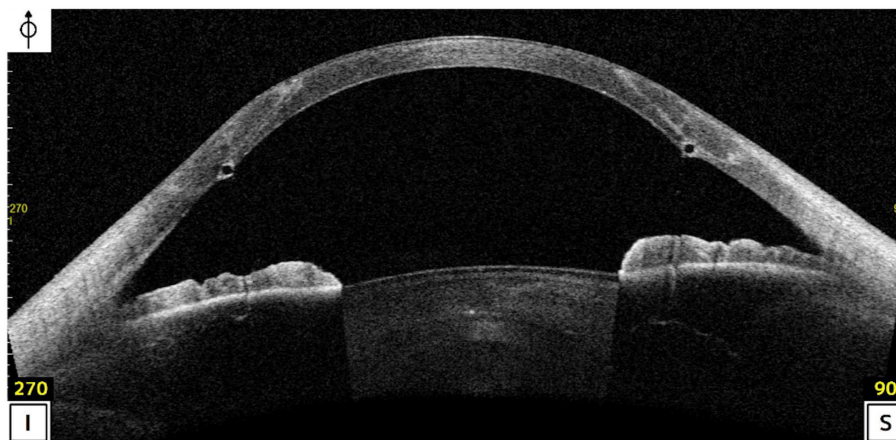


FIGURE 5 | Anterior Segment Optical Coherence Tomography (AS-OCT; Casia II- OCT, Tomey, Japan) 24-months post-operatively.

spherical aberrations were significantly higher before surgery. Besides, our research group has recently shown that long-arc-length intrastromal corneal ring (ICRS) implantation provides significant changes in the anterior and posterior corneal surface morphology of moderate-advanced keratoconus, becoming both surfaces more regular (27). Although both, ICRS and Neoring, have different indications and mechanisms of action, it seems plausible to expect that Neoring might also have a regularization effect on the recipient bed. Moreover, the continuous improvement in CDVA visit by visit (**Table 2**) could be related, obviously, to the removal of the sutures and an ongoing regularization process that, in turn, would be influenced by the healing process around the ring previously explained.

Finally, it is essential to note that the implant added volume to the retained peripheral recipient cornea (**Figure 5**), decreasing the difference between the Tg and Th (Tg-Th). Zhao et al. (16) found that the larger the (Tg-Th) value, the worse the visual and refractive outcomes. The (Tg-Th) value was lower in our study than that reported by Zhao et al. (16) (45.1 and 85.74 μm , respectively). Furthermore, the thickness of the complex (host + Neoring) was thicker than Tg in all cases. All these findings suggest that Neoring implantation in PD-DALK would provide that the posterior corneal surface became more regularized and flattened post-operatively and a smoother transition graft-host junction, providing encouraging outcomes in advanced keratoconus.

In the current study, no complications occurred during surgery or over the entire follow-up time. The most common and significant intraoperative complication is the DM perforation, being mainly associated with the D-DALK technique (2, 7, 8, 15). The endothelial cell count remained stable over the follow-up, suggesting that Neoring implantation did not cause alterations in the endothelium. A late post-operative complication after DALK is the recurrent keratoconus (2, 28, 29). The difference between Tg and Th might provoke a progressive thinning of the graft-host junction over time, which might induce high irregular astigmatism. As previously explained, the implant added volume to the retained peripheral recipient cornea (**Figure 5**), decreasing

the difference between Tg and Th, and making the thickness of the complex (host + Neoring) thicker than Tg. Furthermore, as Krumeich proposed (30), ring implantation might secure the stability of the wound. Hence, the approach of implanting Neoring might minimize the risk for recurrent keratoconus. However, further studies with a larger sample and longer follow-ups are required to address these potential benefits.

Despite the encouraging results in the prospective study, it should be pointed out that this is a pilot study including 10 cases and it only represented a single-center experience. It is important also to note that all surgeries were carried out by an experienced surgeon. Therefore, further prospective, randomized, and multicenter studies with a larger sample and longer follow-ups are required to deeply address the potential benefits of this procedure. Notably, Neoring was initially conceived for the PD-DALK technique because it is implanted in a PD pocket. However, it should be noted that femtosecond laser can be safely and effectively used to create cutting patterns (31) in the host and donor corneas that might allow Neoring implantation in a PD pocket in the periphery, leaving bared a central region of Descemet's membrane. Hence, we consider it interesting to evaluate the outcomes of Neoring implantation in femtosecond laser-assisted DALK using those cutting patterns (31) in future studies.

In conclusion, the findings of this pilot study suggest that Neoring implantation in the PD-DALK procedure might represent a viable option to optimize the post-operative results in moderate-severe keratoconus. Further, long-term follow-up studies, including a larger number of cases, are needed to properly analyze the stability of this surgery and confirm the safety of the procedure.

DATA AVAILABILITY STATEMENT

The original contributions presented in the study are included in the article, further inquiries can be directed to the corresponding author.

ETHICS STATEMENT

The study was approved by the Ethics Committee of the Principado de Asturias (Oviedo, Spain). The patients/participants provided their written informed consent to participate in this study.

AUTHOR CONTRIBUTIONS

BA-B: conception and design of the study, analysis and interpretation of data, writing the manuscript, and critical

revision of the manuscript. CL and LF-V-C: conception and design of the study, analysis and interpretation of data, and critical revision of the manuscript. DM-C and JA: conception and design of the study, analysis and interpretation of data, critical revision of the manuscript, and supervision. All authors read and approved the final manuscript.

FUNDING

Fernández-Vega Ophthalmological Institute has an unrestricted Grant from AJL Ophthalmic.

REFERENCES

- Reinhart WJ, Musch DC, Jacobs DS, Lee WB, Kaufman SC, Shtein RM. Deep anterior lamellar keratoplasty as an alternative to penetrating keratoplasty: a report by the American academy of ophthalmology. *Ophthalmology*. (2011) 118:209–18. doi: 10.1016/j.ophtha.2010.11.002
- Feizi S, Javadi MA, Karimian F, Abolhosseini M, Moshtaghion SM, Naderi A, et al. Penetrating keratoplasty versus deep anterior lamellar keratoplasty in children and adolescents with keratoconus. *Am J Ophthalmol*. (2021) 226:13–21. doi: 10.1016/j.ajo.2021.01.010
- Khattak A, Nakhli FR, Al-Arfaj KM, Cheema AA. Comparison of outcomes and complications of deep anterior lamellar keratoplasty and penetrating keratoplasty performed in a large group of patients with keratoconus. *Int Ophthalmol*. (2018) 38:985–92. doi: 10.1007/s10792-017-0548-9
- Jones MN, Armitage WJ, Ayliffe W, Larkin DF, Kaye SB. Penetrating and deep anterior lamellar keratoplasty for keratoconus: a comparison of graft outcomes in the United Kingdom. *Invest Ophthalmol Vis Sci*. (2009) 50:5625–9. doi: 10.1167/iovs.09-3994
- Huang T, Hu Y, Gui M, Zhang H, Wang Y, Hou C. Large-diameter deep anterior lamellar keratoplasty for keratoconus: visual and refractive outcomes. *Br J Ophthalmol*. (2015) 99:1196–200. doi: 10.1136/bjophthalmol-2014-306170
- Huang T, Zhang X, Wang Y, Zhang H, Huand A, Gao N. Outcomes of deep anterior lamellar keratoplasty using the big-bubble technique in various corneal diseases. *Am J Ophthalmol*. (2012) 154:282–9. doi: 10.1016/j.ajo.2012.02.025
- Sarnicola V, Toro P, Gentile D, Hannush SB. Descemet DALK and predescemet DALK: outcomes in 236 cases of keratoconus. *Cornea*. (2010) 29:53–9. doi: 10.1097/ICO.0b013e3181a31aea
- Abdelkader A, Kaufman HE. Descemet versus pre-descemet lamellar keratoplasty: clinical and confocal study. *Cornea*. (2011) 30:1244–52. doi: 10.1097/ICO.0b013e318219bc1a
- Einan-Lifshitz A, Belkin A, Sorkin N, Mednick Z, Boutin T, Kreimeier M, et al. Evaluation of big bubble technique for deep anterior lamellar keratoplasty in patients with radial keratotomy. *Cornea*. (2019) 38:194–7. doi: 10.1097/ICO.0000000000001811
- Myerscough J, Friehmann A, Bovone C, Mimouni M, Busin M. Evaluation of the risk factors associated with conversion of intended deep anterior lamellar keratoplasty to penetrating keratoplasty. *Br J Ophthalmol*. (2020) 104:764–7. doi: 10.1136/bjophthalmol-2019-314352
- Feizi S, Javadi MA, Kheiri B. Effect of keratoconus severity on clinical outcomes after deep anterior lamellar keratoplasty. *Am J Ophthalmol*. (2019) 202:15–22. doi: 10.1016/j.ajo.2019.01.030
- Ali Javadi M, Kanavi MR, Safi S. A 27-year report from the central eye bank of Iran. *J Ophthalmic Vis Res*. (2020) 15:149–59. doi: 10.18502/jovr.v15i2.6731
- Zare M, Javadi MA, Einollahi B, Baradaran-Rafii A, Zarei Ghanavati S, Farsani MR, et al. Indications for corneal transplantation at a tertiary referral center in Tehran. *J Ophthalmic Vis Res*. (2010) 5:82–6.
- Parker JS, van Dijk K, Melles GR. Treatment options for advanced keratoconus: a review. *Surv Ophthalmol*. (2015) 60:459–80. doi: 10.1016/j.survophthal.2015.02.004
- Anwar M, Teichmann KD. Deep lamellar keratoplasty: surgical techniques for anterior lamellar keratoplasty with and without baring of Descemet's membrane. *Cornea*. (2002) 21:374–83. doi: 10.1097/00003226-200205000-00009
- Zhao Y, Zhuang H, Hong J, Tian L, Xu J. Malapposition of graft-host interface after penetrating keratoplasty (PK) and deep anterior lamellar keratoplasty (DALK): an optical coherence tomography study. *BMC Ophthalmol*. (2020) 20:41. doi: 10.1186/s12886-020-1307-7
- Ardjomand N, Hau S, McAlister JC, Bunce C, Galaretta D, Tuft SJ, et al. Quality of vision and graft thickness in deep anterior lamellar and penetrating corneal allografts. *Am J Ophthalmol*. (2007) 143:228–35. doi: 10.1016/j.ajo.2006.10.043
- Anwar M. Dissection technique in lamellar keratoplasty. *Br J Ophthalmol*. (1972) 56:711–3. doi: 10.1136/bjo.56.9.711
- Tomidokoro A, Oshika T, Amano S, Higaki S, Maeda N, Miyata K. Changes in anterior and posterior corneal curvatures in keratoconus. *Ophthalmology*. (2000) 107:1328–32. doi: 10.1016/S0161-6420(00)00159-7
- Schiano-Lomoriello D, Colabelli-Gisoldi RA, Nubile M, Oddone F, Ducoli G, Villani CM, et al. Descemet and predescemet DALK in keratoconus patients: a clinical and confocal perspective study. *Biomed Res Int*. (2014) 2014:123156. doi: 10.1155/2014/123156
- Lu Y, Grisolia AB, Ge YR, et al. Comparison of femtosecond laser-assisted descemet and predescemet lamellar keratoplasty for keratoconus. *Indian J Ophthalmol*. (2017) 65:19–23. doi: 10.4103/ijo.IJO_688_16
- Javadi MA, Mohammad-Rabei H, Feizi S, Daryabari SH. Visual outcomes of successful versus failed big-bubble deep anterior lamellar keratoplasty for keratoconus. *J Ophthalmic Vis Res*. (2016) 11:32–6. doi: 10.4103/2008-322X.180711
- Song Y, Zhang J, Pan Z. Systematic review and meta-analysis of clinical outcomes of penetrating keratoplasty versus deep anterior lamellar keratoplasty for keratoconus. *Exp Clin Transplant*. (2020) 18:417–28. doi: 10.6002/ect.2019.0123
- Henein C, Nanavaty MA. Systematic review comparing penetrating keratoplasty and deep anterior lamellar keratoplasty for management of keratoconus. *Cont Lens Anterior Eye*. (2017) 40:3–14. doi: 10.1016/j.clae.2016.10.001
- Ibares-Frías L, Gallego P, Cantalapiedra-Rodríguez R, Valsero MC, Mar S, Merayo-Llows J, et al. Tissue reaction after intrastromal corneal ring implantation in an experimental animal model. *Graefes Arch Clin Exp Ophthalmol*. (2015) 253:1071–83. doi: 10.1007/s00417-015-2959-5
- Feizi S, Javadi MA. Factors predicting refractive outcomes after deep anterior lamellar keratoplasty in keratoconus. *Am J Ophthalmol*. (2015) 160:648–53. doi: 10.1016/j.ajo.2015.07.005
- Alfonso JF, Torquetti L, Fernández-Vega-Cueto L, et al. Visual and tomographic outcomes of a 300° arc-length ICRS implantation in moderate to advanced central keratoconus. *J Refract Surg*. (2021) 37:249–55. doi: 10.3928/1081597X-20210115-01
- Feizi S, Javadi MA, Rezaei Kanavi M. Recurrent keratoconus in a corneal graft after deep anterior lamellar keratoplasty. *J Ophthalmic Vis Res*. 2012; 7: 328e31.

29. Patel N, Mearza A, Rostron CK, Chow J. Corneal ectasia following deep lamellar keratoplasty. *Br J Ophthalmol.* (2003) 87:799–800. doi: 10.1136/bjo.87.6.799
30. Krumeich JH, Duncker G. Intrastromal corneal ring in penetrating keratoplasty: evidence-based update 4 years after implantation. *J Cataract Refract Surg.* (2006) 32:993–8. doi: 10.1016/j.jcrs.2006.02.020
31. Gadhvi KA, Romano V, Fernández-Vega Cueto L, Aiello F, Day AC, Gore DM, et al. Femtosecond laser-assisted deep anterior lamellar keratoplasty for keratoconus: multi-surgeon results. *Am J Ophthalmol.* (2020) 220:191–202. doi: 10.1016/j.ajo.2020.07.023

Conflict of Interest: The authors declare that the research was conducted in the absence of any commercial or financial relationships that could be construed as a potential conflict of interest.

Publisher's Note: All claims expressed in this article are solely those of the authors and do not necessarily represent those of their affiliated organizations, or those of the publisher, the editors and the reviewers. Any product that may be evaluated in this article, or claim that may be made by its manufacturer, is not guaranteed or endorsed by the publisher.

Copyright © 2021 Alfonso-Bartolozzi, Lisa, Fernández-Vega-Cueto, Madrid-Costa and Alfonso. This is an open-access article distributed under the terms of the Creative Commons Attribution License (CC BY). The use, distribution or reproduction in other forums is permitted, provided the original author(s) and the copyright owner(s) are credited and that the original publication in this journal is cited, in accordance with accepted academic practice. No use, distribution or reproduction is permitted which does not comply with these terms.



Artificial Cornea: Past, Current, and Future Directions

Gráinne Holland¹, Abhay Pandit², Laura Sánchez-Abella³, Andrea Haiek³, Irida Loinaz³, Damien Dupin³, Maria Gonzalez⁴, Eva Larra⁴, Aritz Bidaguren⁵, Neil Lagali⁶, Elizabeth B. Moloney^{1,2†} and Thomas Ritter^{1,2*†}

¹ School of Medicine, College of Medicine, Nursing and Health Sciences, Regenerative Medicine Institute, National University of Ireland Galway, Galway, Ireland, ² CÚRAM Science Foundation Ireland Research Centre for Medical Devices, National University of Ireland, Galway, Ireland, ³ CIDETEC, Basque Research and Technology Alliance, Parque Científico y Tecnológico de Gipuzkoa, Donostia-San Sebastián, Spain, ⁴ AJL Ophthalmic, Alava, Spain, ⁵ Ophthalmology Department, Donostia University Hospital, San Sebastián, Spain, ⁶ Department of Biomedical and Clinical Sciences, Faculty of Medicine, Linköping University, Linköping, Sweden

OPEN ACCESS

Edited by:

Stefano Ferrari,
Fondazione Banca degli Occhi del
Veneto Onlus - FBOV, Italy

Reviewed by:

Mark Ahearne,
Trinity College Dublin, Ireland
Bert Van Den Bogerd,
University of Antwerp, Belgium

*Correspondence:

Thomas Ritter
thomas.ritter@nuigalway.ie

[†]These authors have contributed
equally to this work

Specialty section:

This article was submitted to
Ophthalmology,
a section of the journal
Frontiers in Medicine

Received: 04 September 2021

Accepted: 15 October 2021

Published: 12 November 2021

Citation:

Holland G, Pandit A,
Sánchez-Abella L, Haiek A, Loinaz I,
Dupin D, Gonzalez M, Larra E,
Bidaguren A, Lagali N, Moloney EB
and Ritter T (2021) Artificial Cornea:
Past, Current, and Future Directions.
Front. Med. 8:770780.
doi: 10.3389/fmed.2021.770780

Corneal diseases are a leading cause of blindness with an estimated 10 million patients diagnosed with bilateral corneal blindness worldwide. Corneal transplantation is highly successful in low-risk patients with corneal blindness but often fails those with high-risk indications such as recurrent or chronic inflammatory disorders, history of glaucoma and herpetic infections, and those with neovascularisation of the host bed. Moreover, the need for donor corneas greatly exceeds the supply, especially in disadvantaged countries. Therefore, artificial and bio-mimetic corneas have been investigated for patients with indications that result in keratoplasty failure. Two long-lasting keratoprotheses with different indications, the Boston type-1 keratoprotheses and osteo-odonto-keratoprotheses have been adapted to minimise complications that have arisen over time. However, both utilise either autologous tissue or an allograft cornea to increase biointegration. To step away from the need for donor material, synthetic keratoprotheses with soft skirts have been introduced to increase biointegration between the device and native tissue. The AlphaCor™, a synthetic polymer (PHEMA) hydrogel, addressed certain complications of the previous versions of keratoprotheses but resulted in stromal melting and optic deposition. Efforts are being made towards creating synthetic keratoprotheses that emulate native corneas by the inclusion of biomolecules that support enhanced biointegration of the implant while reducing stromal melting and optic deposition. The field continues to shift towards more advanced bioengineering approaches to form replacement corneas. Certain biomolecules such as collagen are being investigated to create corneal substitutes, which can be used as the basis for bio-inks in 3D corneal bioprinting. Alternatively, decellularised corneas from mammalian sources have shown potential in replicating both the corneal composition and fibril architecture. This review will discuss the limitations of keratoplasty, milestones in the history of artificial corneal development, advancements in current artificial corneas, and future possibilities in this field.

Keywords: artificial cornea, blindness, biointegration, Boston type-1 keratoprotheses, osteo-odonto-keratoprotheses, AlphaCor™, keratoprosthesis, bio-mimetic cornea

INTRODUCTION

Located at the front of the eye, covering the pupil, iris, and anterior chamber, the cornea is the primary component of the ocular optical system (1). The cornea is made up of three cellular layers- epithelium, stroma, and endothelium; and two acellular layers- Bowman's and Descemet's membranes (**Figure 1**) (2). The outermost layer, the epithelium, which makes up 10% of the total corneal thickness, consists of stratified cells with tight junctions, that form a protective barrier. Between the epithelium and stroma is the Bowman's layer, an acellular layer often known as a modified extension of stroma (3). The stroma makes up 90% of the total corneal thickness. It protects the eye from the external environment while contributing to 65–75% of all light transmission to the retina, enabling vision. Separating the posterior corneal stroma and endothelium is the Descemet's membrane, which is a dense, thick, somewhat transparent, cell-free matrix (4). For those with corneal melting disorders, the Descemet's membrane is sometimes the only layer remaining to keep the eye's integrity. The endothelium is made up of a single layer of hexagonal cells. The function of the endothelium is to regulate and maintain stromal hydration (3). Collectively, the cornea is a highly complex tissue, innervated and avascular.

Corneal diseases are a leading cause of blindness with an estimated 10 million patients diagnosed with bilateral corneal blindness worldwide (5). Furthermore, corneal blindness affects proportionally more children and young adults than any other age-related blinding disease such as macular degeneration (6). Therefore, corneal transplantation, or keratoplasty, is the most common transplant performed globally, with ~185,000 corneal transplants performed every year in 116 countries. Unfortunately, around 1 in 70 patients or 12.7 million people are still awaiting corneal transplantation, given that the demand for donor material far exceeds the supply. This emphasises the need for an innovative solution to supplement the supply of transplantable or implantable tissues for corneal replacement, whether with bio-mimetic or artificial corneas (7).

Abbreviations: 3D, Three-dimensional; ACGR, Australian corneal graft registry; ALK, Anterior lamellar keratoplasty; BCVA, Best-corrected visual acuity; BM, Buccal mucosa; CaP, Calcium phosphate; CDVA, Corrected distance visual acuity; CSK, Corneal stromal keratocytes; DALK, Deep anterior lamellar keratoplasty; DM, Descemet membrane; DMEK, Descemet's membrane endothelial keratoplasty; DSAEK, Descemet's stripping automated endothelial keratoplasty; dsDNA, Double-stranded DNA; ECM, Extracellular matrix; EDC, 1-Ethyl-3-(3-dimethylamino-propyl)-carbodiimide hydrochloride; EK, Endothelial keratoplasty; GA, Glutaraldehyde; HAP, Hydroxyapatite; IOP, Intraocular pressure; IPN, Interpenetrating network; iPSC, Induced pluripotent stem cells; KPro, Keratoprosthesis; L-DOPA, L-3,4-Dihydroxyphenylalanine; LESC, Limbal epithelial stem cell; LK, Lamellar keratoplasty; MDCT/CT, Multi-detector computerised tomography; MMP, Mucous membrane pemphigoid; MOOKP, Modified osteo-odonto-keratoprosthesis; MPC, 2-methacryloyloxyethyl phosphorylcholine; MSC, Mesenchymal stromal cell; Neu5Gc, N-Glycolylneuraminic acid; nHAP, Nano-crystalline hydroxyapatite; OCT, Optical coherence tomography; OOKP, Osteo-odonto-keratoprosthesis; PEG, Polyethylene glycol; PEGDA, Poly(ethylene glycol) diacrylate; PERV, Porcine endogenous retroviruses; PHEMA, Polyhydroxyethyl methacrylate; PK/PKP, Penetrating keratoplasty; PLGA, Poly (lactic-co-glycolic acid); PMMA, Poly (methyl methacrylate); PTFE, Poly(tetrafluoroethylene); RPM, Retroprosthetic membrane; SALK, Superficial anterior lamellar keratoplasty; SJS, Stevens-Johnson syndrome; VA, Visual acuity; α -Gal, Galactose- α -1,3-galactose.

Artificial corneas can be defined as laboratory-made constructs, with or without the help of biological material but typically consisting of manmade materials, designed principally to replace the function of the native human cornea. Typically, keratoprotheses fall into this category. The benefits of artificial corneas tend to outweigh the disadvantages (**Table 1**), especially in difficult and high-risk cases where traditional donor cornea transplantation would have a poor outcome. Production of keratoprotheses (or KPros) is stringent in order to guarantee non-toxic, sterile products with high stability. Moreover, KPros overcome socio-cultural and policy difficulties while preventing viral invasion and immune rejection. These KPros are specialised constructs with limited swelling which results in limited water accumulation and less light scattering from the cornea. Improvement in KPro design is possible due to the continually evolving biomaterial technologies, that enable functionalisation using synthetic materials or surface coating techniques. In addition, reservoir systems such as micro- or nanoparticles can be incorporated into these systems to facilitate biointegration and modulate inflammation. Furthermore, 3D fabrication methods can build a fully functionalised biosynthetic cornea with programmed spatial, optical properties and biomechanical properties which cannot be provided by a human corneal transplant (8).

Keratoplasty and Its Limitations

Throughout the years, keratoplasty has proven to be one of the most successful transplant procedures. For low-risk patients, corneal transplantation is an attractive solution with high success rates: survival of first-time grafts is ~90% at 5 years (9, 10). However, these success rates steadily decrease over time (11). Anshu et al. investigated over one thousand penetrating keratoplasties performed over 20 years and found that corneal grafts remained in only 55.4% of patients at 10 years, 52% at 15 years and 44% at 20 years post-surgery (12). Similarly, the Australian Corneal Graft Registry (ACGR) reported that after 15 years corneal graft survival rates had dropped to 46% for full-thickness grafts and 41% for lamellar grafts (13).

Keratoplasty has proven to work with several conditions, for example, keratoconus, corneal opacities, and bullous keratopathy. However, those with recurrent or chronic inflammatory disorders such as sicca disease states, history of glaucoma and herpetic infections, and those with neovascularisation of the host bed have a low keratoplasty success rate (6, 14, 15). Furthermore, those who have failed their first keratoplasty have a high chance of re-graft failure with about 50% of re-grafts failing at 5 years (9, 16). Given this, surgeons are likely to only give re-grafts to patients with a high chance of graft survival and visual acuity improvement (6).

The need for corneal donor tissue is especially prevalent in developing countries. It is often difficult to meet the required logistics around corneal donor transplantation involving processing, transportation, and storage in developing countries due to a lack of facilities. Additionally, biological tissue can transmit certain infections such as tuberculosis, hepatitis C, and venereal infections. Although artificial corneas, or KPros, can potentially address certain limitations of keratoplasty, at

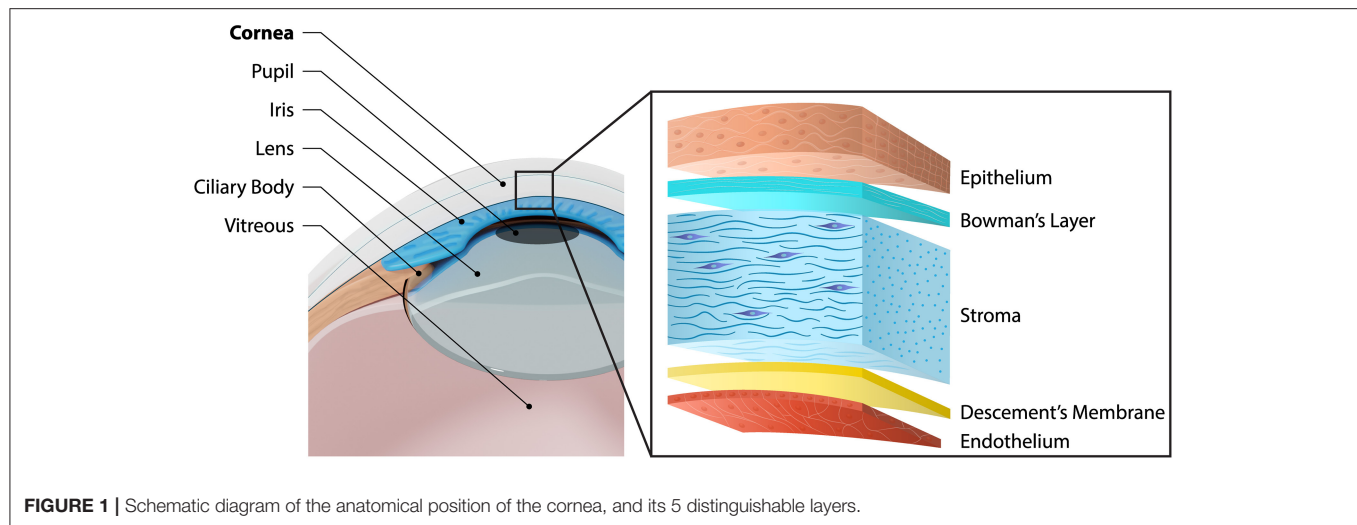


FIGURE 1 | Schematic diagram of the anatomical position of the cornea, and its 5 distinguishable layers.

TABLE 1 | Advantages and disadvantages of keratoprotheses.

Advantages	Disadvantages
Can restore meaningful vision in the most severe cases of corneal blindness where donor corneas fail	Uncomfortable to wear
Avoids religion, culture and policy problems	Transplantation process is complex; multiple surgeries and long-term topical medications often required
Overcomes immune rejection, immune graft risk and ocular surface disease	Limited field of view
Continuously evolving technologies	Unsatisfactory aesthetic appearance
Limited swellability therefore limited water accumulation and less light scattering	Potential for post-operative complications such as extrusion and glaucoma.

present artificial corneas are not seen as an alternative, but more as a last resort. Currently, artificial corneas are only used in end-stage corneal blindness associated with a severe ocular surface disease or as a result of multiple conventional transplantation failures (14). However, advances in KPro technology may lead to KPros being chosen over keratoplasty in the future.

History and Development of Keratoprotheses

Transplantation, including that of corneas, was first referenced around 2000 BC by the Egyptians (17). In 1760, the grandfather of Charles Darwin, Erasmus Darwin, first suggested the removal (trephination) of an opaque cornea and the addition of a KPro to restore vision (18). This was followed by the first full description of a KPro by Guillaume Pellier de Quengsy in 1789 in his monograph on ophthalmology: he suggested a

thin silver-rimmed convex glass disc can be used in place of an opaque cornea with the surgical instruments required for such a procedure (19).

Nonetheless, there was little interest in KPros at that time. In 1853, Nussbaum manufactured a quartz crystal and implanted it into the cornea of rabbits. The first prototype was too large and was rapidly extruded. However, a smaller oblong-shaped prototype was successful in animals and was tried in human patients. These initial KPros had a high failure rate due to infection, leakage, and extrusion of the device (20). Six years later, Heusser successfully implanted a quartz KPro into a blind girl's cornea in Switzerland, who experienced a significant improvement in vision and retained the implant for at least 6 months without complications (21).

In 1862, Abbate made a KPro out of a glass disc surrounded by two rings assembled from natural polymers; gutta-percha and casein. The former was isolated from the exudate of trees and the latter from the precipitation of milk or cheese. The KPro implanted in cats and dogs were only retained for about a week. Although this KPro was quickly extruded, Abbate did emphasise the need for the KPros to be different from glass to allow for incorporation into the host tissue (3, 14). In the early twentieth century, Salzer implanted a quartz disc bounded by a platinum ring with prongs into four humans, with one almost lasting 3 years (22). Much like Abbate, Salzer suggested later that the rim of the KPro should be based on materials that can be incorporated into the host cornea. He also noted that KPros could be made out of materials lighter than glass (3).

Investigation into KPros stalled after Eduard Zirm performed the first successful bilateral keratoplasty in 1905 (23). However, the discovery of poly (methyl methacrylate) (PMMA) in WWII by Harold Ridley refocused attention on artificial corneas. PMMA splinters from crashed Perspex® canopies were found embedded in the cornea of pilots' eyes and were observed to be well-tolerated, thus providing a potential material for subsequent KPros (20, 24). To date PMMA has proven to be the material

of choice, providing a stable and minimally toxic optic. Over time, a two-part “core-skirt” structure was devised for the KPro. Stone took advantage of PMMA to make perforated discs and implant them in corneal lamellae, which were retained for 3 years on average (25, 26). Using a PMMA skirt positioned retrocorneally forming the “nut,” and the threaded optic making up the bolt, Cardona developed the first two-piece nut-and-bolt KPro in 1969 (27). Five years later, Dohlman introduced the collar-button model which had a front and backplate made out of PMMA (28). Aquavella et al. performed a retrospective analysis of implanted Cardona and Dohlman devices, concluding that, although improved device design and surgical procedures reduce the severity of complications, further refinements aimed at KPro biointegration will enhance the long-term clinical outcome for patients (29).

Several scientists took inspiration from Cardona’s nut-and-bolt device but used several different materials as skirts to support biointegration into the host tissue, e.g., Proplast, Teflon, hydrogels, poly-2-hydroxyethyl methacrylate and silicone-carbon (30–32). In this review, various soft and hard KPros and their design, outcomes and recent advances will be reviewed.

HARD KERATOPROSTHESES

Hard keratoprostheses include those made from PMMA as it is a rigid polymer that needs a resilient skirt material to function as a successful implant (Table 2). Moreover, the bonding between PMMA and its skirt must withstand intraocular pressure, and deformations caused by movement of the eye and blinking. Therefore, skirts made from softer materials like Dacron, Teflon and Proplast were extruded (30–32). KPro models like the Boston KPro and osteo-odonto-keratoprosthesis (OOKP), based on harder skirts have been successful in wet blinking eyes and dry or non-blinking eyes, respectively. Although other hard KPros exist, such as the Fyodorov-Zuev KPro (40, 41), this review will focus on the Boston KPro and OOKP as there is an abundance of literature to demonstrate their efficacy in restoring sight, as well as a multitude of studies documenting improvements to their design and/or surgical procedure for enhancing clinical outcomes.

Boston Keratoprosthesis

As mentioned previously, the collar-button model called Dohlman–Doane KPro was a predecessor to the Boston KPro (28). In 1992, the type-I Boston KPro was approved by FDA. Since then it has become the most implanted KPro with over 15,000 devices implanted worldwide. The type II Boston KPro is less popular than its counterpart and is indicated for patients with severe ocular diseases, for example, Stevens-Johnson syndrome (SJS) and mucous membrane pemphigoid (MMP) (33). The main difference consists in the anterior extension which allows implantation through surgically closed eyelids (34).

Design

The Boston KPro consists of a PMMA front plate with a central diameter between 3.5 and 3.7 mm and a backplate made of PMMA or titanium. A titanium locking ring was also added to

secure the backplate (42). Donor corneal tissue acts as a carrier and is placed between the front and backplate. It was found that both frozen and fresh donor corneas could be used for Boston KPro Type 1 (43). It is thus important to consider that these KPros do not eliminate the need for donor human corneas but work in tandem with donor corneas.

Outcomes



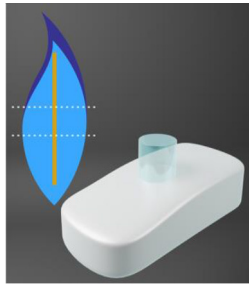
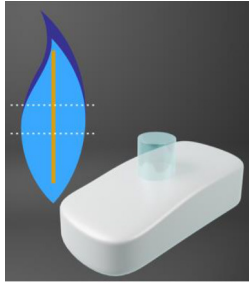

The majority of short-term outcomes of the Boston KPro type-I are favourable. Retention rates are around 90% with post-operative visual acuity (VA) of 20/100 or better in 67% of patients at 6 months and 75% at 1 year (35, 44). However, there is inadequate medium and long-term follow-up data following Boston KPro surgery. This is particularly true for long-term (>5 years) outcomes; both retention rates and complication data are scarce (45). It is important to know the medium- and long-term outcomes as it gives a realistic perspective on the real performance of KPros.

The majority of patients improve their VA following implantation. A meta-analysis of 406 articles found that 60% of patients had 6/60 vision or better at 2 years and 51% at 5 years (45). Kanu et al. found 75 and 66.7% of patients had improved VA at 5 and 10 years, respectively (46). Often, VA improves the longer the KPro has been implanted. Aravena et al. (47) found at 5 years 57% of patients had a corrected distance visual acuity (CDVA) $\geq 20/200$ while at 8 years 82% of patients had a CDVA $\geq 20/200$, while 5% of patients had a CDVA $\geq 20/200$ pre-operatively. In contrast, Szigai et al. (48) found only 36.5% of patients had a VA $\geq 20/200$ post-operatively with 2.4% having a VA $\geq 20/200$ pre-operatively. Szigai et al.’s study had more patients than Aravena’s however (58 vs. 85). Interestingly, Driver et al. investigated 231 eyes: 67 primary KPro procedures and 164 after a failed keratoplasty. They found 78–87% of primary KPro procedures had a CDVA of $\geq 20/200$ after 6 years. In comparison, 56–67% of those given the Boston KPro after failed keratoplasty had a CDVA of $\geq 20/200$ at 6 years (49).

Those with inflammatory diseases like SJS have a high probability of gaining a CDVA of $\geq 20/200$. One study found that 100% of patients with SJS had a CDVA of $\geq 20/200$ after a year (50). Similarly, Brown et al. found 100% of patients with the herpes simplex virus (HSV) had a best-corrected visual acuity (BCVA) $\geq 20/200$. However, only one patient out of four with herpes zoster virus (HZV) had a BCVA $\geq 20/200$ (51). Interestingly, a study investigating patients with chemical or thermal injuries found that after a follow-up of 40.7 months on average, the median best-corrected visual acuity was 20/60 (52).

In general, retention rates for the Boston KPro have been quite high (between 74 and 100%) at the last follow-up (45, 51). The aforementioned meta-analysis review found accumulated retention rates of 88 and 74% at 2 and 5 years, respectively (45). However, conditions that cause cicatrization like SJS or MMP can significantly decrease retention rates (50, 53). Alexander et al. (50) found an increase in post-operative complications for those with SJS which resulted in decreased retention rates. Brown et al. found a similar disparity between the HSV and HZV groups in retention rates as seen with the BCVA.

TABLE 2 | Description of commercial Hard-Keratoprostheses with skirts based on resilient materials, and transparent optic cylinders composed of polymethyl methacrylate (PMMA).

Keratoprosthesis	KPro materials	Schematic	References
Cardona keratoprosthesis	Teflon (skirt) PMMA (optic)		(29, 30)
Boston Keratoprosthesis [type I and type II]	Titanium (skirt) PMMA (optic)		(33–35)
The osteo-odonto-keratoprosthesis (OOKP)	Autologous tooth root and alveolar bone PMMA (optic)		(36, 37)
The modified osteo-odonto-keratoprosthesis (MOOKP)	Osteodental lamina surface PMMA (optic)		(38, 39)
Fyodorov-Zuev keratoprosthesis (MICO)	Titanium (skirt) PMMA (optic)		(40, 41)

The HSV group had a retention rate of 100% whereas the HZV had a retention rate of 25% after around 50 months (51). Phillips et al. (52) found that patients with chemical

or thermal injuries, had an initial retention rate of 77.7% and the remaining KPros were successfully replaced. They did find that for those with severely damaged eyes, the rate

of success can be increased by preparing the ocular surface before implantation with limbal stem cell transplants to reduce sterile ulceration.

Post-operative Complications and Advances

Adjustments in the design of the KPro were introduced to decrease post-operative complications such as the addition of holes to the backplate of the device. The backplate was originally a solid 8 mm PMMA plate which led to high keratolysis and decreased nutritional flow. Keratolysis is defined as the “thinning of peripheral corneal stroma with an overlying epithelial defect due to autoimmune-induced inflammation” (54). Currently, the backplate is 8.5 mm with 16 holes for nutritional support. This led to a decrease in keratolysis from 50 to 10% following transplantation (42). Wearing a large diameter soft or contour contact lens and long-term use of topical antibiotics also decreased sterile keratolysis (14). In 2014, a titanium backplate was introduced as an alternative to PMMA which clicks into the stem without the need for a locking ring, thus easier to assemble. Titanium is well-tolerated by the surrounding tissue and is highly resistant to corrosion and is both light and strong. As it is not magnetic, patients can undergo magnetic resonance imaging (42). Moreover, the titanium backplate can be coloured blue or brown by electrochemical anodisation to help with the cosmetic appeal of the device (55).

There are conflicting reports about whether titanium can cause a reduction in retroprosthetic membrane (RPM) formation, which occurs when fibrovascular tissue grows behind the device. Up to 65% of patients with a Boston KPro form an RPM (56). A study by Todani et al. (57) investigated the potential for RPM formation in 55 eyes with PMMA backplates and 23 with titanium backplates: 41.8% of patients with PMMA backplates developed RPM compared to only 13% for patients with titanium backplates at 6 months post-implantation. However, in the group of patients with PMMA backplates, 39 had threaded PMMA backplates which may, in itself, increase RPM formation (discussed below) (57). In contrast, a study by Talati et al. (58) compared 20 patients with a titanium backplate and 20 with a PMMA backplate with an average follow-up duration of 28.1 or 53.7 months, respectively: 45% of patients with a PMMA backplate developed RPM and 55% of those with a titanium backplate developed RPM. It was concluded that neither material was superior in reducing RPM formation.

In 2007, a newer PMMA stem was produced without screw threads. It was aimed at avoiding damage to the corneal graft associated with the screwing action during surgery and thus possibly reduce RPM formation (59). This newer stem was both easier to use and less expensive to produce as the device was produced by moulding as opposed to machine-made (42). Al Arfaj and Hantera investigated four eyes that underwent Boston type 1 threadless KPro implantation and found no RPM developed at the time of follow-up (i.e., up to 11 months) (60). This is consistent with the observations made by Todani et al. at 6 months post-surgery: 46.1% of eyes implanted with threaded PMMA backplates resulted in RPM, while RPM occurred only in 31.2% of cases implanted with threadless PMMA backplates (57).

Thus, combining a PMMA backplate with a threadless design may reduce the risk for RPM formation (57).

One of the difficulties encountered by many hard KPros is the failure of the corneal graft to adhere to the surface of the PMMA stem. Although PMMA is minimally toxic to corneal stromal cells, poor biointegration between the PMMA and the corneal stroma can lead to corneal melting and graft detachment. Weak interfacial adhesion can create spaces into which bacteria or inflammatory cells can infiltrate (61). In recent years it has been demonstrated that contact between cells and titanium results in increased growth of corneal limbus epithelial cells, alongside a decrease in cell death, thereby providing a superior surface for adhesion (62, 63). Titanium with smooth surface topography was found to enhance cell adhesion and proliferation while roughened titanium can reduce vision-impairing light reflectivity (62).

Several novel techniques have been introduced recently to increase PMMA and corneal tissue adhesion. Sharifi et al. (64) used magnetron sputtering of titanium onto the Boston KPro PMMA stem to show that titanium sputtering can cause an increase in cell adhesion, with an increase in cell growth and collagen deposition, resulting in a more normal corneal stromal cell phenotype. For these reasons, titanium sputtering may improve PMMA-corneal tissue adherence, therefore improving long-term outcomes. Coating the titanium of the KPro with hydroxyapatite (HAp), a constituent from bone and teeth has also resulted in enhanced tissue adherence in rabbit corneas (65, 66). HAp nanoparticles can also be trapped and immobilised on the PMMA surface which results in human corneal fibroblasts adhering and proliferating onto the coated PMMA (61). Similarly, calcium phosphate (CaP) was used to coat PMMA sheets that had dopamine present to induce CaP deposition (61). This resulted in better adhesion, but delamination occurred rather easily. Furthermore, L-3,4-Dihydroxyphenylalanine (L-DOPA) can be covalently bonded to the PMMA surface to support enhanced cellular adhesion, proliferation, and migration, thus improving the compatibility of PMMA (67).

Another post-operative complication that may lead to possible changes in the Boston KPro design is glaucoma. Nonpassopon et al. gathered information from several Boston KPro clinical trials and found 20.2–40% of eyes had an increase in intraocular pressure (IOP), 14–36% developed *de-novo* glaucoma, and 13–33% had progression of previously present glaucoma (42). These results are primarily due to the device being unable to detect elevated IOP early with standard tonometry techniques due to the rigidity of the KPro device (68). Therefore, a potential solution has been introduced by integrating a micro-optomechanical pressure sensor into the Boston KPro device. Hui et al. investigated a fibre-optic Fabry-Perot pressure sensor for its cost-effectiveness and industrial quality control (69). The sensor integrated onto the KPro was stable over long periods and successfully measured IOP. However, pressure sensors implanted in rabbit eyes showed an increase of IOP following RPM formation. It was concluded that RPM formation shortened the optical cavity and caused an artificial IOP increase (69). Another alternative is to use three-dimensional (3D) spectral-domain optical coherence

tomography (OCT) to enhance the evaluation of KPro patients with glaucoma (68).

Cost

In developing countries, the cost of the Boston KPro device can be prohibitive. In 2011, the Aurolab in Madurai, India designed a low-cost version of the Boston KPro, the auroKPro. Basu et al. (70) compared both KPros and found them to be similar in retention rates (70.5 vs. 62.5% for Boston KPro and auroKPro, respectively) and post-operative complications, but more extrusions were observed with the auroKPro. In 2012, the Boston KPro team also produced a less expensive KPro, the Lucia KPro, which was approved by the FDA in 2019 (71, 72). This device had a titanium backplate which was 7.5 mm in diameter with radial petaloid-shaped holes. It was anodized to a brown colour giving a more acceptable appearance to patients. Although efforts are being made towards reducing device manufacturing cost while maintaining ease of implantation, it is important to note that there are many additional costs associated with any corneal procedure, including access to additional clinical resources, and continued post-operative care, and it is ultimately these factors that create a cost-prohibitive option for many patients requiring corneal replacement (70, 73–75).

Osteo-Odonto-Keratoprosthesis

First introduced by Strampelli in 1963, OOKP is one of the longest-lasting KPros available (36). Strampelli used a donor root tooth and alveolar bone to support the PMMA optical cylinder (37). This was further improved upon by Falcinelli in 1998 by adding certain modifications such as using a larger biconvex optic and performing cryo-extraction of the lens. This led to the model which is now known as the modified osteo-odonto-keratoprosthesis (MOOKP) (38). The MOOKP is a device that uses the alveo-dental lamina of a single tooth (usually canine) to support the optical cylinder in its centre. This is covered with a resistant membrane called the buccal mucosa (BM) to give protection and nourishment. It is indicated for patients with bilateral corneal blindness with severe visual loss ($<6/60$) and dry eye or lid damage, as well as poor keratoplasty prognosis. Those with SJS, MMP, chemical or thermal injury view the OOKP as a life-changing surgery (76), and over the last 40 years, centre-based studies across Europe and India have demonstrated excellent anatomical retention of the MOOKP and improvements in visual acuity for the almost 500 patients studied (73).

MOOKP Device Preparation and Implantation

Creating the MOOKP device requires a complex surgical technique and patient counselling, and can only be performed by experienced surgeons. The technique can be separated into two stages: first preparing the bulbar anterior surface and the osteo-odonto-acrylic lamina, and secondly implanting the lamina OOKP into the eye (39, 76).

For those with normal conjunctiva, a 360-degree limbal peritomy is performed, followed by a superficial keratectomy

to remove the epithelium and any scar tissue present (76). Oral mucosa is harvested from below the parotid duct and sutured in place, covering the cornea and sclera (39, 76). To prepare the osteo-odonto-acrylic lamina, a monoradicular tooth and surrounding alveolar bone are removed. Through constant irrigation with a balanced salt solution and with the aid of a dental flywheel, the tooth and alveolar bone are shaped into a 3 mm thick rectangular lamella. A hole is then drilled perpendicularly into the lamina to accommodate an optical cylinder. The PMMA optical cylinder is made up of an anterior stem that ranges in diameter from 3.5 to 4 mm and a posterior section ranging from 4.5 to 5.25 mm in width. The anterior stem protrudes 2–3 mm beyond the alveolar side while the posterior projects through the anterior chamber (76). The completed osteo-odonto-acrylic lamina is then inserted below the lower orbital rim under the skin for ~3 months (39).

In stage 2 the lamina is retrieved from the lower orbital rim and excess soft tissue is removed leaving new vascularisation intact. The mucosal graft is partially detached from top to bottom and the Flieringa ring is placed on the sclera to facilitate attachment of the lamina. A full-thickness disc is made in the cornea to facilitate the optical cylinder of the KPro. A 360-degree iridectomy is performed to remove the iris. This is followed by cryo-extraction of the lens. The lamina is sutured to the sclera and remaining cornea and is covered by the flap of the oral mucosa. Generally, a cosmetic prosthesis is applied which covers the ocular surface, 1 month after surgery (39). Topical broad-spectrum antibiotics must be applied every night for the patient's lifetime (76).

For those with no suitable teeth, a tooth allograft from a related or non-related donor can be used or tibial bone can be used. However, functional survival rates of KPros using tibial bone can be as low as 19% after 10 years (77). Retention of bone strength is reliant on physical stress and so inactivity leads to resorption of the laminae (78). Furthermore, a KPro has been developed for patients with unsuitable teeth for OOKP and no healthy eyelid skin for the Boston KPro type II called the “Lux” KPro (79). It is made up of a PMMA optic, titanium backplate, and a titanium sleeve but it requires a corneal graft. Like the MOOKP, the “Lux” KPro is implanted through, and protected by, a mucous membrane graft (79).

Outcomes

The VA of patients following OOKP surgery can be as good as 6/14. In a systematic review of eight different case studies, Tan et al. found VAs of $\geq 6/18$ in 52% of patients after OOKP (80). Similarly, Liu et al. recorded a VA of $\geq 6/12$ in 53% of all OOKP patients. In the same study, 78% of patients achieved a VA of $\geq 6/60$ (81). Iyer et al. recorded 66% of all patients had a VA $\geq 20/60$ (82). However, complications involving the mucosa, retina, lamina and IOP can occur which affect visual outcomes.

Long- and medium-term anatomical retention rates for OOKP devices are high throughout several studies. Iyer et al. found 96% retention in 50 eyes, with a mean follow-up of 15.4 months (82). Liu et al. reported 72% of patients retained their OOKP after a mean follow-up of 3.9 years (81). De la Paz et al. found 86% of patients with a chemical injury retained their

OOKP while only 65% was retained when the Boston KPro type-I was used (83).

Post-operative Complications

A common cause of OOKP retention failure is resorption. Although there must be a balance between resorption and reformation to preserve the lamina, the osteo-odonto-acrylic lamina is prone to excessive resorption. In a study undertaken by Liu et al., 19% of patients had laminar resorption, resulting in retention failure (81). However, laminar resorption rates are most likely underreported as it tends to progress slowly and is difficult to detect as the lamella resides underneath the oral mucosal membrane graft. Laminar resorption can result in thinning of the lamina which may cause tilting of the optical cylinder, altered refraction, leaking, and endophthalmitis (76).

Advances in imaging have resulted in earlier detection of laminar resorption. Avadhanam et al. (84) found that 40% of all cases of laminar resorption were detected in the first year of follow-up and 66% of cases were found within 3 years of OOKP surgery. They also discovered that laminar thickness did not affect the onset or progression of resorption (84). Multi-detector computerised tomography (MDCT or CT) is widely employed when investigating laminar resorption. Along with imaging, clinical palpation can be carried out by an experienced surgeon to detect resorption early. It seems the best way forward is to implement both methods in the long-term. However, frequent CT scanning is not indicated for the detection of laminar resorption (85).

An autoclavable μ -milling device has been introduced to contour and drill the lamina to increase its stability (86). Iyer et al. introduced a new technique that augments the canine tooth using a mandibular bone graft to boost the labial side of the lamina and therefore decrease laminar resorption (87). In a separate study, Iyer et al. administered a bone morphogenetic protein to 11 eyes with laminar resorption and yet to undergo additional intervention (88). Bone morphogenetic proteins were administered to inhibit further resorption and promote bone generation. However, three eyes had further resorption after protein administration (88). There is uncertainty around the ability of bisphosphonate drugs such as alendronate to decelerate laminar resorption. Several remedies are available that maintain mucosal health and in addition, smoking cessation can have an increased benefit (85).

To decrease laminar resorption, and simplify the surgical procedure, decrease costs, and avoid oral trauma, skirts made of synthetic materials similar to the osteo-odonto-acrylic lamina have been introduced. Avadhanam et al. incorporated nano-crystalline hydroxyapatite (nHAp) coated poly (lactic-co-glycolic acid) PLGA microspheres with a high strength interpenetrating network (IPN) hydrogel to mimic the odonto-acrylic lamina microenvironment (89). They also added poly(ethylene glycol) diacrylate (PEGDA) polymers and agarose to improve the mechanical strength of the hydrogels. This study suggested the PEGDA-agarose based IPN can be used in the future to replace the OOKP lamina (89).

There is a strong correlation between laminar resorption and endophthalmitis, a condition that is caused by a bacterial or

fungal infection of the vitreous and/or aqueous humour (90). A recent study found a 9% incidence rate of endophthalmitis in eyes that had undergone OOKP surgery (91). Falcinelli et al. identified endophthalmitis in 4 out of 181 eyes (2%) following OOKP at a mean 12 years follow-up. Poor pre-operative dental hygiene was reported in these cases (39).

Two common causes of the slowdown in the rate of VA recovery are the presence of air bubbles in the vitreous humour or vitreous haemorrhage. Vitreous haemorrhage was the most common post-operative complication in the systematic review reported by Tan et al., with up to 52% experiencing haemorrhage (80). However, vitreous haemorrhage, and also the problem of choroidal detachment, tend to resolve themselves soon after surgery.

Glaucoma is the main cause of a decrease in VA for those with an OOKP. Tan et al. stated glaucoma rates ranged from 7 to 47% between different studies (80). However, pre-existing glaucoma can be hard to detect pre-operatively (76). Generally, those with glaucoma undergo a trabeculectomy to relieve IOP; however, those with an OOKP will not benefit from this procedure. Kumar et al. found visual field testing and optic disc assessment with optic disc photographs may be used for the monitoring of eyes for glaucoma; but currently, drainage devices are the best method for glaucoma management in those with OOKPs (92, 93). Interestingly, a device called the Ahmed glaucoma drainage device was found to stabilise IOP in three-quarters of OOKP eyes with glaucoma if placed before the mucosal graft (93).






SOFT KERATOPROSTHESES

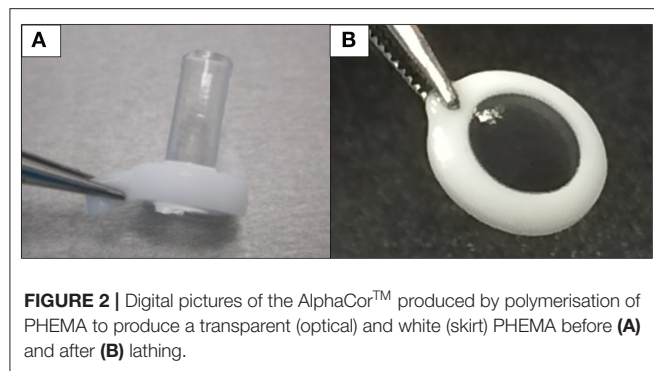
Soft skirt materials have been adopted in recent years to increase biointegration based on a variety of synthetic polymers with or without biofunctionalisation with macromolecules (Table 3). Several skirt and optic type KPros have been brought to clinical trials over the decades, including the Keraklear (94), the MIRO[®] Cornea (95), the Legeais BioKpro III (96) and the Korea Seoul-type KPro (99, 100). However, for the purpose of this review, we will focus on the AlphaCor[™] keratoprosthesis, the first soft KPro to obtain FDA approval almost 20 years ago, while mentioning the two newest soft synthetic KPros that have begun clinical trials in the last year (CorNeat, and EndoArt).

AlphaCor[™] Keratoprosthesis

Chirila et al. at the Lions Eye Institute and the University of Western Australia in Perth aimed to produce an “ideal” KPro. They used cross-linked poly (2-hydroxyethyl methacrylate) (HEMA), to form both the optical and skirt components (101). The hydrophilic PHEMA forms a hydrogel by polymerisation. The skirt and optic are chemically identical with the exception that the skirt has higher water content, meaning it has larger pores to allow for biointegration. The optic and skirt are fused by an IPN to prevent leakage or down growth (102, 103). Formerly known as the Chirila KPro, the AlphaCor[™] KPro (Figure 2) was approved by the FDA in 2003 (97). In 1998, the original Chirila Type-I KPro was first implanted in three people who had failed keratoplasty and had vascularised and/or scarred corneas.

TABLE 3 | Description of commercial Soft-Keratoprostheses with skirts based on soft materials.

Keratoprosthesis	Materials	Schematic	References
Keraklear artificial cornea	PMMA + (polyethylene glycol) PEG		(94)
MIRO® CORNEA UR keratoprosthesis	Hydrophobic acrylic polymer + Genetically engineered fibronectin		(95)
Legeais BioKpro III	Fluorocarbon poly(tetrafluoroethylene) (PTFE)		(96)
Alphacor keratoprosthesis	(Polyhydroxyethyl methacrylate) PHEMA		(97, 98)
Korea Seoul-type keratoprosthesis	PMMA + PEG		(99, 100)



This device required full-thickness removal of the host cornea, and the placement of a conjunctival flap to protect the KPro-corneal interface during post-operative healing; this flap is then removed in a second surgical stage. Unfortunately, two devices were quickly extruded due to retraction of the conjunctival flap. Full-thickness insertion increased the risk of exposing the porous skirt after conjunctival flap failure. In response to these observations, a thinner KPro (the Type II, AlphaCor™ KPro) was developed, allowing for lamellar pocket implantation instead of full-thickness insertion, followed by a subsequent second surgical step several weeks later to trephine the anterior host cornea. A pilot human trial in four patients implanted with the type II KPro observed no post-operative complications, and improved outcomes at seven months follow-up in all individuals (104). This thinner design was subsequently utilised in the larger clinical trials that supported the FDA approval of the AlphaCor™ device (103).

Outcomes

Retention rates reported for the AlphaCor™ have been relatively high. In a phase I trial, 93% of the 14 devices were retained for up to 2.5 years (105). Some years thereafter, Hicks et al. undertook a retrospective study of 322 AlphaCor™ KPros and found at 6 months, 1, and 2 years, 92, 80, and 62% of devices were retained, respectively (97). Of 322 AlphaCor™ KPros implanted, 65.8% were *in situ*, 26.7% had undergone a PK, 6.2% had been replaced with a second AlphaCor™, and 1.2% of patients had lost the eye. Stromal melts occurred in 27% of the cases, from which 65% had resulted in device expulsion (97). Similarly, Jiraskova et al. recorded survival rates of 87, 58, and 42% after 1, 2, and 3 years, respectively (98). Conversely, they found stromal melts occurred in 60% of patients and device removal was necessary in more than half of these patients (98). Topical administration of medroxyprogesterone appeared to protect against melts. On the other hand, protection such as bandage contact lenses could have contributed to this decrease in corneal melts (103).

The high water content and therefore large pores of the AlphaCor™ can lead to inadequate suturing performance and overall poor mechanical strength which causes stromal melts and therefore extrusion. A T-style KPro based on a PHEMA hydrogel was introduced by Xiang et al. to address this problem. They found that adding hyaluronic acid and cationised gelatin

to the skirt promoted cell adhesion and bound the device and native tissue firmly (106). They also added poly(ethylene glycol) (PEG) to the bottom of the optical column and this caused resistance to RPM formation by decreasing cellular attachment and proliferation (106).

Often patients will have pre-existing conditions such as macular disease or glaucomatous cupping which will limit VA improvement. This was the case for many patients in the study carried out by Hicks et al. The average VA was 20/200 and the lowest was light perception. Surprisingly, one patient did achieve a VA of 20/20 (97). Jiraskova et al. found BCVAs ranging from hand movements to 20/25 (98). Although there are promising visual acuity results, regain of sight was often impeded by the occurrence of deposits on the optic and surface spallation of the device. Hicks et al. found that 11% of all patients implanted with an AlphaCor™ had intraoptic calcium or pigment deposition, four cases having white deposition and the other four brown (107). The white deposits had been associated with topical steroid and beta-blocker administration and the brown deposits were correlated with cigarette smoking and topical administration of the beta-blocker levobunolol (107). Interestingly, one study excluded stage 2 of the surgical process, in which corneal tissue is removed from the anterior flap, to find if this could decrease the rate of stromal melts, deposits, and aqueous leakage. All six patients had no stromal melting, infection, aqueous leakage, or extrusion (108).

The AlphaCor™ was developed to address the problems observed in older generations of KPros; namely glaucoma, endophthalmitis, RPM formation, and extrusion. The AlphaCor™ is associated with reduced complications, but corneal stromal melts and optic deposition have been a major setback. Current efforts to improve the clinical outcome include enhancing the stiffness of the skirt material to allow for better suturing of the device into the host eye. Furthermore, the incorporation of gelatin to improve cell attachment and proliferation are also under consideration to enhance device skirt biointegration. In addition, efforts are being made to improve the optics of the AlphaCor™, such as the addition of a UV philtre co-monomer to avoid any UV-associated damage to the retina, as well as the use of an anti-calcification comonomer to reduce the risk of optic depositions that impair visual improvements. It is hoped that these modifications will target the majority of complications previously identified with AlphaCor™, and that future patients will benefit from these improved clinical outcomes.

Synthetic Cornea Alternatives

An interesting alternative to the AlphaCor™ is the CorNeat KPro, a completely synthetic, sterile cornea made using inert materials. Whereas, the AlphaCor™ attempts to somewhat biointegrate with native tissue (stroma), the tissue itself is avascular and is slow to heal. The CorNeat KPro takes advantage of the highly vascularised, fibroblast rich, regenerative environment of the conjunctiva and biointegrates with the tissue.

In contrast to the lengthy MOOKP surgical technique, CorNeat implantation requires just 45 min of surgery using a surgical kit with a marker and snapper. The PMMA lens is

designed to effortlessly snap on into a trephined cornea. If successful, the device should withstand IOP and uphold the eye's integrity. The degradable skirt is implanted subconjunctivally.

The CorNeat KPro is indicated for those who have had keratoplasty failure or an indication that would result in keratoplasty failure (109). The CorNeat has just entered its first-in-human clinical trial in Israel as of January 2021 (ClinicalTrials.gov Identifier: NCT04485858). Several other clinical trials are planned and have a predicted release date of 2023. Moreover, a synthetic endothelial layer has been produced by an Israeli company, EyeYon Medical, known as EndoArt (110). It is a polymer film that acts as a barrier, preventing excess fluid from entering the cornea from the anterior chamber, thereby avoiding corneal oedema and vision loss. The EndoArt is implanted by a minimally-invasive procedure and can reduce pre-existing edema, as evident in pre-clinical studies and in an early clinical trial (ClinicalTrials.gov Identifier: NCT03069521).

FUTURE TRENDS FOR CORNEAL IMPLANTS

In contrast to KPros, a growing area of research and development relates to corneal substitutes aimed at reducing reliance on human donor tissue, in particular for the low-risk cases comprising the majority of corneal transplantations performed worldwide. Various biomaterials have been employed to form full- or partial-thickness corneal substitutes to replicate the structure and function of the cornea. Both natural and synthetic polymers have been used as scaffolds and substitutes for corneal stroma (111). Natural polymers have the advantage of biocompatibility, but synthetic polymers allow for manipulation of chemical and mechanical properties to meet individual needs (112).

Biopolymers of extracellular matrix (ECM) components are being investigated to mimic the corneal microenvironment. In theory, ECM components should be ideal for promoting and supporting regeneration as it is the ECM that supports the growth and embryonic development of an organ. The ideal biomaterial should be biocompatible, transparent, strong (to allow suturing and IOP), non-immunogenic, refractive, permeable to nutrients and oxygen, and resistant to neo-angiogenesis (113).

Collagen and Derivatives

The corneal stroma, which makes up the bulk of the cornea, consists mainly of collagen. Collagen type-I is abundant in several areas of the body, and it is commercially available (112). In the cornea, collagen type-I, III and V form a complex lattice-like structure that provides considerable strength, but this is difficult to replicate in a laboratory setting using purified collagen from different species and tissues. Several treatments have been applied to collagen hydrogels to increase their tensile strength (113). Collagen hydrogels have been plastically compressed to increase density (114), cross-linked chemically (glutaraldehyde, genipin), physically (UV or dehydrothermal treatment) or enzymatically (transglutaminase) (112), and added to other materials capable of forming an IPN or double network (115).

One promising solution for patients with a high-risk of graft failure is a bioengineered corneal implant made from recombinant human collagen type III (RHCIII). In a phase I clinical study, Fagerholm et al. prepared a biosynthetic cornea composed of type III recombinant human collagen crosslinked with the non-toxic zero-length crosslinkers 1-ethyl-3-(3-dimethylamino-propyl)-carbodiimide hydrochloride and N-hydroxysuccinimide (EDC-NHS). It was found that the biomimetic cornea had good biointegration, regenerated the corneal epithelium, partially replaced the corneal stroma and facilitated nerve regeneration, that restored the corneal reflex better than corneal allografts in low-risk patients (116). A 4-year follow-up showed all 10 implants maintained their transparency and no tissue rejection was reported (117). However, these RHCIII implants were only suitable for low-risk patients as they led to neovascularisation in rabbit models with severe pathology (118).

To identify whether the risk of implant-related neovascularisation in high-risk patients could be reduced, modified RHCIII implants were developed to include the synthetic phospholipid methacryloyloxyethyl phosphorylcholine (MPC). These RHCIII-MPC implants had previously been shown to prevent vascularisation in a high-risk alkali burn corneal injury model (118). This device was implanted into three patients with ulceration, decreased corneal integrity, near blindness and associated pain and discomfort (119). Although the implants improved vision in only two of the three patients, in all three cases, the implants remained free of neovascularisation at 1-year follow-up. Functional restoration of corneal integrity was observed, with stable regeneration of both the corneal epithelium and nerves, providing all three patients relief from pain and discomfort (119).

In 2018, Islam et al. grafted cell-free corneal implants consisting of recombinant human collagen and MPC by anterior lamellar keratoplasty (120). The patients were unilaterally blind and at high-risk of graft failure. Three out of six patients gained significant improvement in vision and the corneal stability of the remaining patients was sufficient to allow surgery to improve vision. Grafting outcomes in mini-pig corneas were superior to those in human subjects, indicating that animal models are only predictive for patients with non-severely pathological corneas (120). Another method to combat neovascularisation is to integrate a sustained release nanosystem of bevacizumab (an anti-VEGF drug) into the cell-free biosynthetic scaffolds (121), while ulceration and a neurotrophic deficit could be addressed by sustained release of nerve growth factor, demonstrated recently in a collagen-based scaffold releasing the drug in a controlled manner during a 60-day period (122).

Limbal epithelial stem cells (LESCs) have been successfully cultivated on recombinant human collagen type-I (RHCI) hydrogels (123). LESCs at the junction of the sclera and cornea are responsible for the regeneration of corneal epithelial cells and also prevent invasion by conjunctival epithelial cells (124). Severe limbal stem cell deficiency requires keratolimbal and limbal stem cell allografts but these have poor survival rates and usually require immunosuppression post-surgery (125, 126). One study found that the LESC cultivated hydrogels were biocompatible,

had promising optical characteristics, comparative microbial resistance and successful composite graft generation (123). Additionally, human corneal stromal-derived mesenchymal stromal cells (MSCs) have been shown to culture successfully on a porcine collagen-based hydrogel scaffolds (127).

In 2020, McTiernan et al. introduced the LiQD cornea. The LiQD cornea is made up of short collagen-like peptides conjugated with PEG which are functionally similar to RHCIII implants (128). Fibrinogen was also added to act as a natural adhesive. The LiQD Cornea is liquid at temperatures above 37°C and solidifies to a gel at lower temperatures. It therefore can be used as either a sealant or an alternative to corneal transplants. A 12-month study carried out on pigs found the cornea capable of regeneration and a reduced risk of allergy or immune reaction was observed in traditional corneal transplants or xenogeneic materials, however, all implanted pigs had corneal haze and neovascularisation post-operatively (128).

Alternatively, gelatin, a denatured form of collagen, can be used to construct membranes for corneal cells. It is more pre-disposed to biodegradation and absorption than collagen itself. Gelatin can be cross-linked dehydrothermally or chemically using EDC or glutaraldehyde (GA). Mimura et al. cross-linked a gelatin hydrogel with GA and found the hydrogel was capable of supporting the growth and maintenance of cultured rabbit fibroblasts for 4 weeks (129).

Several other materials beyond collagen or gelatin, such as silk and chitosan are now being investigated to form corneal substitutes with some success (130). This ever-growing area of research has the potential of forming full-thickness corneal biomimetic substitutes in the future.

Decellularised Corneas

Decellularised corneas are one of the most promising forms of replicating the complex structure and function of actual corneas (111, 131). Decellularisation is a process by which cells from mammalian organs or tissues are removed to form a cell-free scaffold with intact ECM integrity. Although hydrogels derived from ECM components such as collagen mimic the cornea's ECM, they may lack its fibril organisation (127) and thereby the tensile strength that the lamellar collagen structure imparts to the stroma.

Decellularised corneas mimic both the fibril architecture and corneal composition and therefore, are a very attractive option. It is the organised and complex architectural structure of the stromal collagen fibrils in the cornea that allow for the appropriate biomechanical properties of the cornea. Collagen fibrils in the anterior part of the cornea are more isotropic and thus allow the IOP to be better withstood and to sustain corneal curvature. Here, spring-like structures extend into deeper fibrils (132). Peripherally the fibrils are circumferentially orientated, more compact and the fibril diameter increases with the merging sclera collagen to reinforce the limbus stabilising the corneal curvature and sustaining its refractive properties (133). The larger and wider fibrils of the posterior cornea and their orthogonal arrangement, as well as the ones of the central cornea, strengthens against strain from extraocular muscles. Narrower bundles in the posterior stroma are directed to the four major

rectus muscles. This complex collagen structure is maintained by proteoglycans and glycosaminoglycans. Decellularised corneas are a promising source for engineering corneal tissue as they retain this complex structure of corneal collagen (132).

The process of decellularisation starts with the isolation of the donor tissue followed by the removal of the cells. New healthy cells can then be added to increase biointegration and finally, the cornea is implanted into the patient (131). Decellularisation can be achieved using physical (freeze-thaw cycle, high hydrostatic pressure, electrophoresis, supercritical CO₂), chemical (Triton X-100, sodium dodecyl sulphate, formic acid, ethanol) and/or biological agents (trypsin, phospholipase A2, Dispase® II). Decellularisation aims to eliminate from the cornea all major histocompatibility complexes to prevent an immune response and therefore rejection once transplanted into the recipient (131). It has been shown that ineffective decellularisation causes macrophages to change into their pro-inflammatory M1 phenotype *in vivo* and *in vitro* (134). Moreover, decellularisation may expose new antigenic sites due to the deformation of the collagen fibrils, which may lead to graft rejection (135). In addition, the process of decellularisation often significantly reduces proteoglycan content. This reduction in proteoglycan content reduces the water holding capacity of these constructs and compromises bioactivity.

Porcine corneas are commonly used for decellularisation studies as they are easily procured and have anatomical similarities with the human cornea. In the case of porcine cells, decellularisation is necessary to eliminate the epitopes Galactose- α -1,3-galactose (α -Gal) and N-glycolylneuraminic acid (Neu5Gc) which are extremely immunogenic to human hosts (136). Suboptimal decellularisation procedures leading to immunogenic reactions are likely the source of inflammation, neovascularization and rejection observed in the first clinical reports of acellular porcine corneas implantation (137).

To address potential issues of xenogeneic transplantation, a potential alternative is to first generate “humanised” pigs. To develop “humanised pigs” one must remove multiple xenoreactive cell surface molecules and porcine endogenous retroviruses (PERV). The revolutionary CRISPR-Cas9 gene-editing technique has been introduced to obtain pigs with GGTA1, CMAH and β 4GalNT2 gene knockouts involved in immunogenic surface glycans (138). PERVs were also inactivated using the same technique (139), possibly making the corneas of transgenic pigs a non-immunogenic alternative. However, the process is very costly compared to using decellularised corneas from “normal” pigs.

Following decellularisation, these matrices may be populated with human cells to generate a viable corneal transplant. There are three parameters used to establish that decellularisation has taken place: staining to verify the absence of intact cell nuclei, quantification of double-stranded DNA (dsDNA), and determination of the maximum length of DNA remnants using agarose gel electrophoresis. The difficulty in choosing the optimal decellularisation technique lies in the fact that researchers have obtained different results using similar techniques. Also increasing decellularisation efficiency is associated with increased damage to the ECM (131).

Recellularisation of the cornea can be achieved using cells from many different origins, all of which are associated with certain advantages and disadvantages. As the cornea is avascular, allogenic cells can be used with a decreased risk of rejection, provided the implanted tissue remains sequestered from the host immune system. Recellularisation of the three different cell types-epithelium, stroma and endothelium- has been carried out using different approaches.

Recellularisation of the stroma is possible using autologous stromal cells by obtaining a biopsy from the uncompromised eye. If both eyes are compromised, adipose-derived MSCs can be activated to produce keratocytes (140). Induced pluripotent stem cells (iPSCs) cultured on cadaveric human corneas have produced cells with a similar phenotype to keratocytes (140).

Different means of achieving cell penetration into the thick densely packed fibril structure of the cornea have been investigated. Human keratocytes seeded directly onto the surface of the scaffold have resulted in distributions resembling human counterparts. In a phase I clinical trial, Ali del Barrio et al. successfully recellularised 120 μ m thick laminas from donor corneas by seeding autologous adipose-derived MSCs which were implanted in four patients (141). Each patient had an improvement in VA and CDVA. However, there was no significant difference between the recellularised and non-recellularised groups, questioning the need to add adipose-derived MSCs, which are obtained from an extra liposuction surgery (141).

Injections of cells into the stroma can damage the stromal fibril structure (131). Freeze-drying creates pores which allow for greater cell penetration (142). Bioreactors have been used where the construct is kept in suspension using a magnetic stirrer and cells, prevented from attaching to other surfaces and promoting the colonisation of the structure. Ma et al. seeded thin sheets of decellularised porcine cornea with keratocytes during transplantation. Cells were added to each sheet, creating a 5-layer recellularised cornea which was then transplanted into rabbits by lamellar keratoplasty (143). Surgery using these recellularised sheets was more successful and had greater transparency than surgeries involving acellular tissue in the model (143).

Epithelial recellularisation was carried out using limbal stem cells isolated from a biopsy of the unaffected eye (144). When both eyes are compromised, oral mucosal allogeneic cells can be used (145). iPSCs could also be used as a non-autogenic cell source due to their ability to differentiate into limbal epithelial stem cell-like cells (146). Xu et al. reported the production of an anterior hemi-cornea using acellular porcine corneal stromata injected with human corneal stromal and epithelial cells (147). These constructs were transfected into dog eyes by lamellar keratoplasty and found to maintain corneal transparency, thickness, and composition (147).

Native corneal endothelial cells are arrested in the G₁ phase, and therefore will not proliferate. However, *in vitro* endothelial cells can proliferate but procedures must be established to restrict the cells from transitioning into MSCs (131). The use of these cells relies on donor corneas. iPSCs can form human corneal endothelial-like cells which can potentially be used for implantation (148). Choi et al. reported the dissection

and sectioning of donor corneal stroma to 120–200 μ m thick (149). Following decellularisation, these stromal sections were seeded with human donor-derived corneal endothelial cells which resulted in a neo-cornea with biomechanical properties comparable to a normal cornea after 14 days in culture (149).

Some reports have questioned the merits of recellularisation as no significant difference had been observed between the acellular and recellularised corneas (141). However, this is a developing field that requires more *in vivo* studies and clinical trials to assess the possible advantages of recellularisation. Nevertheless, decellularised corneas could provide a potential cornea alternative that mimics both its composition as well as its fibril architecture.

3D Bioprinting

3D printing has become an attractive method to manufacture a corneal equivalent. With the emergence of various biomaterials in corneal bioengineering, bio-inks and inks can be made to mimic the corneal microenvironment. Currently, much of the emphasis is on rebuilding a stromal equivalent using several methods which include inkjet printing, extrusion printing, and Laser-assisted printing (8). Duarte Campos et al. (150) bioprinted corneal stromal keratocytes (CSK) in collagen-based bioinks to form stromal equivalents. Theoretically, 3D bioprinting could produce a multi-layered cornea embedded with epithelial cells, keratocytes and endothelial cells.

Isaacson et al. (151) demonstrated the feasibility of engineering an artificial corneal structure using 3D bioprinting. Using an existing 3D digital human corneal model and a composite bio-ink comprising of collagen and alginate, which contained encapsulated corneal keratocytes, 3D constructs anatomically analogous to a human model were produced (151). Keratocytes remained viable for 7 days post-printing. However, the metabolic activity and the protein expression of the keratocyte cells was low which might be linked to the high crosslinking density of the 3D bioprinted scaffold and the lack of a curved geometry (151).

Ulag et al. have 3D printed a cornea suitable for transplantation using an aluminium mould, necessary to achieve the correct shape and a PVA-chitosan construct (152). Scanning electron microscopy and UV spectrometry showed favourable optical properties. Tensile strength could support fluctuations in IOP and the structure remained biocompatible with stem cells after 30 days of degradation (152).

Moreover, decellularised corneal ECM-based bio-inks can be used to mimic the corneal stroma structure. Kim et al. investigated the effects of changing the nozzle diameter and hence the shear stress when extrusion bioprinting was used to bio-print human keratocytes into a bio-ink made from decellularised corneal ECM (153). Widening the nozzle to lower shear stress resulted in non-aligned collagen fibrils. While giving highly structured fibrils, the narrower nozzle and higher shear stress damaged the keratocytes, thereby activating fibroblasts. Finally, the optimal nozzle diameter produced a structure similar to the native human corneal stroma with viable keratocytes (153).

Sorkio et al. produced a scaffold containing a stromal layer and an epithelial layer using laser-assisted bioprinting (154). The

epithelial layer was created using a bio-ink containing human recombinant laminin, hyaluronic acid, and human embryonic stem cells-derived LSCs. The stromal layer was printed with a bio-ink comprised of collagen type 1, blood plasma, thrombin and human adipose tissue-derived stem cells. The structure mimicked the human corneal stroma and supported high cellular viability, but the scaffold lost its shape after a few days. In addition, the supporting membrane added to support the stromal layer led to opacity, rendering the structure non-functional (154).

Finally, Kim et al. bioprinted a scaffold using a gelatin ink in which human corneal endothelial cells were embedded. These cells had been genetically modified to express ribonuclease 5 (R5) which increases endothelial cell proliferation (155). The scaffolds showed transparency and cell viability, and 4 weeks after transplantation of the 3D structures to rabbit corneas, this group showed better transparency than the non-printed group (155). Even though the majority of research focuses on manufacturing a stromal equivalent, 3D bioprinting does have the potential to form a full-thickness, multi-layered cornea model in the future.

CONCLUSIONS

Artificial corneas range from KPros with biological interfaces for treating intractable cases where donor corneas fail, to cell-free medical devices intended to be a primary replacement for donor corneas. The focus of this review was the evolution of KPros and recent developments in corneal substitutes. The Boston KPro and OOKP have stood the test of time by adapting to arising complications. In terms of the Boston KPro, many changes in its design have been implemented to address certain problems: (i) holes were added to the backplate for nutritional support which significantly reduced keratolysis, (ii) titanium sputtering has been introduced to increase PMMA and corneal tissue adhesion, (iii) pressure sensors were investigated to prevent *de-novo* glaucoma, (iv) titanium backplates and a threadless design have shown potential in decreasing RPM formation, and (v) electrochemical anodisation can colour the titanium backplates blue or brown to increase its aesthetic appeal.

In comparison to the Boston KPro, the OOKP has had limited modifications since its creation in 1963, but there have still been several advancements in the surgical procedure involved. Since alterations to the surgical procedure, introduced by Falcinelli, the OOKP has provided the best visual outcomes of any KPro. Some studies have attempted to address the frequent laminar resorption observed with the OOKP, by using an autoclavable μ -milling device, bone morphogenetic proteins, bisphosphonate drugs and/or remedies to maintain mucosal health. The OOKP serves patients with different indications to the Boston KPro. In general, the Boston KPro is for patients with wet, blinking eyes while the OOKP is for patients with dry, non-blinking eyes.

To address the problems of the previous generations of KPros (namely *de-novo* glaucoma, endophthalmitis, RPM formation and extrusion), the AlphaCor™ was developed. This PHEMA-hydrogel-based KPro significantly reduced these complications; however, other complications arose, such as the occurrence

of corneal stromal melts and optic deposits, which have greatly curtailed its use. Some hope comes in the form of synthetic corneas such as the CorNeat which have the potential to completely integrate into the native tissue by joining the conjunctiva, improving both the aesthetic appeal and incidence rate of complications associated with artificial corneas. Nevertheless, the CorNeat has only begun clinical trials.

Although these approaches have focused mainly on artificial corneas made of synthetic materials, much of the interest now lies in using naturally occurring matrix macromolecules such as collagen to form scaffolds for tissue reconstruction and/or delivery of cell-based therapies. These technologies have the advantage of potentially addressing the much larger group of low- to medium-risk indications for corneal transplantation, in contrast to KPros. Decellularised corneas have a potential although a multi-layered corneal alternative and recellularisation using the three corneal cell types has yet to be accomplished. In contrast to biomaterials-based scaffolds, decellularised corneas mimic the complex corneal fibril architecture. However, the immune response to these decellularised constructs is not yet fully understood and initial clinical outcomes have been suboptimal.

First conceived in 1789, artificial corneas have come a long way- from a rudimentary quartz crystal implanted in rabbit eyes to a fully functional, full-thickness KPro implanted in thousands of eyes. Albeit only specified for those who have, or will fail, corneal transplantation, artificial corneas have restored sight to many blind patients. Furthermore, constant improvements in the design have greatly impacted the rate of complications such as RPM formation, glaucoma and endophthalmitis. Soft KPros have demonstrated enormous clinical potential; however, the use of certain biomaterials as components in polymer-based synthetic corneas or 3D printed structures, and the development of decellularised corneas have still presented with serious complications. Concentrated efforts towards improving the biointegration and reducing complications of biofunctionalised soft KPros may hopefully lead to a successful artificial cornea in the near future.

AUTHOR'S NOTE

KPros in general, and particularly the Boston KPro, have shown very good results for vision rehabilitation in eyes where penetrating keratoplasties have failed and where the eye is not severely inflamed. If high levels of inflammation such as in immune disorders (like MMP or SJS) or severe chemical burns are present, however, the KPros are likely to extrude. Drawbacks also include complications such as RPM formation and glaucoma, and KPros often require multiple surgical interventions. A human corneal button is also needed for the implantation, so the KPro does not address the donor cornea shortage, while the expense of the KPro and associated procedures render it unaffordable in many countries. Nonetheless, it should be kept in mind that despite numerous difficulties and limitations, KPros have restored sight and quality

of life to thousands of patients worldwide and continue to do so today.

As KPro outcomes are typically poorer in inflamed eyes, there is a clear need to develop devices and/or protocols to better control the inflammation (e.g., biologics), to prevent extrusion, and improve the retention rate. Here, technologies for sustained release of drugs, either integrated within the KPro itself or implanted within the eye at the time of surgery, could improve outcomes and reduce post-operative complications. Likewise, wireless, or remote monitoring of IOP could aid in the post-operative management of glaucoma.

Although the “classic” KPros will still play an important role in the immediate future for the treatment of serious ocular disorders in high-risk eyes, less technically challenging KPros such as the AlphaCor™ KPro might have an advantage if biointegration can be improved and extrusion can be prevented. We feel, however, that advances in materials, coatings, drug delivery, and 3D (bio)printing could enable a newer generation of KPros to be developed which overcome current limitations. Regarding lower risk eyes where donor corneas could be used if available, several promising approaches exist, although these are still in the development phase. Decellularisation and recellularisation of corneal tissue, from human or non-human sources must still overcome the potential for immunogenicity, and here immunomodulatory cells such as MSCs could play a role. Nonetheless, using intact corneal tissue does not allow for complete control over corneal properties. For this, technologies such as bioprinting and other forms of laboratory-made corneas offer the ability to design a cornea from the “ground up” by choosing the ECM, cell types, and other factors as well as maintaining control over their spatial organisation. This flexibility may prove advantageous, particularly for niche indications. This field, however, is still nascent and very much in an exploratory research phase.

In the more distant future, induced pluripotent stem cell (iPSC) technology might it make possible to generate

human eye organoids *in vitro*, for subsequent transplantation into diseased eyes. However, it remains to be seen how these *in vitro* generated corneal transplants will fare in very diseased human eyes, although, where feasible, an autologous source for iPSCs would render the organoids perfectly immune-compatible. In cases where genetic deficiencies exist, allogeneic iPSC-derived tissues could be tolerated by applying Crispr/Cas gene technology to yield MHC-deficient corneal organoids as a universal source for low-risk corneal transplants.

AUTHOR CONTRIBUTIONS

GH, EM, and TR wrote the manuscript. AP, LS-A, AH, IL, DD, MG, EL, AB, and NL contributed to specific parts of the review and revised and approved the final version of the manuscript. All authors contributed to the article and approved the submitted version.

FUNDING

This project has received funding from the European Union's Horizon 2020 research and innovation programme under Grant Agreement No. 814439. The authors also wish to acknowledge the support of the European Union COST Programme under COST Action CA-18116, ANIRIDIA-NET. In addition, the authors acknowledge the support of Grant Number 13/RC/2073_P2, a research grant from Science Foundation Ireland (SFI) cofunded under the European Regional Development Fund.

ACKNOWLEDGMENTS

Special thanks to Mr. Maciej Doczyk for generating **Figure 1**, and for KPro schematics in **Tables 2, 3**.

REFERENCES

- Kivelä T, Messmer EM BR-J. Cornea. In: Heegaard S, Grossniklaus H, editors. *Eye Pathology*. Berlin; Heidelberg: Springer-Verlag (2015).
- Faye PA, Poumeaud F, Chazelas P, Duchesne M, Rassat M, Miressi F, et al. Focus on cell therapy to treat corneal endothelial diseases. *Exp Eye Res.* (2021) 204:108462. doi: 10.1016/j.exer.2021.108462
- Chirila TV, Hicks CR, Dalton PD, Vijayasekaran S, Lou X, Hong Y, et al. Artificial cornea. *Prog Polym Sci.* (1998) 23:447–73. doi: 10.1016/S0079-6700(97)00036-1
- de Oliveira RC, Wilson SE. Descemet's membrane development, structure, function and regeneration. *Exp Eye Res.* (2020) 197:108090. doi: 10.1016/j.exer.2020.108090
- Pascolini D, Mariotti SP. Global estimates of visual impairment: (2010). *Br J Ophthalmol.* (2012) 96:614–8. doi: 10.1136/bjophthalmol-2011-300539
- Chen M, Ng SM, Akpek EK, Ahmad S. Artificial corneas versus donor corneas for repeat corneal transplants. *Cochrane Database Syst Rev.* (2020) 5:CD009561. doi: 10.1002/14651858.CD009561.pub3
- Gain P, Jullienne R, He Z, Aldossary M, Acquart S, Cognasse F, et al. Global survey of corneal transplantation and eye banking. *JAMA Ophthalmol.* (2016) 134:167–73. doi: 10.1001/jamaophthalmol.2015.4776
- Zhang B, Xue Q, Li J, Ma L, Yao Y, Ye H, et al. 3D bioprinting for artificial cornea: challenges and perspectives. *Med Eng Phys.* (2019) 71:68–78. doi: 10.1016/j.medengphy.2019.05.002
- Thompson RW Jr, Price MO, Bowers PJ, Price FW Jr. Long-term graft survival after penetrating keratoplasty. *Ophthalmology.* (2003) 110:1396–402. doi: 10.1016/S0161-6420(03)00463-9
- NHS. *Survival Rates Following Transplantation*. [Survival rates following transplantation.] (2020). Available online at: <https://www.organdonation.nhs.uk/helping-you-to-decide/about-organ-donation/statistics-about-organ-donation/transplant-activity-report/> (accessed October 5, 2021).
- Armitage WJ, Goodchild C, Griffin MD, Gunn DJ, Hjortdal J, Lohan P, et al. High-risk corneal transplantation: recent developments and future possibilities. *Transplantation.* (2019) 103:2468–78. doi: 10.1097/TP.0000000000002938
- Anshu A, Li L, Htoon HM, de Benito-Llopis L, Shuang LS, Singh MJ, et al. Long-term review of penetrating keratoplasty: a 20-year review in asian eyes. *Am J Ophthalmol.* (2020) 224:254–66. doi: 10.1016/j.ajo.2020.10.014

13. Williams KA, Keane MC, Coffey NE, Jones VJ, Mills RAD, Coster DJ. *The Australian Corneal Graft Registry*. (2018). Available from: <https://dspace.flinders.edu.au/xmlui/bitstream/handle/2328/37917/ACGR%202018%20Report.pdf?sequence=3&isAllowed=y> (accessed October 5, 2021).
14. Avadhanam VS, Smith HE, Liu C. Keratoprostheses for corneal blindness: a review of contemporary devices. *Clin Ophthalmol*. (2015) 9:697–720. doi: 10.2147/OPTH.S27083
15. Williams KA, Lowe M, Bartlett C, Kelly TL, Coster DJ, All Contributors. Risk factors for human corneal graft failure within the Australian corneal graft registry. *Transplantation*. (2008) 86:1720–4. doi: 10.1097/TP.0b013e3181903b0a
16. Ahmad S, Mathews PM, Lindsley K, Alkharashi M, Hwang FS, Ng SM, et al. Boston type 1 keratoprosthesis versus repeat donor keratoplasty for corneal graft failure: a systematic review and meta-analysis. *Ophthalmology*. (2016) 123:165–77. doi: 10.1016/j.ophtha.2015.09.028
17. Moffatt SL, Cartwright VA, Stumpf TH. Centennial review of corneal transplantation. *Clin Exp Ophthalmol*. (2005) 33:642–57. doi: 10.1111/j.1442-9071.2005.01134.x
18. Darwin E. AJO history of ophthalmology series. *Am J Ophthalmol*. (2008) 45:508–13. doi: 10.1016/S0002-9394(08)00351-6
19. de Quengsy GP, Des Herrn D. *Pellier de Quengsy Sammlung von Aufsätzen und Wahrnehmungen sowohl über die Fehler der Augen, als der Theile, die sie umgeben*. Junius. Leipzig (1789).
20. Lam FC, Liu C. The future of keratoprostheses (artificial cornea). *Br J Ophthalmol*. (2011) 95:304–5. doi: 10.1136/bjo.2010.188359
21. Bairo F, Vitale-Brovarone C. Bioceramics in ophthalmology. *Acta Biomater*. (2014) 10:3372–97. doi: 10.1016/j.actbio.2014.05.017
22. Salzer FIV. Ueber den weiteren Verlauf des in meiner Arbeit über den künstlichen Hornhaut-Ersatz mitgeteilten Falles von Cornea arteficialis, sowie des von Schröder'schen Falles. *Ophthalmologica*. (1900) 3:504–9. doi: 10.1159/000278187
23. Armitage WJ, Tullo AB, Larkin DF. The first successful full-thickness corneal transplant: a commentary on Eduard Firm's landmark paper of 1906. *Br J Ophthalmol*. (2006) 90:1222–3. doi: 10.1136/bjo.2006.101527
24. Williams HP. Sir Harold Ridley's vision. *Br J Ophthalmol*. (2001) 85:1022–3. doi: 10.1136/bjo.85.9.1022
25. Stone W Jr. Alloplasty in surgery of the eye. *N Engl J Med*. (1958) 258:486–90. doi: 10.1056/NEJM195803062581007
26. Stone W Jr, Herbert E. Experimental study of plastic material as replacement for the cornea; a preliminary report. *Am J Ophthalmol*. (1953) 36:168–73. doi: 10.1016/0002-9394(53)90167-6
27. Cardona H. Mushroom transcorneal keratoprosthesis (bolt and nut). *Am J Ophthalmol*. (1969) 68:604–12. doi: 10.1016/0002-9394(69)91239-2
28. Dohlman CH, Schneider HA, Doane MG. Prostrokeratoplasty. *Am J Ophthalmol*. (1974) 77:694–70. doi: 10.1016/0002-9394(74)90534-0
29. Aquavella JV, Qian Y, McCormick GJ, Palakuru JR. Keratoprosthesis: current techniques. *Cornea*. (2006) 25:656–62. doi: 10.1097/01.icc.0000214226.36485.d2
30. Vijayasekaran S, Robertson T, Hicks C, Hirst L. Histopathology of long-term Cardona keratoprosthesis: a case report. *Cornea*. (2005) 24:233–7. doi: 10.1097/01.icc.0000134192.26239.62
31. Legeais JM, Rossi C, Renard G, Salvoldelli M, D'Hermies F, Pouliquen YJ, et al. new fluorocarbon for keratoprosthesis. *Cornea*. (1992) 11:538–45. doi: 10.1097/00003226-199211000-00010
32. Chammartin M, Goldblum D, Fruh B, Wilkens L, Bosshardt D, Sarra GM. Case report of osteo-odonto keratoprosthesis (Strampelli) and of Dacron keratoprosthesis (Pintucci). *Klin Monbl Augenheilkd*. (2009) 226:180–3. doi: 10.1055/s-2008-1027997
33. Lee R, Khoueir Z, Tsikata E, Chodosh J, Dohlman CH, Chen TC. Long-term visual outcomes and complications of boston keratoprosthesis type II implantation. *Ophthalmology*. (2017) 124:27–35. doi: 10.1016/j.ophtha.2016.07.011
34. Pujari S, Siddique SS, Dohlman CH, Chodosh J. The Boston keratoprosthesis type II: the Massachusetts eye and ear infirmary experience. *Cornea*. (2011) 30:1298–303. doi: 10.1097/ICO.0b013e318215207c
35. Aldave AJ, Kamal KM, Vo RC, Yu F. The Boston type I keratoprosthesis: improving outcomes and expanding indications. *Ophthalmology*. (2009) 116:640–51. doi: 10.1016/j.ophtha.2008.12.058
36. Liu C, Paul B, Tandon R, Lee E, Fong K, Mavrikakis I, et al. The osteo-odonto-keratoprosthesis (OOKP). *Semin Ophthalmol*. (2005) 20:113–28. doi: 10.1080/088205305090931386
37. Strampelli B. Keratoprosthesis with osteodental tissue. *Am J Ophthalmol*. (1963) 89:1029–39.
38. Falcinelli GC. Personal changes and innovations in Strampelli's osteo-odonto-keratoprosthesis. *An Inst Barraquer (Barc)*. (1998) 28:47–8.
39. Falcinelli G, Falsini B, Taloni M, Colliardo P, Falcinelli G. Modified osteo-odonto-keratoprosthesis for treatment of corneal blindness: long-term anatomical and functional outcomes in 181 cases. *Arch Ophthalmol*. (2005) 123:1319–29. doi: 10.1001/archophth.123.10.1319
40. Huang Y, Yu J, Liu L, Du G, Song J, Guo H. Moscow eye microsurgery complex in Russia keratoprosthesis in Beijing. *Ophthalmology*. (2011) 118:41–6. doi: 10.1016/j.ophtha.2010.05.019
41. Ghaffariyeh A, Honarpisheh N, Karkhaneh A, Abudi R, Moroz ZI, Peyman A, et al. Fyodorov-Zuev keratoprosthesis implantation: long-term results in patients with multiple failed corneal grafts. *Graefes Arch Clin Exp Ophthalmol*. (2011) 249:93–101. doi: 10.1007/s00417-010-1493-8
42. Nonpassopon M, Niparugs M, Cortina MS. Boston type 1 keratoprosthesis: updated perspectives. *Clin Ophthalmol*. (2020) 14:1189–200. doi: 10.2147/OPTH.S219270
43. Robert MC, Biernacki K, Harissi-Dagher M. Boston keratoprosthesis type 1 surgery: use of frozen versus fresh corneal donor carriers. *Cornea*. (2012) 31:339–45. doi: 10.1097/ICO.0b013e31823e6110
44. Ciolino JB, Belin MW, Todani A, Al-Arfaj K, Rudnisky CJ. Boston keratoprosthesis type 1 study G. Retention of the Boston keratoprosthesis type 1: multicenter study results. *Ophthalmology*. (2013) 120:1195–200. doi: 10.1016/j.ophtha.2012.11.025
45. Priddy J, Bardan AS, Tawfik HS, Liu C. Systematic review and meta-analysis of the medium- and long-term outcomes of the Boston type 1 keratoprosthesis. *Cornea*. (2019) 38:1465–73. doi: 10.1097/ICO.0000000000002098
46. Kanu LN, Niparugs M, Nonpassopon M, Karas FI, de la Cruz JM, Cortina MS. Predictive factors of Boston type I keratoprosthesis outcomes: a long-term analysis. *Ocul Surf*. (2020) 18:613–9. doi: 10.1016/j.jtos.2020.07.012
47. Aravena C, Yu F, Aldave AJ. Long-term visual outcomes, complications, and retention of the Boston type I keratoprosthesis. *Cornea*. (2018) 37:3–10. doi: 10.1097/ICO.00000000000001405
48. Sziagiato AA, Bostan C, Nayman T, Harissi-Dagher M. Long-term visual outcomes of the Boston type I keratoprosthesis in Canada. *Brit J Ophthalmol*. (2020) 104:1601–7. doi: 10.1136/bjophthalmol-2019-315345
49. Driver TH, Aravena C, Duong HNV, Christenbury JG, Yu F, Basak SK, et al. Outcomes of the Boston type I keratoprosthesis as the primary penetrating corneal procedure. *Cornea*. (2018) 37:1400–7. doi: 10.1097/ICO.00000000000001735
50. Alexander JK, Basak SK, Padilla MD, Yu F, Aldave AJ. International outcomes of the Boston type I keratoprosthesis in Stevens-Johnson syndrome. *Cornea*. (2015) 34:1387–94. doi: 10.1097/ICO.0000000000000619
51. Brown CR, Wagoner MD, Welder JD, Cohen AW, Goins KM, Greiner MA, et al. Boston keratoprosthesis type 1 for herpes simplex and herpes zoster keratopathy. *Cornea*. (2014) 33:801–5. doi: 10.1097/ICO.0000000000000164
52. Phillips DL, Hager JL, Goins KM, Kitzmann AS, Greiner MA, Cohen AW, et al. Boston type 1 keratoprosthesis for chemical and thermal injury. *Cornea*. (2014) 33:905–9. doi: 10.1097/ICO.0000000000000204
53. Palioura S, Kim B, Dohlman CH, Chodosh J. The Boston keratoprosthesis type I in mucous membrane pemphigoid. *Cornea*. (2013) 32:956–61. doi: 10.1097/ICO.0b013e318286fd73
54. Betts B. Keratolysis (corneal melting), marginal, systemic immune-mediated disease. In: Schmidt-Erfurth U, Kohnen T, editors. *Encyclopedia of Ophthalmology*. Berlin, Heidelberg: Springer Berlin Heidelberg (2018). p. 1001–2.
55. Paschalis EI, Chodosh J, Spurr-Michaud S, Cruzat A, Tauber A, Behlau I, et al. *In vitro* and *in vivo* assessment of titanium surface modification for coloring the backplate of the Boston keratoprosthesis. *Invest Ophthalmol Vis Sci*. (2013) 54:3863–73. doi: 10.1167/iiov.13-11714
56. Park J, Phruksaodomchai P, Cortina MS. Retroprosthetic membrane: a complication of keratoprosthesis with broad consequences. *Ocul Surf*. (2020) 18:893–900. doi: 10.1016/j.jtos.2020.09.004

57. Todani A, Ciolino JB, Ament JD, Colby KA, Pineda R, Belin MW, et al. Titanium back plate for a PMMA keratoprosthesis: clinical outcomes. *Graefes Arch Clin Exp Ophthalmol.* (2011) 249:1515–8. doi: 10.1007/s00417-011-1684-y
58. Talati RK, Hallak JA, Karas FI, de la Cruz J, Cortina MS. Retroprosthetic membrane formation in boston keratoprosthesis: a case-control-matched comparison of titanium versus PMMA backplate. *Cornea.* (2018) 37:145–50. doi: 10.1097/ICO.0000000000001462
59. Chew HF, Ayres BD, Hammersmith KM, Rapuano CJ, Laibson PR, Myers JS, et al. Boston keratoprosthesis outcomes and complications. *Cornea.* (2009) 28:989–96. doi: 10.1097/ICO.0b013e3181a186dc
60. Al Arfaj K, Hantera M. Short-term visual outcomes of Boston keratoprosthesis type I in Saudi Arabia. *Middle East Afr J Ophthalmol.* (2012) 19:88–92. doi: 10.4103/0974-9233.92121
61. Riau AK, Venkatraman SS, Dohlman CH, Mehta JS. Surface modifications of the PMMA Optic of a keratoprosthesis to improve Biointegration. *Cornea.* (2017) 36(Suppl. 1):S15–25. doi: 10.1097/ICO.0000000000001352
62. Zhou C, Lei F, Chodosh J, Paschalis EI. The role of titanium surface microtopography on adhesion, proliferation, transformation, and matrix deposition of corneal cells. *Invest Ophthalmol Vis Sci.* (2016) 57:1927–38. doi: 10.1167/iiov.15-18406
63. Ament JD, Spurr-Michaud SJ, Dohlman CH, Gipson IK. The Boston Keratoprosthesis: comparing corneal epithelial cell compatibility with titanium and PMMA. *Cornea.* (2009) 28:808–11. doi: 10.1097/ICO.0b013e31819670ac
64. Sharifi S, Islam MM, Sharifi H, Islam R, Nilsson PH, Dohlman CH, et al. Sputter deposition of titanium on poly(methyl methacrylate) enhances corneal biocompatibility. *Transl Vis Sci Technol.* (2020) 9:41. doi: 10.1167/tvst.9.13.41
65. Li L, Jiang H, Wang LQ, Huang YF. Experimental study on the biocompatibility of keratoprosthesis with improved titanium implant. *Int J Ophthalmol.* (2018) 11:1741–5. doi: 10.18240/ijo.2018.11.02
66. Dong Y, Yang J, Wang L, Ma X, Huang Y, Qiu Z, et al. An improved biofunction of titanium for keratoprosthesis by hydroxyapatite-coating. *J Biomater Appl.* (2014) 28:990–7. doi: 10.1177/0885328213490312
67. Sharifi R, Mahmoudzadeh S, Islam MM, Koza D, Dohlman CH, Chodosh J, et al. Covalent functionalization of PMMA surface with L-3,4-dihydroxyphenylalanine (L-DOPA) to enhance its biocompatibility and adhesion to corneal tissue. *Adv Mater Interfaces.* (2020) 7:1900767. doi: 10.1002/admi.201900767
68. Khoueiri Z, Jassim F, Braaf B, Poon LY, Tsikata E, Chodosh J, et al. Three-dimensional optical coherence tomography imaging for glaucoma associated with boston keratoprosthesis type I and II. *J Glaucoma.* (2019) 28:718–26. doi: 10.1097/IJG.0000000000001280
69. Hui PC, Shtyrkova K, Zhou C, Chen X, Chodosh J, Dohlman CH, et al. Implantable self-aligning fiber-optic optomechanical devices for *in vivo* intraocular pressure-sensing in artificial cornea. *J Biophotonics.* (2020) 13:e202000031. doi: 10.1002/jbio.202070018
70. Basu S, Serna-Ojeda JC, Senthil S, Pappuru RR, Bagga B, Sangwan V. The aurolab keratoprosthesis (KPro) versus the Boston type I Kpro: 5-year clinical outcomes in 134 cases of bilateral corneal blindness. *Am J Ophthalmol.* (2019) 205:175–83. doi: 10.1016/j.ajo.2019.03.016
71. Bakshi SK, Paschalis EI, Graney J, Chodosh J. Lucia and beyond: development of an affordable keratoprosthesis. *Cornea.* (2019) 38:492–7. doi: 10.1097/ICO.0000000000001880
72. Chodosh J. *FDA Approval Obtained for the Boston Keratoprosthesis Type I Lucia Design.* (2019). Available online at: https://eye.hms.harvard.edu/files/eye/files/kpro_2019_newsletterfinalweb.pdf (accessed October 5, 2021).
73. Iyer G, Srinivasan B, Agarwal S, Talele D, Rishi E, Rishi P, et al. Keratoprosthesis: current global scenario and a broad Indian perspective. *Indian J Ophthalmol.* (2018) 66:620–9. doi: 10.4103/ijo.IJO_22_18
74. Hirneiss C, Neubauer AS, Niedermeier A, Messmer EM, Ulbig M, Kampik A. Cost utility for penetrating keratoplasty in patients with poor binocular vision. *Ophthalmology.* (2006) 113:2176–80. doi: 10.1016/j.opthta.2006.05.060
75. Ament JD, Strykowski TP, Ciolino JB, Todani A, Chodosh J, Dohlman CH. Cost-effectiveness of the Boston keratoprosthesis. *Am J Ophthalmol.* (2010) 149:221–8.e2. doi: 10.1016/j.ajo.2009.08.027
76. Zarei-Ghanavati M, Avadhanam V, Vasquez Perez A, Liu C. The osteo-odonto-keratoprosthesis. *Curr Opin Ophthalmol.* (2017) 28:397–402. doi: 10.1097/ICO.0000000000000388
77. Charoenrook V, Michael R, de la Paz MF, Ding A, Barraquer RI, Temprano J. Osteokeratoprosthesis using tibial bone: surgical technique and outcomes. *Ocul Surf.* (2016) 14:495–506. doi: 10.1016/j.jtos.2016.07.002
78. Avadhanam VS, Zarei-Ghanavati M, Bardan AS, Iyer G, Srinivasan B, Agarwal S, et al. When there is no tooth - looking beyond the Falcinelli MOOKP. *Ocul Surf.* (2019) 17:4–8. doi: 10.1016/j.jtos.2018.08.006
79. Bakshi SK, Graney J, Paschalis EI, Agarwal S, Basu S, Iyer G, et al. Design and outcomes of a novel keratoprosthesis: addressing unmet needs in end-stage cicatricial corneal blindness. *Cornea.* (2020) 39:484–90. doi: 10.1097/ICO.0000000000002207
80. Tan A, Tan DT, Tan XW, Mehta JS. Osteo-odonto keratoprosthesis: systematic review of surgical outcomes and complication rates. *Ocul Surf.* (2012) 10:15–25. doi: 10.1016/j.jtos.2012.01.003
81. Liu C, Okera S, Tandon R, Herold J, Hull C, Thorp S. Visual rehabilitation in end-stage inflammatory ocular surface disease with the osteo-odonto-keratoprosthesis: results from the UK. *Br J Ophthalmol.* (2008) 92:1211–7. doi: 10.1136/bjo.2007.130567
82. Iyer G, Pillai VS, Srinivasan B, Falcinelli G, Padmanabhan P, Guruswami S, et al. Modified osteo-odonto keratoprosthesis—the Indian experience—results of the first 50 cases. *Cornea.* (2010) 29:771–6. doi: 10.1097/ICO.0b013e3181ca31fc
83. de la Paz MF, Salvador-Culla B, Charoenrook V, Temprano J, Alvarez de Toledo J, Grabner G, et al. Osteo-odonto-, tibial bone and Boston keratoprosthesis in clinically comparable cases of chemical injury and autoimmune disease. *Ocul Surf.* (2019) 17:476–83. doi: 10.1016/j.jtos.2019.04.006
84. Avadhanam VS, Chervenoff JV, Zarei-Ghanavati M, Liu C. Clinical study of laminar resorption: part 1 - factors affecting laminar resorption. *Ocul Surf.* (2020) 18:699–705. doi: 10.1016/j.jtos.2020.07.010
85. Avadhanam VS, Smith J, Poostchi A, Chervenoff J, Al Raqqad N, Francis I, et al. Detection of laminar resorption in osteo-odonto-keratoprostheses. *Ocul Surf.* (2019) 17:78–82. doi: 10.1016/j.jtos.2018.09.004
86. Aguilar M, Sawatari Y, Gonzalez A, Lee W, Rowaan C, Sathiah D, et al. Improvements in the modified osteo-odonto keratoprosthesis (MOOKP) surgery technique. *Investig Ophthalmol Visual Sci.* (2013) 54:3481.
87. Iyer G, Srinivasan B, Agarwal S, Rishi E, Rishi P, Rajan G, et al. Bone augmentation of the osteo-odonto alveolar lamina in MOOKP—will it delay laminar resorption? *Graefes Arch Clin Exp Ophthalmol.* (2015) 253:1137–41. doi: 10.1007/s00417-015-3055-6
88. Iyer G, Srinivasan B, Agarwal S, Shanmugasundaram S, Rajan G. Structural & functional rehabilitation in eyes with lamina resorption following MOOKP—can the lamina be salvaged? *Graefes Arch Clin Exp Ophthalmol.* (2014) 252:781–90. doi: 10.1007/s00417-014-2598-2
89. Avadhanam V, Ingavle G, Zheng Y, Kumar S, Liu C, Sandeman S. Biomimetic bone-like composites as osteo-odonto-keratoprosthesis skirt substitutes. *J Biomater Appl.* (2021) 35:1043–60. doi: 10.1177/0885328220972219
90. Durand ML. Endophthalmitis. *Clin Microbiol Infect.* (2013) 19:227–34. doi: 10.1111/1469-0691.12118
91. Rishi P, Rishi E, Manchegowda P, Iyer G, Srinivasan B, Agarwal S. Endophthalmitis in eyes with osteo-odonto keratoprosthesis. *Ocul Immunol Inflamm.* (2020) 1–5. doi: 10.1080/09273948.2020.1770807
92. Kumar RS, Tan DT, Por YM, Oen FT, Hoh ST, Parthasarathy A, et al. Glaucoma management in patients with osteo-odonto-keratoprosthesis (OOKP): the Singapore OOKP Study. *J Glaucoma.* (2009) 18:354–60. doi: 10.1097/IJG.0b013e3181845644
93. Iyer G, Srinivasan B, Agarwal S, Shetty R, Krishnamoorthy S, Balekudaru S, et al. Glaucoma in modified osteo-odonto-keratoprosthesis eyes: role of additional stage 1A and Ahmed glaucoma drainage device-technique and timing. *Am J Ophthalmol.* (2015) 159:482–9.e2. doi: 10.1016/j.ajo.2014.11.030
94. Farid M, Sabeti S, Minckler DS. Histopathological study of an explanted novel artificial corneal device. *Cornea.* (2020) 39:915–8. doi: 10.1097/ICO.0000000000002261

95. Duncker GIW, Storsberg J, Moller-Lierheim WGK. The fully synthetic, bio-coated MIRO® CORNEA UR keratoprosthesis: development, preclinical testing, and first clinical results. *Spektrum Augenheilkd.* (2014) 28:250–60. doi: 10.1007/s00717-014-0243-4
96. Hollick EJ, Watson SL, Dart JK, Luthert PJ, Allan BD. Legeais BioKpro III keratoprosthesis implantation: long term results in seven patients. *Br J Ophthalmol.* (2006) 90:1146–51. doi: 10.1136/bjo.2006.092510
97. Hicks CR, Crawford GJ, Dart JK, Grabner G, Holland EJ, Stulting RD, et al. AlphaCor: clinical outcomes. *Cornea.* (2006) 25:1034–42. doi: 10.1097/01.icc.0000229982.23334.6b
98. Jiraskova N, Rozsival P, Burova M, Kalfertova M. AlphaCor artificial cornea: clinical outcome. *Eye (Lond).* (2011) 25:1138–46. doi: 10.1038/eye.2011.122
99. Kim MK, Lee JL, Wee WR, Lee JH. Seoul-type keratoprosthesis: preliminary results of the first 7 human cases. *Arch Ophthalmol.* (2002) 120:761–6. doi: 10.1001/archophth.120.6.761
100. Lee JH, Wee WR, Chung ES, Kim HY, Park SH, Kim YH. Development of a newly designed double-fixed Seoul-type keratoprosthesis. *Arch Ophthalmol.* (2000) 118:1673–8. doi: 10.1001/archophth.118.12.1673
101. Chirila TV. An overview of the development of artificial corneas with porous skirts and the use of PHEMA for such an application. *Biomaterials.* (2001) 22:3311–7. doi: 10.1016/S0142-9612(01)00168-5
102. Hicks CR, Crawford GJ, Lou X, Tan DT, Snibson GR, Sutton G, et al. Corneal replacement using a synthetic hydrogel cornea, AlphaCor: device, preliminary outcomes and complications. *Eye (Lond).* (2003) 17:385–92. doi: 10.1038/sj.eye.6700333
103. Crawford GJ. The development and results of an artificial cornea: AlphaCor™. In: Chirila TV, Harkin DG, editors. *Biomaterials and Regenerative Medicine in Ophthalmology*. 2nd ed. Woodhead Publishing (2016). p. 443–62.
104. Hicks C, Crawford G, Chirila T, Wiffen S, Vijayasekaran S, Lou X, et al. Development and clinical assessment of an artificial cornea. *Prog Retin Eye Res.* (2000) 19:149–70. doi: 10.1016/S1350-9462(99)00013-0
105. Crawford GJ, Hicks CR, Lou X, Vijayasekaran S, Tan D, Mulholland B, et al. The Chirila Keratoprosthesis: phase I human clinical trial. *Ophthalmology.* (2002) 109:883–9. doi: 10.1016/S0161-6420(02)00958-2
106. Xiang J, Sun J, Hong J, Wang W, Wei A, Le Q, et al. T-style keratoprosthesis based on surface-modified poly (2-hydroxyethyl methacrylate) hydrogel for cornea repairs. *Mater Sci Eng C Mater Biol Appl.* (2015) 50:274–85. doi: 10.1016/j.msec.2015.01.089
107. Hicks CR, Chirila TV, Werner L, Crawford GJ, Apple DJ, Constable IJ. Deposits in artificial corneas: risk factors and prevention. *Clin Exp Ophthalmol.* (2004) 32:185–91. doi: 10.1111/j.1442-9071.2004.00781.x
108. Ngakeng V, Hauck MJ, Price MO, Price FW, Jr. AlphaCor keratoprosthesis: a novel approach to minimize the risks of long-term postoperative complications. *Cornea.* (2008) 27:905–10. doi: 10.1097/ICO.0b013e3181705cbe
109. *Corneal Kpro*[Synthetic Cornea- Revolutionary Innovation in Corneal Replacement Therapy: Corneal Vision. Available online at: https://92eebc15-6bb4-42ef-8befc7443168a4e2.filesusr.com/ugd/cd910f_8fa896afce4e4234993f5c576590bed4.pdf (accessed October 5, 2021).
110. *About EyeYon Medical: EyeYon Medical.* Available online at: <https://eye-yon.com/about> (accessed October 5, 2021).
111. Brunette I, Roberts CJ, Vidal F, Harissi-Dagher M, Lachaine J, Sheardown H, et al. Alternatives to eye bank native tissue for corneal stromal replacement. *Prog Retin Eye Res.* (2017) 59:97–130. doi: 10.1016/j.preteyeres.2017.04.002
112. Chen Z, You J, Liu X, Cooper S, Hodge C, Sutton G, et al. Biomaterials for corneal bioengineering. *Biomed Mater.* (2018) 13:032002. doi: 10.1088/1748-605X/aa92d2
113. Griffith M, Poudel BK, Malhotra K, Akla N, González-Andrades M, Courtman D, et al. Biosynthetic alternatives for corneal transplant surgery. *Expert Rev Ophthalmol.* (2020) 15:129–43. doi: 10.1080/17469899.2020.1754798
114. Mi S, Chen B, Wright B, Connors CJ. Plastic compression of a collagen gel forms a much improved scaffold for ocular surface tissue engineering over conventional collagen gels. *J Biomed Mater Res A.* (2010) 95:447–53. doi: 10.1002/jbm.a.32861
115. Li F, Carlsson D, Lohmann C, Suuronen E, Vascotto S, Kobuch K, et al. Cellular and nerve regeneration within a biosynthetic extracellular matrix for corneal transplantation. *Proc Natl Acad Sci USA.* (2003) 100:15346–51. doi: 10.1073/pnas.2536767100
116. Fagerholm P, Lagali NS, Merrett K, Jackson WB, Munger R, Liu Y, et al. A biosynthetic alternative to human donor tissue for inducing corneal regeneration: 24-month follow-up of a phase I clinical study. *Sci Transl Med.* (2010) 2:46ra61. doi: 10.1126/scitranslmed.3001022
117. Fagerholm P, Lagali NS, Ong JA, Merrett K, Jackson WB, Polarek JW, et al. Stable corneal regeneration four years after implantation of a cell-free recombinant human collagen scaffold. *Biomaterials.* (2014) 35:2420–7. doi: 10.1016/j.biomaterials.2013.11.079
118. Hackett JM, Lagali N, Merrett K, Edelhauser H, Sun Y, Gan L, et al. Biosynthetic corneal implants for replacement of pathologic corneal tissue: performance in a controlled rabbit alkali burn model. *Invest Ophthalmol Vis Sci.* (2011) 52:651–7. doi: 10.1167/iov.10-5224
119. Buznyk O, Pasyechnikova N, Islam MM, Iakymenko S, Fagerholm P, Griffith M. Bioengineered corneas grafted as alternatives to human donor corneas in three high-risk patients. *Clin Transl Sci.* (2015) 8:558–62. doi: 10.1111/cts.12293
120. Islam MM, Buznyk O, Reddy JC, Pasyechnikova N, Alarcon EI, Hayes S, et al. Biomaterials-enabled cornea regeneration in patients at high risk for rejection of donor tissue transplantation. *NPJ Regen Med.* (2018) 3:2. doi: 10.1038/s41536-017-0038-8
121. Buznyk O, Azharuddin M, Islam MM, Fagerholm P, Pasyechnikova N, Patra HK. Collagen-based scaffolds with infused anti-VEGF release system as potential cornea substitute for high-risk keratoplasty: a preliminary *in vitro* evaluation. *Heliyon.* (2020) 6:e05105. doi: 10.1016/j.heliyon.2020.e05105
122. Xeroudaki M, Thangavelu M, Lennikov A, Ratnayake A, Bisevac J, Petrovski G, et al. A porous collagen-based hydrogel and implantation method for corneal stromal regeneration and sustained local drug delivery. *Sci Rep.* (2020) 10:16936. doi: 10.1038/s41598-020-73730-9
123. Haagdorens M, Liszka A, Ljunggren M, Fagerholm P, Valiokas R, Cepela V, et al. Recombinant human collagen type I hydrogels as superior cell carriers for corneal epithelial stem cells and corneal transplantation. *Investig Ophthalmol Visual Sci.* (2019) 60:4139.
124. Atallah MR, Palioura S, Perez VL, Amescua G. Limbal stem cell transplantation: current perspectives. *Clin Ophthalmol.* (2016) 10:593–602. doi: 10.2147/OPTH.S83676
125. Ilari L, Daya SM. Long-term outcomes of keratolimbal allograft for the treatment of severe ocular surface disorders. *Ophthalmology.* (2002) 109:1278–84. doi: 10.1016/S0161-6420(02)01081-3
126. Solomon A, Ellies P, Anderson DF, Touhami A, Grueterich M, Espana EM, et al. Long-term outcome of keratolimbal allograft with or without penetrating keratoplasty for total limbal stem cell deficiency. *Ophthalmology.* (2002) 109:1159–66. doi: 10.1016/S0161-6420(02)00960-0
127. Koulikovska M, Rafat M, Petrovski G, Vereb Z, Akhtar S, Fagerholm P, et al. Enhanced regeneration of corneal tissue via a bioengineered collagen construct implanted by a nondisruptive surgical technique. *Tissue Eng Part A.* (2015) 21:1116–30. doi: 10.1089/ten.tea.2014.0562
128. McTiernan CD, Simpson FC, Haagdorens M, Samarawickrama C, Hunter D, Buznyk O, et al. LiQD Cornea: pro-regeneration collagen mimetics as patches and alternatives to corneal transplantation. *Sci Adv.* (2020) 6:eaba2187. doi: 10.1126/sciadv.aba2187
129. Mimura T, Amano S, Yokoo S, Uchida S, Yamagami S, Usui T, et al. Tissue engineering of corneal stroma with rabbit fibroblast precursors and gelatin hydrogels. *Mol Vis.* (2008) 14:1819–28. Available online at: <http://www.molvis.org/molvis/v14/a215/>
130. Ahearne M, Fernández-Pérez J, Masterton S, Madden PW, Bhattacharjee P. Designing scaffolds for corneal regeneration. *Adv Funct Mat.* (2020) 30:996. doi: 10.1002/adfm.201908996
131. Fernandez-Perez J, Ahearne M. Decellularisation and Recellularisation of cornea: progress towards a donor alternative. *Methods.* (2020) 171:86–96. doi: 10.1016/j.jymeth.2019.05.009

132. Zhou HY, Cao Y, Wu J, Zhang WS. Role of corneal collagen fibrils in corneal disorders and related pathological conditions. *Int J Ophthalmol.* (2017) 10:803–11. doi: 10.18240/ijo.2017.05.24
133. Boote C, Kamma-Lorger CS, Hayes S, Harris J, Burghammer M, Hiller J, et al. Quantification of collagen organization in the peripheral human cornea at micron-scale resolution. *Biophys J.* (2011) 101:33–42. doi: 10.1016/j.bpj.2011.05.029
134. Keane TJ, Londono R, Turner NJ, Badyalak SF. Consequences of ineffective Decellularisation of biologic scaffolds on the host response. *Biomaterials.* (2012) 33:1771–81. doi: 10.1016/j.biomaterials.2011.10.054
135. Chakraborty J, Roy S, Murab S, Ravani R, Kaur K, Devi S, et al. Modulation of macrophage phenotype, maturation, and graft integration through chondroitin sulfate cross-linking to decellularised cornea. *ACS Biomater Sci Eng.* (2019) 5:165–79. doi: 10.1021/acsbomaterials.8b00251
136. Yoon CH, Choi HJ, Kim MK. Corneal xenotransplantation: where are we standing? *Prog Retin Eye Res.* (2021) 80:100876. doi: 10.1016/j.preteyeres.2020.100876
137. Lagali N. Corneal stromal regeneration: current status and future therapeutic potential. *Curr Eye Res.* (2020) 45:278–90. doi: 10.1080/02713683.2019.1663874
138. Wang RG, Ruan M, Zhang RJ, Chen L, Li XX, Fang B, et al. Antigenicity of tissues and organs from GGT1/CMAH/beta4GalNT2 triple gene knockout pigs. *J Biomed Res.* (2018) 33:235–43. doi: 10.7555/JBR.32.20180018
139. Niu D, Wei HJ, Lin L, George H, Wang T, Lee IH, et al. Inactivation of porcine endogenous retrovirus in pigs using CRISPR-Cas9. *Science.* (2017) 357:1303–7. doi: 10.1126/science.aan4187
140. Naylor RW, McGhee CN, Cowan CA, Davidson AJ, Holm TM, Sherwin T. Derivation of corneal keratocyte-like cells from human induced pluripotent stem cells. *PLoS ONE.* (2016) 11:e0165464. doi: 10.1371/journal.pone.0165464
141. Alio Del Barrio JL, El Zarif M, Azaar A, Makdissy N, Khalil C, Harb W, et al. Corneal stroma enhancement with decellularised stromal laminas with or without stem cell Recellularisation for advanced keratoconus. *Am J Ophthalmol.* (2018) 186:47–58. doi: 10.1016/j.ajo.2017.10.026
142. Pang K, Du L, Wu X. A rabbit anterior cornea replacement derived from acellular porcine cornea matrix, epithelial cells and keratocytes. *Biomaterials.* (2010) 31:7257–65. doi: 10.1016/j.biomaterials.2010.05.066
143. Ma XY, Zhang Y, Zhu D, Lu Y, Zhou G, Liu W, et al. Corneal stroma regeneration with acellular corneal stroma sheets and keratocytes in a rabbit model. *PLoS ONE.* (2015) 10:e0132705. doi: 10.1371/journal.pone.0132705
144. Rama P, Matuska S, Paganoni G, Spinelli A, De Luca M, Pellegrini G. Limbal stem-cell therapy and long-term corneal regeneration. *N Engl J Med.* (2010) 363:147–55. doi: 10.1056/NEJMoa0905955
145. Kolli S, Ahmad S, Mudhar HS, Meeny A, Lako M, Figueiredo FC. Successful application of ex vivo expanded human autologous oral mucosal epithelium for the treatment of total bilateral limbal stem cell deficiency. *Stem Cells.* (2014) 32:2135–46. doi: 10.1002/stem.1694
146. Mikhailova A, Ilmarinen T, Uusitalo H, Skottman H. Small-molecule induction promotes corneal epithelial cell differentiation from human induced pluripotent stem cells. *Stem Cell Reports.* (2014) 2:219–31. doi: 10.1016/j.stemcr.2013.12.014
147. Xu B, Song Z, Fan T. Construction of anterior hemi-corneal equivalents using nontransfected human corneal cells and transplantation in dog models. *Artif Organs.* (2017) 41:1004–16. doi: 10.1111/aor.12878
148. Wagoner MD, Bohrer LR, Aldrich BT, Greiner MA, Mullins RF, Worthington KS, et al. Feeder-free differentiation of cells exhibiting characteristics of corneal endothelium from human induced pluripotent stem cells. *Biol Open.* (2018) 7:102. doi: 10.1242/bio.032102
149. Choi JS, Williams JK, Greven M, Walter KA, Laber PW, Khang G, et al. Bioengineering endothelialized neo-corneas using donor-derived corneal endothelial cells and decellularised corneal stroma. *Biomaterials.* (2010) 31:6738–45. doi: 10.1016/j.biomaterials.2010.05.020
150. Duarte Campos DF, Rohde M, Ross M, Anvari P, Blaaser A, Vogt M, et al. Corneal bioprinting utilizing collagen-based bioinks and primary human keratocytes. *J Biomed Mater Res A.* (2019) 107:1945–53. doi: 10.1002/jbma.a.36702
151. Isaacson A, Swioklo S, Connon CJ. 3D bioprinting of a corneal stroma equivalent. *Exp Eye Res.* (2018) 173:188–93. doi: 10.1016/j.exer.2018.05.010
152. Ulag S, Ilhan E, Sahin A, Karademir Yilmaz B, Kalaskar DM, Ekren N, et al. 3D printed artificial cornea for corneal stromal transplantation. *Eur Polymer J.* (2020) 133:109744. doi: 10.1016/j.eurpolymj.2020.109744
153. Kim H, Jang J, Park J, Lee KP, Lee S, Lee DM, et al. Shear-induced alignment of collagen fibrils using 3D cell printing for corneal stroma tissue engineering. *Biofabrication.* (2019) 11:035017. doi: 10.1088/1758-5090/ab1a8b
154. Sorkio A, Koch L, Koivusalo L, Deiwick A, Miettinen S, Chichkov B, et al. Human stem cell based corneal tissue mimicking structures using laser-assisted 3D bioprinting and functional bioinks. *Biomaterials.* (2018) 171:57–71. doi: 10.1016/j.biomaterials.2018.04.034
155. Kim KW, Lee SJ, Park SH, Kim JC. Ex vivo functionality of 3D bioprinted corneal endothelium engineered with ribonuclease 5-overexpressing human corneal endothelial cells. *Adv Healthc Mater.* (2018) 7:e1800398. doi: 10.1002/adhm.201800398

Conflict of Interest: The authors declare that the research was conducted in the absence of any commercial or financial relationships that could be construed as a potential conflict of interest.

Publisher's Note: All claims expressed in this article are solely those of the authors and do not necessarily represent those of their affiliated organizations, or those of the publisher, the editors and the reviewers. Any product that may be evaluated in this article, or claim that may be made by its manufacturer, is not guaranteed or endorsed by the publisher.

Copyright © 2021 Holland, Pandit, Sánchez-Abella, Haiek, Loinaz, Dupin, Gonzalez, Larra, Bidaguren, Lagali, Moloney and Ritter. This is an open-access article distributed under the terms of the Creative Commons Attribution License (CC BY). The use, distribution or reproduction in other forums is permitted, provided the original author(s) and the copyright owner(s) are credited and that the original publication in this journal is cited, in accordance with accepted academic practice. No use, distribution or reproduction is permitted which does not comply with these terms.



Ultrastructural Analysis of Rehydrated Human Donor Corneas After Air-Drying and Dissection by Femtosecond Laser

Emilio Pedrotti¹, Erika Bonacci¹, Adriano Fasolo^{1,2*}, Arianna De Rossi¹, Davide Camposampiero², Gary L. A. Jones², Paolo Bernardi³, Flavia Merigo³, Diego Ponzin², Giorgio Marchini¹ and Andrea Sbarbati³

¹ Ophthalmology Unit, Department of Neurosciences, Biomedicine and Movement Sciences, University of Verona, Verona, Italy, ² Research Unit, The Veneto Eye Bank Foundation, Venice, Italy, ³ Anatomy and Histology Section, Department of Neurosciences, Biomedicine and Movement Sciences, University of Verona, Verona, Italy

OPEN ACCESS

Edited by:

Hannah Levis,
University of Liverpool,
United Kingdom

Reviewed by:

Rodolfo Mastropasqua,
University of Modena and Reggio
Emilia, Italy

Giuseppe Giannaccare,
Università Magna Grecia di
Catanzaro, Italy

*Correspondence:

Adriano Fasolo
adriano.fasolo@fbvov.it

Specialty section:

This article was submitted to
Ophthalmology,
a section of the journal
Frontiers in Medicine

Received: 01 October 2021

Accepted: 24 November 2021

Published: 21 December 2021

Citation:

Pedrotti E, Bonacci E, Fasolo A, De Rossi A, Camposampiero D, Jones GLA, Bernardi P, Merigo F, Ponzin D, Marchini G and Sbarbati A (2021) Ultrastructural Analysis of Rehydrated Human Donor Corneas After Air-Drying and Dissection by Femtosecond Laser. *Front. Med.* 8:787937. doi: 10.3389/fmed.2021.787937

Purpose: To evaluate the efficiency of femtosecond laser (FSL) incision of rehydrated human donor corneas after air-drying and its effects on corneal structure.

Methods: We compared the rehydrated and fresh-preserved corneas by microscopy following Victus-Tecnolas FSL treatment for straight-edge anterior lamellar keratoplasty (ALK). The corneas were dehydrated at room temperature under a laminar-flow hood.

Results: To obtain the horizontal cut in rehydrated corneas, we increased the FSL pulse energy to 1.2 μJ from 0.80 μJ applied for the fresh corneas and obtained a clear-cut separation of the lamellar lenticule cap from the corneal bed. Light microscopy showed regular arrangement of stromal collagen lamellae, with spaces in between the fibers in the corneal stroma in the fresh and the rehydrated corneas, but the uppermost epithelial layers in the rehydrated corneas were lost. Transmission electron microscopy (TEM) revealed no signs of thermal or mechanical damage to the corneal structure. The epithelial basal membrane and Bowman's layer maintained their integrity. The epithelial basal layer and cells were separated by large spaces due to junction alteration in the rehydrated corneas. There were gaps between the lamellar layers in the stroma, especially in the rehydrated corneas. Keratocytes displayed normal structure in the fresh corneas but were devoid of microorganules in the rehydrated corneas. Minor irregularities were observed in the vertical incision and the horizontal stroma appeared smooth on scanning electron microscopy.

Conclusion: The corneal stroma of rehydrated corneas maintained morphology and integrity, while corneal cellular components were generally altered. When corneas are intended for FSL-assisted ALK, effective stromal bed incision is best achieved at a laser power higher than that currently adopted for fresh corneas.

Keywords: dehydrated cornea, electron microscopy, femtosecond laser, light microscopy, rehydrated cornea

INTRODUCTION

Hypothermia and organ culture are the two most important storage methods employed by the American and European eye banks for the preservation of human donor corneas for up to 2 and 4 weeks, respectively (1, 2).

Longer storage periods may become necessary when there is an unexpected rise in supply or a fall in demand of corneal tissue, as has occurred during the COVID-19 pandemic (3, 4), during annual recess periods, or in low-income countries where appropriate healthcare structures and eye-banking frameworks are sometimes lacking.

The conventional preservation times of whole corneas and stromal lenticules can be lengthened by cryopreservation/vitrification (5), dehydration without freezing (6), glycerolization (7–9), lyophilization (or *freeze-drying*) (10–12), and sterilization by gamma irradiation (13).

Such methods, however, can disrupt tissue and cell structures (14, 15). Non-viable whole corneas or anterior stromal lenticules can be employed to treat corneal stroma diseases not involving the endothelial layer or for reconstructive indications, thus allowing subsequent visual grafting. Whereas the application of corneas after cryopreservation can result in poor graft quality (5), lyophilized or silica gel-dehydrated corneal lenticules have been successfully employed in treating epikeratophakia, corneal scars, and keratoconus without negative clinical outcome after keratoplasty (6, 12, 16).

With the introduction of the femtosecond laser (FSL) for corneal trephination, lamellar techniques have become an easier and more predictable choice to place lamellar cuts at the desired plane (17). FSL-assisted anterior lamellar keratoplasty (ALK) allows for a precise and controlled incision, which is key to the successful pneumatic dissection and graft-host interface, with superior visual recovery and/or reduced complications (18).

In this study, we tested the feasibility of air-drying and FSL-assisted dissection of rehydrated corneas to obtain an anterior lamellar graft, and analyzed the quality of the stromal surface at the horizontal and the side cuts by light and electron microscopy.

MATERIALS AND METHODS

Donor Corneas

Human donor corneas were obtained from *Fondazione Banca degli Occhi del Veneto* (The Veneto Eye Bank Foundation, FBOV, Venice, IT). Written consent was obtained from the next kin of donor for the tissues evaluated as being unsuitable for therapeutic application, to be used for research purposes (Protocol no. CRT/19 rev. 02, 24 May 2018). The study adhered to the tenets of the Declaration of Helsinki.

The study materials were corneas with a clear and uncompromised stroma and without apparent irregularities, nonetheless unsuitable for transplantation because of donor serology or poor endothelial cell density. Four corneas were dehydrated after preservation in sterile *Storage* solution (MEM-Earle with HEPES 25 mM, antibiotics, dextran T500) at 31°C. Two corneas, used as controls (CTRL), were maintained in

hypothermic storage at 2–6°C in a sterile *Cold* solution (MEM-Earle with HEPES 25 mM, antibiotics, dextran T500); conditions that do not influence the proper physical characteristics of the corneas, though the cornea swells to about two times its normal thickness and the number of layers of epithelial cells are reduced (19).

Dehydration and Rehydration Process

The corneas were dehydrated in the eye bank laboratory by positioning them on a Teflon base, endothelial side up, and then air-dried overnight (12–15 h) at room temperature under a laminar-flow biohazard hood.

The dehydrated corneas were transferred to a 25-mm sterile plastic Petri dish (Falcon 3001, Becton Dickinson, Waltham, MA, USA) and placed inside a 60-ml sterile single-use storage plastic jar (Nalgene, Nalge Nunc International, Rochester, NY, USA). The Petri dish containing the dehydrated cornea was positioned over two other 25-mm Petri dishes; the bottom one was empty and served simply to reduce the space in the jar, the middle one contained 2–6 mm silica gel beads (Chameleon, VWR Chemicals, Leuven, Belgium). The jar was closed with a screw top cap and stored at 4–6°C for up to 6 months (**Figure 1**), following the European rules for corneal tissues in the presence of silica gel (20).

On delivery to the surgical center, dehydrated corneas were transferred into sterile *Deswelling-Transport* solution (same composition as the *Cold* solution) to rehydrate and recover their physiological thickness for a minimum of 24 h before use.

Sterility Testing

Sterility testing was achieved by sampling the *Storage* solution before the dehydration process, 6 days after the preservation in organ culture, and testing the *Deswelling-Transport* solution 24 h after the transfer of the dehydrated cornea prior to shipment to the surgical center. Microbial growth was screened in the media by means of two validated automated systems: Bactec 9240 (Becton-Dickinson, Franklin Lakes, NJ, USA) and HB&L (Alifax, Padua, Italy) (21).

Maintenance of sterile conditions during the dehydration process was assessed by a gelatin membrane filter (Gelatine Disposables, Sartorius, Gottingen, Germany) next to the Teflon base to collect airborne microbes that were then cultivated on blood agar plates for 7 days. In the event of positive results for microbial contamination of any of the tests, the cornea is discarded.

FSL Incision

We used a Victus FSL (Technolas, Perfect Vision, Munich, Germany), which generates 290–550 fs pulses at 1,040 nm wavelength at 80 kHz repetition rate, to obtain ALK incisions with a straight-edge configuration. The rehydrated (RHD) corneas were mounted on an artificial anterior chamber (Network Medical Products, Coronet House, Ripon, UK) connected to a bottle of balanced salt solution (Alcon Laboratories Inc., Fort Worth, TX, USA) positioned at a height of 50 cm to maintain a pressure of 20 mmHg

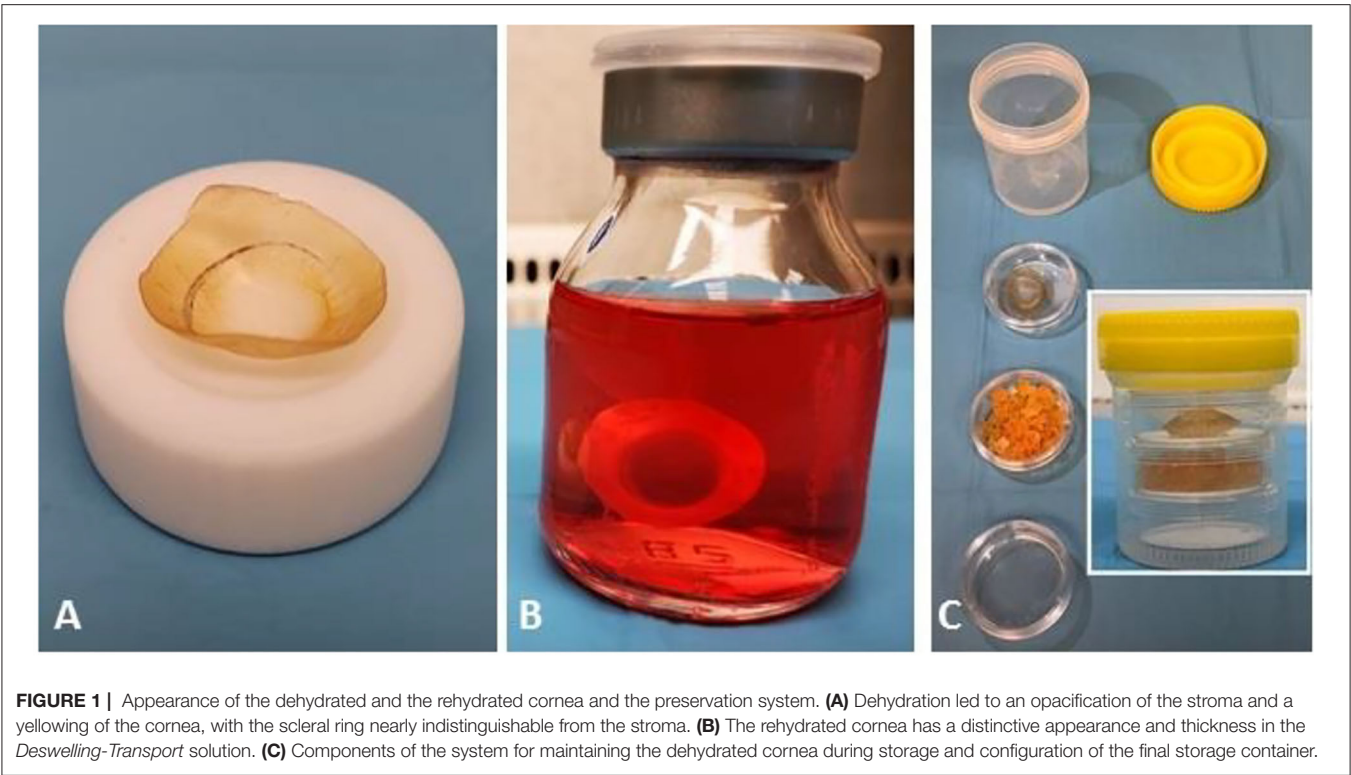


FIGURE 1 | Appearance of the dehydrated and the rehydrated cornea and the preservation system. **(A)** Dehydration led to an opacification of the stroma and a yellowing of the cornea, with the scleral ring nearly indistinguishable from the stroma. **(B)** The rehydrated cornea has a distinctive appearance and thickness in the *Deswelling-Transport* solution. **(C)** Components of the system for maintaining the dehydrated cornea during storage and configuration of the final storage container.

TABLE 1 | FSL straight-edge configuration parameters for anterior lamellar keratoplasty.

Common parameters		
Anterior diameter	8.2 mm	Anterior diameter value
Depth ratio	79%	Ratio of cutting depth to pachymetry
Posterior diameter	7.5 mm	Posterior diameter value
Vertical incision parameters—rim incision		
Line spacing	2.0 μm	Distance between spots of adjacent lines
Spot spacing	4.0 μm	Distance between adjacent spots on a line
Side cut angle	70°	Angle between the corneal surface tangent and the rim cut
Top bonus	100 μm	Extension of the rim cut at the anterior side of the cornea to ensure exit of laser cut out of the eye
Bottom bonus	−10 μm	Extension of the rim cut inside the cornea to ensure that rim and bed cut overlap
Pulse energy	1.80 μJ	Energy level of each single pulse
Horizontal incision parameters—bed incision		
Line spacing	6.0 μm	Distance between spots of adjacent lines
Spot spacing	6.0 μm	Distance between adjacent spots on a line
Pulse energy	adjusted 0.8–1.8 μJ	Energy level of each single pulse

similar to that of the natural eye and sufficient to support the tissue.

Two lamellar incisions were made, a vertical rim incision and a horizontal bed incision, to assess the suturing of graft-to-receiver corneal edges and the quality of the graft-host interface, respectively. The FSL pulse energy was set at the level currently implemented to shape donor and receiver corneas for FSL-assisted ALK (**Table 1**) (22).

At the end of the procedure, the samples obtained under the cutting plane (posterior portion of the stroma, Descemet's membrane, and endothelium) served as bed samples, while those obtained from above the incision plane (epithelium, Bowman's layer, and anterior portion of the stroma) served as cap samples. All samples were examined using light microscopy, transmission electron microscopy (TEM) and scanning electron microscopy (SEM).

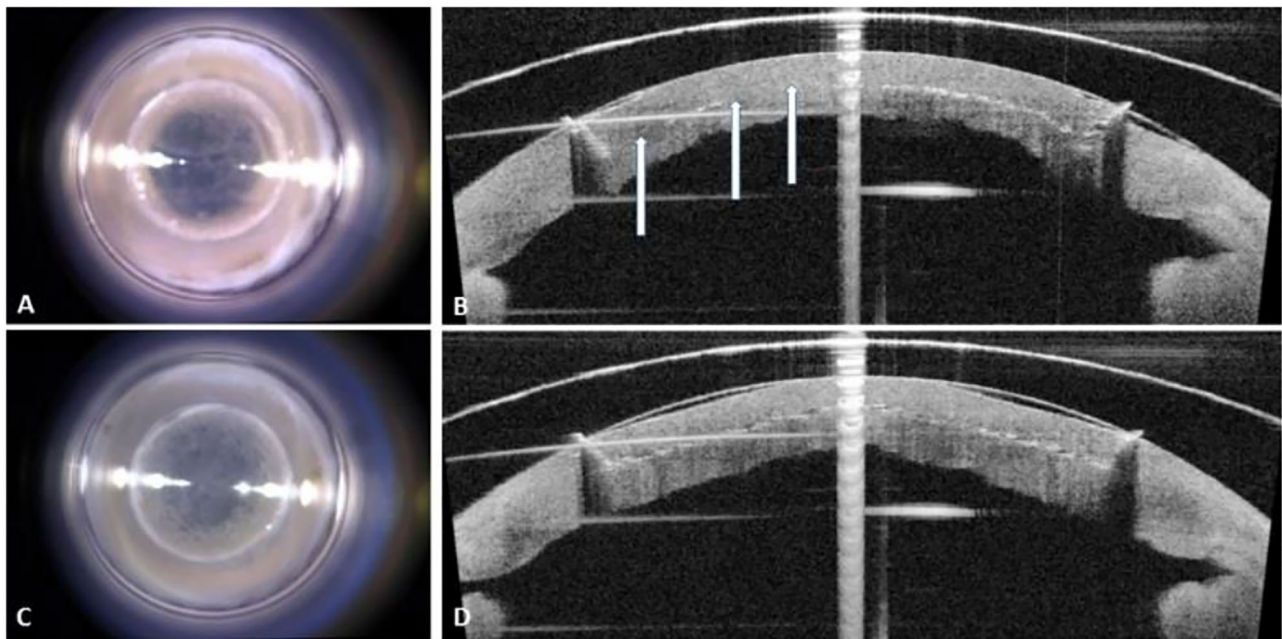


FIGURE 2 | Surgical microscopy and integrated optical coherence tomography images of the rehydrated cornea following femtosecond laser (FSL) lamellar incision. **(A)** Frontal view of the failed incisions at 0.8 μJ . **(B)** Cut of the internal horizontal layer is largely absent (arrows). **(C)** Frontal view of the successful incisions. **(D)** Anterior, middle, and posterior views of the lamellar cut following straight-edge configuration.

Light Microscopy and TEM

The cornea samples were fixed by immersion in 2% glutaraldehyde in 0.1 M phosphate buffer, pH 7.4, for 2 h at 4°C. After three 5-min washes with phosphate buffer, they were post-fixed with 1% OsO_4 diluted in 0.2 M potassium hexa-cyanoferrate for 1 h and then, after rinsing in 0.1 M phosphate buffer, dehydrated in graded concentrations of acetone, and embedded in a mixture of Epon and Araldite (Electron Microscopic Sciences, Fort Washington, PA, USA). Semi-thin sections of 1 μm thick were stained with toluidine blue and examined under an Olympus BX51 fluorescence microscope (Olympus, Tokyo, Japan) equipped with a digital camera (DKY-F58 CCD JVC, Yokohama, Japan). Digital images were analyzed with Image-Pro Plus 7.0 software (Media Cybernetics, Silver Spring, MD, USA).

For ultrastructural examination, ultrathin 70-nm sections were cut on an Ultracut E Ultramicrotome (Reichert-Jung, Heidelberg, Germany), contrasted with lead citrate, and observed on a Philips Morgagni 268 D transmission electron microscope (FEI Company, Eindhoven, The Netherlands), equipped with a MegaView 2 camera for the acquisition of digital images.

Scanning Electron Microscopy

The corneal samples were fixed in 2% glutaraldehyde in 0.1 M phosphate for 2 h at 4°C, post-fixed with 1% OsO_4 in the same buffer for 1 h at 4°C and dehydrated in graded concentrations of ethanol. They were then processed by critical point-drying (CPD 030, Balzers, Vaduz, Liechtenstein), mounted on stubs

with colloidal silver, sputtered with gold by a MED 010 coater (Balzers), and examined with an XL30 scanning electron microscope (FEI Company).

RESULTS

Before FSL processing, the corneas displayed a normal physiological thickness. We shaped one rehydrated cornea by FSL at the pulse energy currently used to obtain a stroma lamellar cut for anterior keratoplasty, 1.80 and 0.80 μJ for rim and horizontal incision, respectively. The FSL procedure proved ineffective and was tricky to separate the lamellar cap from the posterior corneal bed because thin tissue bridges were formed in the corneal stroma at the horizontal plane cut (**Figure 2A**). To shape the subsequent RHD corneas, we increased the FSL energy for the horizontal incision to 1.0, 1.20, and 1.80 μJ , aligning rim and bed incision power. In all three cases, we obtained a clear-cut separation of the incised lamellar lenticule cap from the donor cornea bed, with the 1.2 μJ cut as good as the 1.8 μJ (**Figure 2B**), while residual stromal tissue bridges in the 1.0 μJ cut were recognized by the surgeon.

We successfully cut the CTRL corneas at 1.80 and 0.80 μJ for the rim and the bed incision, respectively (**Figures 2C,D**).

Light microscopy of the toluidine blue-stained sections showed a well-preserved overall structure, well-defined incision borders, and distinct corneal layers (**Figures 3A–C,F–H**). The stromal collagen lamellae layers displayed a regular arrangement, with gaps in between lamellae in the corneal

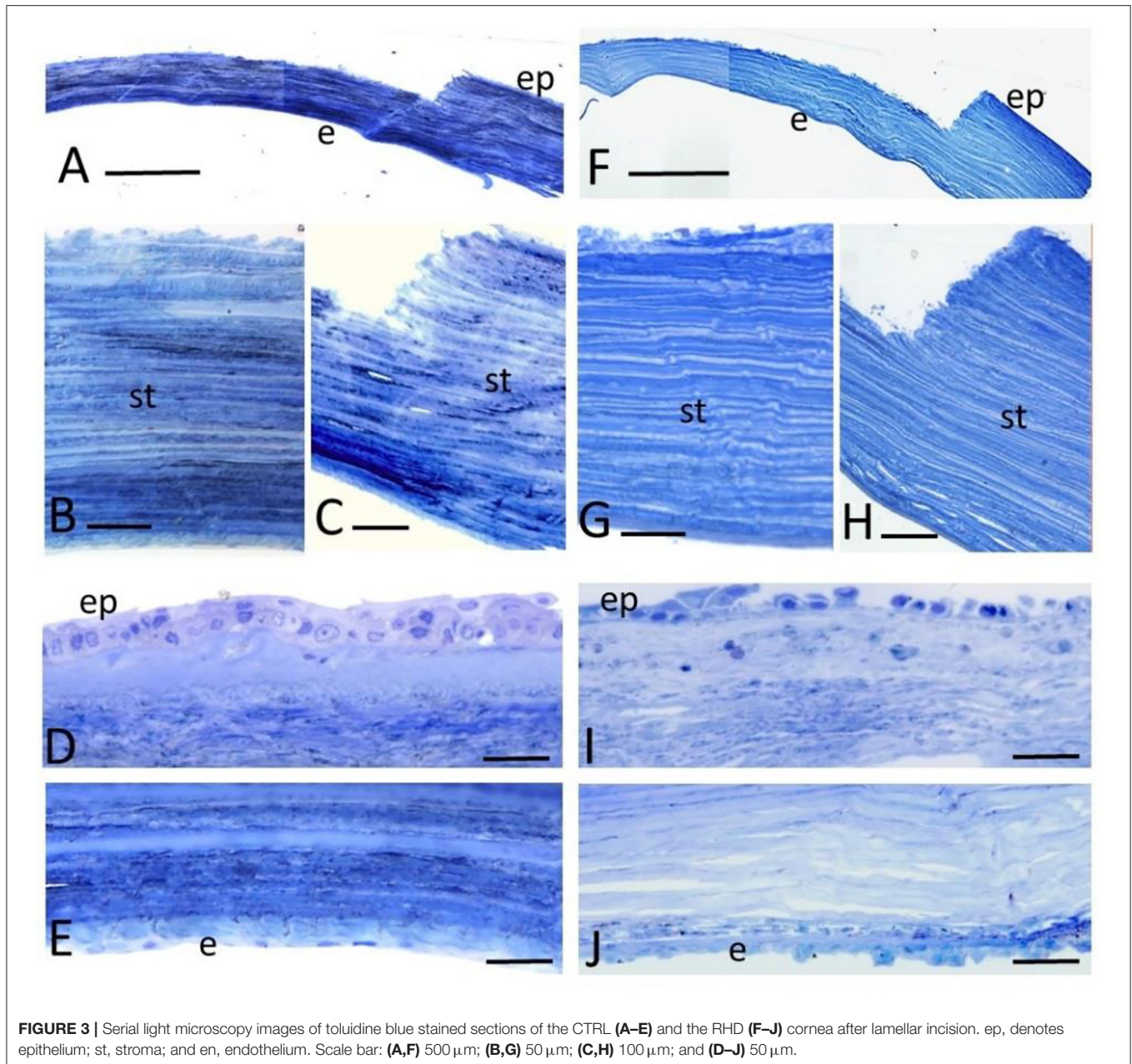


FIGURE 3 | Serial light microscopy images of toluidine blue stained sections of the CTRL (A–E) and the RHD (F–J) cornea after lamellar incision. ep, denotes epithelium; st, stroma; and en, endothelium. Scale bar: (A,F) 500 μ m; (B,G) 50 μ m; (C,H) 100 μ m; and (D–J) 50 μ m.

stroma in the CTRL and the RHD cornea. Compared with the CTRL cornea, the uppermost superficial epithelial layers of the RHD cornea were almost fully depleted (Figures 3D,I, respectively). The endothelium showed its typical organization, though detached from the Descemet's membrane in some areas in the CTRL and the RHD cornea (Figures 3E,J, respectively).

Ultrastructural TEM revealed no signs of thermal or mechanical damage to the corneal structure after FSL incision in either the CTRL or the RHD cornea. The epithelial basal membrane and Bowman's layer maintained their integrity in the CTRL (Figure 4A) and the RHD cornea; however, only the

columnar basal layer of the epithelium and cells separated by large spaces due to junction alteration were retrieved in the RHD cornea (Figure 4D). No changes were noted in the organization of the lamellar layers in the stroma; an alternating light and dark staining pattern highlighted regular disposition of the collagen lamellae (Figures 4B,E). Gaps between the lamellar architecture were detectable throughout the stroma, particularly in the RHD cornea. Keratocytes were normal in structure and regularly distinguishable between the stroma lamellae in the CTRL cornea (Figure 4C), but sparse electron-dense with distinct organelles and damaged devoid keratocytes were detected in the RHD cornea (Figure 4F).

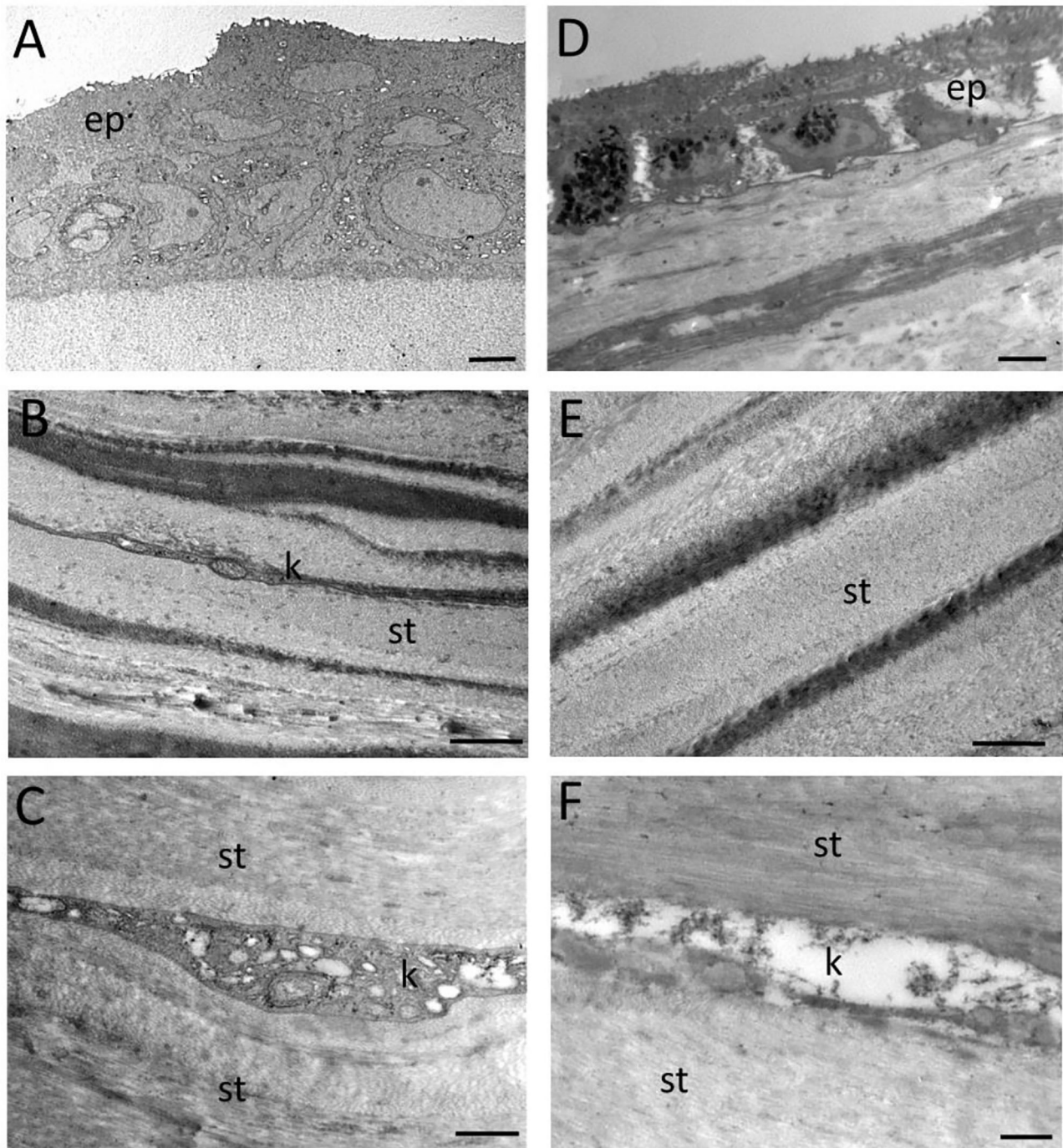


FIGURE 4 | Transmission electron micrographs showing the epithelial surface not involved by laser incision and the deep corneal stroma of the CTRL (A–C) and the RHD (D–F) cornea. ep denotes epithelium; st, stroma; and k, keratocyte. Scale bar: (A,D) 2 μ m; (B,E) 1 μ m; and (C,F) 500 nm.

Comparable results were obtained with SEM, which showed that the corneal surface not involved by the incision was covered with a proper multilayered intact epithelium in the CTRL cornea (Figure 5A), whereas that of the RHD

cornea was devoid of the uppermost superficial epithelial layers, and large spaces were noted among the residual basal epithelial columnar cells (Figure 5E). A regular cutting surface with slightly irregular organization of the

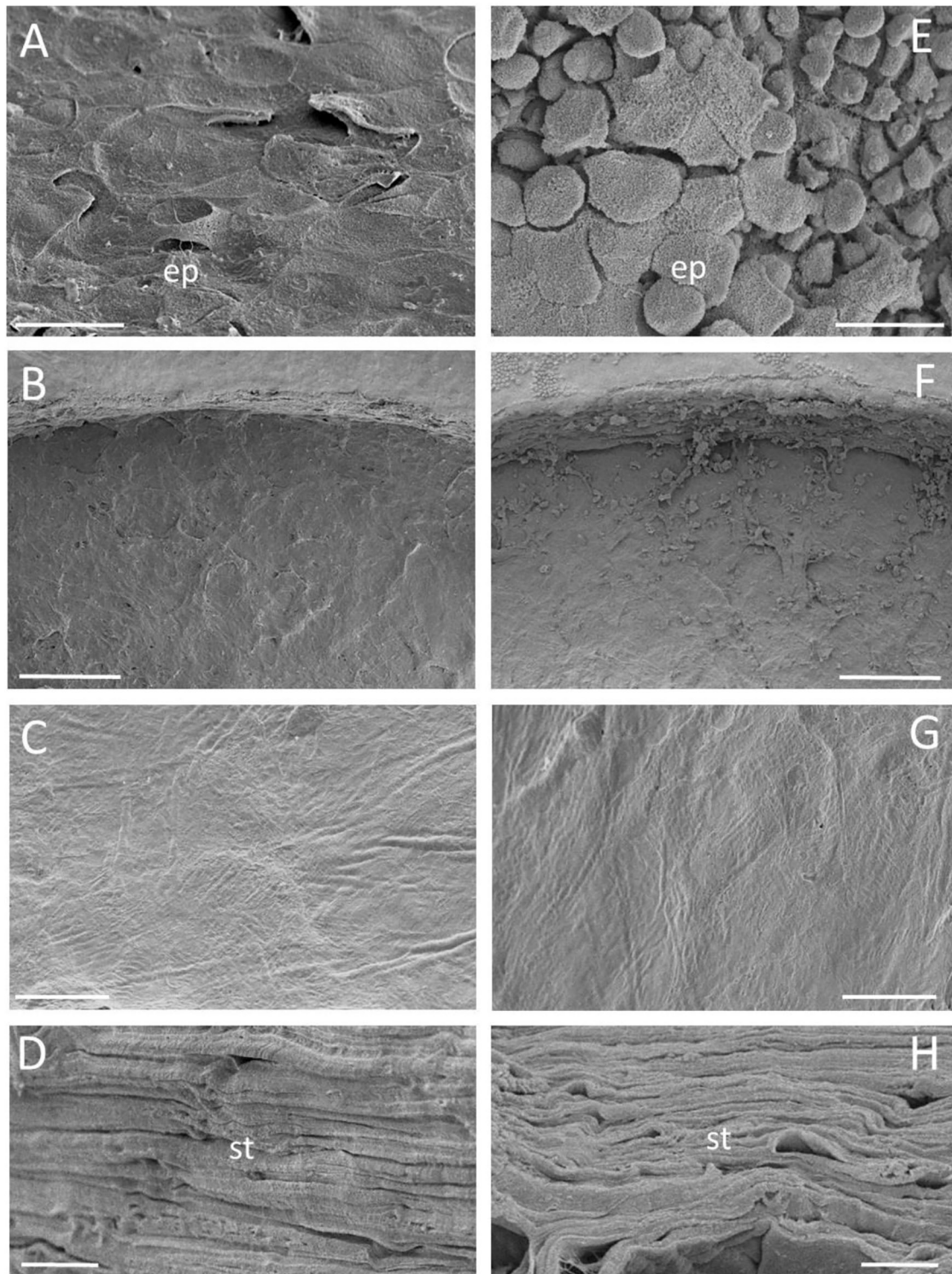


FIGURE 5 | Scanning electron micrographs showing the epithelial surface not involved by laser incision (**A,E**) and the stromal surface after vertical and horizontal cuts in the CTRL (**B–D**) and the rehydrated (**F–H**) cornea. No differences were found between 1.2 and 1.8 μJ pulse energy horizontal incisions. Scale bar: (**A,E**) 20 μm ; (**B,F**) 200 μm ; (**C,G**) 50 μm ; and (**D,H**) 10 μm .

collagen lamellae was observed in the vertical incision in the CTRL (**Figures 5B,C**) and the RHD cornea (**Figures 5E,G**). The lamellar arrangement at the stroma appeared regular and smooth in both the CTRL and the RHD cornea (**Figures 5D,H**, respectively).

DISCUSSION

This study showed that air-dried corneas rehydrated in a solution containing dextran kept their overall corneal architecture, such as the Bowman's layer, endothelial basal membranes, and the organization of the stromal layer. Changes occurred in the spaces in between the collagen lamellae, without major alteration in corneal thickness, while some features at the cellular level appeared lost or altered.

Compared with the fresh cornea, the RHD cornea maintained epithelial basement membrane and the columnar basal epithelial cells only; the endothelial cells layer showed depletion in both fresh and RHD, a condition likely resulting from the manipulation during mounting of the cornea onto the artificial anterior chamber for FSL ablation; and the anatomical structure and vitality of the stromal keratocytes were found to have deteriorated.

The maintenance of integrity of the epithelial basement membrane and Bowman's layer is essential for effective epithelial renewal after grafting, when the donor epithelium is replaced by that of the receiver.

Degeneration of keratocytes with necrotic and apoptotic changes due to the dehydration process is expected. It has been observed with ultrastructural evaluation in dehydrated corneas after lyophilization or cryopreservation, with or without the use of a cryoprotective agent (10, 23). For this reason, it was not necessary to include a control group to compare air-drying with other procedures for dehydrating corneal tissue. However, the absence of vital keratocytes in RHD corneas intended for ALK or reconstructive keratoplasty is not an issue, as migration of host keratocytes into the donor stroma with the promotion of gradual replacement of keratocytes and maintenance of the synthesis of new collagen is expected (24).

Finally, the vitality of endothelial cells is not an issue as only the anterior part of the cornea is intended for transplantation.

We observed no negative effects following rehydration with the *Deswelling-Transport* solution containing dextran, artifacts after dehydration, metallization for TEM and SEM observations, or negative FSL sequelae. What we did find significant for

application in FSL-assisted keratoplasty is that the laser pulse energy needs to be increased compared with fresh corneas used as control to obtain the horizontal stromal incision. Irregularities in the fibril arrangement in the RHD cornea, albeit slight compared with the CTRL cornea, and focal regions of irregularly spaced collagen lamellae induced by dehydration-rehydration may increase Rayleigh scattering resulting in reduced beam quality and depth of penetration (25).

Since the light scattering mechanism is wavelength-dependent, increasing the wavelength could improve incision quality, as our findings show. Clinical systems, such as the Victus 80 KHz FSL use a wavelength of 1,040 nm, which assures satisfactory incision penetration and prevents unwanted thermal side effects. The pulse energy can be adjusted, however, and we improved the horizontal cut by raising it from 0.8 to 1.0 μJ and 1.2 μJ . At the high pulse energies of 1.2 and 1.8 μJ , we observed a remarkably smooth surface without major abnormalities, such as melted-like photo-disrupted collagen fibrils (26); the ultrastructural result ensures optical quality of the graft performed using corneas after dehydration-rehydration, and FSL parameters. A smooth surface generated by an effective FSL-assisted incision provides for an excellent interface and apposition of donor and recipient surfaces, with a clean incision border for suturing a graft-to-host edge in precise apposition. Such broad and close contact between donor and host parenchyma could further benefit keratocyte repopulation of the dehydrated tissue.

Our data show that dehydration by air-drying is associated with minor changes in corneal structure and that following rehydration corneas are a reliable source of tissues for FSL-assisted optical or reconstructive ALK.

Compared with other techniques for dehydrating corneal tissue, air-drying closely resembles the method currently applied for processing amniotic membrane (27), it is simple, cheap, and can be easily incorporated into routine eye bank protocols.

DATA AVAILABILITY STATEMENT

The raw data supporting the conclusions of this article will be made available by the authors, without undue reservation.

AUTHOR CONTRIBUTIONS

All authors listed have made a substantial, direct, and intellectual contribution to the work and approved it for publication.

REFERENCES

- Armitage WJ. Preservation of human cornea. *Transfus Med Hemother*. (2011) 38:143–7. doi: 10.1159/000326632
- Clairhout I, Maas H, Pels E. *European Eye Bank Association Directory Report*. 18th ed. (2010). Available online at: www.europeaneyebanks.org (accessed March 26, 2021).
- dell'Omo R, Filippelli M, Virgili G, Bandello F, Querques G, Lanzetta P, et al. Effect of COVID-19-related lockdown on ophthalmic practice in Italy: a report from 39 institutional centers. *Eur J Ophthalmol*. (2021) 2021:11206721211002442. doi: 10.1177/11206721211002442
- Franch A, Fasolo A, Carraro P, Favarato M, Birattari F, Leon PE, et al. Corneal transplantation during the COVID-19 pandemic: an operational guide. *Eur J Ophthalmol*. (2021) 2021:11206721211006565. doi: 10.1177/11206721211006565
- Canals M, Costa J, Potau JM, Merindano MD, Pita D, Ruano D. Long-term cryopreservation of human donor corneas. *Eur J Ophthalmol*. (1996) 6:234–41. doi: 10.1177/112067219600600302

6. Bonci P, Della Valle V, Bonci P, Lodi R, Russo A. Deep anterior lamellar keratoplasty with dehydrated, 4 °C-stored, and rehydrated lenticules. *Eur J Ophthalmol.* (2011) 21:368–73. doi: 10.5301/EJO.2010.5972
7. Gupta N, Upadhyay P. Use of glycerol-preserved corneas for corneal transplants. *Indian J Ophthalmol.* (2017) 65:569–73. doi: 10.4103/ijo.IJO_56_17
8. Lin HC, Ong SJ, Chao AN. Eye preservation tectonic graft using glycerol-preserved donor cornea. *Eye.* (2012) 26:1446–450. doi: 10.1038/eye.2012.192
9. Tripathi H, Mehdi MU, Gupta D, Sen S, Kashyap S, Nag TC, et al. Long-term preservation of donor corneas in glycerol for keratoplasty: exploring new protocols. *Br J Ophthalmol.* (2016) 100:284–90. doi: 10.1136/bjophthalmol-2015-306944
10. Farias RJM, Sousa LB, Lima Filho AAS, Lourenço ACS, Tanakai MH, Freymuller E. Light and transmission electronic microscopy evaluation of lyophilized corneas. *Cornea.* (2008) 27:791–4. doi: 10.1097/ICO.0b013e31816ed54c
11. Chau GK, Dilly SA, Sheard CE, Roston CK. Deep lamellar keratoplasty on air with lyophilized tissue. *Br J Ophthalmol.* (1992) 76:646–50. doi: 10.1136/bjo.76.11.646
12. Coombes AG, Kirwan JF, Roston CK. Deep lamellar keratoplasty with lyophilized tissue in the management of keratoconus. *Br J Ophthalmol.* (2001) 85:788–91. doi: 10.1136/bjo.85.7.788
13. Daoud YJ, Smith R, Smith T, Akpek EK, Ward DE, Stark WJ. The intraoperative impression and postoperative outcomes of gamma-irradiated corneas in corneal and glaucoma patch surgery. *Cornea.* (2011) 30:1387–91. doi: 10.1097/ICO.0b013e31821c9c09
14. Klop A, Vester M. The effect of repeated freeze-thaw cycles on human muscle tissue visualised by postmortem computed tomography. *Clin Anat.* (2017) 30:799–804. doi: 10.1002/ca.22917
15. Chaurasia S, Das S, Roy A. A review of long-term corneal preservation techniques: relevance and renewed interests in the COVID-19 era. *Indian J Ophthalmol.* (2020) 68:1357–63. doi: 10.4103/ijo.IJO_1505_20
16. Tan DT, Mehta JS. Future directions in lamellar corneal transplantation. *Cornea.* (2007) 26:S21–28. doi: 10.1097/ICO.0b013e31812f685c
17. Singh NP, Said DG, Dua HS. Lamellar keratoplasty techniques. *Indian J Ophthalmol.* (2018) 66:1239–50. doi: 10.4103/ijo.IJO_95_18
18. Adeyolu J, Konstantopoulos A, Mehta JS, Hossain P. Femtolaser-assisted keratoplasty: surgical outcomes and benefits. *J EU Cornea.* (2020) 8:1–13. doi: 10.1016/j.xjec.2020.05.001
19. Pels L, Rijnveld WJ. Organ culture preservation for corneal tissue. Technical and quality aspects. In: Bredehorn-Mayr T, Duncker GIW, Armitage WJ, editors. *Eye Banking*. Basel: Karger (2009). p. 31–46.
20. EUR-Lex. Directive 2004/23/EC of the European Parliament and of the Council of 31 March 2004 on setting standards of quality and safety for the donation, procurement, testing, processing, preservation, storage and distribution of human tissues and cells (2004). Available online at: <https://eur-lex.europa.eu/legal-content/EN/TXT/?uri=celex%3A32004L0023> (accessed September 30, 2020).
21. Camposampiero D, Fasolo A, Saccon G, Donisi PM, Zanetti E, Ponzin D. Gram stain and addition of amphotericin b to improve the microbial safety of human donor corneas. *Cell Tissue Bank.* (2021). doi: 10.1007/s10561-021-09981-1
22. Pedrotti E, Bonacci E, De Rossi A, Bonetto J, Chierigo C, Fasolo A, et al. Femtosecond laser-assisted big-bubble deep anterior lamellar keratoplasty. *Clin Ophthalmol.* (2021) 15:645–50. doi: 10.2147/OPHT. S294966
23. Villalba R, Peña J, Luque E, Villalba JM, Gomez-Villagran JL. Keratocyte migration in human corneas cryopreserved under standard conditions. *Cell Tissue Bank.* (2004) 5:201–4. doi: 10.1007/s10561-004-1091-2
24. Russo A, Bonci P, Leonetti P, Cortecchia S, Nannini R, Bonci P. Long-term dehydrated donor lamella survival in anterior keratoplasty: keratocyte migration and repopulation of corneal stroma. *Cornea.* (2015) 34:1044–51. doi: 10.1097/ICO.0000000000000536
25. Crotti C, Deloison F, Alahyane F, Aptel F, Kowalczyk L, Legeais JM, et al. Wavelength optimization in femtosecond laser corneal surgery. *Invest Ophthalmol Vis Sci.* (2013) 54:3340–9. doi: 10.1167/iovs.12-10694
26. Jumelle C, Hamri A, Egaud G, Maclair C, Reynaud S, Dumas V, et al. Comparison of four methods of surface roughness assessment of corneal stromal bed after lamellar cutting. *Biomed Opt Express.* (2017) 8:4974–86. doi: 10.1364/BOE.8.004974
27. Marsit N, Dwejen S, Saad I, Abdalla S, Shaab A, Salem S, et al. Substantiation of 25 kGy radiation sterilization dose for banked air dried amniotic membrane and evaluation of personnel skill in influencing finished product bioburden. *Cell Tissue Bank.* (2014) 15:603–11. doi: 10.1007/s10561-014-9433-1

Conflict of Interest: The authors declare that the research was conducted in the absence of any commercial or financial relationships that could be construed as a potential conflict of interest.

Publisher's Note: All claims expressed in this article are solely those of the authors and do not necessarily represent those of their affiliated organizations, or those of the publisher, the editors and the reviewers. Any product that may be evaluated in this article, or claim that may be made by its manufacturer, is not guaranteed or endorsed by the publisher.

Copyright © 2021 Pedrotti, Bonacci, Fasolo, De Rossi, Camposampiero, Jones, Bernardi, Merigo, Ponzin, Marchini and Sbarbati. This is an open-access article distributed under the terms of the Creative Commons Attribution License (CC BY). The use, distribution or reproduction in other forums is permitted, provided the original author(s) and the copyright owner(s) are credited and that the original publication in this journal is cited, in accordance with accepted academic practice. No use, distribution or reproduction is permitted which does not comply with these terms.



The Effects of Donor-Recipient Age and Sex Compatibility in the Outcomes of Deep Anterior Lamellar Keratoplasties

Hon Shing Ong^{1,2,3*}, Nathalie Chiam¹, Hla Myint Htoon^{2,3}, Ashish Kumar¹, Anshu Arundhati^{1,3} and Jodhbir S. Mehta^{1,2,3,4*}

¹ Corneal and External Diseases Department, Singapore National Eye Centre, Singapore, Singapore, ² Singapore Eye Research Institute, Singapore, Singapore, ³ Duke-NUS Medical School, Singapore, Singapore, ⁴ School of Material Science and Engineering, Nanyang Technological University, Singapore, Singapore

OPEN ACCESS

Edited by:

Mohit Parekh,
University College London,
United Kingdom

Reviewed by:

Vishal Jhanji,
University of Pittsburgh, United States
Mehran Zarei Ghanavati,
Tehran University of Medical
Sciences, Iran

*Correspondence:

Jodhbir S. Mehta
jodmehta@gmail.com
Hon Shing Ong
honshing@gmail.com

Specialty section:

This article was submitted to
Ophthalmology,
a section of the journal
Frontiers in Medicine

Received: 25 October 2021

Accepted: 20 December 2021

Published: 27 January 2022

Citation:

Ong HS, Chiam N, Htoon HM, Kumar A, Arundhati A and Mehta JS (2022) The Effects of Donor-Recipient Age and Sex Compatibility in the Outcomes of Deep Anterior Lamellar Keratoplasties. *Front. Med.* 8:801472. doi: 10.3389/fmed.2021.801472

Purpose: Corneal transplantations are the commonest allogenic transplant surgeries performed worldwide. Transplantable grade donor cornea is a finite resource. There is thus an impetus for eye banks to optimize the use of each harvested cornea, and clinicians to minimize the risks of graft rejection and failure. With better survival and lower rejection rates, anterior lamellar keratoplasty has gained popularity as an alternative technique to full-thickness penetrating keratoplasty, for the treatment of corneal stromal diseases. This study evaluated the effects of donor-recipient age- and sex-matching on the outcomes of eyes that had undergone deep anterior lamellar keratoplasty (DALK) surgeries.

Design: Observational cross-sectional study (national corneal graft registry data).

Subjects: All DALK surgeries performed in a tertiary ophthalmic hospital over an 11-year period.

Methods: To analyse the effects of donor-recipient sex-matching, transplantations were classified as “presumed H-Y incompatible” (male donor to female recipient) or “presumed H-Y compatible” (all other donor-recipient sex combinations). For age-matching, differences in donor and recipient ages were calculated. Cox proportional hazards regressions were used to evaluate the influence of donor-recipient sex-matching and age-matching on graft failure and rejection.

Main Outcome Measures: Rates of graft failure and rejection within each group.

Results: 401 eyes were included. 271 (67.6%) transplants were presumed H-Y compatible. 29 (7.2%) grafts failed and 9 (2.2%) grafts rejected. There were trends of lower hazard ratios (HRs) in graft failure and rejection in the presumed H-Y compatible group [HRs: 0.59 (95% CI 0.20–1.77, $p = 0.34$) and 0.93 (95% CI 0.22–3.89, $p = 0.926$), respectively]. Median difference in age between recipients and donors was 15.0 years (IQR –2.8–34.3). The HRs of graft failure and rejection were not influenced by donor-recipient age [HRs per 1-year increase in age difference: 0.995 (95% CI 0.98–1.01, $p = 0.483$) and 1.01 (95% CI 0.99–1.03, $p = 0.394$), respectively].

Conclusion: In eyes that had undergone DALK surgeries, no significant influence of donor-recipient sex- or age-matching on graft rejection and failure was observed. Without strong evidence and the limitations of obtaining sample sizes required for an adequately powered study, the benefits of sex- and age-matching of donors and recipients during graft allocation for DALK surgeries is currently inconclusive.

Keywords: corneal transplantation, keratoplasty, eye banking, anterior lamellar keratoplasty, HLA compatibility, graft rejection, graft survival, graft failure

INTRODUCTION

Corneal transplantations are the most common allogenic transplant surgeries performed worldwide (1, 2). A global report indicated that in 2012, a total of 283 530 donor corneas were harvested annually and stored in 742 eye banks worldwide (3). Of these, 184,576 were used to perform corneal transplantation surgeries in 116 countries (3). Similarly, the Eye Bank Association of America reported that in 2018, of the 133,576 donor corneas procured by 57 eye banks in the United States, 85,441 were used to perform transplantation surgeries (2). As the cornea is thought to be immunologically privileged, (4) compared to other forms of solid organ transplantations, corneal tissue allografts are associated with comparatively lower risks of immunological rejection and less requirements for prolonged systemic immunosuppression (5–11).

Penetrating keratoplasty (PKP) is a full-thickness corneal transplantation technique where all layers of the corneas are replaced. Since its introduction in 1905, for more than a century, PKP has been the predominant procedure for the treatment of visual loss from corneal diseases. Over the past two decades however, there has been a paradigm shift in the surgical treatment of corneal diseases to perform selective tissue transplantation i.e., anterior lamellar keratoplasty (ALK) or endothelial keratoplasty (EK), where only diseased layers of the cornea are replaced (2, 9, 12–14). In ALK, the anterior diseased layers of the recipient's cornea are replaced (15); in EK, a posterior lamellar keratoplasty technique, the diseased corneal endothelium of the recipient is replaced (16). These two “lamellar” keratoplasty techniques, have been shown to achieve lower risks of immunological graft rejection and improved graft survival rates (9, 17–22). With these advantages, lamellar keratoplasties have thus gradually been adopted as preferred corneal transplantation techniques in various institutions (2, 9, 13). Nevertheless, graft rejection and failure do occur following all types of corneal transplantations (23, 24).

With only one in 70 of the global demands of corneal transplantations being met, there is a shortage of suitable donor corneas (3). Indeed, transplantable grade donor corneal tissue is a finite and scarce resource. There is therefore a strong impetus for eye banks to optimize the use of each harvested donor corneal tissue, and clinicians to minimize the risks of graft rejection and failure. Attempts to lower the risks of graft rejection can begin pre-operatively during donor tissue allocation. In allogeneic solid organ transplantations, donor-recipient human

major histocompatibility antigens / human leukocyte antigens (HLA) matching is one of the most important considerations in donor tissue allocations. This is particularly important for kidney and bone marrow transplantations (25). On the contrary, HLA matching is not routinely performed in corneal transplantations, as existing evidence suggests that this practice does not confer a significant graft survival benefit (23, 26–29). Some studies have, however, investigated the effects of donor-recipient age- or sex-matching in corneal graft allocations (30–34). In age-matching, recipients are assigned grafts from donors who are of the same age group. This is commonly practiced in many eye banks, (30, 35) despite a lack of evidence on whether grafts from older donors perform as well as grafts from younger donors in young recipients, and vice versa (30). In sex-matching, donor corneal tissues are allocated to recipients of the same sex (32, 34, 36). Additionally, a further subtype of sex-matching is H-Y compatibility. The H-Y antigen, which is HLA-A1 restricted, is expressed by the Y chromosome and is found in A1-positive males (36–39). H-Y incompatible grafts refer to grafts from A1-positive male donors being transplanted into female recipients or into A1-negative male recipients, whilst H-Y compatible grafts refer to the other possible donor-recipient combinations (i.e., A1-positive male donor grafts to A1-positive male recipients, female donor grafts to female or male recipients).

Published literature on donor-recipient age or sex compatibility has thus far mainly been focused on the outcomes of PKP procedures (31, 34, 36, 40–43). Studies on PKP have reported beneficial effects of sex or H-Y matching in lowering the risks of graft rejection and improving graft survival (31, 34, 36). Nevertheless, the current evidence for donor-recipient sex-matching is still considered equivocal, as several other studies have failed to show significant benefit in sex- or H-Y antigen matching (40, 42, 43). Such varying results have been attributed to differences in study designs, diversities in ethnic populations, or inadequate sample sizes (31, 34, 36, 40, 42, 43). With the shift away from performing PKP procedures, investigators have set out to evaluate the effects of sex-matching in eyes undergoing lamellar keratoplasties, in particular, EKs (32, 33). However, the evidence of donor-recipient sex-matching in EK has also so far been inconsistent, (32–34) with some studies observing lower rates of graft survival with male donors (33) but others failing to show similar associations (32).

Anterior lamellar keratoplasty (ALK), the other selective tissue transplant procedure, has gained popularity as an alternative to PKP to treat corneal stromal diseases (15, 17, 44). Examples

of such diseases include keratoconus, corneal dystrophies, or stromal scars caused by a variety of insults (e.g., infection, trauma). In ALK, the recipient's own Descemet membrane (DM) and corneal endothelium are retained. As endothelial graft rejection is the most commonly encountered form of immunological rejection following corneal transplantations, the observed rates of graft rejection in ALK are therefore significantly lower compared to PKP or EK (9, 19, 22, 44). Despite being less common, immunological rejections, namely epithelial, subepithelial, or stromal rejections, still do occur following ALK (22). Stromal rejection rates after ALK have been reported to be ~5% but can be as high as 25% within the first 18 months following transplantation (45–47). Nonetheless, the significance of donor-recipient age- or sex- matching specifically for ALK surgery, has yet to be explored. Using data from the Singapore national transplant registry, we evaluated the effects of donor-recipient age- and sex- matching on the surgical outcomes of eyes that had undergone deep anterior lamellar keratoplasty (DALK) surgeries.

METHODS

Study Population

This was a cross-sectional analysis of consecutive DALK surgeries performed in the Singapore National Eye Center from 2004 to 2015. Data was obtained from the Singapore Corneal Transplant Study (SCTS) database. This national transplant registry database is maintained by the Singapore Eye Bank where the surgical outcomes of all corneal transplants performed in Singapore are prospectively collected. The study protocol adhered to the tenets of the Declaration of Helsinki and is approved by the SingHealth Centralized Institutional Review Board (CIRB reference: 2018/2688).

The Singapore National Eye Center is a tertiary referral center that performs approximately 80% of corneal transplants in Singapore. The DALK surgeries were performed by a group of corneal surgeons in our center, including trained corneal specialists and corneal fellows-in-training. All surgeons used the same techniques of DALK. DALK surgeries were performed using either the modified big bubble technique or a pre-Descemetic manual layer-by-layer dissection technique (48). Post-operatively, topical steroids (*Guttae* prednisolone acetate 1% or Dexamethasone 0.1%) together with topical fluoroquinolone antibiotics (*Guttae* levofloxacin 0.5% or moxifloxacin 0.5%) were administered at 3-hourly intervals and gradually tapered over 6–8 months. Sutures were removed between post-operative month 4–18, guided by visual acuities and corneal astigmatism.

As is standard practice at the Singapore Eye Bank, donor-recipient ages were matched as closely as possible, where recipients were allocated corneal tissues from donors of approximately the same age groups. No donor-recipient matching for sex was performed in the allocation of corneal grafts to the recipients. In our study, we only included cases of DALKs performed for optical indications. As DALKs that are performed for tectonic or therapeutic reasons tend to have poorer outcomes compared to grafts performed for optical indications, (49) these

cases were excluded to avoid adding unnecessary heterogeneity into the data. For eyes that had undergone repeat grafts, the outcome data of the first (primary) corneal grafting of these eyes were analyzed.

Data Collected and Primary Outcomes

Pre-operative variables collected included age and sex of both recipients and donors. Recipient eye characteristics collected included indications for transplant surgeries, co-existing ocular diseases, and the presence of risk factors for graft failure or rejection (such as cornea vascularisation, ocular surface disease, active ocular inflammation, and glaucoma). High-risk grafts were defined as cases with at least one of the aforementioned risk factors for graft failure or rejection. Post-operative data collected included the presence and recorded date of occurrence of graft rejection, graft failure, and any other post-operative complications. From this data, the duration of rejection-free period and graft survival were extrapolated. Graft rejection was defined as corneal oedema and the presence of epithelial or stromal inflammation in a graft that was previously clear (50). Graft failure was defined as persistent graft oedema that compromised vision for a minimum of three consecutive months (50).

Statistical Analysis

All statistical analyses were performed using Stata version 15.0 (StataCorp, College Station, Texas, USA). The unit of analysis was outcomes for eyes. To account for the cluster effect of within-patient inter-eye correlations in patients who had DALK surgeries performed in both eyes, cluster-correlated analysis was performed. The primary outcomes were graft rejection and graft failure. To analyse the effects of donor-recipient age-matching on graft rejection and failure, the donor-recipient age gap was calculated. Donor age gap = age of recipient – age of donor in years. To analyse the effects of donor-recipient sex-matching and presumed H-Y compatibility on graft rejection and failure, we looked at presumed H-Y incompatible grafts [male donor to female recipient (M-F)] and compared them to presumed H-Y compatible grafts [male donor to male recipient (M-M), female donor to male recipient (F-M), female donor to female recipient (F-F)]. The term “presumed compatibility” was used as the H-Y antigen is HLA-A1 restricted; it is only expressed by the Y-chromosome in A1-positive males (36–39) and the frequencies of the A1 allele varies amongst different ethnic populations (51).

Kaplan-Meier curves of graft survival time and rejection-free survival time were generated; the differences between presumed H-Y compatible and incompatible groups were also assessed with log-rank tests. Additionally, Cox proportional hazards regression were used to evaluate the influence of age- and sex-matching on the hazards of graft rejection and failure. Univariable and multivariable analyses were also conducted. The multivariable cox regression model was adjusted for donor age, recipient age, donor sex, recipient sex, indications of graft, and whether the graft was considered low or high risk. Using the observed rates of events and hazard ratios determined in this study, Cox regression power analyses were used to estimate the sample sizes required to achieve sufficient power (80%) to show a significant difference if

any, in rates of graft survival and graft rejection. A $p < 0.05$ was considered statistically significant.

RESULTS

A total of 540 DALK surgeries were performed over the 11-year study period. Of these, 56 surgeries were performed for tectonic or therapeutic indications and were excluded. Of the 484 surgeries performed for optical indications, 24 were repeat transplants; no follow-up data were available in 59 cases. Thus, a total of 401 eyes that underwent DALK surgeries for optical indications were included in our analyses. The characteristics of our donor and recipient population is reported in **Table 1**. The most common indications for DALKs were keratoconus ($n = 167$, 41.6%), corneal dystrophies ($n = 42$, 10.5%), cornea scar from infective keratitis ($n = 50$, 12.5%), and cornea scar from interstitial keratitis ($n = 22$, 5.5%). The remaining cases were performed for less common indications such as corneal scar from chemical injuries or ocular surface diseases. Amongst the recipients, the median age was 33.3 (IQR: 22.8–53.9) years and 192 (47.9%) were female. Amongst the donors, the median age was 55.0 (IQR: 40.0–66.0) years and 126 (31.4%) were female. The median difference in age between recipients and donors was 15.0 years (IQR: –2.8–34.3). With regard to donor-recipient sex-matching, 130 (32.4%), 145 (36.2%), 64 (15.9%), and 62 (15.5%) were M-F, M-M, F-M, and F-F, respectively. Ninety-six grafts (23.9%) were classified as high risk grafts.

Effects of Sex-Matching on Graft Survival

29 (7.2%) of DALK grafts had failed. Of the grafts that failed, the median time to graft failure was 0.38 years (IQR 0.15–0.84). Presumed H-Y incompatible grafts (M-F grafts) showed a trend of worse survival compared to presumed H-Y compatible grafts (M-M, F-M, F-F), although this was not statistically significant ($p = 0.345$) (**Figure 1**).

Effects of Sex-Matching on Graft Rejection

Rejection episodes were recorded in 9 (2.2%) grafts. Of the grafts that suffered rejection, the median time to rejection was 1.1 years (IQR 0.93–3.0). There was no significant difference in rejection-free duration in presumed H-Y incompatible grafts (M-F grafts) compared to presumed H-Y compatible grafts (M-M, F-M, F-F) ($p = 0.439$) (**Figure 2**).

Table 2 presents the hazard ratios (HR) of graft failure and rejection in our analyses of donor-recipient sex-matching. The HRs of graft failure were lower in presumed H-Y compatible grafts (M-M, F-M, F-F grafts) compared to presumed H-Y incompatible grafts (M-F grafts), although this was not statistically significant in both univariable and multivariable analyses ($p = 0.329$ and $p = 0.347$, respectively). Similarly, there were trends that the HRs of graft rejection were lower in presumed H-Y compatible grafts (M-M, F-M, F-F grafts) compared to presumed H-Y incompatible grafts (M-F grafts), although this was not statistically significant in both univariable and multivariable analyses ($p = 0.842$ and $p = 0.926$, respectively). **Table 3** presents the HR of graft failure and rejection in our analyses of donor-recipient age-matching. The

donor-recipient differences in age did not have a significant influence on graft failure or rejection in both univariable and multivariable analyses.

DISCUSSION

In this study, we evaluated the effects of donor-recipient sex- and age-matching on the risks of graft failure and rejection in eyes that had undergone DALK surgeries. In our cohort of 401 consecutive DALK grafts performed over an 11-year period (2004–2015), there were trends of improved graft survival in presumed H-Y compatible grafts (**Figure 1**). Through univariable and multivariable regression models on risks of graft rejection and failure, we also showed trends of a protective effect when presumed H-Y compatible grafts were used (**Table 2**). Overall however, our results did not achieve statistical significance. When we evaluated donor-recipient age-matching in our series, such trends seen in sex-matching on graft rejection and survival, were not observed.

A potential graft survival benefit of donor-recipient sex-matching was first reported by Völker-Dieben et al. (31). Reporting on the clinical outcomes of 539 PKP procedures, the authors observed that female donor corneas had significantly better one-year graft survival in female recipients compared to male recipients (31). More recently, interest in the concept of sex-matching for corneal transplantations was renewed after two studies independently reported lower rates of graft rejection and failure amongst donor-recipient sex-matched or H-Y antigen compatible transplantations (34, 36). In a series evaluating 229 HLA-A1 donor positive keratoplasties, Bohringer et al. showed a significant benefit in rejection-free graft survival in H-Y compatible transplantations. In a subsequent UK based study which included 18,171 patients who had undergone predominantly PKP procedures, Hopkinson et al. showed that in certain pathologies, such as Fuchs' endothelial dystrophy and keratoconus, patients receiving biological sex-mismatched donor tissues were at greater risk of graft rejection and failure (34).

Not all studies have reported similar beneficial effects of sex-matching (40, 42, 43). Even in the initial 1982 series by Völker-Dieben et al. showing graft survival benefits of female to female transplantations, male donors to male or female recipients did not influence graft survival (31). Furthermore, when the same investigators incorporated a larger number of grafts in their 1987 report, sex-matching no longer had a significant association with graft failure (43). Similarly, a Japanese study of 396 eyes that had undergone PKP procedures found no additional benefit in lowering the risks of rejection with sex-matching (42). In another study based on a Korean population, their presumed H-Y compatible group was not associated with improved rejection-free PKP graft survival (40).

The evidence of sex-matching in lamellar keratoplasties, is even much less clear. In 2017, a Swedish based study investigating 1,789 EK procedures showed that male donor sex was associated with lower rates of graft survival in a univariate regression model (33). Although the authors explained their finding through immunological mechanisms, they believed that other

TABLE 1 | Descriptive data of both donors and recipients.

	Entire study population	Presumed HY Incompatible (M-F)	Presumed HY compatible (M-M, F-M, F-F)
Number of eyes	401	130	271
Graft failure <i>n</i> (%)	29 (7.2)	11 (8.5)	18 (6.6)
Graft rejection <i>n</i> (%)	9 (2.2)	3 (2.3)	6 (2.2)
Donor demographic characteristics*			
Age, years median (IQR)	55 (40–66)	53 (36–63)	56 (42–68)
Female gender, <i>n</i> (%)	126 (31.4)	–	–
Race, <i>n</i> (%)	389	128	261
Chinese	73 (18.8)	24 (18.8)	49 (18.8)
Malay	7 (1.8)	2 (1.6)	5 (1.9)
Indian	46 (11.8)	18 (14)	35 (13.4)
Others	263 (67.6)	84 (65.6)	172 (65.9)
Recipient demographic characteristics†			
Age, years median (IQR)	33.3 (22.8–53.9)	35.6 (23.5–55.7)	32.9 (22.5–53)
Female gender, <i>n</i> (%)	192 (47.9)	–	–
Race, <i>n</i> (%)			
Chinese	148 (36.9)	52 (40)	96 (35.4)
Malay	57 (14.2)	20 (15.4)	37 (13.7)
Indian	73 (18.2)	21 (16.1)	52 (19.2)
Others	123 (30.7)	37 (28.5)	86 (31.7)
Recipient ocular characteristics† Low or high-risk graft, <i>n</i> (%)			
Low risk	305 (76.1)	97 (74.6)	208 (76.8)
High risk	96 (23.9)	33 (25.4)	63 (23.2)
Optical indication for corneal transplant, <i>n</i> (%)			
Keratoconus	167 (41.6)	47 (36.2)	120 (44.3)
Corneal dystrophies	42 (10.5)	15 (11.5)	27 (10.0)
Scar from previous infective keratitis	50 (12.5)	22 (16.9)	28 (10.3)
Scar from previous interstitial keratitis	22 (5.5)	7 (5.4)	15 (5.5)
Miscellaneous (e.g., scars from other pathologies)	120 (29.9)	39 (30.0)	81 (29.9)
Donor-recipient matching characteristics†			
Donor-recipient sex matching (4 groups), <i>n</i> (%)			
Male to Female (M-F)	130 (32.4)	130 (100.0)	0
Male to Male (M-M)	145 (36.1)	0	145 (53.5)
Female to Male (F-M)	64 (16.0)	0	64 (23.6)
Female to Female (F-F)	62 (15.5)	0	62 (22.9)
Difference in donor vs. recipient age	15.0 (–2.8–34.3)	10.8 (–6.9–30.1)	17.3 (0.14–35.5)

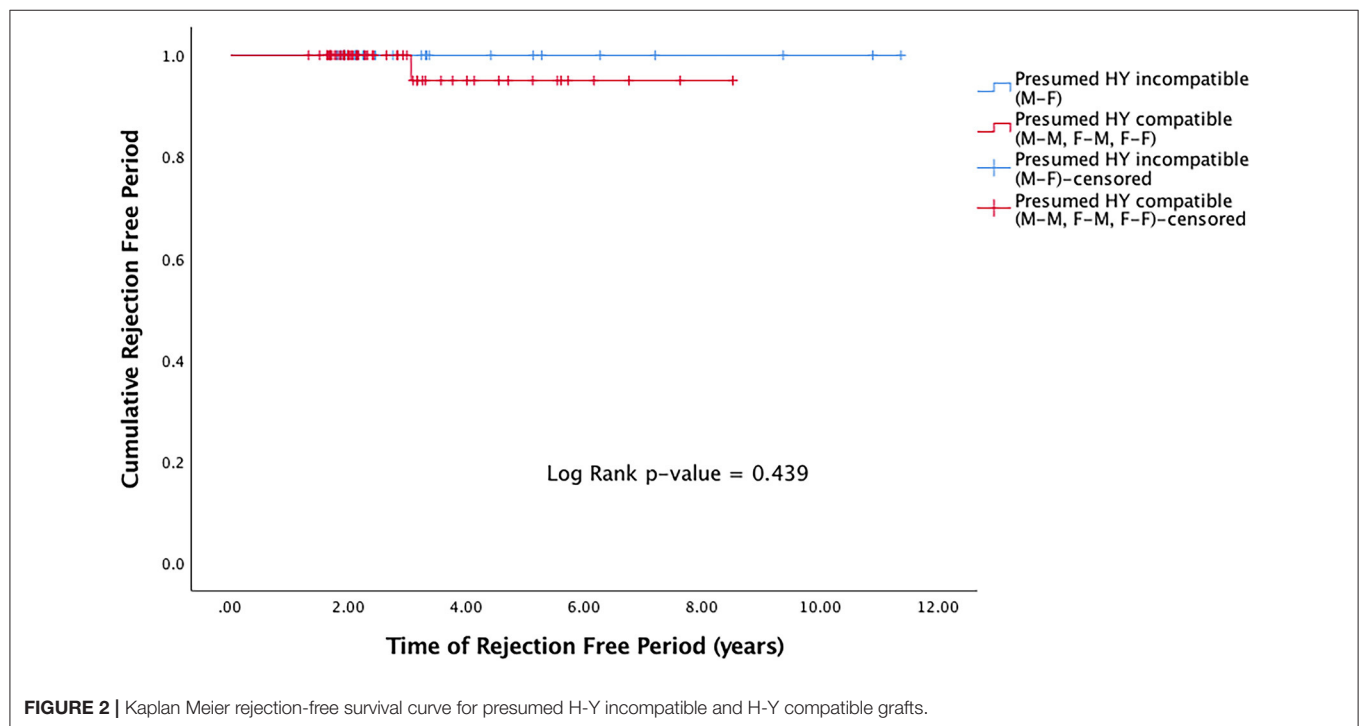
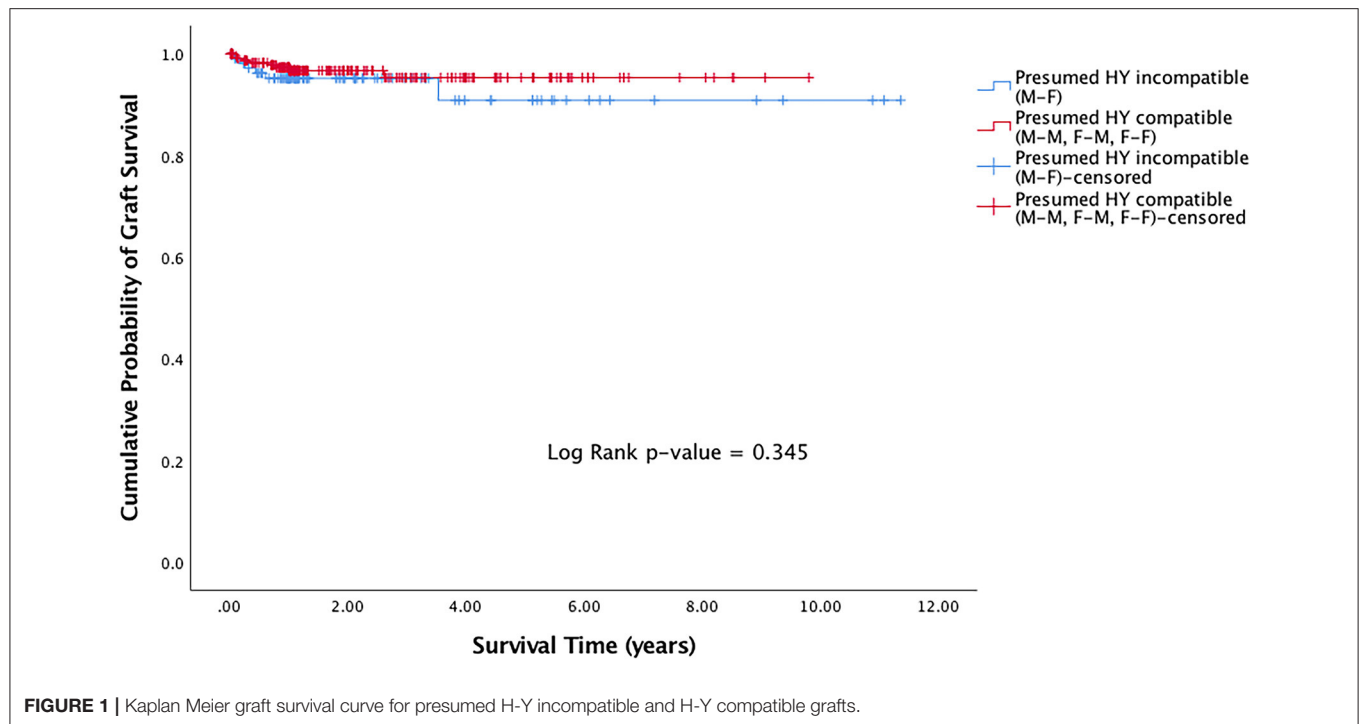
*Data are presented as median (interquartile range, IQR) or *n* (%) as appropriate.

†Eye-specific variables.

undetermined mechanisms may also be involved (33). Studies have reported that adrenaline can affect corneal endothelial function (52, 53). Unintentional injuries (which includes trauma from falls, burns, road traffic accidents etc.) are associated higher systemic release of adrenaline, and account for more male deaths (7.6%) (54) compared to female deaths (4.4%) (55); this could thus potentially explain the lower EK graft survival rates observed with male donors (33). Nevertheless, when covariate models were applied in the Swedish study, sex-matching failed to be predictive of graft failure (33). Furthermore, donor sex was not associated with risks of graft rejection (33). Similarly, in a 2018 study reporting outcomes of over 2,000 EK procedures, the investigators failed to show significant effects of reducing graft rejection and improving graft survival in sex-matched

transplantations (32). Our study, being the first to investigate the effects on anterior lamellar procedures alone, similarly supports the other studies on EK, in the notion that in lamellar surgery, sex-mismatching is less of a concern.

Several factors may explain why the beneficial effects of sex-matching have been observed in studies involving PKP but not in studies of lamellar keratoplasties, such as ours. It has been well-reported that the risks of graft rejection and failure, are significantly lower in lamellar keratoplasty procedures compared to full-thickness PKPs (9, 17–22). Depending on the pre-operative diagnoses for performing PKP, five-year graft survival rates have been reported to be as low as 21% and graft rejection rates to be as high as 68% in some series (56, 57). As a result of higher incidences of graft rejections and failures in PKP



procedures, the effects of sex-matching are therefore more likely to be observed. In our study of DALK surgeries, the rates of graft failure and rejection were low at 7.2 and 2.2%, respectively. A much larger sample size would thus be required to show a

beneficial effect, if any, of sex-matching in lamellar keratoplasties. It would indeed be beyond the practicality of most institutions to obtain the required number of lamellar transplantations to show statistical significance. To illustrate this, with our current

TABLE 2 | Associations of donor-recipient sex-matching with graft failure and rejection.

	Total	Events	Univariable model			Multivariable model ^a		
	N	N (%)	HR	95% CI	P	HR	95% CI	P
Graft failure								
Donor-recipient sex-matching								
Presumed HY-incompatible	130	11 (8.5)	Reference	—	—	Reference	—	—
Presumed HY-compatible	271	18 (6.6)	0.59	0.21–1.69	0.329	0.59	0.20–1.77	0.347
Graft rejection								
Donor-recipient sex-matching								
Presumed HY-incompatible	130	3 (2.3)	Reference	—	—	Reference	—	—
Presumed HY-compatible	271	6 (2.2)	0.87	0.21–3.56	0.842	0.93	0.22–3.89	0.926

HR, hazards ratio; CI, confidence interval.

^aMultivariable model adjusts for high risk graft, indications of graft, age of donor, and age of recipient.

TABLE 3 | Associations of donor-recipient age-matching with graft failure and rejection.

	Total	Events	Univariable model			Multivariable model ^a		
	N	N (%)	HR	95% CI	P	HR	95% CI	P
Graft failure								
Difference in donor vs. recipient age, per 1-year increase	401	29 (7.2)	0.994	0.98–1.01	0.453	0.995	0.98–1.01	0.483
Graft rejection								
Difference in donor vs. recipient age, per 1-year increase	401	9 (4.2)	1.01	0.99–1.02	0.302	1.01	0.99–1.03	0.394

HR, hazards ratio; CI, confidence interval.

^aMultivariable model adjusts for high risk graft, indications of graft, sex of donor, and sex of recipient.

observed rates of events and hazard ratios (Table 2), using Cox regression power analyses (α -level = 0.05), the numbers of DALK surgeries required for the study to have 80% power to show significant effects of sex-matching (aiming to detect a 50% difference between the groups), if any, on rates of graft survival and graft rejection are 25,951 and 596,034, respectively (58). Obtaining such numbers of performed DALK surgeries would not be possible, even when multicentred graft registry data are used (7, 34). This limitation was also observed in the large UK-based study using national registry data reported by Hopkinson et al. (34). Although authors demonstrated that the protective effects of H-Y antigen compatibility were significant for PKPs, they acknowledged that the benefits of donor-recipient matching in lamellar keratoplasties (ALK and EK surgeries) were not conclusive due to inadequate numbers (34). From the report however, the overall numbers of lamellar keratoplasties included in their study were unclear.

Another factor explaining the disparity of results between studies evaluating the effects of sex-matched corneal transplantations relates to H-Y compatibility and the prevalence of male individuals who are HLA-A1 positive (31, 34, 36). The H-Y antigen, is expressed by the Y chromosome and is found in HLA-A1 positive male individuals (36–39). All female recipients and A1 negative male recipients may thus theoretically develop an alloimmune response against the H-Y antigens when they receive grafts from A1 positive male donors (59). As H-Y antigens are expressed in A1-positive males, donor-recipient sex-matching has thus been used as a surrogate for H-Y

antigen compatibility, as opposed to expensive tests required to detect other major and minor histocompatibility antigens. Indeed, studies have assumed H-Y antigen incompatibility as “all male donor grafts to female recipients”, with all the other possible donor-recipient combinations as H-Y compatible (40, 42). However, this may not be entirely accurate (60). Racial heterogeneity of a population is a confounder when comparing between different datasets. Indeed, the frequencies of the A1 allele varies between different geographical and ethnic populations (51). For example, in our Singapore cohort comprising mostly of patients with Chinese, Malay, and Indian origins, the frequencies of the A1 allele could range between 0.7 and 28.8% (using Singapore-Malaysia allele frequency data), with the prevalence being lower in individuals of Chinese origins and higher in those of Indian origins (51). This may explain why studies investigating donor-recipient sex-matching as a surrogate for presumed H-Y compatibility have failed to show significant effects in graft rejection and survival rates (40, 42, 60). This is especially the case in populations where the frequencies of A1 allele are low (40, 42, 51). Many of the transplants reported in these studies are therefore in fact H-Y compatible.

In addition to sex- or H-Y matching for DALK grafts, we also explored the hypothesis that age-matching may affect graft failure or rejection. It is the practice of many cornea eye banks and surgeons to match donor and recipient grafts for age (24). This practice originated in the early days of penetrating keratoplasties, as it was hypothesized that younger donor grafts had better endothelial cell counts (compared to older donor grafts) and

hence should be reserved for younger recipients with longer average life expectancies (61). In our study, we found that older recipient age and older donor age were in fact both associated with lower hazards of graft rejections. However, the difference between donor and recipient age was not associated with the hazards of graft rejection or failure (Table 3). The Cornea Donor study has also investigated the effect of donor-recipient age differences on graft outcomes of penetrating keratoplasty (61). Similarly, they did not observe any adverse graft outcomes when donor-recipient ages were not matched (61). In a study on EK, donor age was also not found to be an independent risk factor for graft survival (33). Thus, there appears to be a lack of evidence of donor-recipient age matching in graft allocation.

Our study has its limitations. Firstly, the retrospective nature of our data limits any inferences of causality, with respect to age- and sex-matching and risks of graft failure and rejection, for which a randomized clinical trial would have served best. Secondly, as mentioned above, because of our low rates of graft failure and rejection, a larger sample size is required to have sufficient power to detect significance differences between matched and unmatched groups. In this study, we used data obtained from the Singapore national transplant registry, where the surgical outcomes of all corneal transplantations performed in Singapore are prospectively collected. This allowed us to obtain data on the 401 DALKs cases performed for optical indications over an 11-year period. As the surgical technique of DALK is challenging and not performed by all corneal surgeons, this large sample size of DALK cases will not be easily replicated by many other institutions. Obtaining the required numbers through other study designs, such as a randomized controlled trial, would not have been possible. Future work may involve combining data from different corneal graft registries to increase the sample size to achieve sufficient statistical power. However, as indicated in

our power analyses, obtaining the required number of cases may be difficult even when such registry data are combined.

In conclusion, in our large cohort, in eyes that had undergone DALK surgeries, no significant influence of donor-recipient sex- or age-matching on graft rejection and failure was observed. This adds to the current literature which has thus far been focused on PKP and EK procedures. Without strong evidence and the limitations of obtaining numbers required for an adequately powered study, the benefits of sex- and age-matching of donors and recipients during graft allocation for DALK surgeries remains inconclusive.

DATA AVAILABILITY STATEMENT

The raw data supporting the conclusions of this article will be made available by the authors, without undue reservation.

ETHICS STATEMENT

This study was reviewed and approved by SingHealth Centralized Institutional Review Board.

AUTHOR CONTRIBUTIONS

HO, AA, and JM: conceptualization and supervision. HO, NC, HH, and AK: data curation, formal analysis, investigation, and methodology. HO, NC, and JM: writing draft, review, and editing. All authors approved the manuscript.

FUNDING

This work was partially supported by the Lee Foundation SingHealth Transplant Grant (No. SHTX/LFG/001/2019).

REFERENCES

- Gaum L, Reynolds I, Jones MN, Clarkson AJ, Gillan HL, Kaye SB. Tissue and corneal donation and transplantation in the UK. *Br J Anaesth*. (2012) 108(Suppl. 1):i43–7. doi: 10.1093/bja/aer398
- EBAA. *Eye Banking Statistical Report*. (2018). Available online at: <https://restoresight.org/what-we-do/publications/statistical-report/> (accessed June 15, 2021).
- Gain P, Jullienne R, He Z, Aldossary M, Acquart S, Cognasse F, et al. Global survey of corneal transplantation and eye banking. *JAMA Ophthalmol*. (2016) 134:167–73. doi: 10.1001/jamaophthalmol.2015.4776
- Chong EM, Dana MR. Graft failure IV. Immunologic mechanisms of corneal transplant rejection. *Int Ophthalmol*. (2008) 28:209–22. doi: 10.1007/s10792-007-9099-9
- Waldock A, Cook SD. Corneal transplantation: how successful are we? *Br J Ophthalmol*. (2000) 84:813–5. doi: 10.1136/bjo.84.8.813
- Tan DT, Dart JK, Holland EJ, Kinoshita S. Corneal transplantation. *Lancet*. (2012) 379:1749–61. doi: 10.1016/S0140-6736(12)60437-1
- Coster DJ, Lowe MT, Keane MC, Williams KA, Australian Corneal Graft Registry C. A comparison of lamellar and penetrating keratoplasty outcomes: a registry study. *Ophthalmology*. (2014) 121:979–87. doi: 10.1016/j.ophtha.2013.12.017
- Dickman MM, Peeters JM, van den Biggelaar FJ, Ambergen TA, van Dongen MC, Kruit PJ, et al. Changing practice patterns and long-term outcomes of endothelial versus penetrating keratoplasty: a prospective dutch registry study. *Am J Ophthalmol*. (2016) 170:133–42. doi: 10.1016/j.ajo.2016.07.024
- Tan D, Ang M, Arundhati A, Khor WB. Development of selective lamellar keratoplasty within an asian corneal transplant program: the Singapore corneal transplant study (an American ophthalmological society thesis). *Trans Am Ophthalmol Soc*. (2015) 113:T10.
- Jones MN, Armitage WJ, Ayliffe W, Larkin DE, Kaye SB, Group NOTA, et al. Penetrating and deep anterior lamellar keratoplasty for keratoconus: a comparison of graft outcomes in the United Kingdom. *Invest Ophthalmol Vis Sci*. (2009) 50:5625–9. doi: 10.1167/iops.09-3994
- Greenrod EB, Jones MN, Kaye S, Larkin DE, National Health Service B, Transplant Ocular Tissue Advisory G, et al. Center and surgeon effect on outcomes of endothelial keratoplasty versus penetrating keratoplasty in the United Kingdom. *Am J Ophthalmol*. (2014) 158:957–66. doi: 10.1016/j.ajo.2014.07.037
- Park CY, Lee JK, Gore PK, Lim CY, Chuck RS. Keratoplasty in the United States: a 10-year review from 2005 through 2014. *Ophthalmology*. (2015) 122:2432–42. doi: 10.1016/j.ophtha.2015.08.017
- Flockerzi E, Maier P, Bohringer D, Reinshagen H, Kruse F, Cursiefen C, et al. Trends in corneal transplantation from 2001 to 2016 in Germany: a report of the DOG-section cornea and its keratoplasty registry. *Am J Ophthalmol*. (2018) 188:91–8. doi: 10.1016/j.ajo.2018.01.018

14. Kim BZ, Meyer JJ, Brookes NH, Moffatt SL, Twohill HC, Pendergrast DG, et al. New Zealand trends in corneal transplantation over the 25 years 1991–2015. *Br J Ophthalmol.* (2017) 101:834–8. doi: 10.1136/bjophthalmol-2016-309021
15. Nanavaty MA, Vijjan KS, Yvon C. Deep anterior lamellar keratoplasty: a surgeon's guide. *J Curr Ophthalmol.* (2018) 30:297–310. doi: 10.1016/j.joco.2018.06.004
16. Ong HS, Mehta JS. Corneal Endothelial Reconstruction: Current and Future Approaches in Agarwal A. *Video Atlas of Anterior Segment Repair and Reconstruction - Managing Challenges in Cornea, Glaucoma, and Lens Surgery.* Stuttgart, New York, NY: Thieme Publishing Group (2019). p. 41–52.
17. Reinhart WJ, Musch DC, Jacobs DS, Lee WB, Kaufman SC, Shtein RM. Deep anterior lamellar keratoplasty as an alternative to penetrating keratoplasty a report by the american academy of ophthalmology. *Ophthalmology.* (2011) 118:209–18. doi: 10.1016/j.ophtha.2010.11.002
18. Woo JH, Ang M, Htoon HM, Tan D. Descemet membrane endothelial keratoplasty versus descemet stripping automated endothelial keratoplasty and penetrating keratoplasty. *Am J Ophthalmol.* (2019) 207:288–303. doi: 10.1016/j.ajo.2019.06.012
19. Song Y, Zhang J, Pan Z. Systematic review and meta-analysis of clinical outcomes of penetrating keratoplasty versus deep anterior lamellar keratoplasty for keratoconus. *Exp Clin Transplant.* (2020) 18:417–28. doi: 10.6002/ect.2019.0123
20. Krumeich JH, Knulle A, Krumeich BM. [Deep anterior lamellar (DALK) vs. penetrating keratoplasty (PKP): a clinical and statistical analysis]. *Klin Monbl Augenheilkd.* (2008) 225:637–48. doi: 10.1055/s-2008-1027485
21. Panda A, Bageshwar LM, Ray M, Singh JP, Kumar A. Deep lamellar keratoplasty versus penetrating keratoplasty for corneal lesions. *Cornea.* (1999) 18:172–5. doi: 10.1097/00003226-199903000-00005
22. Hos D, Matthaai M, Bock F, Maruyama K, Notara M, Clahsen T, et al. Immune reactions after modern lamellar (DALK, DSAEK, DMEK) versus conventional penetrating corneal transplantation. *Prog Retin Eye Res.* (2019) 73:100768. doi: 10.1016/j.preteyeres.2019.07.001
23. Bohringer D, Grotejohann B, Ihorst G, Reinshagen H, Spierings E, Reinhard T. Rejection prophylaxis in corneal transplant. *Dtsch Arztebl Int.* (2018) 115:259–65. doi: 10.3238/arztebl.2018.0259
24. Stulting RD, Sugar A, Beck R, Belin M, Dontchev M, Feder RS, et al. Effect of donor and recipient factors on corneal graft rejection. *Cornea.* (2012) 31:1141–7. doi: 10.1097/ICO.0b013e31823f77f5
25. Sheldon S, Poulton K. HLA typing and its influence on organ transplantation. *Methods Mol Biol.* (2006) 333:157–74. doi: 10.1385/1-59745-049-9:157
26. Boisjoly HM, Roy R, Bernard PM, Dube I, Laughrea PA, Bazin R. Association between corneal allograft reactions and HLA compatibility. *Ophthalmology.* (1990) 97:1689–98. doi: 10.1016/S0161-6420(90)32360-6
27. Fink N, Stark WJ, Maguire MG, Stulting D, Meyer R, Foulks G, et al. Effectiveness of histocompatibility matching in high-risk corneal transplantation: a summary of results from the collaborative corneal transplantation studies. *Cesk Oftalmol.* (1994) 50:3–12.
28. Vail A, Gore SM, Bradley BA, Easty DL, Rogers CA, Armitage WJ. Conclusions of the corneal transplant follow up study. Collaborating Surgeons. *Br J Ophthalmol.* (1997) 81:631–6. doi: 10.1136/bjo.81.8.631
29. Reinhard T, Bohringer D, Enczmann J, Kogler G, Mayweg S, Wernet P, et al. Improvement of graft prognosis in penetrating normal-risk keratoplasty by HLA class I and II matching. *Eye.* (2004) 18:269–77. doi: 10.1038/sj.eye.6700636
30. Cornea Donor Study Investigator Group, Gal RL, Dontchev M, Beck RW, Mannis MJ, Holland EJ, et al. The effect of donor age on corneal transplantation outcome results of the cornea donor study. *Ophthalmology.* (2008) 115:620–6 e6. doi: 10.1016/j.ophtha.2008.01.003
31. Volker-Dieben HJ, Kok-van Alphen CC, Lansbergen Q, Persijn GG. Different influences on corneal graft survival in 539 transplants. *Acta Ophthalmol.* (1982) 60:190–202. doi: 10.1111/j.1755-3768.1982.tb08373.x
32. Price DA, Kelley M, Price FW Jr, Price MO. Five-year graft survival of descemet membrane endothelial keratoplasty (EK) versus descemet stripping EK and the effect of donor sex matching. *Ophthalmology.* (2018) 125:1508–14. doi: 10.1016/j.ophtha.2018.03.050
33. Potapenko IO, Samolov B, Armitage MC, Bystrom B, Hjortdal J. Donor endothelial cell count does not correlate with descemet stripping automated endothelial keratoplasty transplant survival after 2 years of follow-up. *Cornea.* (2017) 36:649–54. doi: 10.1097/ICO.0000000000001189
34. Hopkinson CL, Romano V, Kaye RA, Steger B, Stewart RM, Tsagkatakis M, et al. The influence of donor and recipient gender incompatibility on corneal transplant rejection and failure. *Am J Transplant.* (2017) 17:210–7. doi: 10.1111/ajt.13926
35. McGlumphy EJ, Margo JA, Haidara M, Brown CH, Hoover CK, Munir WM. Predictive value of corneal donor demographics on endothelial cell density. *Cornea.* (2018) 37:1159–62. doi: 10.1097/ICO.0000000000001664
36. Bohringer D, Spierings E, Enczmann J, Bohringer S, Sundmacher R, Goulmy E, et al. Matching of the minor histocompatibility antigen HLA-A1/H-Y may improve prognosis in corneal transplantation. *Transplantation.* (2006) 82:1037–41. doi: 10.1097/01.tp.0000235908.54766.44
37. de Bueger M, Bakker A, Van Rood JJ, Van der Woude F, Goulmy E. Tissue distribution of human minor histocompatibility antigens. Ubiquitous versus restricted tissue distribution indicates heterogeneity among human cytotoxic T lymphocyte-defined non-MHC antigens. *J Immunol.* (1992) 149:1788–94.
38. Cantrell MA, Bogan JS, Simpson E, Bicknell JN, Goulmy E, Chandler P, et al. Deletion mapping of H-Y antigen to the long arm of the human Y chromosome. *Genomics.* (1992) 13:1255–60. doi: 10.1016/0888-7543(92)90043-R
39. Pierce RA, Field ED, den Haan JM, Caldwell JA, White FM, Marto JA, et al. Cutting edge: the HLA-A*0101-restricted HY minor histocompatibility antigen originates from DFFRY and contains a cysteinylated cysteine residue as identified by a novel mass spectrometric technique. *J Immunol.* (1999) 163:6360–4.
40. Kim MJ, Kim JH, Jeon HS, Wee WR, Hyon JY. Effect of histocompatibility Y antigen matching on graft survival in primary penetrating keratoplasty. *Cornea.* (2018) 37:33–8. doi: 10.1097/ICO.0000000000001394
41. Barraquer RI, Pareja-Arco L, Gomez-Benlloch A, Michael R. Risk factors for graft failure after penetrating keratoplasty. *Medicine.* (2019) 98:e15274. doi: 10.1097/MD.00000000000015274
42. Inoue K, Amano S, Oshika T, Tsuru T. Histocompatibility Y antigen compatibility and allograft rejection in corneal transplantation. *Eye.* (2000) 14 (Pt 2):201–5. doi: 10.1038/eye.2000.54
43. Volker-Dieben HJ, D'Amato J, Kok-van Alphen CC. Hierarchy of prognostic factors for corneal allograft survival. *Aust N Z J Ophthalmol.* (1987) 15:11–8. doi: 10.1111/j.1442-9071.1987.tb00300.x
44. Price MO, Price FW Jr. Deep anterior lamellar keratoplasty: coming of age. *Br J Ophthalmol.* (2010) 94:1275–6. doi: 10.1136/bjo.2010.182519
45. Giannaccare G, Weiss JS, Sapigni L, Bovone C, Mattioli L, Campos EC, et al. Immunologic stromal rejection after deep anterior lamellar keratoplasty with grafts of a larger size (9 mm) for various stromal diseases. *Cornea.* (2018) 37:967–72. doi: 10.1097/ICO.0000000000001584
46. Gonzalez A, Price MO, Feng MT, Lee C, Arbelaez JG, Price FW Jr. Immunologic rejection episodes after deep anterior lamellar keratoplasty: incidence and risk factors. *Cornea.* (2017) 36:1076–82. doi: 10.1097/ICO.0000000000001223
47. Olson EA, Tu EY, Basti S. Stromal rejection following deep anterior lamellar keratoplasty: implications for postoperative care. *Cornea.* (2012) 31:969–73. doi: 10.1097/ICO.0b013e31823f8a99
48. Tan DT, Mehta JS. Future directions in lamellar corneal transplantation. *Cornea.* (2007) 26(9 Suppl. 1):S21–8. doi: 10.1097/ICO.0b013e31812f685c
49. Ang M, Mehta JS, Sng CC, Htoon HM, Tan DT. Indications, outcomes, and risk factors for failure in tectonic keratoplasty. *Ophthalmology.* (2012) 119:1311–9. doi: 10.1016/j.ophtha.2012.01.021
50. Lass JH, Szczotka-Flynn LB, Ayala AR, Benetz BA, Gal RL, Aldave AJ, et al. Cornea preservation time study: methods and potential impact on the cornea donor pool in the United States. *Cornea.* (2015) 34:601–8. doi: 10.1097/ICO.0000000000000417
51. Gonzalez-Galarza FF, Takeshita LY, Santos EJ, Kempson F, Maia MH, da Silva AL, et al. Allele frequency net 2015 update: new features for HLA epitopes, KIR and disease and HLA adverse drug reaction associations. *Nucleic Acids Res.* (2015) 43:D784–8. doi: 10.1093/nar/gku1166
52. Edelhauser HE, Hyndiuk RA, Zeeb A, Schultz RO. Corneal edema and the intraocular use of epinephrine. *Am J Ophthalmol.* (1982) 93:327–33. doi: 10.1016/0002-9394(82)90534-7

53. Hull DS, Chemotti MT, Edelhauser HF, Van Horn DL, Hyndiuk RA. Effect of epinephrine on the corneal endothelium. *Am J Ophthalmol.* (1975) 79:245–50. doi: 10.1016/0002-9394(75)90078-1
54. Prevention CfDCA. *Leading Causes of Death - Males - All races and origins - United States.* (2017). Available online at: <https://www.cdc.gov/healthequity/lcod/men/2017/all-races-origins/index.htm> (accessed June 15, 2021).
55. Prevention CfDCA. *Leading Causes of Death - Females - All races and origins - United States.* (2017). Available online at: <https://www.cdc.gov/women/lcod/2017/all-races-origins/index.htm> (accessed June 15, 2021).
56. Dandona L, Naduvilath TJ, Janarthanan M, Ragu K, Rao GN. Survival analysis and visual outcome in a large series of corneal transplants in India. *Br J Ophthalmol.* (1997) 81:726–31. doi: 10.1136/bjo.81.9.726
57. Panda A, Vanathi M, Kumar A, Dash Y, Priya S. Corneal graft rejection. *Surv Ophthalmol.* (2007) 52:375–96. doi: 10.1016/j.survophthal.2007.04.008
58. Schoenfeld DA. Sample-size formula for the proportional-hazards regression model. *Biometrics.* (1983) 39:499–503. doi: 10.2307/2531021
59. Tan JC, Wadia PP, Coram M, Grumet FC, Kambham N, Miller K, et al. H-Y antibody development associates with acute rejection in female patients with male kidney transplants. *Transplantation.* (2008) 86:75–81. doi: 10.1097/TP.0b013e31817352b9
60. Larkin DFP. Letter to the editor in response to Kim et al., “Effect of histocompatibility Y antigen matching on graft survival in primary penetrating keratoplasty”. *Cornea.* (2018) 37:e29. doi: 10.1097/ICO.0000000000001539
61. Mannis MJ, Holland EJ, Gal RL, Dontchev M, Kollman C, Raghinaru D, et al. The effect of donor age on penetrating keratoplasty for endothelial disease: graft survival after 10 years in the Cornea Donor Study. *Ophthalmology.* (2013) 120:2419–27. doi: 10.1016/j.ophtha.2013.08.026

Conflict of Interest: The authors declare that the research was conducted in the absence of any commercial or financial relationships that could be construed as a potential conflict of interest.

Publisher’s Note: All claims expressed in this article are solely those of the authors and do not necessarily represent those of their affiliated organizations, or those of the publisher, the editors and the reviewers. Any product that may be evaluated in this article, or claim that may be made by its manufacturer, is not guaranteed or endorsed by the publisher.

Copyright © 2022 Ong, Chiam, Htoon, Kumar, Arundhati and Mehta. This is an open-access article distributed under the terms of the Creative Commons Attribution License (CC BY). The use, distribution or reproduction in other forums is permitted, provided the original author(s) and the copyright owner(s) are credited and that the original publication in this journal is cited, in accordance with accepted academic practice. No use, distribution or reproduction is permitted which does not comply with these terms.



Donor-Related Risk Factors for Graft Decompensation Following Descemet's Stripping Automated Endothelial Keratoplasty

Sota Nishisako¹, Takefumi Yamaguchi², Masatoshi Hirayama², Kazunari Higa¹, Dai Aoki¹, Chiaki Sasaki¹, Hisashi Noma³ and Jun Shimazaki^{1,2*}

¹ Cornea Center and Eye Bank, Tokyo Dental College, Ichikawa General Hospital, Chiba, Japan, ² Department of Ophthalmology, Tokyo Dental College, Ichikawa General Hospital, Chiba, Japan, ³ Department of Data Science, The Institute of Statistical Mathematics, Tokyo, Japan

OPEN ACCESS

Edited by:

Hannah Levis,
University of Liverpool,
United Kingdom

Reviewed by:

Giulia Coco,
Università di Roma Tor Vergata, Italy
Vito Romano,
University of Brescia, Italy

*Correspondence:

Jun Shimazaki
jun@eyebank.or.jp

Specialty section:

This article was submitted to
Ophthalmology,
a section of the journal
Frontiers in Medicine

Received: 07 November 2021

Accepted: 11 January 2022

Published: 04 February 2022

Citation:

Nishisako S, Yamaguchi T,
Hirayama M, Higa K, Aoki D, Sasaki C,
Noma H and Shimazaki J (2022)
Donor-Related Risk Factors for Graft
Decompensation Following
Descemet's Stripping Automated
Endothelial Keratoplasty.
Front. Med. 9:810536.
doi: 10.3389/fmed.2022.810536

Aims: To identify donor-related risk factors associated with graft endothelial failure and postoperative endothelial cell density (ECD) reduction after Descemet's stripping automated endothelial keratoplasty (DSAEK).

Methods: This was a single-center retrospective study conducted from July 2006–December 2016. We included 584 consecutive eyes (482 patients) that underwent DSAEK for the treatment of laser iridotomy-related bullous keratopathy (192 eyes), pseudophakic bullous keratopathy (137 eyes), regrant (96 eyes), Fuchs' endothelial corneal dystrophy (FECD; 59 eyes) and others (100 eyes). Twenty-three donor- and recipient-related risk factors potentially associated with graft failure and ECD reduction were assessed using Cox hazard models and linear mixed effect models.

Results: The median age of the patients was 73.5 years (male; 35.6%). After DSAEK, ECD decreased from 2,674 cells/mm² (95% confidence interval [CI]; 2,646–2,701) to 1,132 (1,076–1,190) at 12 months and 904 (845–963) at 24 months ($P < 0.001$). Fifty-five eyes (9.4%) had graft endothelial failure without rejection. This failure was associated with donor pseudophakic lens status (hazard ratio [HR]; 2.67, CI; 1.50–4.76, $P = 0.001$) and preoperative endothelial folds (HR; 2.82, CI; 1.20–6.62, $P = 0.02$). The incidence of graft endothelial failure in non-FECD patients was significantly higher among those receiving donor grafts with a pseudophakic lens status and preoperative presence of endothelial folds ($P < 0.001$). Postoperative ECD loss was significantly greater in eyes with these risk factors compared to those without ($P = 0.007$).

Conclusions: Pseudophakic status and/or presence of preoperative endothelial folds are the significant donor risk factors for endothelial failure in non-FECD patients.

Keywords: donor-related risk factors, donor pseudophakic lens status, preoperative endothelial folds, Descemet's stripping automated endothelial keratoplasty (DSAEK), non-fuchs' endothelial corneal dystrophy patients

INTRODUCTION

Corneal endothelial dysfunction is one of the leading causes of blindness among patients with corneal diseases (1). Selective replacement of the damaged corneal endothelium by Descemet's stripping automated endothelial keratoplasty (DSAEK) or Descemet's membrane endothelial keratoplasty (DMEK) allow rapid visual recovery (2, 3), resistance to trauma, and minimum astigmatism in comparison with conventional penetrating keratoplasty (PKP), and were able to improve the prognosis of corneal transplantation for bullous keratopathy (BK) eyes (4–6). However, late corneal endothelial failure owing to chronic loss of corneal endothelial cells remains a clinically relevant issue that should be addressed to improve the long-term prognosis of endothelial keratoplasty (7).

Previous clinical studies have shown various risk factors, including donor and recipient factors, associated with endothelial cell density (ECD) loss and graft failure (8–13). However, these results for donor risk factors after DSAEK were obtained in the United States or Europe, where Fuchs' endothelial corneal dystrophy (FECD) is the most common indication in recipient cohorts. In contrast, the indications for DSAEK in Asian countries are different: 70% of endothelial keratoplasties in these countries were performed for treating pseudophakic bullous keratopathy (PBK) or laser-iridotomy-related bullous keratopathy (LIBK), and the number of cases involving FECD accounted for approximately 10% of all transplants (14–16). Although a thorough assessment of donor-related risk factors to improve graft survival after DSAEK is essential, the data for cases involving non-FECD corneal edema disease in Asian countries have been scarce. Therefore, this study aimed to evaluate donor-related factors that may be associated with corneal endothelial failure and reduction in ECD after DSAEK, especially for recipients with non-FECD.

MATERIALS AND METHODS

This study was conducted according to the tenets of the Declaration of Helsinki, and it received approval from the Institutional Ethics Reviewer Board of Tokyo Dental College Ichikawa General Hospital (Acceptance No. I 18-19). Our Institutional Review Board waived the requirement for informed consent for this retrospective study. Patient data were anonymized before access and/or analysis.

Data Collection and Analysis

From July 2006 through December 2016, 587 eyes of 485 patients who underwent DSAEK at the Tokyo Dental College Ichikawa General Hospital were enrolled. All eligible donor corneas met the medical standards of the Eye Bank Association of America or Cornea Center and Eye Bank (CCEB, Chiba, Japan). All domestic corneas were donated to Japanese eye banks and were transported to Tokyo Dental College Ichikawa General Hospital via CCEB. Imported corneas were prepared at an eye bank in the United States of America (Sight-Life, Seattle, WA) and were shipped internationally by airplane. All donor corneas were preserved in a viewing storage chamber and kept in cold-storage

TABLE 1 | Demographics of all samples (N = 584).

Donor and donor cornea characteristics	
Donor age, median (IQR), range, y	66.0 (58, 72), 18–96
Donor sex, male, <i>n</i> (%)	373 (63.9)
Imported graft, <i>n</i> (%)	427 (73.1)
History of diabetes mellitus, <i>n</i> (%)	140 (24.0)
Cigarettes smoking, <i>n</i> (%)	323 (55.3)
Alcohol consumption, <i>n</i> (%)	206 (35.3)
Drug abuse, <i>n</i> (%)	73 (12.5)
History of LASIK, <i>n</i> (%)	34 (5.8)
Donor lens status, <i>n</i> (%)	
Phakic	487 (84.0)
IOL	97 (16.6)
Cause of death, <i>n</i> (%)	
Cardiac disease	148 (25.3)
Cancer	147 (25.2)
Cerebrovascular accident	86 (14.8)
Respiratory disease	99 (17.0)
Others	104 (17.7)
Refrigerated/on ice, <i>n</i> (%)	343 (58.7)
Time from death to the preservation, median (IQR), range, h	8.0 (5.9, 11.9), 1.8–26.9
Time from death to operation, median (IQR), range, d	6.9 (6.0, 7.7), 2.0–9.6
Graft ECD, median (IQR), range, cells/mm ²	2,637 (2,415, 2,921), 2,010–3,812
Endothelial folds, <i>n</i> (%) [*]	
None	157 (26.9)
Mild to moderate	427 (73.1)
Recipient and surgical characteristics	
Recipient age at DSAEK, median (IQR), range, y	73.5 (67, 79), 15–99
Recipient sex, male, <i>n</i> (%)	208 (35.6)
Etiology, <i>n</i> (%)	
FECD	59 (10.1)
LIBK	192 (32.9)
PBK	137 (23.5)
Regraft [†]	96 (16.4)
Others	100 (17.1)
Recipient lens status at DSAEK, <i>n</i> (%)	
Phakic	244 (41.8)
IOL/Aphakic	340 (58.2)
Simultaneous cataract surgery, <i>n</i> (%)	189 (32.4)
Re-bubbling, <i>n</i> (%)	79 (13.5)
Central graft thickness, median (IQR), range, μm^{\ddagger}	143 (123, 161), 53–270

(Continued)

TABLE 1 | Continued

Graft diameter, <i>n</i> (%), mm	
6.75–7.75	144 (24.7)
8.0–8.75	440 (75.3)

DSAEK, Descemet's stripping automated endothelial keratoplasty; ECD, endothelial cell density; FECD, Fuchs' endothelial corneal dystrophy; IOL, intraocular lens; IQR, interquartile range; LASIK, laser-assisted in situ keratomileusis; LIBK, laser-iridotomy-related bullous keratopathy; PBK, pseudophakic bullous keratopathy.

*Grafts without folds were defined as having "no graft folds," "mild graft folds" were defined by the presence of graft folds limited to <25% of the area of the total cornea, and "moderate graft folds" were defined by the presence of graft folds that occupied more than 25% of the area of the total cornea.

[†]Regraft is included in re-DSAEK (56 eyes), post penetrating keratoplasty (36 eyes), post-deep anterior lamellar keratoplasty (2 eyes) and post-Descemet's membrane endothelial keratoplasty (2 eyes).

[‡]Central graft thickness data was obtained in 503 eyes.

corneal preservation medium (Optisol-GS solution; Bausch and Lomb Surgical, Rochester, NY, USA) at a temperature of 2°–8°C. In the eye bank, the central corneal ECD of all tissues was measured using specular microscopy and slit-lamp microscopy was performed by eye bank technicians or eye doctors to evaluate transplant suitability (i.e., epithelial/stromal/endothelial cells/endothelial folds/cutting issue). ECDs of all the grafts used for DSAEK in this study were more than 2,000 cells/mm² preoperatively. The DSAEK procedure was performed using the double-glaze technique in a standardized manner (17, 18). Briefly, Descemet stripping was performed using a reverse-bent Sinsky hook (ASICO, Westmont, IL), and the recipient's endothelium and Descemet's membrane were carefully removed with forceps. A pre-cut donor tissue was trephined, and was gently inserted into the anterior chamber using the Busin glide spatula (ASICO). Air was carefully injected into the anterior chamber to unfold the graft. Ten minutes after the air injection, half of the air was replaced with a balanced salt solution (Alcon, Fort Worth, TX). Postoperatively, topical 0.1% betamethasone (Sanbetazon; Santen, Osaka, Japan) qid was prescribed for 6 months. Six months after DSAEK, 0.1% fluorometholone (Flumetholone 0.1; Santen) was prescribed three times a day for up to 12 months after surgery. ECD was measured by blinded ophthalmologists at 1, 3, 6, 12, and 24 months after DSAEK using a specular microscopy system (EM-4000; TOMEY, Nagoya, Japan). Approximately 50 cells were analyzed for mean ECD (17). In some patients, direct ECD measurement was difficult due to corneal edema or interface irregularity. Therefore, ECD in eyes with irreversible edema due to endothelial decompensation was defined as 300 cells/mm² as previously reported (7, 17, 19). To evaluate the association between postoperative ECD and risk factors, we analyzed ECD as absolute ECD and percentage of 24-month ECD loss (%ECD loss = [24-month ECD – graft ECD]/graft ECD × 100) (10). Graft survival periods were defined as from DSAEK surgery to the date of the clinical visit when irreversible corneal edema refractory to subsequent topical steroid use was noted. Graft survival time or time to censor (end of the study/loss of contact/withdrawal from the study) was calculated as the number of days between the date of DSAEK

surgery and endothelial failure or censor. Three eyes of three patients with a follow-up period of < 1 month were excluded. We treated 13 eyes involving graft rejection episodes, four eyes with ocular infections, and nine eyes in which the procedure failed because of ocular surface complications or irregular graft thickness as censors. A total of 584 eyes of 482 patients were finally included. We selected the following 15 variables based on previous studies and our knowledge of donor-related factors (7–13) that can potentially affect graft survival and reduction in ECD after DSAEK: donor age, sex, domestic/imported graft, history of diabetes mellitus, cigarette smoking, alcohol consumption, drug abuse, history of laser-assisted *in situ* keratomileusis, lens status (phakic/intraocular lens [IOL]), cause of death (cardiac disease/cancer/cerebrovascular accident/respiratory disease/other diseases), refrigerated body/eyes, time from death to the preservation, time from death to operation, ECD, and graft endothelial folds (none/mild/moderate). The graft endothelial fold severity grade for each patient was determined based on slit-lamp microscopic examination findings before DSAEK. Briefly, grafts without folds were defined as having "no graft folds," "mild graft folds" were defined by the presence of graft folds limited to <25% of the area of the total cornea, and "moderate graft folds" were defined by the presence of graft folds occupying more than 25% of the area of the total cornea. Among recipient/surgical factors, we evaluated age, sex, etiologies of bullous keratopathy, lens status at DSAEK, simultaneous cataract surgery, re-bubbling, central graft thickness, and graft diameter. Thus, a total of 23 potential preoperative risk factors (15 donor-related and eight recipient-related factors) were evaluated (Table 1).

Statistical Analysis

The required sample size was based on previous studies (5, 7–13) which estimated that approximately 10% of grafts used DSAEK develop graft failure postoperatively. Given approximately 30% of withdrawal from the study, we determined that a sample size of at least 521 would provide 80% power to detect a difference in a hazard ratio of 0.60 or greater at an alpha value of 0.05 (two-sided). The cumulative probability of graft survival at the 2-year follow-up was calculated using the Kaplan–Meier method. In survival analysis, the collected categorical data were transformed into dummy and continuous variables and dichotomized with the median for use as categorical data. Recipient etiologies were investigated under non-FECD groups. A log-rank test was used to assess the association of each baseline factor with endothelial failure in univariate analysis. Factors with *P* < 0.05 in univariate analysis underwent proportional hazard analyses by log-log plot and Schoenfeld residuals tests and were included in multivariate Cox proportional hazard regression analysis for estimation of the independent predictors of endothelial failure in all patients. The prognostic model was prepared by combining the extracted risk factors (20, 21). Cumulative probability of graft survival was compared between the grafts with no risk factors and grafts with one or two risk factors. The Kaplan–Meier curves were plotted with non-FECD.

To evaluate the associations between postoperative ECD changes and risk factors adjusted for the effects of patient

TABLE 2 | Association between baseline factors and graft endothelial failure.

Prognostic factor	n	2-year graft survival (95% CI)	Log-rank test	Multivariate models*	
			P	HR (95% CI)	P
Donor age, y					
18–65	281	0.91 (0.86–0.94)	0.04	1 [reference]	0.48
66–96	303	0.85 (0.80–0.89)		1.23 (0.69–2.19)	
Donor sex					
Male	373	0.90 (0.86–0.93)	0.13		
Female	211	0.86 (0.79–0.90)			
Imported graft					
No	157	0.89 (0.85–0.92)	0.48		
Yes	427	0.87 (0.79–0.92)			
History of diabetes mellitus					
No	444	0.91 (0.87–0.93)	0.007	1 [reference]	0.09
Yes	140	0.81 (0.72–0.87)		1.63 (0.93–2.86)	
Cigarettes smoking					
No	323	0.87 (0.82–0.91)	0.42		
Yes	261	0.90 (0.84–0.93)			
Alcohol consumption					
No	378	0.87 (0.82–0.90)	0.22		
Yes	206	0.91 (0.85–0.94)			
Drug abuse					
No	511	0.89 (0.85–0.91)	0.55		
Yes	73	0.85 (0.72–0.92)			
History of LASIK					
No	550	0.88 (0.85–0.91)	0.92		
Yes	34	0.89 (0.70–0.96)			
Donor lens status					
Phakic	487	0.91 (0.88–0.94)	<0.001	1 [reference]	0.001
IOL	97	0.73 (0.62–0.81)		2.67 (1.50–4.76)	
Cause of death					
Cancer	147	0.87 (0.83–0.90)	0.22		
Non-cancer	437	0.93 (0.86–0.96)			
Refrigerated/on ice					
No	241	0.89 (0.84–0.93)	0.68		
Yes	343	0.88 (0.83–0.91)			
Time from death to the preservation, h					
1.8–7.9	287	0.89 (0.84–0.92)	0.49		
8.0–26.9	297	0.87 (0.82–0.91)			
Time from death to operation, d					
1.8–6.8	289	0.88 (0.82–0.91)	0.47		
6.9–9.6	295	0.89 (0.84–0.92)			
Graft ECD, cells/mm ²					
2,010–2,636	292	0.85 (0.80–0.89)	0.06		
2,637–3,812	292	0.91 (0.87–0.94)			
Endothelial folds [†]					
None	157	0.95 (0.89–0.98)	0.003	1 [reference]	0.02
Mild to moderate	427	0.86 (0.81–0.89)		2.82 (1.20–6.62)	

(Continued)

TABLE 2 | Continued

Prognostic factor	n	2-year graft survival (95% CI)	Log-rank test	Multivariate models*		
			P	HR (95% CI)	P	
Recipient age at DSAEK, y						
15–72	259	0.87 (0.82–0.91)	0.56			
73–92	325	0.89 (0.84–0.92)				
Recipient sex						
Male	208	0.85 (0.78–0.90)	0.23			
Female	376	0.90 (0.86–0.93)				
Etiology						
FECD	59	0.98 (0.85–1.00)	0.04	1 [reference]	0.09	
Non-FECD	525	0.87 (0.83–0.90)				
Recipient lens status						
Phakic	244	0.90 (0.84–0.93)	0.53			
IOL/Aphakic	340	0.88 (0.83–0.91)				
Simultaneous CS						
No	395	0.87 (0.83–0.90)	0.15			
Yes	189	0.92 (0.86–0.95)				
Re-bubbling						
No	505	0.88 (0.85–0.91)	0.18			
Yes	79	0.82 (0.67–0.91)				
Central graft thickness, μm^\ddagger						
53–130	167	0.85 (0.75–0.91)	0.93			
131–270	336	0.89 (0.84–0.92)				
Graft diameter, mm						
6.75–7.75	144	0.89 (0.85–0.91)	0.80			
8.00–8.75	440	0.89 (0.81–0.93)				

CI, confidence interval; CS, cataract surgery; DSAEK, Descemet's stripping automated endothelial keratoplasty; ECD, endothelial cell density; FECD, Fuchs' endothelial corneal dystrophy; HR, hazard ratio; LASIK, laser-assisted in situ keratomileusis; IOL = intraocular lens.

*Cox proportional hazard regression analysis.

[†]Grafts without folds were defined as having "no graft folds," "mild graft folds" were defined by the presence of graft folds limited to <25% of the area of the total cornea, and "moderate graft folds" were defined by the presence of graft folds occupying more than 25% of the area of the total cornea.

Bold numbers indicate $P < 0.05$.

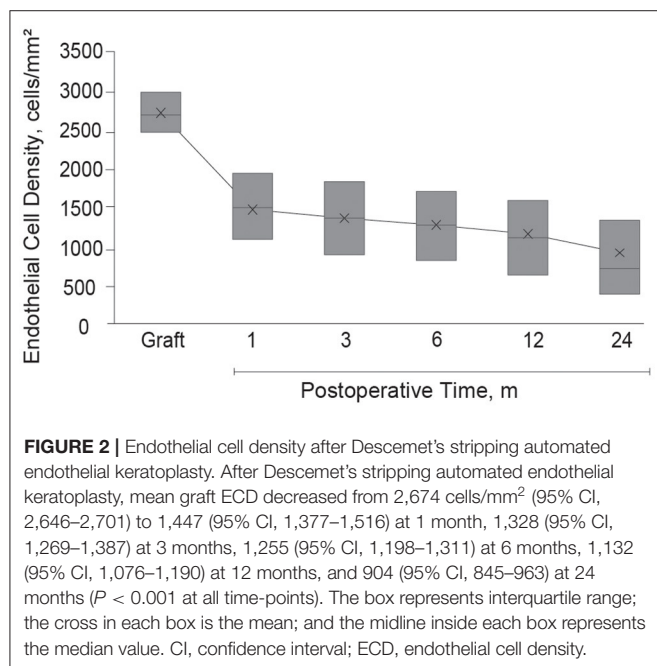
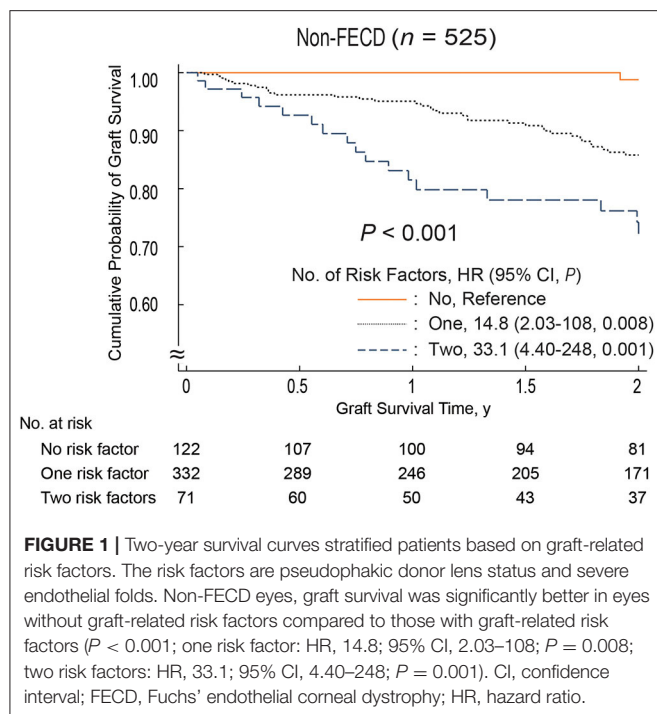
[‡]Central graft thickness data was obtained in 503 eyes.

and surgeon factors, we used linear mixed effect models with random intercepts for recipient and surgeon effect. In the univariate model, the interaction of all potential risk factors and postoperative time were analyzed. Potential risk factors from univariate models with $P < 0.10$ were evaluated in a multivariate model, with %ECD loss after DSAEK. In the final model, the differences in postoperative ECD were compared between the grafts with no risk factors and grafts with one or two risk factors using a linear mixed effect model adjusted for etiology (fixed effect) and recipient and surgeon (random effect). Continuous variables were included in all ECD models in continuous form but were categorized for display in tables. Missing data were not imputed. Statistical analyses for graft survival were conducted using STATA/IC 16.0 for Windows (StataCorp LP, College Station, TX) and R version 4.3.0 for Windows (lme4 package, R Foundation for Statistical Computing, Vienna, Austria) was used for ECD analysis. All reported P values were 2-sided, and values < 0.05 were considered statistically significant.

RESULTS

Demographics

In 584 eyes of 482 patients (Table 1), the median follow-up period was 24 months (interquartile range [IQR], 12–24 months). The recipients' age at DSAEK ranged from 15 to 99 years (median, 73.5 years), and 208 (35.6%) were male, while 582 were Asian (99.9%). The etiologies of BK included LIBK in 192 eyes (32.9%), PBK in 137 eyes (23.5%), re-graft (re-DSAEK, 56 eyes [58.3%]; post-PKP, 36 eyes, [37.5%]; post-deep anterior lamellar keratoplasty, two eyes, [2.1%] and post-DMEK, two eyes, [2.1%]) in 96 eyes (16.4%), FECD in 59 eyes (10.1%), and other conditions (birth injury, chronic uveitis, endotheliitis, etc.) in 100 eyes (17.1%). The recipients' lens status at DSAEK was pseudophakic in 340 eyes (58.2%), and simultaneous DSAEK and cataract surgery was performed in 189 eyes (32.4%). Median central graft thickness was 143 μm (range, 53–270 μm) and the most common graft diameter was 8.0 mm in the current study. There were 373 (63.9%) male donors aged 18–96 years (median, 66.0 years). A total of 427 corneas (73.1%) were



imported (157 corneas [26.9%] were domestic). A history of diabetes mellitus was present in 140 (24.0%) grafts, and the donor lens status was pseudophakic in 97 grafts (16.6%). The median donor ECD was 2,637 cells/mm² (range, 2,010–3,812 cells/mm²), 157 grafts (26.9%) had no endothelial folds, while 427 grafts (73.1%) had mild to moderate endothelial folds before DSAEK.

Graft Survival and Cox Proportional Hazards Analysis

During the 2-year follow-up period, endothelial failure occurred in 55 eyes (9.4%). The cumulative probability of endothelial failure after DSAEK in the entire cohort was 0.94 (95% confidence interval [CI], 0.91–0.96) at 1 year and 0.88 (95% CI, 0.84–0.91) at 2 years (**Supplementary Figure 1**). Among the 23 variables selected as potential preoperative risk factors and tested in a univariate analysis using the log-rank test, donor age ($P = 0.04$), history of diabetes mellitus ($P = 0.007$), donor lens status ($P < 0.001$), endothelial folds ($P = 0.003$), and etiology ($P = 0.04$) were found to be statistically significant. These five variables were added to a multivariate model. Cox proportional hazard regression analysis revealed that donor lens status (IOL, hazard ratio [HR], 2.67; 95% CI, 1.50–4.76; $P = 0.001$) and endothelial folds (mild to moderate, HR, 2.82; 95% CI, 1.20–6.62; $P = 0.02$) were risk factors associated with endothelial failure (**Table 2**). **Figure 1** shows the influence of pseudophakic donor lens state and endothelial folds on graft survival in non-FECD eyes. In eyes with non-FECD, the outcome for grafts with one or two risk factors was significantly worse than that for those with no risk factor (one risk factor: HR, 14.8; 95% CI, 2.03–108; $P = 0.008$; two risk factors: HR, 33.1; 95% CI, 4.40–248; $P = 0.001$).

Endothelial Cell Density Analysis

Endothelial images were obtained and analyzable in 332 eyes (56.8%) at 1 month, 415 eyes (71.1%) at 3 months, 442 eyes (75.6%) at 6 months, 454 eyes (77.7%) at 12 months, and 383 eyes (65.5%) at 24 months after DSAEK. Mean postoperative ECD was associated with postoperative time and decreased from 2,674 cells/mm² (95% CI, 2,646–2,701) to 1,447 (95% CI, 1,377–1,516) at 1 month, 1,328 (95% CI, 1,269–1,387) at 3 months, 1,255 (95% CI, 1,198–1,311) at 6 months, 1,132 (95% CI, 1,076–1,190) at 12 months, and 904 (95% CI, 845–963) at 24 months ($P < 0.001$ at all timepoints, **Figure 2**). Factors associated with postoperative ECD reduction are shown in **Table 3** and **Supplementary Table 1**. In a univariate model, donor age ($P = 0.08$), donor lens status ($P = 0.02$), graft ECD ($P = 0.07$), endothelial folds ($P = 0.04$), recipient sex ($P = 0.05$) and etiology ($P = 0.06$) had statistically significant association with postoperative ECD. Multivariable models showed that the risk factors independently associated with %ECD loss included donor lens status ($P < 0.001$), endothelial folds ($P = 0.002$) and etiology ($P = 0.001$). When the patients were stratified based on graft risk factors (pseudophakic donor lens state and endothelial folds), ECD after DSAEK was significantly greater in eyes receiving grafts from phakic eyes and without preoperative endothelial folds compared to those receiving grafts from pseudophakic eyes and/or with preoperative endothelial folds, in the mixed effect model adjusted with etiology ($P = 0.007$, **Table 4**).

DISCUSSION

We identified donor lens status and preoperative graft endothelial folds as risk factors associated with graft endothelial failure and ECD reduction after DSAEK. Furthermore, we demonstrated

TABLE 3 | Factors associated with postoperative endothelial cell density.

Prognostic factor	n	Univariate models ^{*,†}		Multivariate models ^{*,‡}	
		Mean ECD at 24-month (95% CI)	p	Mean %ECD loss at 24-month (95% CI)	p
Donor age, y					
18–59	107	992 (883–1,100)	0.08	63.4 (59.6–67.3)	0.21
60–69	128	981 (870–1,092)		64.1 (60.3–68.0)	
70–79	116	767 (672–862)		70.7 (67.1–74.1)	
80–95	32	799 (577–1,022)		71.3 (64.0–78.7)	
Donor lens status					
Phakic	312	967 (900–1,033)	0.02	64.3 (61.9–66.6)	<0.001
IOL	71	628 (522–734)		76.5 (72.7–80.2)	
Graft ECD, cells/mm ²					
2,010–2,499	111	669 (590–747)	0.07	70.8 (67.3–74.2)	0.08
2,500–2,749	123	845 (752–938)		67.4 (63.8–71.0)	
2,750–2,999	75	1013 (881–1,145)		64.7 (60.1–69.3)	
3,000–3,812	74	1244 (1,073–1,414)		60.5 (54.9–66.0)	
Endothelial folds [§]					
None	105	1069 (959–1,179)	0.04	60.2 (56.2–64.3)	0.002
Mild to moderate	278	842 (773–911)		68.9 (66.5–71.3)	
Recipient sex					
Male	133	828 (729–927)	0.05	69.4 (65.9–72.8)	0.07
Female	250	944 (871–1,018)		65.0 (62.4–67.6)	
Etiology					
FECD	35	1245 (1,043–1,448)	0.06	54.7 (47.8–61.6)	0.001
Non-FECD	348	867 (808–931)		67.7 (65.6–69.8)	

CI, confidence interval; ECD, endothelial cell density; FECD, Fuchs' endothelial corneal dystrophy; IOL, intraocular lens.

^{*}Adjusted for recipient and surgeon (random effect).

[†]The interaction of potential risk factors and postoperative time were analyzed.

[‡]The percentage ECD loss at 24-month is calculated as (24-month ECD – graft ECD)/graft ECD × 100.

[§]Grafts without folds were defined as having “no graft folds,” “mild graft folds” were defined by the presence of graft folds limited to <25% of the area of the total cornea, and “moderate graft folds” were defined by the presence of graft folds occupying more than 25% of the area of the total cornea.

Bold numbers indicate $P < 0.05$.

that these risk factors were clinically relevant especially in non-FECD and not in FECD, since these were associated with endothelial failure after DSAEK in non-FECD eyes. Although the prognosis of endothelial keratoplasty has been reported to be poor in eyes with PBK (8, 10, 12) especially in BK eyes after glaucoma surgery, in comparison with FECD (7, 12, 22), grafting is the only solution for such eyes with graft failure. Our results suggested that selecting better grafts with no endothelial folds or from phakic eyes for non-FECD patients may prolong graft survival after DSAEK. Our results also indicated that differences in imported or domestic donors did not have an adverse influence on endothelial failure after DSAEK.

Corneal transplants are performed in 116 countries, and imported grafts are used in 70 countries (23). The international organ-sharing program for corneal transplants has successfully grown because corneal tissue can be preserved for more than 1 week (24). Thus, understanding the donor-related risk factors from the global/transnational perspective and optimization of corneal donor tissues is important for both exporting and importing countries.

Previous studies identified several factors, including lower graft ECD (10, 12), history of glaucoma surgery (12, 13, 25), preoperative diagnosis (8, 10, 12), presence of donor diabetes mellitus (8, 10), preservation time of donor tissues (11), pre-existing iris damage (7), age (13, 26), race (4), sex (22, 26), graft size (7, 27), and pre-lamellar dissection corneal thickness (9), as risk factors for graft failure and/or rapid ECD loss after DSAEK. In contrast, long-term graft survival is known to be greater in eyes with relatively healthy peripheral endothelial cells (i.e., FECD/keratoconus) than those with BK (28, 29). Endothelial cells may migrate from the donor to the recipient eyes without peripheral endothelium (i.e., non-FECD), resulting in lower graft ECD and earlier graft failure, whereas ECD is greater in the periphery than in the center and peripheral regions of the cornea and cell migration from the host to the donor graft have been documented in corneal transplants (27, 29, 30). In the current study, we revealed that graft survival in eyes with non-FECD was significantly greater in eyes from donors with a phakic eye (HR: 2.67) and no endothelial folds (HR: 2.82). Furthermore, postoperative ECD decrease was significantly associated with donor lens status (IOL) and endothelial folds.

TABLE 4 | Endothelial cell density after Descemet's stripping automated endothelial keratoplasty by graft-related risk factors.

Postoperative time	No risk factor*		One risk factor		Two risk factors	
	<i>n</i>	Mean (95% CI)	<i>n</i>	Mean (95% CI)	<i>n</i>	Mean (95% CI)
Graft	108	2,717 (2,651–2,783)	321	2,677 (2,639–2,714)	155	2,638 (2,586–2,690)
1 month	70	1,639 (1,508–1,770)	180	1,461 (1,366–1,557)	82	1,251 (1,107–1,395)
3 months	78	1,552 (1,429–1,674)	225	1,316 (1,237–1,395)	112	1,197 (1,078–1,315)
6 months	83	1,507 (1,386–1,628)	238	1,258 (1,183–1,334)	121	1,074 (966–1,183)
12 months	88	1,454 (1,319–1,589)	244	1,114 (1,039–1,188)	122	940 (836–1,044)
24 months	73	1,166 (1,033–1,298)	200	931 (847–1,014)	110	682 (589–776)
<i>p</i> [†]				0.007		

CI, confidence interval.

*The risk factors are pseudophakic donor lens status and severe endothelial folds.

[†]Analyzed with a linear mixed-effect model adjusted for etiology (fixed effect) and recipient and surgeon (random effect).

We identified pseudophakic donor lens status as a risk factor associated with ECD reduction and graft de-compensation after DSAEK, in contrast, the recipients' lens status did not show a statistically significant difference. This may be related to the relatively short follow-up period of 2 years after DSAEK. The annual ECD reduction rate in normal eyes is 0.9%, which can increase up to 2.5% per year after cataract surgery (31). Kawai et al. reported elevated levels of inflammatory cytokines such as interleukin-8 and monocyte-chemotactic protein-1 after cataract surgery (32). Our recent prospective studies have shown that an aqueous humor (AqH) microenvironment with elevated levels of inflammatory cytokines is associated with rapid loss of ECD after PKP and DSAEK (17, 18, 25, 33, 34). Our multi-omics analyses of human corneal endothelial cells identified stress-induced cell senescence as an upregulated biological process in BK (35). Collectively, these results suggest that the pseudophakic donor corneal endothelium shows deterioration in quality, such as cell aging or vulnerability to the pathological microenvironment in the AqH, that potentially leads to rapid ECD loss and endothelial failure after DSAEK.

In the current study, the preoperative presence of graft folds was associated with endothelial failure and lower ECD after DSAEK. Previous studies have reported the existence of dead cells in donor corneal endothelium preserved in Optisol-GS and stored at a temperature between 4°C and 8°C before transplantation (36). Corneal folding has been shown to be significantly correlated with a reduction in corneal endothelial cells, and various studies using cell staining techniques have observed a higher concentration of dead/apoptotic endothelial cells along areas with corneal folds (37, 38). We checked the ECD before surgeries in all donor grafts, but the area of ECD measurement is very limited, approximately 0.24 × 0.35 mm (39), and ECD cannot be measured in the area with endothelial folds. A series of these studies suggested the difference between ECD values obtained by eye bank specular microscopy and the actual viable endothelial cells on the donor graft. The origin/mechanism of donor corneal folds has not been closely explored (40). In our sub-analysis, we found that donor age and time from death to the preservation were associated with the severity grade of the graft endothelial folds (Supplementary Table 2). There was

no statistically significant difference between fold severe levels (mild folds vs. moderate folds) in endothelial failure after DSAEK ($p = 0.91$, data not shown). Further studies are necessary to evaluate the association between the presence of graft folds and reduction in viable corneal endothelial cells. Other potential risk factors discussed in previous studies (2, 4, 7–13, 22, 26, 27) were not associated with endothelial failure in this study: such as donor age ($P = 0.48$, in graft survival analysis), donor sex ($P = 0.13$), history of diabetes mellitus ($P = 0.09$), graft ECD ($P = 0.06$), gender matching ($P = 0.12$, data not shown), re-bubbling ($P = 0.18$), graft thickness ($P = 0.93$), and graft diameter ($P = 0.80$). This may have reflected differences in the cohort of recipients.

This study had some limitations. First, heterogeneous etiologies, such as FECD, PBK, LIBK, and regraft, could potentially have caused bias. We found that pseudophakic donor lens status/preoperative endothelial folds were risk factors for poor prognosis of DSAEK in the non-FECD group. Further analysis that stratified the patients based on etiology for BK was attempted. DSAEK using a graft from pseudophakic donor eyes with preoperative endothelial folds showed a trend of poor prognosis in a non-FECD group, but there was no statistically significant difference for BK other than LIBK (Supplementary Figure 2). A larger sample size and longer follow-up period are needed to further assess risk factors and donor-recipient matching. Second, almost all the subjects in this study were Japanese, and future studies will be needed to substantiate the results in other populations. Third, we could not identify the exact pathological mechanism involved in ECD loss and endothelial failure in eyes with these risk factors. We recently showed that pathological alterations in the microenvironment of AqH due to iris damage predisposed to ECD loss via exacerbated stress-induced cell senescence (35).

In conclusion, grafts from pseudophakic donor eyes with preoperative endothelial folds are identified as risk factors for endothelial failure after DSAEK in recipients with non-FECD. The results of this study suggest that optimization of corneal donor tissues for patients undergoing endothelial keratoplasty is important, especially for non-FECD patients.

DATA AVAILABILITY STATEMENT

The raw data supporting the conclusions of this article will be made available by the authors, without undue reservation.

ETHICS STATEMENT

The studies involving human participants were reviewed and approved by the Institutional Ethics Reviewer Board of Tokyo Dental College Ichikawa General Hospital (Acceptance No. I 18-19). The patients/participants provided their written informed consent to participate in this study.

AUTHOR CONTRIBUTIONS

SN and TY had full access to all the data in the study and take responsibility for the integrity of the data and the accuracy of the data analysis, study concept and design, and drafting of the manuscript. SN, TY, MH, HN, JS, and KH critical revision of the manuscript for important intellectual content. SN, TY, and HN statistical analysis. JS and SN obtained funding. JS, TY, and MH study supervision. All authors acquisition, analysis, or

interpretation of data and administrative, technical, or material support.

FUNDING

This study received funding from a Novartis Research Grant. The funder was not involved in the study design, collection, analysis, interpretation of data, the writing of this article or the decision to submit it for publication.

ACKNOWLEDGMENTS

We thank Editage company for English language editing.

MEETING PRESENTATION

Presented at the Japan Cornea Conference, Tokyo, Japan, April 2020.

SUPPLEMENTARY MATERIAL

The Supplementary Material for this article can be found online at: <https://www.frontiersin.org/articles/10.3389/fmed.2022.810536/full#supplementary-material>

REFERENCES

1. Eye Bank Association of America. 2019 Eye Banking Statistical Report. Available online at: <https://restoresight.org/wp-content/uploads/2020/04/2019-EBAA-Stat-Report-FINAL.pdf> (accessed May 10, 2020).
2. Mencucci R, Favuzza E, Marziali E, Cennamo M, Mazzotta C, Lucenteforte E, et al. Ultrathin descemet stripping automated endothelial keratoplasty versus Descemet membrane endothelial keratoplasty: a fellow-eye comparison. *Eye Vis.* (2020) 7:25. doi: 10.1186/s40662-020-00191-6
3. Dickman MM, Kruit PJ, Remeijer L, Van RJ, Van DLA, Wijdh RHJ, et al. A randomized multicenter clinical trial of ultrathin Descemet stripping automated endothelial keratoplasty (DSAEK) versus DSAEK. *Ophthalmology.* (2016) 123:2276–84. doi: 10.1016/j.ophtha.2016.07.036
4. Price MO, Jordan CS, Moore G, Price FW Jr. Graft rejection episodes after Descemet stripping with endothelial keratoplasty: part two: the statistical analysis of probability and risk factors. *Br J Ophthalmol.* (2009) 93:391–5. doi: 10.1136/bjo.2008.140038
5. Ang M, Soh Y, Htoon HM, Mehta JS, Tan D. Five-year graft survival comparing Descemet stripping automated endothelial keratoplasty and penetrating keratoplasty. *Ophthalmology.* (2016) 123:1646–52. doi: 10.1016/j.ophtha.2016.04.049
6. Price MO, Price FW Jr. Endothelial keratoplasty - a review. *Clin Exp Ophthalmol.* (2010) 38:128–40. doi: 10.1111/j.1442-9071.2010.02213.x
7. Ishii N, Yamaguchi T, Yazu H, Satake Y, Yoshida A, Shimazaki J. Factors associated with graft survival and endothelial cell density after Descemet's stripping automated endothelial keratoplasty. *Sci Rep.* (2016) 6:25276. doi: 10.1038/srep25276
8. Terry MA, Aldave AJ, Szczotka-Flynn LB, Liang W, Ayala AR, Maguire MG, et al. Donor, recipient, and operative factors associated with graft success in the Cornea Preservation Time Study. *Ophthalmology.* (2018) 125:1700–9. doi: 10.1016/j.ophtha.2018.08.002
9. Ross KW, Stoeger CG, Rosenwasser GOD, O'Brien RC, Szczotka-Flynn LB, Ayala AR, et al. Prelamellar dissection donor corneal thickness is associated with Descemet stripping automated endothelial keratoplasty operative complications in the Cornea Preservation Time Study. *Cornea.* (2019) 38:1069–76. doi: 10.1097/ICO.0000000000002040
10. Lass JH, Benetz BA, Patel SV, Szczotka-Flynn LB, O'Brien R, Ayala AR, et al. Donor, recipient, and operative factors associated with increased endothelial cell loss in the Cornea Preservation Time Study. *JAMA Ophthalmol.* (2019) 137:185–93. doi: 10.1001/jamaophthalmol.2018.5669
11. Lass JH, Benetz BA, Verdier DD, Szczotka-Flynn LB, Ayala AR, Liang W, et al. Corneal endothelial cell loss 3 years after successful Descemet stripping automated endothelial keratoplasty in the Cornea Preservation Time Study: a randomized clinical trial. *JAMA Ophthalmol.* (2017) 135:1394–400. doi: 10.1001/jamaophthalmol.2017.4970
12. Price MO, Fairchild KM, Price DA, Price FW Jr. Descemet's stripping endothelial keratoplasty five-year graft survival and endothelial cell loss. *Ophthalmology.* (2011) 118:725–9. doi: 10.1016/j.ophtha.2010.08.012
13. Mity D, Bhogal M, Patel AK, Lee BS, Chai SM, Price MO, et al. Descemet stripping automated endothelial keratoplasty after failed penetrating keratoplasty: survival, rejection risk, and visual outcome. *JAMA Ophthalmol.* (2014) 132:742–49. doi: 10.1001/jamaophthalmol.2014.352
14. Shimazaki J, Amano S, Uno T, Maeda N, Yokoi N, Japan Bullous Keratopathy Study Group. National survey on bullous keratopathy in Japan. *Cornea.* (2007) 26:274–8. doi: 10.1097/ICO.0b013e31802c9e19
15. Nishino T, Kobayashi A, Yokogawa H, Mori N, Masaki T, Sugiyama K. A 10-year review of underlying diseases for endothelial keratoplasty (DSAEK/DMEK) in a tertiary referral hospital in Japan. *Clin Ophthalmol.* (2018) 12:1359–65. doi: 10.2147/OPHT.S170263
16. Takahashi A, Yamaguchi T, Tomida D, Nishisako S, Sasaki C, Shimazaki J. Trends in surgical procedures and indications for corneal transplantation over 27 years in a tertiary hospital in Japan. *Jpn J Ophthalmol.* (2021) 65:608–15. doi: 10.1007/s10384-021-00849-1
17. Yazu H, Yamaguchi T, Aketa N, Higa K, Suzuki T, Yagi-Yaguchi Y, et al. Preoperative aqueous cytokine levels are associated with endothelial cell loss after Descemet's stripping automated endothelial keratoplasty. *Invest Ophthalmol Vis Sci.* (2018) 59:612–20. doi: 10.1167/iops.17-23049
18. Yamaguchi T, Higa K, Tsubota K, Shimazaki J. Elevation of preoperative recipient aqueous cytokine levels in eyes with primary graft failure after corneal transplantation. *Mol Vis.* (2018) 24:613–20.

19. Ibrahim O, Yagi-Yaguchi Y, Kakisu K, Shimazaki J, Yamaguchi T. Association of iris damage with reduction in corneal endothelial cell density after penetrating keratoplasty. *Cornea*. (2019) 38:268–74. doi: 10.1097/ICO.0000000000001819
20. Polee MB, Hop WC, Kok TC, Eskens FA, van der Burg ME, Splinter TA, et al. Prognostic factors for survival in patients with advanced oesophageal cancer treated with cisplatin-based combination chemotherapy. *Br J Cancer*. (2003) 89:2045–50. doi: 10.1038/sj.bjc.6601364
21. Ikeda M, Natsugoe S, Ueno S, Baba M, Aikou T. Significant host- and tumor-related factors for predicting prognosis in patients with esophageal carcinoma. *Ann Surg*. (2003) 238:197–202. doi: 10.1097/01.sla.0000080822.22415.cb
22. Potapenko IO, Samolov B, Armitage MC, Byström B, Hjortdal J. Donor endothelial cell count does not correlate with Descemet stripping automated endothelial keratoplasty transplant survival after 2 Years of follow-up. *Cornea*. (2017) 36:649–54. doi: 10.1097/ICO.0000000000001189
23. Gain P, Jullienne R, He Z, Aldossary M, Acquart S, Cognasse F, et al. Global survey of corneal transplantation and eye banking. *JAMA Ophthalmol*. (2016) 134:167–73. doi: 10.1001/jamaophthalmol.2015.4776
24. Shimazaki J, Shinozaki N, Shimmura S, Holland EJ, Tsubota K. Efficacy and safety of international donor sharing: a single-center, case-controlled study on corneal transplantation. *Transplantation*. (2004) 78:216–20. doi: 10.1097/01.TP.0000128329.28962.4A
25. Yagi-Yaguchi Y, Yamaguchi T, Higa K, Suzuki T, Aketa N, Dogru M, et al. Association between corneal endothelial cell densities and elevated cytokine levels in the aqueous humor. *Sci Rep*. (2017) 7:13603. doi: 10.1038/s41598-017-14131-3
26. Romano V, Parekh M, Virgili G, Coco G, Leon P, Islein, K et al. Gender matching did not affect 2-year rejection or failure rates following DSAEK for Fuchs endothelial corneal dystrophy. *Am J Ophthalmol*. (2021) 235:204–10. doi: 10.1016/j.ajo.2021.09.029
27. Romano V, Tey A, Hill NM, Ahmad S, Britten C, Batterbury M, et al. Influence of graft size on graft survival following Descemet stripping automated endothelial keratoplasty. *Br J Ophthalmol*. (2015) 99:784–8. doi: 10.1136/bjophthalmol-2014-305648
28. Dirisamer M, Yeh R-Y, van Dijk K, Ham L, Dapena I, Melles GRJ. Recipient endothelium may relate to corneal clearance in Descemet membrane endothelial transfer. *Am J Ophthalmol*. (2012) 154:290–96.e1. doi: 10.1016/j.ajo.2012.02.032
29. Lagali N, Stenevi U, Claesson M, Fagerholm P, Hanson C, Weijdegard B, et al. Donor and recipient endothelial cell population of the transplanted human cornea: a two-dimensional imaging study. *Invest Ophthalmol Vis Sci*. (2010) 51:1898–904. doi: 10.1167/iovs.09-4066
30. Price MO, Baig KM, Brubaker JW, Price FW Jr. Randomized, prospective comparison of pre-cut vs surgeon-dissected grafts for descemet stripping automated endothelial keratoplasty. *Am J Ophthalmol*. (2008) 146:36–41. doi: 10.1016/j.ajo.2008.02.024
31. Bourne WM, Nelson LR, Hodge DO. Continued endothelial cell loss ten years after lens implantation. *Ophthalmology*. (1994) 101:1014–22; discussion 1022–1023. doi: 10.1016/S0161-6420(94)31224-3
32. Kawai M, Inoue T, Inatani M, Tsuboi N, Shobayashi K, Matsukawa A, et al. Elevated levels of monocyte chemoattractant protein-1 in the aqueous humor after phacoemulsification. *Invest Ophthalmol Vis Sci*. (2012) 53:7951–60. doi: 10.1167/iovs.12-10231
33. Yamaguchi T, Higa K, Suzuki T, Nakayama N, Yagi-Yaguchi Y, Dogru M, et al. Elevated cytokine levels in the aqueous humor of eyes with bullous keratopathy and low endothelial cell density. *Invest Ophthalmol Vis Sci*. (2016) 57:954–62. doi: 10.1167/iovs.16-20187
34. Yagi-Yaguchi Y, Yamaguchi T, Higa K, Suzuki T, Yazu H, Aketa N, et al. Preoperative aqueous cytokine levels are associated with a rapid reduction in endothelial cells after penetrating keratoplasty. *Am J Ophthalmol*. (2017) 181:166–73. doi: 10.1016/j.ajo.2017.07.005
35. Yamaguchi T, Higa K, Yagi-Yaguchi Y, Ueda K, Noma H, Shibata S, et al. Pathological processes in aqueous humor due to iris atrophy predispose to early corneal graft failure in humans and mice. *Sci Adv*. (2020) 6:eaz5195. doi: 10.1126/sciadv.aaz5195
36. Kitazawa K, Inatomi T, Tanioka H, Kawasaki S, Nakagawa H, Hieda O, et al. The existence of dead cells in donor corneal endothelium preserved with storage media. *Br J Ophthalmol*. (2017) 101:1725–30. doi: 10.1136/bjophthalmol-2017-310913
37. Pipparelli A, Thuret G, Toubeau D, He Z, Piselli S, Lefèvre S, et al. Pan-corneal endothelial viability assessment: application to endothelial grafts predissected by eye banks. *Invest Ophthalmol Vis Sci*. (2011) 52:6018–25. doi: 10.1167/iovs.10-6641
38. Nartey IN, Ng W, Sherrard ES, Steele AD. Posterior corneal folds and endothelial cell damage in human donor eyes. *Br J Ophthalmol*. (1989) 73:121–5. doi: 10.1136/bjo.73.2.121
39. McCarey BE, Edelhauser HF, Lynn MJ. Review of corneal endothelial specular microscopy for FDA clinical trials of refractive procedures, surgical devices, and new intraocular drugs and solutions. *Cornea*. (2008) 27:1–16. doi: 10.1097/ICO.0b013e31815892da
40. Annadanam A, Stoeger CG, Galloway JD, Hikes MT, Jun AS. Optical coherence tomography assessment of the cornea during corneal swelling: should the term “Descemet membrane folds” be reconsidered? *Cornea*. (2019) 38:754–7. doi: 10.1097/ICO.0000000000001908

Conflict of Interest: The authors declare that the research was conducted in the absence of any commercial or financial relationships that could be construed as a potential conflict of interest.

Publisher's Note: All claims expressed in this article are solely those of the authors and do not necessarily represent those of their affiliated organizations, or those of the publisher, the editors and the reviewers. Any product that may be evaluated in this article, or claim that may be made by its manufacturer, is not guaranteed or endorsed by the publisher.

Copyright © 2022 Nishisako, Yamaguchi, Hirayama, Higa, Aoki, Sasaki, Noma and Shimazaki. This is an open-access article distributed under the terms of the Creative Commons Attribution License (CC BY). The use, distribution or reproduction in other forums is permitted, provided the original author(s) and the copyright owner(s) are credited and that the original publication in this journal is cited, in accordance with accepted academic practice. No use, distribution or reproduction is permitted which does not comply with these terms.



Extracellular Vesicles Derived From Human Corneal Endothelial Cells Inhibit Proliferation of Human Corneal Endothelial Cells

Mohit Parekh¹, Hefin Rhys², Tiago Ramos¹, Stefano Ferrari³ and Sajjad Ahmad^{1,4*}

¹ Institute of Ophthalmology, Faculty of Brain Sciences, University College London, London, United Kingdom, ² Flow Cytometry Science Technology Platform, Francis Crick Institute, London, United Kingdom, ³ International Center for Ocular Physiopathology, Fondazione Banca Degli Occhi del Veneto, Venice, Italy, ⁴ Cornea and External Eye Disease, Moorfields Eye Hospital NHS Foundation Trust, London, United Kingdom

OPEN ACCESS

Edited by:

Ravirajsinh Jadeja,
Augusta University, United States

Reviewed by:

Min Wu,
The Affiliated Hospital of Yunnan
University, China
Chua Kien Hui,
National University of
Malaysia, Malaysia

*Correspondence:

Sajjad Ahmad
sajjad.ahmad@ucl.ac.uk

Specialty section:

This article was submitted to
Ophthalmology,
a section of the journal
Frontiers in Medicine

Received: 05 August 2021

Accepted: 16 December 2021

Published: 04 February 2022

Citation:

Parekh M, Rhys H, Ramos T, Ferrari S
and Ahmad S (2022) Extracellular
Vesicles Derived From Human Corneal
Endothelial Cells Inhibit Proliferation of
Human Corneal Endothelial Cells.
Front. Med. 8:753555.
doi: 10.3389/fmed.2021.753555

Corneal endothelial cells (CEncs) are a monolayer of hexagonal cells that are responsible for maintaining the function and transparency of the cornea. Damage or dysfunction of CEncs could lead to blindness. Human CEncs (HCEncs) have shown limited proliferative capacity *in vivo* hence, their maintenance is crucial. Extracellular vesicles (EVs) are responsible for inter- and intra-cellular communication, proliferation, cell-differentiation, migration, and many other complex biological processes. Therefore, we investigated the effect of EVs (derived from human corneal endothelial cell line-HCEC-12) on corneal endothelial cells. HCEC-12 cells were starved with serum-depleted media for 72 h. The media was ultracentrifuged at 100,000xg to isolate the EVs. EV counting, characterization, internalization and localization were performed using NanoSight, flow cytometry, Dil labeling and confocal microscopy respectively. HCEC-12 and HCEncs were cultured with media supplemented with EVs. Extracted EVs showed a homogeneous mixture of exosomes and microvesicles. Cells with EVs decreased the proliferation rate; increased apoptosis and cell size; showed poor wound healing response *in vitro* and on *ex vivo* human, porcine, and rabbit CECs. Thirteen miRNAs were found in the EV sample using next generation sequencing. We observed that increased cellular uptake of EVs by CECs limit the proliferative capacity of HCEncs. These preliminary data may help in understanding the pathology of corneal endothelial dysfunction and provide further insights in the development of future therapeutic treatment options.

Keywords: cornea, eye, exosomes, extracellular vesicles, corneal endothelial cells

INTRODUCTION

The cornea is the anterior tissue of the eye that refracts incident light to the lens, further converging it to the retina and optic nerve (1). Corneal clarity is essential for normal visual function. Corneal transparency is supported by its structural anatomy and physiology, mainly the endothelium. Human corneal endothelial cells (HCEncs) line the under surface of the cornea. The cornea is avascular and receives its hydration and nutrients from the tear film and the aqueous humor from both sides of the eye. Excess accumulation of fluid, known as corneal oedema, affects

corneal transparency and results in visual impairment. A mechanism to maintain corneal deturgescence is therefore required. This is performed by the corneal endothelium. The corneal endothelium acts as a barrier to fluid movement with the corneal endothelial cells actively pumping ions to move water osmotically from the aqueous humor to the corneal stroma and vice versa (2, 3). This combination of leaky barrier and fluid pump function is termed the pump-leak mechanism (2, 3).

HCECs have no mitotic activity *in vivo*, although they can be induced to divide in cultured corneal cells (4, 5). Human corneas at birth are characterized by a considerable endothelial cell reserve, with HCEC density being 6,000 cells/mm² at birth and declining to approximately 2,600 cells/mm² or even low during the eighth decade of life (6, 7). HCECs have an almost perfect hexagonal shape which enables the formation of a tight cobblestone cell layer. The percentage of HCECs with a hexagonal shape also decreases from 75 to 60% with age (8). Other than age, there are several pathologies which result in accelerated HCEC loss and dysfunction, resulting in loss of corneal clarity and blindness. These include viral infections, inflammation, and surgical procedures within the eye. However, dystrophies [Fuchs' dystrophy (9), posterior polymorphous dystrophy (10), congenital hereditary dystrophy (11)] or other conditions like iridocorneal endothelial syndrome (12) can also contribute toward partial or total blindness. Fuchs' endothelial corneal dystrophy (FECD) remains one of the common causes of corneal blindness resulting from the loss of endothelial cells. In FECD, the pump function of the endothelial cell decreases followed by a reduction in barrier function (9).

Several pathological processes require the migration and spreading of viable HCECs (13). In doing this, HCECs grow in size and lose their typical hexagonal shape. Endothelial wound healing is associated with a transient acquisition of fibroblast morphology, known as endothelial-mesenchymal transformation (14). In the later stages of endothelial healing, the number of tight junctions and pump sites return to physiological levels, corneal thickness as a result of corneal oedema returns to normal, and corneal transparency and vision is restored. When HCEC density decreases below 500 cells/mm², there is a significant risk of chronic and irreversible corneal oedema (15). In this scenario, the only treatment available is the replacement of the corneal endothelium by corneal transplantation (keratoplasty) from donor cadavers. Corneal endothelial failure remains one of the commonest reasons for requiring keratoplasty. Despite recent advances in surgical techniques, corneal transplantation has its limitations like transplant rejection and shortage of global donor cornea supply (16). Hence, HCEC culture was introduced as a potential therapeutic option (17–19). However, HCECs are difficult to proliferate *in vitro* due to multiple factors like donor variability, cell source, age, preservation time (20), and tissue supply, which further challenges the conventional cell-based treatment option indicating the need of a parallel therapeutic approach.

Interestingly, while HCEC's lack of proliferative capacity *in vivo* appears to be a feature found in humans, felines,

and primates, many species such as rabbits and pigs have shown cell proliferation *in vivo*. Rabbits retain the ability to proliferate and regenerate *in vivo* following trauma (21–24). Pig corneal endothelial cells have also shown a higher proliferation potential compared to humans (25). Although pig corneal endothelium appears to have limited proliferative capacity *in vivo* compared to rabbits, their proliferative capacity remains better than HCECs (26). Hence, investigating the reasons for the proliferative capacity of these species and lack of proliferation in HCECs becomes important to develop new treatment options.

Extracellular vesicle (EV) trafficking is an important mechanism of intercellular communication in multicellular organisms (13–27). However, only a small collection of studies has examined EV function in the eye and the cornea in general (13, 28). Produced by different mechanisms with different subcellular origins and size distributions, three types of EVs have been classified: apoptotic bodies (1 to 5 μm in diameter); microvesicles (up to 1 μm in diameter); and exosomes (40 to 150 nm in diameter) (29). Exosomes are intraluminal membrane vesicles that form from the inward budding of the endosomal membrane. They contain different constituents of the parent cell, such as DNA, RNA, mRNA, micro-RNA, transcription factors, cytokines, lipids, metabolites, cytosolic and cell-surface proteins, and growth factors. Although the transfer of cargo between the cells is not completely understood, exosomes may be crucial in understanding cell trans-differentiation, proliferation, mechanisms or causes of disease, and to finding potential new therapies (29).

Due to the difficulties and limitations such as the global shortage of donor corneas, it is important to find alternative therapeutic strategies for treating corneal endothelial failure in humans. This requires basic understanding of the mechanisms that enable corneal endothelial maintenance in health and disease. As EVs have shown an important role in reprogramming normal/injured cells, the aim of this study was to investigate the role of EVs on HCECs and in other higher animals and identify the factors that inhibit the proliferation of these cells in humans *in vivo*.

MATERIALS AND METHODS

Ethical Statement

Human donor corneas were shipped from Fondazione Banca degli Occhi del Veneto (FBOV, Venice, Italy) to UCL Institute of Ophthalmology (London, UK) with written consent for research use as the tissues were not suitable for transplantation due to poor endothelial cell count (<2200 cells/mm²). The tissues were utilized and discarded as per the Human Tissue Authority (HTA, UK) guidelines. The experiments were approved by the UCL ethics committee (10/H0106/57-2011ETR10) and were performed in accordance with the Declaration of Helsinki. The porcine and rabbit corneas were obtained from whole eyes shipped by a local abattoir and did not qualify for any special animal handling approval / ARVO guidelines for animal handling.

HCEC-12 Cell Culture and Extraction of EVs

HCEC-12 cell lines were cultured on T-175 flasks (Nunc EasYFlask Delta surface, ThermoFisher Scientific, Waltham, MA, USA) using cell culture media (CCM-Ham's F12:Medium 199 (1:1) supplemented with 5% FBS; ThermoFisher Scientific, Waltham, MA, USA). Upon 95% confluence, the cells were starved with serum-depleted media (CCM without FBS; 10 mL per T-175 flask) every 24 h up to 72 h at 37°C, 5% CO₂. Following starving, the conditioned media (CM) was collected every 24 h and centrifuged at 112 x g for 5 min at 4°C (centrifuge 5417, Eppendorf, Hamburg, Germany) to remove the dead cells and large debris. The supernatant was collected and re-centrifuged at 699xg for 10 min at 4°C to remove any potential media remnants. The CM was then filtered through a 0.22 µm filter (Merck Millipore, Burlington, Massachusetts, USA). Approximately 9 mL of the final volume from the flask was obtained. 4.5 mL of the filtered media was gently transferred to each sterile OptiSeal tube (Beckman Coulter, Brea, California, USA), capped and ultracentrifuged at 100,000xg in a TLA 100.4 fixed angle rotor (Beckman Coulter, Brea, California, USA) in an Optima Max-E ultracentrifuge machine (Beckman Coulter, Brea, California, USA) for 2 h at 4°C. The resulting pellet (volume dependent on experiment) was re-suspended and washed with sterile PBS followed by a second round of ultracentrifugation using the same settings as mentioned above, to obtain a pellet free of any media remnants. The resulting pellet was re-suspended in sterile PBS and either used directly for experiments or stored at -80°C. The entire procedure was carried out in the laminar flow hood to maintain sterility. The stored EV suspension was thawed in water bath at 37°C before use.

Quantification, Characterization, Visualization, and Uptake of EVs

Quantification of EVs

From the EV suspension, 1 mL of the solution containing EVs was used for quantification and sizing following manufacturer's instructions (NanoSight NS300 instrument, Amesbury, UK). The temperature was kept constant at 22°C and the water viscosity kept at 0.953cP. For analysis, 1,498 frames were used at a rate of 25 frames per second. Sterile PBS was used as controls to ensure there was no contamination of any small visible molecules.

Characterization of EVs by Flow Cytometry

The EVs-containing suspension was ultra-centrifuged using the same settings as mentioned earlier and the resulting pellet was incubated with 10 µL of aldehyde/sulfate latex beads (ThermoFisher Scientific, Waltham, Massachusetts, USA) for 15 min at room temperature (RT). PBS was added to make up a final volume of 1 mL and the entire solution was incubated at 4°C overnight on a test tube rotator wheel fixed at 20 rpm (Stuart® Equipment, Saffordshire, ST15 OSA, UK). Glycine (Sigma-Aldrich, Darmstadt, Germany) was added to a final concentration of 100 mM and the resulting solution incubated at RT for 30 min. The solution was then centrifuged (Note:

all centrifugation steps were performed for 3 min at 1800 x g in RT). The supernatant was removed, and the remaining pellet was washed thrice in 1 mL of 0.5% bovine serum albumin (BSA, Sigma-Aldrich, Darmstadt, Germany) in PBS. The pellet was re-suspended in 100 µL of primary antibody (**Supplementary Table 1**) diluted in 0.5% BSA and incubated in the dark for 30 min at 4°C. After washing and centrifugation, the resulting pellet was re-suspended in 100 µL of appropriate secondary antibody (**Supplementary Table 2**) diluted in 0.5% BSA. This suspension was then incubated in the dark for 30 min at 4°C. After washing and centrifugation steps, the resulting pellet was re-suspended in 500 µL of 0.5% BSA. This final suspension was analyzed using Fortessa X-20 (BD Biosciences, San Jose, CA, USA) flow cytometer (Laser 488 nm, filter 533/30) and the results were analyzed using BD FACSDiva software.

Cellular Uptake of EVs

The stored suspension of EVs was labeled with 1,1'-Diiododecyl-3,3',3'-Tetramethylindocarbocyanine Perchlorate (DiI) fluorescent dye (V228885, ThermoFisher, Waltham, Massachusetts, USA). Briefly, the EV solution was gently mixed with DiI in PBS (1:1000) and incubated for 30 min in the dark at RT followed by a single wash with PBS and ultracentrifugation (100,000xg) for 2 h at 4°C. The DiI-labeled EVs were diluted in the CCM supplemented with exosome depleted FBS (ThermoFisher Scientific) and used for qualitative and time point analysis.

For confocal microscopy, approximately 50,000 cells (HCEC-12) per well of 4-well lab-Tek II chamber slides (Thermo Fisher Scientific) and for Imagestream flow cytometry analysis, approximately 150,000 cells per well of a 12 well plate (Thermo Fisher Scientific) was cultured for 48 h. HCEC-12 cells were refreshed with the CM (fetal bovine serum (FBS) replaced with exosome-free serum) supplemented with 40 µL of EVs (obtained from 1 mL of the EV suspension i.e., ~5 X 10⁶ particles) with 360 µL of CM (10% EVs). The cells were monitored at different time points i.e., 3, 6, 12, 24, and 48 h. The media was not refreshed after adding the EVs throughout the entire course of this experiment. Negative control was cells with standard FBS.

Cellular Uptake and Localization of EVs-Time Point Analysis Using Confocal Microscope

The cells (control and with EVs) were washed with PBS and fixed with 4% paraformaldehyde (PFA) at 3, 6, 12, 24, and 48 h following addition of DiI-positive EVs. Hoechst 33342 (ThermoFisher Scientific) (0.5 µg/mL) was added on the cells to stain the nucleus at RT for 30 min. After each step, the cells were washed at least twice with PBS. After detaching the walls of the Lab-Tek slides, the cells were covered with mounting media (Vectashield, Vector Laboratories, Burlingame, CA, USA) and cover slips. The cells with EV uptake were imaged using the LSM 700 confocal microscope (Carl Zeiss, Cambridge, UK) and captured using a built-in Zen software. Localization was observed using 3D view feature of the confocal microscope following z-stacking of the image.

Internalization and Cellular Uptake of EVs Using ImageStream

The cells (control and with EVs) were washed with PBS and detached from the plate using TrypLE Express (1X), phenol red (Life Technologies, Monza, Italy) treatment for 5 min at 37°C to dissociate the clumps into single cells. The collected cells were centrifuged at 194xg for 5 min, washed and fixed with 4% PFA. The fixed cells were labeled with Hoechst 33342 (as described above) in 1.5 mL Eppendorf tubes, washed with PBS, and re-suspended in 50 µL of PBS. Samples were acquired on an ImageStream[®] MkII (Austin, Texas, USA) at 60x magnification on low flow rate. The 405, 561, and 785 nm (for scatter) lasers were switched on and set to 30, 200, and 1.0–1.2 mW, respectively. Laser powers were chosen that maximized resolution while avoiding pixel saturation. Channels 1 and 9 were reserved for brightfield images. Using the IDEAS analysis software, single cells were gated using Area vs. Aspect ratio (a measure of object roundness). The gradient RMS feature of the brightfield images was used to gate on focused events. Percentage of Dil+ events were identified from the different phases after gating on non-clipped objects using the Raw Centroid X and Hoechst 33342-positive events. The quantification of internalization, total EV+ population and total internalization score was obtained from these positive events. The internalization feature is defined as the ratio of the intensity inside the cell to the intensity of the entire cell. The higher the score, the greater the concentration of intensity inside the cell. All pixels were background-subtracted and an Adaptive Erode (M01, Ch01 BF1, 78) mask was created to define the inside of the cell for this feature. The Bright Detail Intensity R3 and Bright Detail Intensity R7 features computed the intensity of localized bright spots within the masked area in the image. Bright Detail Intensity R3 and R7 features compute the intensity of bright spots that are 3 pixels or 7 pixels in radius or less, respectively. In each case, the local background around the spots was removed before the intensity computation.

Human Corneal Endothelial Cell Line (HCEC-12) Culture With EVs

Human corneal endothelial cells from a certified cell line (HCEC-12) were cultured on 75 cm² culture flasks (Nunc, Thermo Fisher Scientific, Rochester, NY, USA) to reach 95% confluence using CCM as mentioned above. The cells were trypsinised and cultured on Lab-Tek II chamber slides (8 chambers, 25 x 75 mm, 0.7 cm² culture area, Thermo Fisher Scientific). Upon confluence, the CCM was removed and the HCEC-12 cells were washed with sterile PBS. The cells were refreshed with CCM (as control) and media supplemented with 10% EVs, as described above (CCM with exo-free serum-as experimental group). The cells were analyzed for proliferation rate, doubling time, viability, apoptosis and endothelial cell specific markers at different time points.

Human Corneal Endothelial Cell Culture From Old-Aged Donor Tissues With EVs Endothelial Cell Evaluation

Donor endothelium of all the tissues was stained with trypan blue (0.25% w/v) to determine the viability of the cells. Approximately 100 µL of trypan blue was applied topically on the endothelial surface for 20 s and washed with sterile phosphate buffered saline (PBS). The endothelium was exposed to a hypotonic sucrose solution (1.8%) to count the number of endothelial cells using a reticule (10 x 10) fixed to the eyepiece of an inverted microscope (Nikon Eclipse TS100, Nikon, Surrey, UK). An average of five different counts was recorded (30).

Cell Culture

The Descemet's membrane-endothelial complex of the tissues were stripped in multiple pieces to ensure quick enzymatic digestion. The excised pieces were digested in 2 mg/mL collagenase Type 1 (Thermo Fisher Scientific, Rochester, NY, USA) for 2 h at 37°C and 5% CO₂. The resulting solution was centrifuged for 5 min at 194xg and the pellet was re-suspended with TrypLE Express (1X), phenol red (Life Technologies, Monza, Italy) for 5 min at 37°C to further dissociate into single cells. The supernatant was discarded, and the cells were re-suspended in 200 µL of the HCEC culture medium (HCM), which is a formulation of 1:1 Ham's F12:M199 (Sigma-Aldrich), 5% FBS, 20 µg/ml ascorbic acid (Sigma-Aldrich), 1% Insulin Transferrin Selenium (Gibco), 10 ng/ml recombinant human FGF basic (Gibco), 10 µM ROCK inhibitor (Y-27632; Miltenyi Biotech) and 1% PenStrep (Sigma-Aldrich) (18, 31–35). The cells were counted using haemocytometer. Lab-Tek II chamber slides (8-well) were coated with 50 µL Fibronectin Collagen (FNC) coating mix (US Biological Life Sciences, Salem, Massachusetts, USA) for 30–45 min at 37°C and 5% CO₂. The residual coating was removed before plating cells. 200 µL of the cell suspension from each cornea was divided into two equal halves and plated on each chamber a) without EVs and b) with EVs (10%). The media was topped up to make a final volume of 400 µL. The HCM (with/without EVs) was replaced, and the cells were monitored every alternate day until confluence followed by end-stage characterization.

Proliferation Rate, Cell Doubling Numbers and Time on HCEC-12 and HCECs

The proliferation rate was measured every alternate day using an in-built reticule (10 x 10) attached to an inverted microscope (Nikon Eclipse TS100; Nikon). The number of endothelial cells/mm² were counted using the same reticule determined by counting the number of blocks filled by the cells every alternate day represented as percentage of proliferation rate in the given area. This also facilitated in calculating the cell doubling time and doubling numbers.

Hoechst 33342, Ethidium Homodimer and Calcein AM (HEC) Staining to Determine Live/Dead HCEC-12 Cells and HCEncs

Cells at confluence were washed with PBS after preservation prior to the assay. 5 μ L of Hoechst 33342 (H) (Thermo Fisher Scientific), 4 μ L of Ethidium Homodimer EthD-1 (E) and 2 μ L Calcein AM (C) (Live/Dead viability/cytotoxicity kit, Thermo Fisher Scientific) was mixed in 1 mL of PBS. 100 μ L of the final solution was directly added on the cells and incubated at room temperature in dark for 45 min, followed by a single washing step with PBS. The walls of the Lab-Tek slides were detached and the cells were mounted with mounting media (without DAPI). The Zeiss LSM 700 confocal microscope (Carl Zeiss, Cambridge, UK) was used to image the cells that were captured using built-in Zen software. The measurements and data analysis were performed using ImageJ (FIJI) bundled with 64-bit Java 1.8.0 112. Viability of cells was measured as the number of Calcein AM-Hoechst-positive cells (double stained) compared with the number of only Hoechst-positive cells. The images were split and the Hoechst positive cells were overlayed with numbers. Calcein AM positive cells were patched on the overlayed image to calculate the number of cells with no calcein positivity and converted to percentage for statistical analysis.

Cell Apoptosis Using Terminal Deoxynucleotidyl Transferase Deoxyuridine Triphosphate Nick-End Labeling Assay on HCEC-12 and HCEncs

Cell apoptosis was performed as described in the manufacturer's protocol for TACS 2 terminal deoxynucleotidyl transferase (TdT) diaminobenzidine (DAB) *in situ* apoptosis detection kit (Cat# 4810-30-K; Trevigen, Maryland, USA). One separate positive sample was induced with apoptosis using TACS nuclease and all the samples were viewed and imaged using inverted light microscope (Nikon Eclipse TS100, Nikon, Surrey, UK). The apoptotic cells were manually counted, and an average was recorded from five random areas (36).

Immunostaining of Zonula Occludens-1 (ZO-1) and Na⁺/K⁺ATPase

Cells at confluence were washed with PBS and fixed in 4% paraformaldehyde (PFA) at RT for 20 min. The cells were permeabilized with 0.25% Triton X-100 in PBS for 30 min. After blocking with 10% goat serum for 1 h at RT, the cells were incubated overnight at 4°C with primary antibody anti-ZO-1 (ZO-1-1A12, Alexa Fluor 488; Thermo Fisher Scientific, Rochester, NY, USA) (HCEC-12 and HCEncs), 1:200 and; anti-Na/K ATPase (Sodium Potassium ATPase Alpha 1 Antibody (464.6)-FITC; Novus Biologicals, Centennial, CO) (HCEncs only), 1:50. Hoechst 33342 (0.5 μ g/mL) was diluted in PBS and 100 μ L of the solution was added on the cells to stain the nucleus. After each step, the cells were washed 3 times with PBS. After detaching the walls of the Lab-Tek slides, the cells were covered with mounting medium and cover slips. Expression of these markers were examined using the LSM 700 confocal

microscope (Carl Zeiss) and images were captured using an in-built Zen software.

For hexagonality, ZO-1-positive images were converted to overlay masks using pre-determined macroinstructions to define the parameters of both hexagonality and polymorphism within a particular area (37). The images were auto-converted and the total number of cells in the investigated area were counted using the macros for ZO-1. The hexagonal and polymorphic cells were counted manually depending on the cellular structure comprising 6 borders per cell for hexagonal cells and < 4 borders for severely polymorphic cells in the investigated area. Cell area (μ m²) was measured by marking the borders of the cell using a free-hand tool followed by the area measurement tool. The numbers were converted into percentage for statistical analysis.

Effect of EVs on Wound Healing (Scratch Assay)—*in vitro* and *ex vivo* (Human, Porcine and Rabbit Corneal Tissues)

In vitro Wound Healing of HCEC-12 Cells

HCEC-12 cells were cultured on standard 12 well plates. Upon confluence, the center of the wells was scratched using a 1 mL pipette tip to create a wound. The well was washed using sterile PBS and the cells were refreshed with CCM supplemented with EVs (10% EVs), as described above. The cells in exo-free serum CCM were considered as control. The wounded area was monitored every 24 h till the wound healing was complete. The images were loaded on ImageJ and the total area of the wounded zone was measured at different time point leading to calculation of percentage wound closure at each time point.

Ex vivo Wound Healing on Human Donor Cornea

Like the *in vitro* wound healing assay, a scratch was made at the center of the tissue using a 1 mL pipette tip. The tissue was washed and placed in HCM supplemented with/without EVs. The tissues with exo-free HCM were considered as control. The wound healing was monitored every 24 h and calculated as mentioned above.

Ex vivo Wound Healing on Porcine and Rabbit Corneas

Porcine and rabbit eyes were obtained from a local abattoir. The corneas were excised and preserved in CCM before the experiments. Using the same technique as described above, the corneal endothelium was scratched at the center. The tissues (donor-matched i.e., OD vs. OS) were washed and preserved in the media supplemented with exo-free CCM and the other tissues were preserved with 10% HCEC-12 derived EVs. The wound healing was monitored every 24 h and calculated as mentioned above.

Cargo Characterization by Next Generation Sequencing

One μ L of total EV-RNA was utilized for measurement of small RNA concentration by Agilent Bioanalyzer Small RNA Assay using Bioanalyzer 2100 Expert instrument (Agilent Technologies, Santa Clara, CA). Next generation sequencing libraries were generated with the TailorMix Micro RNA Sample Preparation

version 2 protocol (SeqMatic LLC, Fremont, CA). Briefly, 3'-adapter was ligated to the RNA sample and excess 3'-adapters were removed subsequently. 5'-adapter was then ligated to the 3'-adapter ligated samples, followed by first strand cDNA synthesis. cDNA library was amplified and barcoded via enrichment PCR. Final RNA library was size-selected on an 8% TBE polyacrylamide gel. Sequencing was performed on the Illumina NextSeq 500 platform at a read length of 1 x 75 bp single-end at SR50. FASTQ files for each sample were generated using bcl2fastq software (Illumina Inc., San Diego, CA). FASTQ data were checked using FastQC tool and Bowtie2 used to map the spike-in DNA. RNA adapters were trimmed off using FastqMcf and cutadapt, with PRINSEQ used in the quality filtering step. Bowtie was used to map against the human reference genome (GRCh37). DEseq was used for abundance determination and differential expression analysis (38–41). The miRNA database was added, and the pathway analysis was performed using TarBase v7.0 of KEGG analysis (mirPath v.2, Diana tools). The heatmap was created after adding all the miRNAs in the KEGG analysis and selecting pathways union with settings of *p*-Value threshold at 0.05 using enrichment analysis method of Fisher's Exact Test (Hypergeometric Distribution).

Statistical Analysis

A two-tailed Wilcoxon signed rank test for paired test and Mann-Whitney test was used to evaluate the evidence of a

difference between the cells *in vitro* and *ex vivo* with and without EVs. All statistical analyses were conducted using GraphPad Prism 5.01 software.

RESULTS

Data From Human Donor Corneal Endothelial Cells (*n* = 40)

Average age of 62.75 ± 6.22 (mean \pm SD) years, endothelial cell density of $1,800 \pm 95.34$ cells/mm², post-mortem interval of 12.48 ± 5.68 h with preservation time of 12.08 ± 4.76 days from the donor corneas was recorded.

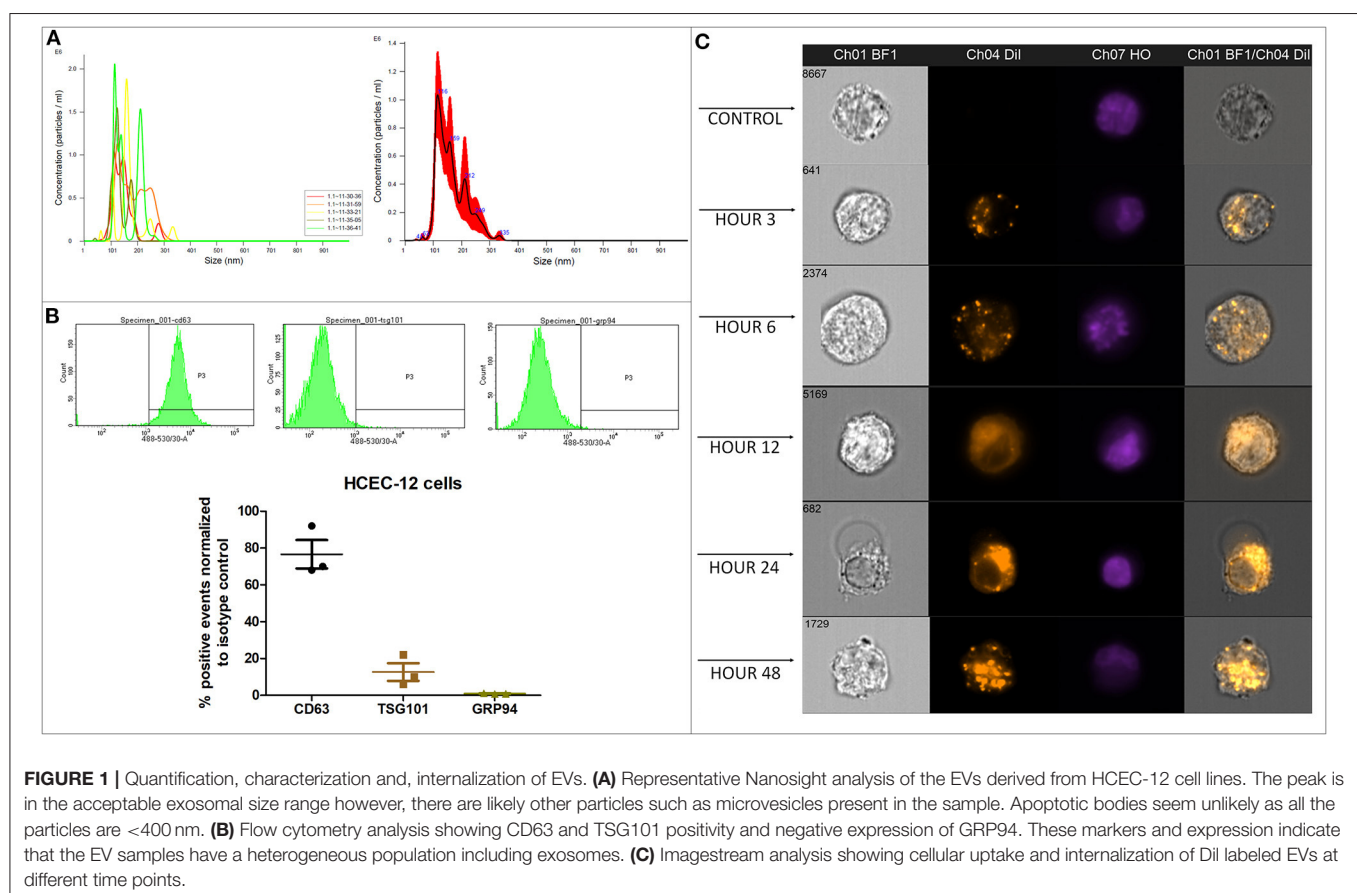
Quantification and Characterization of EVs From HCEC-12 Cells

NanoSight Analysis (*n* = 3)

Average concentration of $1.23 \times 10^9 \pm 5.63 \times 10^7$ particles/mL were found from approximately 18 million cells using Nanosight analysis i.e., ~68 EVs per cell. The particles were distributed in the size range of exosomes and microvesicles (**Figure 1A**, **Supplementary Video 1**).

Flow Cytometry (*n* = 3)

Flow cytometry analysis showed that the EV samples were positive for CD63 and TSG101 and did not express GRP94 (**Figure 1B**).



Quantification and characterization indicated that the extracted EV solution contained a heterogeneous population of exosomes and microvesicles.

Cellular Uptake and Internalization of EVs Using Dil Labeling and Imagestream Analysis on HCEC-12 Cells

Confocal Imaging (n = 3)

Dil labeled the lipid bilayer of the EVs. The 3D image showed that the EVs were internalized inside the cell either on or surrounding the nucleus or in the cytoplasmic region within 24 h (Supplementary Figure 1A). The EVs were visible inside the cells as early as 3 h after addition (Supplementary Figure 1B). A gradual increase in the uptake of EVs was observed between 3 and 48 h (Supplementary Figure 1B).

Imagestream Analysis (n = 3)

Dil-labeled EVs showed internalization by 3 h. However, Dil uptake and internalization of EVs was at its peak at 48 h (Figure 1C, Supplementary Figure 1C). The localization was not specific to a particular cellular organelle and was distributed throughout the cell.

Effect of EV Uptake on Proliferation, Cell Numbers and Doubling Time of HCEC-12 Cells and HCEncs

HCEC-12 (n = 40)

Proliferation rate of HCEC-12 cells without EVs was significantly higher compared to the cells with EVs at 12, 24, and 48 h (Figures 2A,B). The cell numbers significantly increased from 80,000 cells to 145,000 in cells without EVs compared to 115,000 in cells with EVs (Figure 2C). Cell doubling time from the cells without EVs group was significantly less i.e., <4 days compared with the EVs group, which was over 6 days (Figure 2D) (Table 1).

HCEncs (n = 40)

HCEncs without EVs showed 99% confluency by day 9 compared to 88% confluency observed in cells with EVs (Figure 2E). Proliferation rate was significantly higher in cells without EVs compared to the cells with EVs at days 3, 5, 7 and 9 (Figure 2F). The cell numbers significantly increased from 70,000 cells to 200,000 in cells without EVs compared to 160,000 in cells with EVs (Figure 2G). Cell doubling time from the cells without EVs was significantly less i.e., <4 days compared with the EVs group, which was over 4 days (Figure 2H) (Table 1).

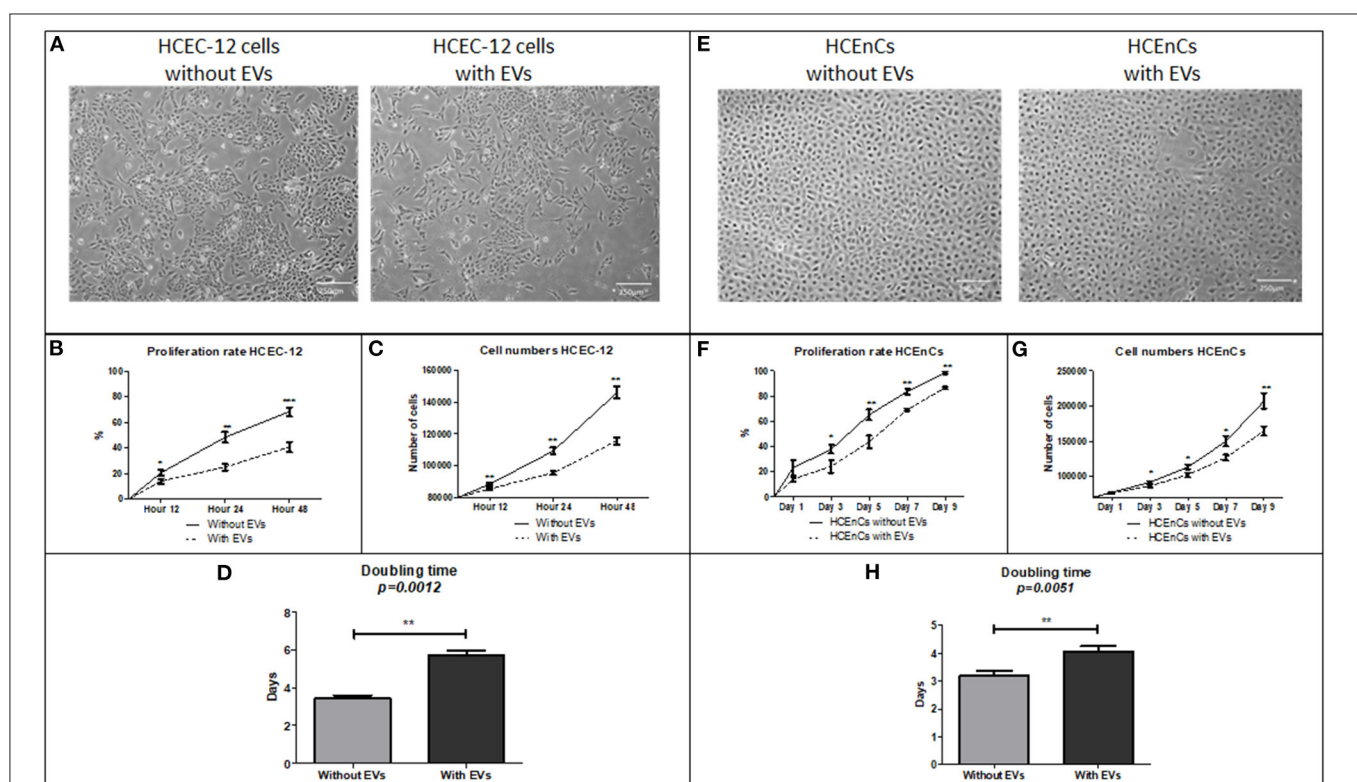


FIGURE 2 | Morphology, proliferation rate, cell doubling time and rate on HCEC-12 and HCEncs. **(A)** Morphology of cells was found to be normal without much changes in cellular shape or size. This also helped in checking the confluency rate of cells. **(B)** Statistically significantly higher proliferation rate was observed in cells without EVs. **(C)** Cell numbers significantly increased and **(D)** cell doubling time significantly decreased in the absence of EVs. **(E)** morphological difference was observed in cells with EVs. However, the cells were fully confluent by day 9 without EVs. **(F)** Statistically significantly higher proliferation rate was observed in cells without EVs. **(G)** Cell numbers significantly increased and **(H)** cell doubling time significantly decreased in the absence of EVs. Scale = 250 μ m. * $p < 0.05$; ** $p < 0.01$; *** $p < 0.001$.

TABLE 1 | Analysis of parameters such as proliferation rate, doubling time and rate, live/dead and apoptosis, hexagonality and cell area.

HCEC-12	Without EVs	With EVs	HCEncs	Without EVs	With EVs
Proliferation (%)			Proliferation (%)		
Hour 12	21 ± 2	14 ± 3	Day 1	23 ± 6	14 ± 2
Hour 24	48 ± 4	25 ± 3	Day 3	38 ± 3	24 ± 5
Hour 48	68 ± 3	40 ± 4	Day 5	65 ± 4	44 ± 6
			Day 7	84 ± 2	69 ± 2
			Day 9	98 ± 2	87 ± 1
Cell doubling (no. of cells)			Cell doubling (no. of cells)		
Hour 12	88,400 ± 690	85,333 ± 832	Day 1	77,250 ± 760	75,800 ± 483
Hour 24	109,180 ± 2,106	95,433 ± 1,322	Day 3	91,370 ± 1,655	86,116 ± 1,794
Hour 48	145,760 ± 3,678	115,615 ± 2,196	Day 5	113,010 ± 3,214	101,910 ± 2,854
			Day 7	149,832 ± 7,238	126,516 ± 4,190
			Day 9	207,050 ± 11,010	164,616 ± 6,294
Doubling time (days)	3 ± 1	6 ± 1	Doubling time (days)	3 ± 2	4 ± 1
Live (%)	96 ± 1	94 ± 2	Live (%)	95 ± 1	92 ± 2
Dead (%)	1 ± 1	2 ± 1	Apoptotic (%)	4 ± 2	8 ± 3
Apoptotic (%)	2 ± 1	3 ± 1	Hexagonality (%)	72 ± 3	67 ± 5
Hexagonality (%)	72 ± 6	69 ± 7	Cell area (%)	401 ± 25	443 ± 33
Cell area (%)	407 ± 18	427 ± 16			

Corneal endothelial cells with EVs inhibited the proliferation of cells and increased the cell doubling time.

Effect of EV Uptake on Viability of Cells Using HEC Staining

HCEC-12 (n = 6)

HEC staining showed viability (calcein AM positive cells) in both, cells without (Figure 3A) and with EVs (Figure 3B). The cells without EVs showed a higher number of viable cells compared to the cells with EVs (Figure 3C), although it was found to be non-significant.

HCEncs (n = 6)

HEC staining showed viable cells (calcein am positive cells) in both, cells without (Figure 3D) and with EVs (Figure 3E). The cells without EVs showed a higher number of viable cells compared to the cells with EVs (Figure 3F), but not found to be significantly different.

This indicated that addition of 10% EVs in the cells does not affect the cell viability (Table 1).

Effect of EVs on Cell Apoptosis Using TUNEL Assay

HCEC-12 (n = 6)

Cells without EVs (Figure 4A) and with EVs (Figure 4B) showed apoptotic cells. However, they were not found to be statistically significantly different (Figure 4C) (Table 1).

HCEncs (n = 6)

Cells from human donor tissues cultured without EVs (Figure 4D) showed a significantly lower number of

apoptotic cells compared with the cells containing EVs (Figures 4E,F).

The data indicated that EVs could contain pro-apoptotic factors that induce apoptosis in human donor corneal endothelial cells.

Effect of EVs on Expression of Specific Proteins-ZO-1 Staining for Tight Junctions and Analysis of Hexagonality and Cell Area, and Na⁺/K⁺-ATPase for Pump Functions

ZO-1 Staining on HCEC-12 (n = 6)

HCEC-12 cells without EVs (Figure 5A) and with EVs (Figure 5B) showed the expression of ZO-1. As corneal endothelial cells are a monolayer of hexagonal cells, it is important to determine the hexagonality of these cells, which further indicates whether the cells are differentiating into other cell types or maintaining their phenotype after addition of EVs. There was no significant difference between the cells with and without EVs in terms of hexagonality (Figure 5C) or cell area (Figure 5D) (Table 1). ZO-1 expression was lost at multiple sites in both groups.

ZO-1 Staining on HCEncs (n = 6)

HCEncs without EVs (Figure 5E) and with EVs (Figure 5F) expressed ZO-1. Although there was no significant difference between the cells with and without EVs in terms of hexagonality (Figure 5G), the cells without EVs showed significantly smaller cell area compared to the cells with EVs (Figure 5H) (Table 1). ZO-1 expression was found to be homogeneously distributed at the intercellular junctions in the sample without EVs compared

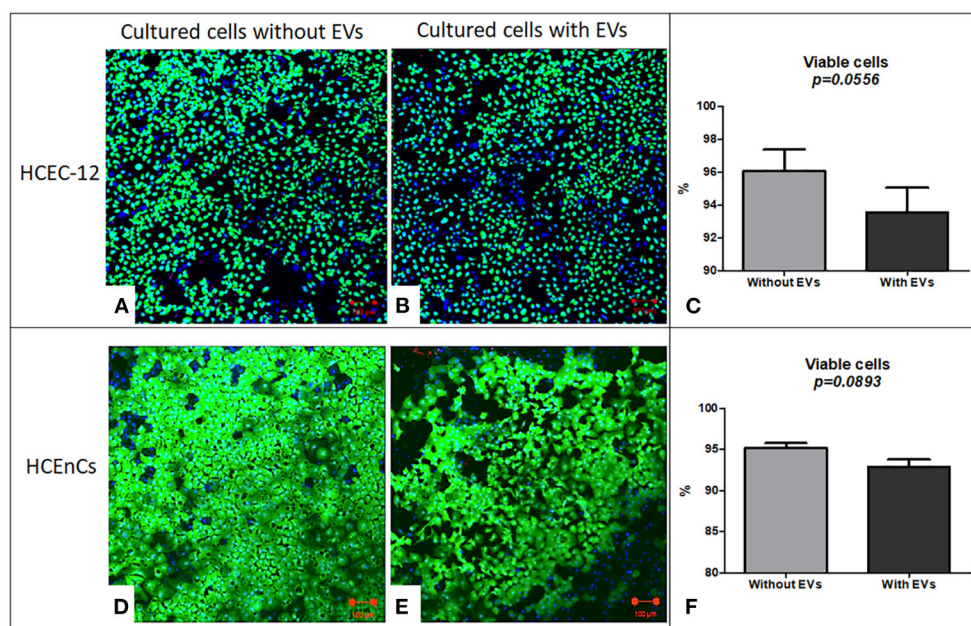


FIGURE 3 | Live/dead analysis using Hoechst, Ethidium homodimer and Calcein AM staining (HEC) / triple labeling. In HCEC-12 lines (A) higher number of viable cells were observed in cells without EVs compared with that (B) with EVs. (C) The percentage viability was not found to be significantly different in cells with or without EVs. In HCEnC, a similar trend was observed i.e., a higher number of viable cells (D) without EVs compared to (E) with EVs showing no statistical significance in (F) viability. Ethidium homodimer positive cells were not observed. (Hoechst, nuclear in blue staining and Calcein AM, live cells in green staining). Scale = 100 μ m.

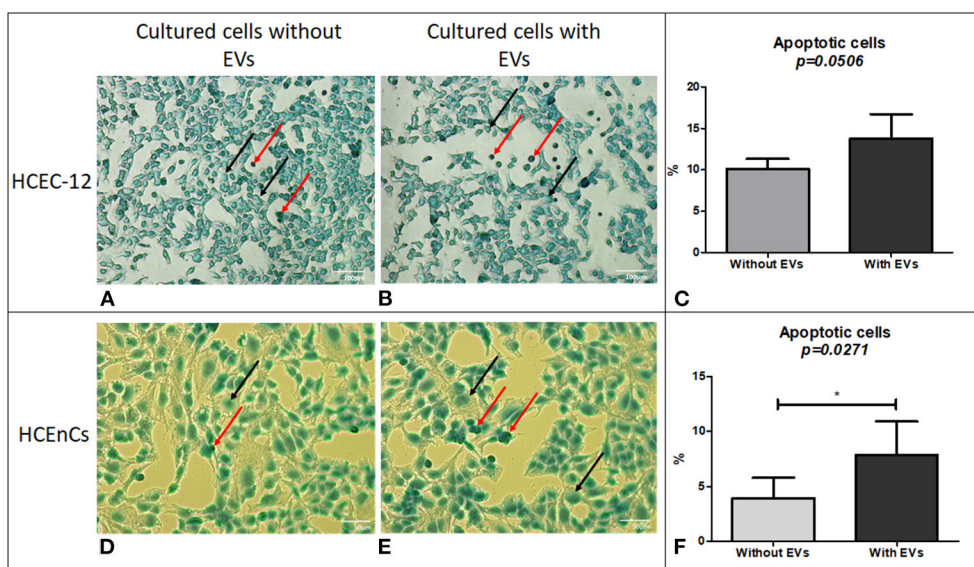
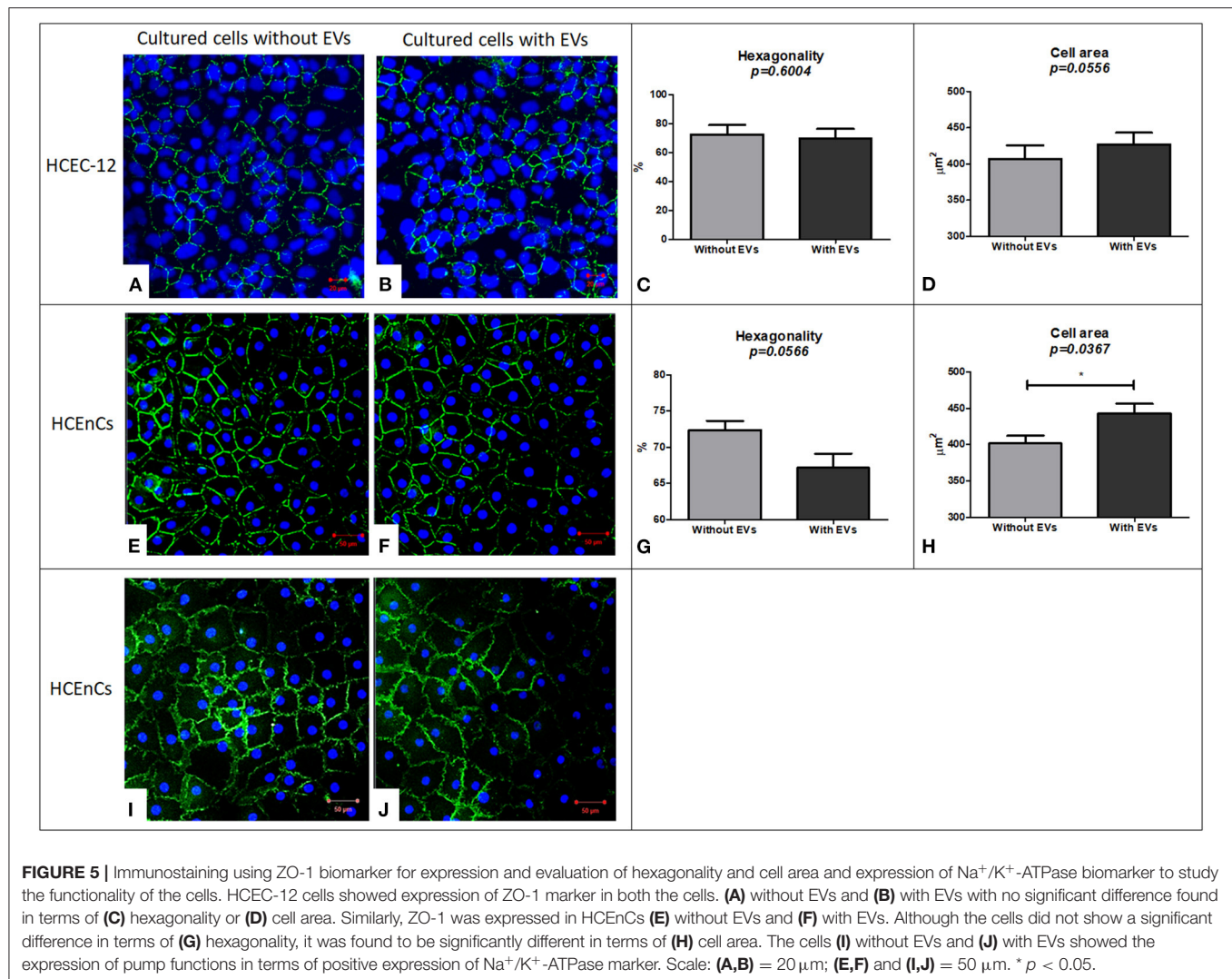


FIGURE 4 | Cell apoptosis using TUNEL assay. Although a lower number of cells were found to be apoptotic in HCEC-12 (A) without EVs compared (B) with EVs, (C) a statistical significance was not observed between the two groups. However, HCEnC showed lower number of apoptotic cells (D) without EVs compared to (E) with EVs and was found to be (F) significantly different. (Black arrow, Methyl green counterstain; red arrow, apoptotic cells). Scale: (A,B) = 100 μ m; (D,E) = 50 μ m. * $p < 0.05$.

to loss of ZO-1 expression at multiple sites with EVs indicating that the EVs may influence the development and maintenance of tight junctions. However, this must be further investigated as it is a subjective evaluation.

Na⁺/K⁺-ATPase Staining on HCEnC (n = 6)

As a functional marker, Na⁺/K⁺-ATPase was expressed in cells without EVs (Figure 5I) and with EVs (Figure 5J). However, it was not expressed throughout the sample in the presence of



EVs indicating that EVs may also influence the pump-function outcomes of HCEncs. This staining was not performed on cell lines as it was only used to determine the effect of EVs on the function of HCEncs.

Effect of EVs on Corneal Endothelial Wound Healing

Wound Healing Rate on HCEC-12 Cells (n = 6)

HCEC-12 with EVs slowed down the wound healing response (Figure 6A) and, it was found to be statistically significantly different at day 1 (Figure 6B). Wound was completely healed within 3 days in both the groups (Table 2).

Wound Healing Rate on ex vivo Human Donor Corneas (n = 6)

Human donor corneas without EVs showed faster wound healing response compared with the cells with EVs (Figure 6C). A statistical significance was observed at day 3 and 4 where the cells

without EVs showed faster wound healing compared to the cells with EVs (Figure 6D) (Table 2).

Wound Healing Response on ex vivo Porcine and Rabbit Corneas With and Without HCEC-12 Derived EVs (n = 6 Each)

Porcine corneas with human EVs showed a slow wound healing response (Figure 7A) that was statistically significant at days 2 and 3 (Figure 7B). Rabbit corneas with human EVs slowed the wound healing response (Figure 7C) and was found to be significantly different at day 2 (Figure 7D) (Table 2). This indicated that human EVs affect the migration of endothelial cells of other species that have otherwise shown to possess natural capacity to proliferate *in vivo*.

Next Generation Sequencing of EVs Derived From HCEC-12 Cells

Next generation sequencing showed 13 microRNAs (Figure 8A) from HCEC-12 derived EVs. It was observed that some of these

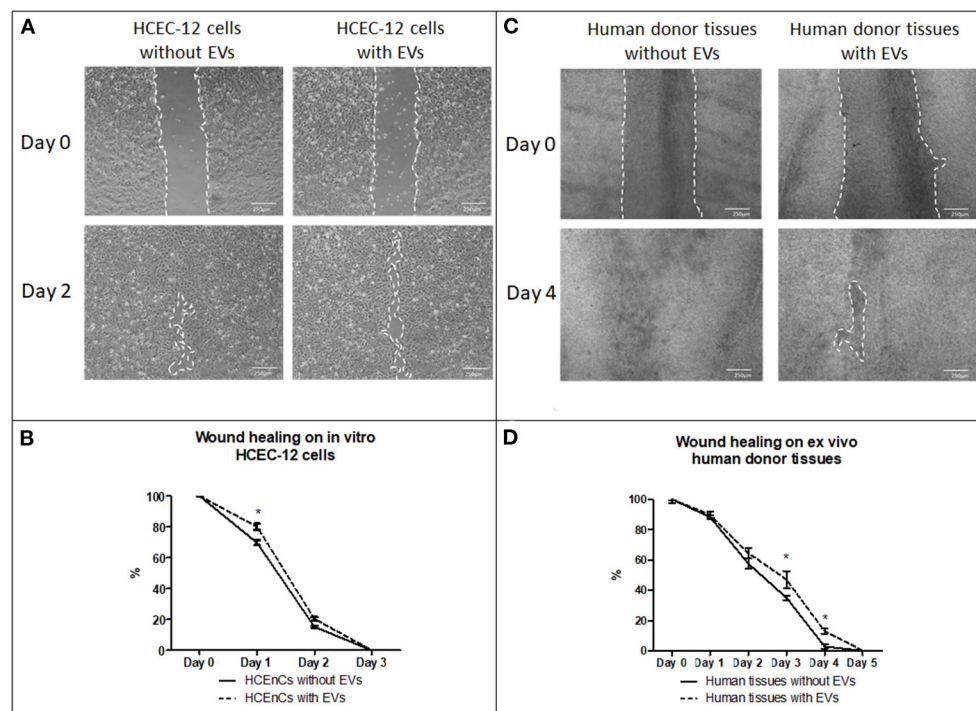


FIGURE 6 | Effect of EVs derived from HCEC-12 cells on *in vitro* cells and *ex vivo* human donor corneas –scratch assay. **(A)** wound healing on HCEC-12 cell line showing slow response in presence of EVs. **(B)** data showing early slow wound healing response on HCEC-12 cells in presence of EVs. **(C)** Wound healing response on *ex vivo* human donor tissues without and with EVs. **(D)** data showing statistically significantly slow wound healing response of HCECs on donor tissues in presence of EVs. * $p < 0.05$.

TABLE 2 | Percentage wound healing *in vitro* and on *ex vivo* human, pig and rabbit tissues.

Wound healing (%)	HCEC-12 cells without EVs	HCEC-12 cells with EVs
Day 1	70 ± 2	80 ± 2
Day 2	15 ± 1	20 ± 1
Day 3	0 ± 0	0 ± 0
Wound healing (%)	Human tissues without EVs	Human tissues with EVs
Day 1	88 ± 1	90 ± 2
Day 2	57 ± 3	65 ± 3
Day 3	35 ± 1	47 ± 6
Day 4	3 ± 1	13 ± 2
Day 5	0 ± 0	0 ± 0
Wound healing (%)	Pig tissue without human EVs	Pig tissue with human EVs
Day 1	77 ± 5	92 ± 4
Day 2	33 ± 5	78 ± 6
Day 3	2 ± 2	26 ± 1
Day 4	0 ± 0	0 ± 0
Wound healing (%)	Rabbit tissue without human EVs	Rabbit tissue with human EVs
Day 1	81 ± 17	77 ± 12
Day 2	3 ± 2	18 ± 4
Day 3	0 ± 0	3 ± 1

microRNAs were actively involved in cell cycle pathway and inducing cellular apoptosis (Figure 8B).

DISCUSSION

Exosomes derived from different cell types has been involved in a wide panoply of therapeutic functions (13). Exosomes are enriched in major histocompatibility complexes and do not respond to immunosuppressive molecules thus encouraging their use as therapeutic agents (42–45). This is mainly due to their critical role in the transfer of bioactive molecules within and between tissues. However, the challenge remains in learning the effect of EVs derived from corneal endothelial cells. Anatomically, the posterior cornea is placed in an enclosed environment compared to the ocular surface. EVs therefore have a higher chance of retention in the anterior chamber than on the surface as they get washed by continuous tear flow. Therefore, the release and the effects of the EVs derived from corneal endothelial cells remain an interesting area of investigation.

In our study, the characterization i.e., size distribution and, positive expression of CD63 and TSG101 and, negative expression of GRP94 indicated that the isolated sample had a heterogeneous mixture of EVs, including exosomes. However, purifying and enriching exosomes will be crucial if intended

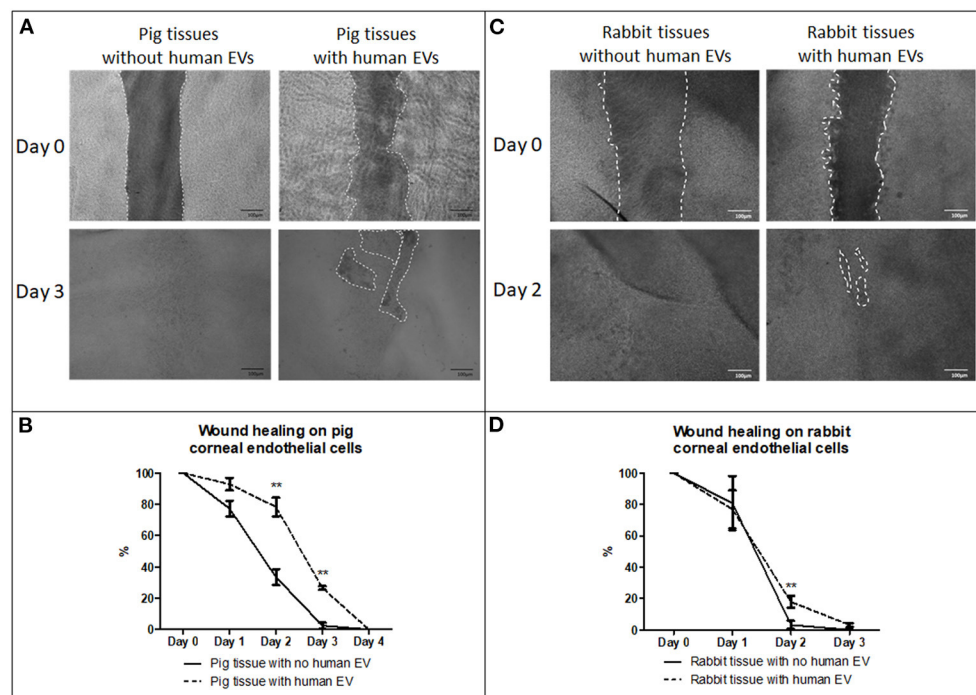


FIGURE 7 | Effect of EVs derived from HCEC-12 cells on ex vivo porcine and rabbit corneas. **(A)** slow wound healing response was observed on porcine corneal endothelial cells when exposed to HCEC-12 derived EVs, **(B)** which showed statistical significance. Similar trend was observed on, **(C)** the rabbit tissues when exposed to EVs with **(D)** significantly slow wound healing response when exposed to HCEC-12 derived EVs. * $p < 0.05$; ** $p < 0.01$.

for re-modeling the exosomal cargo for therapeutic purpose. Dil labeling showed that the cells take up small number of EVs at 3, 6, and 12 h however, a higher cellular uptake of EVs was observed at 24 and 48 h. EVs require longer time to be completely internalized in the cells (**Supplementary Figure 1C**) however, the localization appears to be dispersed, as the EVs were observed both, on the surface, in the cytoplasm and on the nucleus (**Supplementary Figures 1A,B**). The EVs did not show any change in cell proliferation after 48 h (unpublished data) therefore, to observe the chronic effect, the EVs were added every alternate day while refreshing the media. This showed that the EVs have a shorter life span to deliver the cargo inside the cell and continuous addition of EVs is required to see a long-lasting detrimental effect. This would be extremely important for the development of EV therapy. Continuous presence and uptake of EVs in the cell inhibits proliferation, cell doubling time and rate, further highlighting that the continuous release and uptake of EVs may result in reduced proliferative capacity of CECs *in vivo*. EVs at 10% concentration did not induce mortality to the normal functioning cell however, 100% concentration of EVs showed mortality of cells during the dose response study (data not shown). In addition, the expression of tight junction or pump function proteins are not significantly affected although the expression was not consistent throughout the surface. However, in an attempt to survive and function, the cells enlarged to cover the vacant space available due to loss of surrounding cells thus increasing polymorphism and pleomorphism. These features are like FECD cells i.e., the cells show polymegathism,

further indicative of increased exosomal activity under stressed environment. Although EVs are released by the cells routinely, stress of any form could release excessive EVs from the CECs in the anterior chamber of the eye. This continuous release of EVs could result into uptake of more EVs by the cells resulting into overexpression of certain miRNAs that could possibly inhibit the proliferation of cells.

FECD which is one of the leading causes of corneal blindness and transplant has shown to be susceptible to oxidative DNA damage and oxidative stress-induced apoptosis than normal corneal endothelial cells. Increased activation of p53 in FECD has suggested that it mediates cell death in susceptible corneal endothelial cells. This means that p53 plays a critical role in complex mechanisms regulating oxidative-stress-induced apoptosis in FECD (46). Studies have also reported that excessive apoptosis may be an important mechanism in the pathogenesis of FECD (47). The cargo analysis in our study using NGS showed that hsa-miR-196b-5p is involved in p53 pathway. In addition, it has been observed that EVs influence immune activation through cell-to-cell communication, while oxidative stress enhances exosome release from stressed cells. In our study, we starved the cells to obtain a higher quantity of EVs for experiments with serum depleted media to enhance the release of EVs. This means that the cells, when stressed, release excess EVs (48–50). Our hypothesis here is that following oxidative stress, normal corneal cells start releasing excessive EVs, which contain factors that promote apoptosis. In addition, as endothelial cells are in a closed environment,

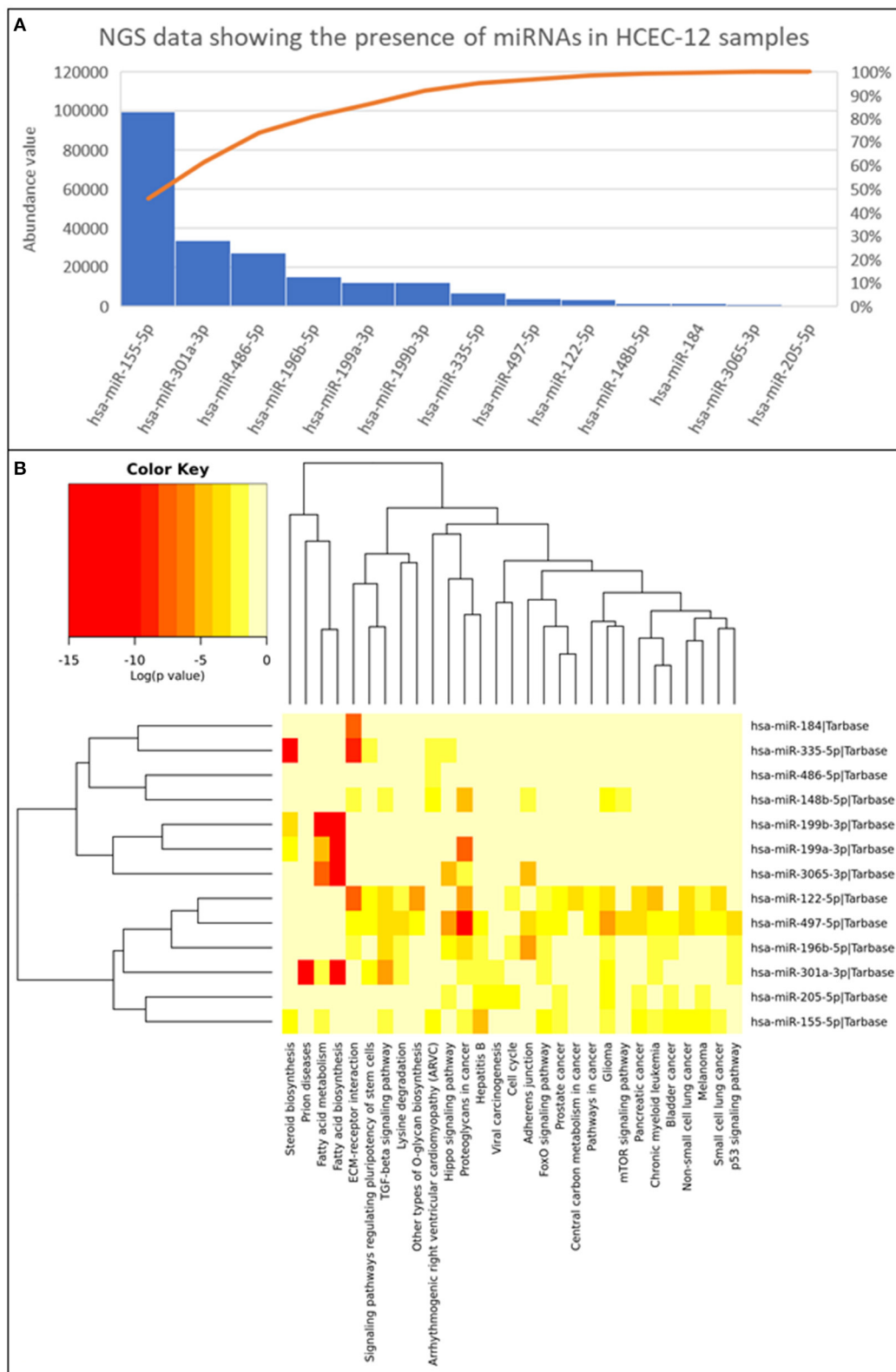


FIGURE 8 | Next generation sequencing data showing the presence of 13 miRNAs and their abundance values derived from HCEC-12 cells. **(A)** The Pareto chart plot shows the distribution of the data in descending order of frequency with a cumulative line on a secondary axis as a percentage of the total. **(B)** Heatmap of all the miRNAs and their associated pathways.

continuous release of EVs and cellular uptake of excessive EVs may result in FECD. Therefore, the next challenge will be to investigate the specifics of each miRNA and reverse the inhibiting factor to increase the proliferation rate of these cells and to understand the pathogenesis of EV derived FECD.

CECs have shown specific properties with regards to wound healing. Primarily, the endothelium heals by cell migration followed by increased cell spreading. This process may be followed by endothelial-mesenchymal transformation. Cell proliferation, however, plays a secondary role (51). This could be a reason of the larger cell area induced by EVs. Moreover, the cells reached confluence with lower cell count which again highlights that the cells expanded in size but not in numbers. In terms of migration and wound healing response, cells supplemented with EVs showed reduced cell migration or wound closure compared to the cells without EVs, *in vitro*. These results were translated to *ex vivo* human corneas as well. It has been shown that porcine and rabbit corneal endothelial cells have a greater proliferative capacity than humans (23, 24, 26, 52). This baseline difference leads to earlier wound closure of these species compared to the humans. Both, porcine and rabbit endothelial cells treated with human EVs slowed the wound healing response. This further indicated that there are factors in the exosomal cargo of HCEC-12 derived EVs that reduce the proliferative and migration capability of the known proliferative cells of different species. Slow wound healing could be a result of stress induced by human EVs changing the microenvironment of the CECs in animal tissues and not necessarily the exosomal cargo itself *per se*. However, the EV crosstalk mechanism between human and porcine/rabbit needs to be further investigated.

EVs transfer the cargo from the originating cell to the receiving cell and influence various biological processes such as differentiation, migration, proliferation etc. The cargo, that includes DNA, RNA, mRNA, miRNA, proteins, and lipids, can modulate the cellular fate (53). miRNA have been found to be in abundance and responsible for the functions of multiple EV populations. It has been demonstrated that miRNAs act toward biological characteristics including proliferation, cellular apoptosis, migration, and tumorigenesis. In our study, we reported 13 miRNAs with their abundance values (Figure 8). Some of which were found to have key roles in cell cycle (hsa-miR-205-5p; hsa-miR-196b-5p; hsa-miR-122-5p), adherence junction (hsa-miR-196b-5p; hsa-miR-497-5p; hsa-miR-3065-3p; hsa-miR-148b-5p) and p53 signaling pathway (hsa-miR-301a-3p; hsa-miR-196b-5p; hsa-miR-497-5p). hsa-miR-196b-5p was found in all three biological functions however, its role is mainly known in the progression of cancer cells (54–57). It has not been studied in the ocular research thus needing extensive research.

The therapeutic efficacy of corneal endothelial cell derived EVs have not been studied and their secretions to restore tissue homeostasis enhancing tissue recovery, reparation, and regeneration needs attention. While many functions of EVs

have been identified, investigations about EV functions in many specialized tissues of the eye are just at the preliminary stage. However, as we observed that the EVs inhibit the growth of HCECs, as an alternative, reprogramming the EVs to induce growth and proliferation of cells could be a potential future therapeutic approach. Enriching exosomes from EVs and utilizing them as a carrier for a desired therapeutic molecule/miRNA would further supplement the future development for the corneal endothelial treatment.

DATA AVAILABILITY STATEMENT

The datasets presented in this article are not readily available because they are in the internal server of UCL Institute of Ophthalmology. Requests to access the datasets should be directed to Sajjad Ahmad.

ETHICS STATEMENT

Ethical review and approval was not required for the animal study because the study was performed on tissues from dead animals.

AUTHOR CONTRIBUTIONS

All authors listed have made a substantial, direct, and intellectual contribution to the work and approved it for publication.

FUNDING

This study was fully funded by Moorfields Eye Charity grant (R170041A) to SA (Nov 2016-Oct 2021). The publication and open access of this article has been enabled by a grant from Moorfields Eye Charity [GR001457].

ACKNOWLEDGMENTS

Dr. Alice Davidson, UCL Institute of Ophthalmology, London, UK for generously gifting HCEC-12 cell line. Moorfields NIHR Biomedical Research Centre, London, UK. The authors thank Mr. Owen Hughes and Mr. PJ Chana from Luminex corporation, Newcastle upon Tyne, UK, for their help and expertise in setting up the flow cytometry experiments.

SUPPLEMENTARY MATERIAL

The Supplementary Material for this article can be found online at: <https://www.frontiersin.org/articles/10.3389/fmed.2021.753555/full#supplementary-material>

Supplementary Figure 1 | Cellular uptake and 3D imaging using confocal microscopy. (A) A z-stack 3D image showing internalization / localization of EVs in the cell. (B) Cellular uptake of Dil labeled EVs (stained in red) at different time points. (C) Imagestream analysis showing the uptake and internalization of Dil labeled EVs at different time points.

Supplementary Video 1 | Nanosight analysis showing the presence of EVs derived from HCEC-12 cells.

REFERENCES

- Parekh M, Romano V, Hassani K, Testa V, Wongvisavavit R, Ferrari S, et al. Biomaterials for corneal endothelial cell culture and tissue engineering. *J Tissue Eng.* (2021) 12:2041731421990536. doi: 10.1177/2041731421990536
- Bourne WM. Biology of the corneal endothelium in health and disease. *Eye.* (2003) 17:912–8. doi: 10.1038/sj.eye.6700559
- Stiemke MM, Edelhauser HF, Geroski DH. The developing corneal endothelium: correlation of morphology, hydration and Na/K ATPase pump site density. *Curr Eye Res.* (2009) 10:145–56. doi: 10.3109/02713689109001742
- Senoo T, Joyce NC. Cell cycle kinetics in corneal endothelium from old and young donors. *Invest Ophthalmol Vis Sci.* (2000) 41:660–7.
- Joyce NC, Navon SE, Roy S, Zieske JD. Expression of cell cycle-associated proteins in human and rabbit corneal endothelium in situ. *Invest Ophthalmol Vis Sci.* (1996) 37:1566–75.
- Bahn CF, Glassman RM, MacCallum DK, Lillie JH, Meyer RF, Robinson BJ, et al. Postnatal development of corneal endothelium. *Invest Ophthalmol Vis Sci.* (1986) 27:44–51.
- Nucci P, Brancato R, Mets MB, Shevell SK. Normal endothelial cell density range in childhood. *Arch Ophthalmol.* (1990) 108:247–8. doi: 10.1001/archoph.1990.01070040099039
- Yee RW, Matsuda M, Schultz RO, Edelhauser HF. Changes in the normal corneal endothelial cellular pattern as a function of age. *Curr Eye Res.* (2009) 4:671–8. doi: 10.3109/02713688509017661
- Wilson SE, Bourne WM, Brubaker RF. Effect of dexamethasone on corneal endothelial function in Fuchs' dystrophy. *Invest Ophthalmol Vis Sci.* (1988) 29:357–61.
- Krachmer JH. Posterior polymorphous corneal dystrophy: a disease characterized by epithelial-like endothelial cells which influence management and prognosis. *Trans Am Ophthalmol Soc.* (1985) 83:413–75.
- Pandrowala H, Bansal A, Vemuganti GK, Rao GN. Frequency, distribution, and outcome of keratoplasty for corneal dystrophies at a tertiary eye care center in South India. *Cornea.* (2004) 23:541–6. doi: 10.1097/01.ic.0000126324.58884.b9
- Levy SG, McCartney ACE, Baghai MH, Barrett MC, Moss J. Pathology of the iridocorneal-endothelial syndrome. the ICE-cell. *Invest Ophthalmol Vis Sci.* (1995) 36:2592–601.
- Nuzzi R, Buono L, Scalabrin S, DeIulio M, Bussolati B. Effect of stem cell-derived extracellular vesicles on damaged human corneal endothelial cells. *Stem Cells Int.* (2021) 2021:6644463. doi: 10.1155/2021/6644463
- Miyamoto T, Sumioka T, Saika S. Endothelial mesenchymal transition: a therapeutic target in retrocorneal membrane. *Cornea.* (2010) 29:S52–6. doi: 10.1097/ICO.0b013e3181efe36a
- Pulse KS, Brand RJ, Cohen SR, Guillon M. Hypoxic effects on corneal morphology and function. *Invest Ophthalmol Vis Sci.* (1990) 31:1542–54.
- Gain P, Jullienne R, He Z, Aldossary M, Acquart S, Cognasse F, et al. Global survey of corneal transplantation and eye banking. *JAMA Ophthalmol.* (2016) 134:167–73. doi: 10.1001/jamaophthalmol.2015.4776
- Okumura N, Koizumi N, Ueno M, Sakamoto Y, Takahashi H, Tsuchiya H, et al. ROCK inhibitor converts corneal endothelial cells into a phenotype capable of regenerating in vivo endothelial tissue. *Am J Pathol.* (2012) 181:268–77. doi: 10.1016/j.ajpath.2012.03.033
- Peh GSL, Ang HP, Lwin CN, Adnan K, George BL, Seah XY, et al. Regulatory compliant tissue-engineered human corneal endothelial grafts restore corneal function of rabbits with bullous keratopathy. *Sci Rep.* (2017) 7:14149. doi: 10.1038/s41598-017-14723-z
- Kinoshita S, Koizumi N, Ueno M, Okumura N, Imai K, Tanaka H, et al. Injection of cultured cells with a ROCK inhibitor for bullous keratopathy. *N Engl J Med.* (2018) 378:995–1003. doi: 10.1056/NEJMoa1712770
- Parekh M, Peh GSL, Mehta JS, Ahmad S, Ponzin D, Ferrari S. Effects of corneal preservation conditions on human corneal endothelial cell culture. *Exp Eye Res.* (2019) 179:93–101. doi: 10.1016/j.exer.2018.11.007
- Van Horn DL, Hyndrick RA. Endothelial wound repair in primate cornea. *Exp Eye Res.* (1975) 21:113–24. doi: 10.1016/0014-4835(75)90076-7
- Khodadoust AA, Green K. Physiological function of regenerating endothelium. *Invest Ophthalmol Vis Sci.* (1976) 15:96–101.
- Van Horn DL, Sendele DD, Seidemen S, Buco PJ. Regenerative capacity of the corneal endothelium in rabbit and cat. *Invest Ophthalmol Visual Sci.* (1977) 17:597–613.
- Gospodarowicz D, Greenburg G, Alvarado J. Transplantation of cultured bovine corneal endothelial cells to rabbit cornea: clinical implications for human studies. *Proc Natl Acad Sci U S A.* (1979) 76:464–8. doi: 10.1073/pnas.76.1.464
- Marquez-Curtis LA, McGann LE, Elliott JAW. Expansion and cryopreservation of porcine and human corneal endothelial cells. *Cryobiology.* (2017) 77:1–13. doi: 10.1016/j.cryobiol.2017.04.012
- Nicholls S, Bailey M, Mitchard L, Dick AD. Can the corneal endothelium of the pig proliferate in vivo? *ACTA Ophthalmol.* (2009). doi: 10.1111/j.1755-3768.2009.2271.x
- Grange C, Tritta S, Tapparo M, Cedrino M, Tetta C, Camussi G, et al. Stem cell-derived extracellular vesicles inhibit and revert fibrosis progression in a mouse model of diabetic nephropathy. *Sci Rep.* (2019) 9:1–13. doi: 10.1038/s41598-019-41100-9
- Giebel B, Kordelas L, Börger V. Clinical potential of mesenchymal stem/stromal cell-derived extracellular vesicles. *Stem Cell Investigation.* (2017) 4:84. doi: 10.21037/sci.2017.09.06
- Kalluri R, LeBleu VS. The biology, function, and biomedical applications of exosomes. *Science.* (2020) 367:eaau6977. doi: 10.1126/science.aau6977
- Parekh M, Peh G, Mehta JS, Ramos T, Ponzin D, Ahmad S, et al. Passaging capability of human corneal endothelial cells derived from old donors with and without accelerating cell attachment. *Exp Eye Res.* (2019) 189:107814. doi: 10.1016/j.exer.2019.107814
- Parekh M, Graceffa V, Bertolin M, Elbadawy H, Salvalaio G, Ruzza A, et al. Reconstruction and regeneration of corneal endothelium: a review on current methods and future aspects. *J Cell Sci Ther.* (2013) 4:146. doi: 10.4172/2157-7013.1000146
- Parekh M, Ferrari S, Sheridan C, Kaye S, Ahmad S. Concise review: an update on the culture of human corneal endothelial cells for transplantation. *Stem Cells Transl Med.* (2016) 5:258–64. doi: 10.5966/sctm.2015-0181
- Parekh M, Romano V, Ruzza A, Kaye SB, Ponzin D, Ahmad S, et al. Culturing discarded peripheral human corneal endothelial cells from the tissues deemed for preloaded DMEK transplants. *Cornea.* (2019) 38:1175–81. doi: 10.1097/ICO.0000000000001998
- Peh GS, Beuerman RW, Colman A, Tan D, Mehta JS. Human corneal endothelial cell expansion for corneal endothelium transplantation: an overview. *Transplantation.* (2011) 91:811–9. doi: 10.1097/TP.0b013e3182111f01
- Peh GSL, Chng Z, Ang HP, Cheng TYD, Adnan K, Seah XY, et al. Propagation of human corneal endothelial cells: a novel dual media approach. *Cell Transplant.* (2013) 24:287–304. doi: 10.3727/096368913X675719
- Parekh M, Ruzza A, Ferrari S, Ponzin D. Preservation of preloaded DMEK lenticles in dextran and non-dextran-based organ culture medium. *J Ophthalmol.* (2016) 2016:5830835. doi: 10.1155/2016/5830835
- Parekh M, Ramos T, O'Sullivan F, Meleady P, Ferrari S, Ponzin D, et al. Human corneal endothelial cells from older donors can be cultured and passaged on cell-derived extracellular matrix. *Acta Ophthalmol.* (2021) 99:e512–22. doi: 10.1111/aos.14614
- Livak KJ, Schmittgen TD. Analysis of relative gene expression data using real-time quantitative PCR and the 2^{−(Delta Delta C(T))} method. *Methods.* (2011) 25:402–8. doi: 10.1006/meth.2001.1262
- Kuhn RM, Haussler D, Kent WJ. The UCSC genome browser and associated tools. *Brief Bioinform.* (2013) 14:144–61. doi: 10.1093/bib/bbs038
- Langmead B, Salzberg SL. Fast gapped-read alignment with Bowtie 2. *Nat Methods.* (2012) 9:357–9. doi: 10.1038/nmeth.1923
- Li H, Handsaker B, Wysoker A, Fennell T, Ruan J, Homer N, et al. The sequence alignment/map format and SAMtools. *Bioinformatics.* (2009) 25:2078–9. doi: 10.1093/bioinformatics/btp352
- Escudier B, Dorval T, Chaput N, Andre F, Caby MP, Novault S, et al. Vaccination of metastatic melanoma patients with autologous dendritic cell (DC) derived-exosomes: results of the first phase I clinical trial. *J Transl Med.* (2005) 3:10. doi: 10.1186/1479-5876-3-10
- Ratajczak J, Meikus K, Kucia M, Zhang J, Reza R, Dvorak P, et al. Embryonic stem cell-derived microvesicles reprogram hematopoietic

- progenitors: evidence for horizontal transfer of mRNA and protein delivery. *Leukemia*. (2006) 20:847. doi: 10.1038/sj.leu.2404132
44. Ratajczak J, Wysoczynski M, Hayek F, Janowska-Wieczorek A, Ratajczak MZ. Membrane-derived microvesicles: important and underappreciated mediators of cell-to-cell communication. *Leukemia*. (2006) 20:1487–95. doi: 10.1038/sj.leu.2404296
 45. Katsman D, Stackpole EJ, Domin DR, Farber DB. Embryonic stem cell-derived microvesicles induce gene expression changes in Muller cells of the retina. *PLoS ONE*. (2012) 7:e50417. doi: 10.1371/journal.pone.0050417
 46. Azizi B, Fuchsluger T, Schmedt T, Chen Y, Jurkunas U. p53-regulated increase in oxidative-stress-induced apoptosis in fuchs endothelial corneal dystrophy: a native tissue model. *Invest Ophthalmol Vis Sci*. (2011) 52:9291–7. doi: 10.1167/iovs.11-8312
 47. Li QJ, Ashraf MF, Shen DF, Green WR, Stark WJ, Chan CC, et al. The role of apoptosis in the pathogenesis of fuchs endothelial dystrophy of the cornea. *Arch Ophthalmol*. (2001) 119:1597–604. doi: 10.1001/archoph.119.11.1597
 48. Eldh M, Ekström K, Valadi H, Sjöstrand M, Olsson B, Jernäs M, et al. Exosomes communicate protective messages during oxidative stress; possible role of exosomal shuttle RNA. *PLoS ONE*. (2010) 5:e15353. doi: 10.1371/journal.pone.0015353
 49. Hedlund M, Nagaeva O, Kargl D, Baranov V, Nilsson ML. Thermal- and oxidative stress causes enhanced release of NKG2D ligand-bearing immunosuppressive exosomes in leukemia/lymphoma T and B cells. *PLoS ONE*. (2011) 6:e16899. doi: 10.1371/journal.pone.0016899
 50. Chettimada S, Lorenz DR, Misra V, Dillon ST, Reeves RK, Manickam C, et al. Exosome markers associated with immune activation and oxidative stress in HIV patients on antiretroviral therapy. *Sci Rep*. (2018) 8:7227. doi: 10.1038/s41598-018-25515-4
 51. Lubinov AV, Saghizadeh M. Progress in corneal wound healing. *Prog Retin Eye Res*. (2015) 49:17–45. doi: 10.1016/j.preteyeres.2015.07.002
 52. Smeringaiova I, Merjava SR, Stranak Z, Studeny P, Bednar J, Jirsova K. Endothelial wound repair of the organ-cultured porcine corneas. *Curr Eye Res*. (2018) 43:856–65. doi: 10.1080/02713683.2018.1458883
 53. Valadi H, Ekstrom K, Bossios A, Sjostrand M, Lee JJ, Lotvall JO. Exosome-mediated transfer of mRNAs and microRNAs is a novel mechanism of genetic exchange between cells. *Nat Cell Biol*. (2007) 9:654–9. doi: 10.1038/ncb1596
 54. Xin H, Wang C, Chi Y, Liu Z. MicroRNA-196b-5p promotes malignant progression of colorectal cancer by targeting ING5. *Cancer Cell Int*. (2020) 20:119. doi: 10.1186/s12935-020-01200-3
 55. Zhang L, Luo B, Dang YW, He RQ, Peng ZG, Chen Z, et al. Clinical significance of microRNA-196b-5p in hepatocellular carcinoma and its potential molecular mechanism. *J Cancer*. (2019) 10:5355–70. doi: 10.7150/jca.29293
 56. Lee SW, Park KC, Kim JG, Moon SJ, Kang SB, Lee DS, et al. Dysregulation of MicroRNA-196b-5p and MicroRNA-375 in gastric cancer. *J Gastric Cancer*. (2016) 16:221–9. doi: 10.5230/jgc.2016.16.4.221
 57. Li J, Wang L, He F, Li B, Han R. Long noncoding RNA LINC00629 restrains the progression of gastric cancer by upregulating AQP4 through competitively binding to miR-196b-5p. *J Cell Physiol*. (2020) 235:2973–85. doi: 10.1002/jcp.29203

Conflict of Interest: The authors declare that the research was conducted in the absence of any commercial or financial relationships that could be construed as a potential conflict of interest.

Publisher's Note: All claims expressed in this article are solely those of the authors and do not necessarily represent those of their affiliated organizations, or those of the publisher, the editors and the reviewers. Any product that may be evaluated in this article, or claim that may be made by its manufacturer, is not guaranteed or endorsed by the publisher.

Copyright © 2022 Parekh, Rhys, Ramos, Ferrari and Ahmad. This is an open-access article distributed under the terms of the Creative Commons Attribution License (CC BY). The use, distribution or reproduction in other forums is permitted, provided the original author(s) and the copyright owner(s) are credited and that the original publication in this journal is cited, in accordance with accepted academic practice. No use, distribution or reproduction is permitted which does not comply with these terms.



Impact of the COVID-19 Pandemic on Corneal Transplantation: A Report From the Italian Association of Eye Banks

Rita Mencucci^{1*}, Michela Cennamo¹, Diego Ponzin², Federico Genzano Besso³, Giulio Pocobelli⁴, Matilde Buzzi¹, Carlo Nucci⁴ and Francesco Aiello⁴
on behalf of Italian Society Eye Bank Group (SIBO)

¹ Department of Neurosciences, Psychology, Pharmacology and Child Health, Eye Clinic, University of Florence, Florence, Italy, ² The Veneto Eye Bank Foundation, Venice, Italy, ³ Eye Bank of Piedmont, SSD Tissue Banks and Biorepository, Città della Salute e della Scienza, Turin, Italy, ⁴ Ophthalmology Unit, Department of Experimental Medicine, University of Rome "Tor Vergata", Rome, Italy

OPEN ACCESS

Edited by:

Hannah Levis,
University of Liverpool,
United Kingdom

Reviewed by:

Yousef Ahmed Fouad,
Ain Shams University, Egypt
Mo Ziaei,
The University of Auckland,
New Zealand

*Correspondence:

Rita Mencucci
rita.mencucci@unifi.it

Specialty section:

This article was submitted to
Ophthalmology,
a section of the journal
Frontiers in Medicine

Received: 28 December 2021

Accepted: 09 February 2022

Published: 22 March 2022

Citation:

Mencucci R, Cennamo M, Ponzin D, Genzano Besso F, Pocobelli G, Buzzi M, Nucci C and Aiello F (2022) Impact of the COVID-19 Pandemic on Corneal Transplantation: A Report From the Italian Association of Eye Banks. *Front. Med.* 9:844601. doi: 10.3389/fmed.2022.844601

Purpose: To analyze the impact of COVID-19 on Italian corneal transplantation from March-2020 to February 2021 compared to the same timeframe of the 2 previous years, in order to identify potential consequences of a global pandemic on corneal procurement and transplantation services during this time.

Methods: This national, multicentric, retrospective cohort study evaluated data collected from 12 (100%) Italian eye banks from March 2020 to February 2021 (Group A). The number of tissues collected, distributed and discarded were compared with the same time-frame of the 2 previous years: 2019 and 2018 (group B and C, respectively). The different type of transplants performed were reported. Data were analyzed using a non-parametric Friedman test.

Results: Corneal procurement and the percentage of distributed tissues reduced in 2020 by more than 30 and 15%, respectively, compared to the 2 previous years. During the pandemic corneal transplant surgery showed only a modest drop: the number of the penetrating keratoplasties (PKs) and the anterior lamellar keratoplasties (ALKs) decreased by about 30 and 20% in comparison with groups B and C, respectively; between the Endothelial Keratoplasties (EKs), the Descemet membrane endothelial keratoplasty (DMEK) increased slightly from March 2020 to February 2021.

Conclusions: Italy was one of the first countries most affected by the outbreak of COVID-19, and the Italian government adopted severe measures to limit viral transmission. The pandemic generated several implications in corneal transplant activity during the first lockdown. Then an efficacious reaction with constant, vigorous work led to a resumption of transplant surgery to a near-normal standard. The increase of EKs, despite the pandemic, is a sign that the advance in corneal transplantation has gone ahead and it continues to evolve.

Keywords: SARS-CoV-2, eye bank guidelines, corneal transplant, eye donor screening, endokeratoplasty

INTRODUCTION

The difficult scenario, experienced during the first COVID-19 pandemic wave, and that negatively impacted the National Health System by diverting resources to contain this infection, influenced the “second wave” which started around 1st October 2020. The lessons learned from the first wave led to a less confused and more organized access path to intensive care units (1).

COVID-19 has become a constant threat for solid organ transplantation; as a result, the pandemic has generated significant challenges to Italian procurement and transplantation programs. It has been recorded a substantial decrease during the most critical weeks of the early COVID-19 spread, with a 25% reduction in total donations at a national level, partly due to the unknown relationship between the virus and tissues (2).

In Italy, after an initial period of uncertainty relating to the risk of transmission, corneal transplantation activity has been encouraged by the national regulatory authorities and Italian corneal scientific societies, in order to avoid tissue waste. A previous retrospective study comparing the Italian Eye Bank activity during the lockdown period with the same timeframe of 2018 and 2019 has shown a dramatic reduction in corneal transplant activity, resulting in a significant waste of resources (3).

In this study, we analyzed the impact of COVID-19 on Italian corneal transplantation in the whole year “annus horribilis” from March 2020 to February 2021. We therefore compared the aforementioned period with the same timeframe of the two previous years (2018 and 2019), in order to describe the effects of a global pandemic on Italian corneal procurement and transplantation services during this time.

Our study aimed to analyze the clinical relevance and the potential consequences of the COVID-19 pandemic on corneal transplant activity.

MATERIALS AND METHODS

In this national multicentric, retrospective cohort study, we analyzed data from 12 (100%) Italian eye banks, collected by the Italian Eye Bank Society “Società Italiana Banche degli Occhi” (SIBO), in order to report the eye bank activity between March 2020 and February 2021, comparing it with two previous years. To simplify data reporting we classified the three main different time-frames into 3 groups as follows: Group A: from March 2020 to February 2021; Group B: from March 2019 to February 2020; Group C: from March 2018 to February 2019.

We compared the number of corneas collected and distributed by the eye banks after the completion of the screening tissue process. The decrease in the number of corneas procured and distributed was calculated as a percentage of the average. We also reported the number of wasted corneas (returned back and expired).

Finally, we measured the impact of the COVID-19 pandemic on corneal transplant surgery in Italy, comparing the type of transplants performed: penetrating keratoplasty (PK), anterior lamellar keratoplasty (ALK), Descemet stripping

TABLE 1 | Data summary from Italian Eye Bank Associations.

	Group C	Group B	Group A
N° of collected tissues	17,099	17,930	11,241
N° of distributed tissues	7,074	7,266	5,928
N° PK	3,403	3,198	2,294
N° DALK	675	778	587
N° DSAEK	2,437	2,619	2,431
N° DMEK	559	671	616
N° EP	315	338	424
N° of discarded tissues	857	847	940
N° of COVID-19 + tissues	0	15	151
N° of canceled procedures	127	145	208
N° of expired tissues	623	591	436
N° of requested albeit not transplanted corneas	107	96	42

PK, Penetrating keratoplasty; ALK, anterior lamellar keratoplasty; DSAEK, Descemet stripping automated endothelial keratoplasty; DMEK, Descemet membrane endothelial keratoplasty; EP, Emergency procedures.

Group A: March 2020–February 2021.

Group B: March 2019–February 2020.

Group C: March 2018–February 2019.

automated endothelial keratoplasty (DSAEK), Descemet membrane endothelial keratoplasty (DMEK) and emergency procedures (EP).

STATISTICAL ANALYSIS

Data were recorded and analyzed using Microsoft Excel (2021). The mean number of corneas collected, and those discarded, from March 2020 to February 2021 was compared with the previous 2 years using a non-parametric Friedman test (Stata/IC 16, StataCorp, USA). Statistical significance was defined as a $p < 0.05$. Data are resumed in **Table 1**.

RESULTS

Italian Eye Bank Procurement and Distribution Activity

From the 1st March 2020 to the 28th February 2021, 11,241 donor corneas were collected and harvested. Compared to the previous 2 years the number of corneas in Group A appears significantly reduced (Group A: 11,241; Group B: 17,930, (−37.3%); Group C: 17,099, (−34.4%); $p = 0.0009$) (**Figure 1**).

Moreover, we noticed a substantial reduction in the number of distributed tissues when comparing Group A data with the previous 2 years (Group B: −16.2%; Group C: −18.4%) ($p = 0.0009$) (**Figure 2**).

Discarded Tissues

The number of total discarded corneas declined from 857 in Group C to 847 in Group B (−1.17%) and to 837 in Group A (−2.33%) ($p = 0.008$) (**Figure 3**).

Among the discharged tissues in Group A, 151 (18%) were dismissed because considered at risk for SARS-CoV-2 contamination. Nonetheless, the percentage of discarded tissues

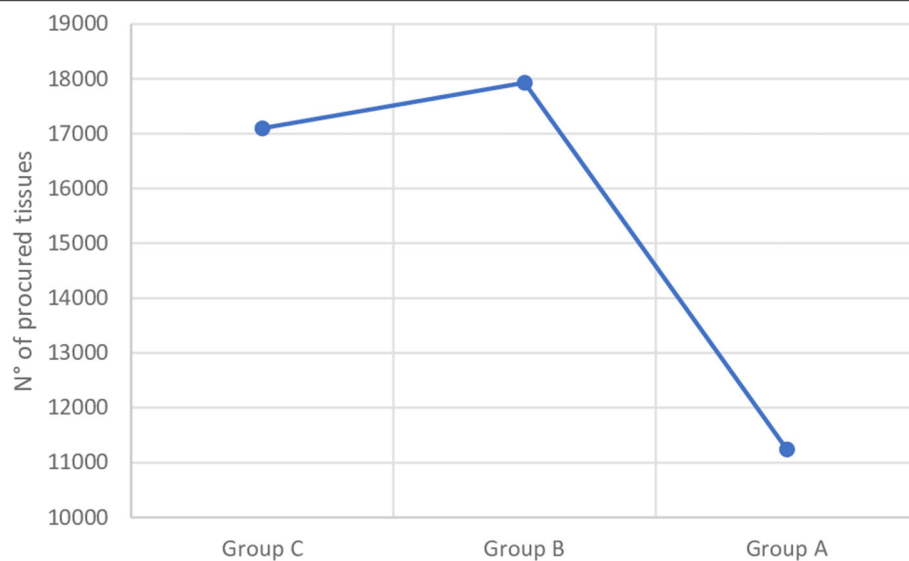


FIGURE 1 | Corneal procurement trend of Italian Association of Eye Banks. Group A, March 2020–February 2021; Group B, March 2019–February 2020; Group C, March 2018–February 2019.

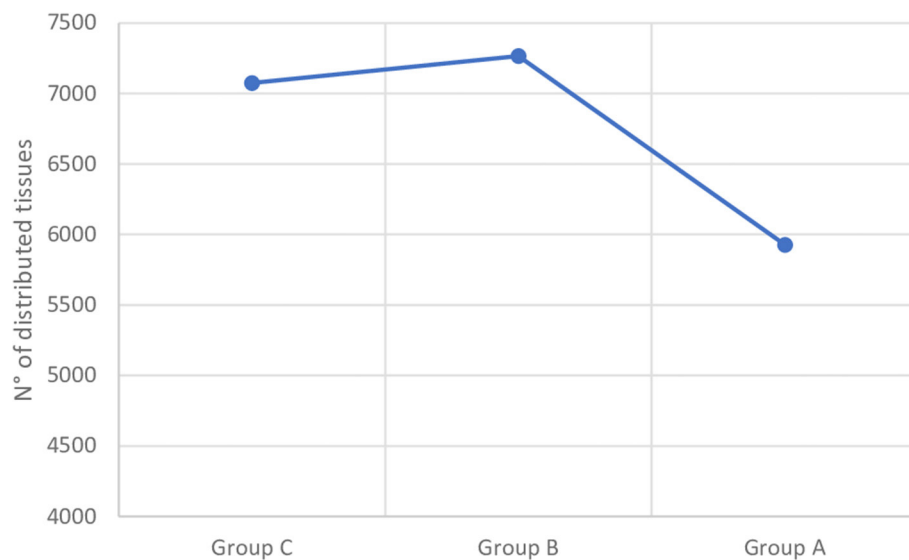


FIGURE 2 | Corneal distribution trend of Italian Association of Eye Banks. Group A, March 2020–February 2021; Group B, March 2019–February 2020; Group C, March 2018–February 2019.

due to a suspicion of SARS-CoV-2 contamination, over the total number of retrieved corneas in Group A, accounted for 1.34%.

Notably, in Group A, 208 surgical procedures were canceled resulting in a 63.8% and 43.5% increase of canceled procedure compared to Group C and Group B, respectively ($p = 0.003$). Nonetheless, the number of expired tissues decreased from 623 in Group C to 591 in Group B and 436 in Group A (−5.1 and −30% respectively) ($p = 0.001$) probably due to a lower number of procured tissues. Similarly, the number of corneas requested, albeit not used by surgeons, declined from 107 to 96 (−10.28%)

and to 42 (−60.75%), in Group C, Group B and Group A, respectively ($p = 0.002$).

Pandemic Impact on Corneal Transplant Surgery

We observed different trends when analyzing the different subtypes of corneal grafts. In particular, the number of PKs significantly decreased from 3,403 in Group C and 3,198 in Group B to 2,294 in Group A ($p = 0.0006$).

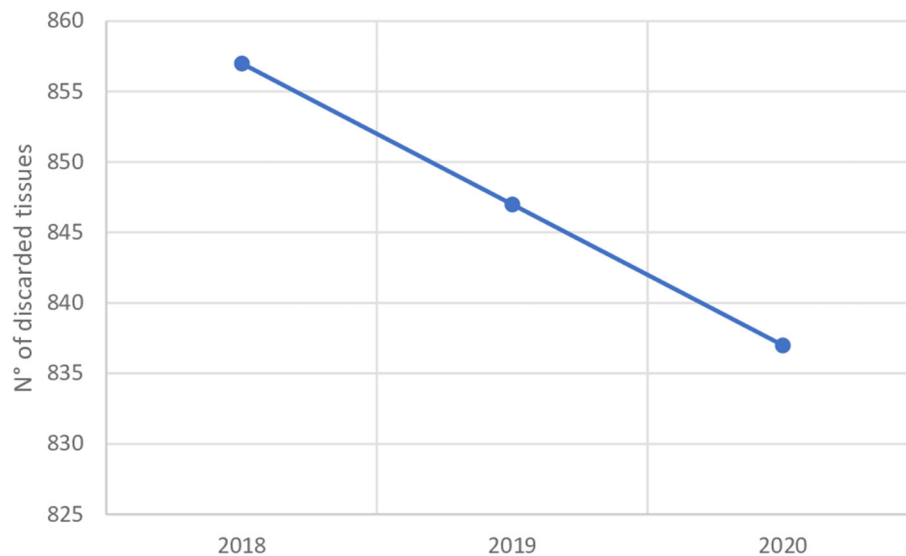


FIGURE 3 | Discarded corneal tissue trend of Italian Association of Eye Banks. Group A, March 2020–February 2021; Group B, March 2019–February 2020; Group C, March 2018–February 2019.

Similarly, the ALK numbers changed from 675 and 778 to 587 in Group C, Group B and Group A, respectively ($p = 0.001$). Interestingly, the endothelial keratoplasties were only partially affected, with 2,437 procedures performed in Group C, 2,619 in Group B and 2,431 in Group A. Nonetheless, the number of DMEKs increased during the study period, from 559 in Group C to 671 (+20%) and 616 (+10.2%) in Group B and A, respectively ($p = 0.006$) (Figure 4).

Among all the surgeries, 424 (7.6%) were performed as emergency procedures in Group A, whose number significantly increased from 315 in Group C (+34.6%) and 338 in Group B (+25.4%).

DISCUSSION

Early in the outbreak period of 2020, organ and tissue procurement and transplantation were dramatically affected by the COVID-19 pandemic in the United States and Europe. This was due to the lack of information on the risk of SARS-CoV-2 transmission from donor tissue to recipient. Indeed, no information was available on the effects of the COVID-19 infection on transplanted patients. After the initial deferral of elective surgical activity, the transplant rate began to increase, encouraged by local governments and in agreement with the national transplant Societies (4). At the beginning of the pandemic, an European multinational survey involving 64 eye banks showed a significant reduction in the number of corneas procured and distributed per month from March to May 2020, compared with the two previous years. Despite a wide variation in the international stringency of recommendations for corneal donor screening, negative correlation between the decrease in procurement and stringency were found (5).

Due to COVID-19, eye banks have globally developed different guidelines and criteria for evaluating the viability of donor corneas (6). The European Eye Bank Association (EEBA) has developed its own guidelines: first PCR test is required; if the PCR test is positive 14 days prior to death, the donor is ineligible; in addition, a nasopharyngeal swab postmortem is performed. However, individual risk assessment is necessary to assess the eligibility of the donor (7). The level of precautions adopted in the various countries ranged from automatic exclusion to retrieval if nasopharyngeal swab was negative in three categories of patients: (1) suspected to have COVID-19 but died from another cause; (2) recovered from COVID-19 and died later on from another cause; (3) asymptomatic at risk (5). For suspected donors, in European countries with the least stringent recommendations on retrieval tissues, the guidelines imposed a 14-day quarantine interval between recovery and death or between last symptom and death. The Countries with the most stringent donor guidelines, such as Austria, Belgium, France, Spain, imposed a prolonged period of up to 28 days free interval between recovery and death or between last symptom and death. No country made serology testing mandatory, but Italy recommended to be performed for epidemiologic reasons (5).

In Italy, one of the nations with the highest cornea procurement, the selection criteria released by the competent health Authority and therefore adopted by SIBO for donor screening, are summarized in Table 2.

For all the corneas collected by the eye banks, the use of 5% povidone-iodine (PVP-I) disinfection protocol was recommended during their retrieval. This has been shown to be effective at inactivating SARS-CoV-2 (as well as other viruses) (8).

The findings of this study confirmed that the COVID-19 pandemic partially reduced the number of cornea donations in comparison with the two previous years. From our data, which

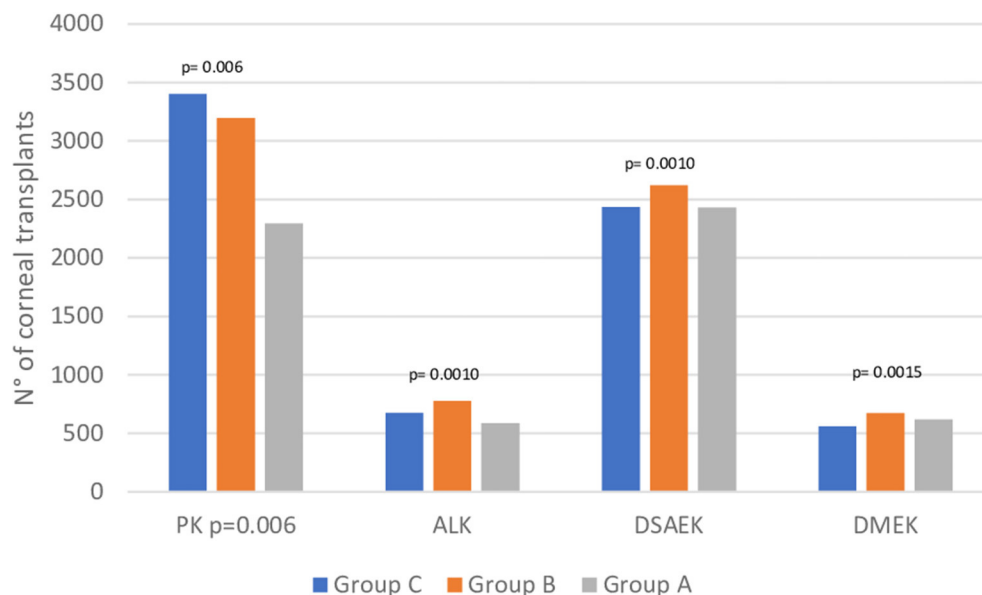


FIGURE 4 | Corneal transplant activity. PK, Penetrating keratoplasty; ALK, Anterior Lamellar Keratoplasty; DSAEK, Descemet Stripping Automated Endothelial Keratoplasty; DMEK, Descemet Membrane Endothelial Keratoplasty. Group A, March 2020–February 2021; Group B, March 2019–February 2020; Group C, March 2018–February 2019.

TABLE 2 | Italian screening criteria COVID-19 donor screening.

Donor status	Recommendations for donor screening
History of COVID-19/symptoms compatible with COVID-19 but swab not performed, or negative, or serological antibody to SARS-CoV-2	Tissues should be collected 14 days after a documented virological recovery (resolution of symptoms and/or negative swab), and following a nasopharyngeal (genetic) swab for SARS-CoV-2 performed within 24 h of death*
History of close contact with COVID-19 patients (absence of clinical symptoms or with negative nasopharyngeal swab)	Tissues could be collected 14 days after the last close contact and following a nasopharyngeal (genetic) swab performed within 24 h of death, with negative results available before tissue distribution*.
Vaccinated	No contraindication

* or, where present, a nasopharyngeal swab performed within 48 h prior to collection.

also analyzed the months following the lockdown, a reduction of 38 and 20% of corneal procurement and distributed tissues respectively emerged, compared to the 2019 and 2018.

The number of procured corneas represent, in our opinion, one of the main indexes of Eye Bank activity throughout each country. In this context, the apparent reduction in the number of retrieved corneas (more than 30%) during the last 12 months, compared to the previous 2 years, poses a number of considerations. In fact, this proportion appeared substantially contracted when compared to the one reported by the SIBO group, which presented a nearly 60% reduction in

the number of retrieved corneas during the Italian lockdown period (3). Nonetheless, a nearly 30% reduction in a 1-year estimate of working activity might simply be related to the first 3-month of lockdown period, due to a dramatic reduction of surgical activity.

Early in the pandemic, before the introduction of Italian donor screening guidelines to exclude tissues potentially infected by SARS-CoV-2, an increase in discarded corneas considered at risk of contamination was reported (3). Current evidence indicates that SARS-CoV-2 transmission via corneal transplants from an infected donor to a healthy recipient host is a very rare event (9). Though, many studies speculate that the eye may be a possible entry route for SARS-CoV-2, due to co-expression of SARS-CoV-2 entry receptors (ACE2 and TMPRSS2); the risk of transmission associated with cornea transplantation is very low. Therefore, the benefit of decedent testing would appear to be negligible (10, 11). In our opinion, the stringent screening and the proper manipulation of corneal tissues according to the guidelines provided by the competent health regulatory Authorities appear to be sufficient to prevent the transmission of SARS-CoV-2 to cornea transplant recipients.

During the pandemic a substantial reduction in overall eye surgical procedures were reported in the first 2 months of pandemic corresponding to the Italian national lockdown (10 March–9 May 2020). The reduction included predominantly elective surgeries. However, urgent procedures and intravitreal injections were also heavily affected (12). The deferral of elective surgery resulted in a significant increase in expired tissues to be used for corneal transplants compared to the previous 2 years. Against a relative reduction in the procurement and the distribution, the percentage of the transplants carried out

during the “annus horribilis” was not dramatically affected. During the first 3 months of the COVID-19 lockdown period, the number of performed transplants both PK and EK were reduced by more than 50% compared to the same months of the previous 2 years (3). In our report, the number of PKs decreased of 29 and 33% compared to 2019 and 2018 respectively. The ALKs reduced of 25 and 14% compared to group B and C, respectively. Instead, between the EKs, the DMEK increased slightly compared to previous years. The reduction in the number of PKs in Group A compared to the previous 2 years may have been only partially affected by the COVID-19 pandemic; on one hand, the introduction of lamellar keratoplasty techniques has led to a general decrease in the percentage of PKs in recent years (13); on the other hand, the concomitant reduction of ALKs, although less than the PKs, could be justified by the suspension or deferral of elective surgical activity and by the delay in the treatment of pathologies that during the lockdown have been underestimated as reported for the rhegmatogenous retinal detachment (12). The relative increase of EKs, even during the pandemic, confirms the trend of recent years, with a progressive increase in endothelial selective corneal transplants and can be explained by the higher likelihood of this procedure being performed under local anesthesia and not requiring access to anesthetic facilities (14, 15). A recent report from India confirms that there was a gradual and incremental increase in all types of keratoplasties in the unlock phase, which exceeded the preceding years’ monthly numbers in February and March 2021 (16).

Despite the difficult period, in relative terms, transplant activities have not suffered a profound negative impact. The possible explanation for this positive report may depend both on the guidelines adopted by eye bank that helped to improve screening by avoiding a loss of tissue, and on the competent authorities that encouraged transplantation activity. Therefore, the whole system from eye banks to surgery has

held up well, and the advance in corneal transplantation has gone ahead.

CONCLUSIONS

In conclusion, while the lockdown-related restrictions caused tremendous impact on eye banking/corneal transplant organization, our data support the hypothesis of an efficacious reaction with a constant and vigorous working activity resumption. Moreover, the increase in endothelial keratoplasty surgery, despite the pandemic, is a sign that corneal transplant surgery continues to evolve.

ITALIAN SOCIETY EYE BANK (SIBO) GROUP

Imola: Paola Bonci; Cosenza: Giuseppe Calabrò; Pavia: Roberto Ceccuzzi; Fabriano: Massimiliano Corneli; L'Aquila: Germano Genitti; Lucca: Claudio Giannarini; Monza: Raffaella Mistò; Rome: Augusto Pocobelli; Naples: Achille Tortori; Genoa: Davide Venzano.

DATA AVAILABILITY STATEMENT

The raw data supporting the conclusions of this article will be made available by the authors, without undue reservation.

AUTHOR CONTRIBUTIONS

RM, MC, FG, DP, and FA: conceptualization. RM, MC, FA, FG, GP, MB, and CN: methodology. FA, GP, and CN: formal analysis. RM, MC, FA, MB, GP, and DP: investigation. RM, MC, FA, FG, GP, and DP: data curation. RM, MC, FA, and DP: writing-original draft preparation and writing-review and editing. All authors contributed to the article and approved the submitted version.

REFERENCES

- Mantica G, Riccardi N, Terrone C, Gratarola A. Non-COVID-19 admissions to the emergency department during the pandemic second wave in Italy: what is changed from the first wave? *Am J Emerg Med.* (2020) 45:625–6. doi: 10.1016/j.ajem.2020.11.046
- Angelico R, Trapani S, Manzia TM, Lombardini L, Tisone G, Cardillo M. The COVID-19 outbreak in Italy: Initial implications for organ transplantation programs. *Am J Transplant.* (2020) 20:1780–4. doi: 10.1111/ajt.15904
- Aiello F, Genzano Besso F, Pocobelli G, Gallo Afflitto G, Colabelli Gisoldi RAM, Nucci C, et al. Corneal transplant during COVID-19 pandemic: the Italian Eye Bank national report. *Cell Tissue Bank.* (2021) 22:697–702. doi: 10.1007/s10561-021-09934-8
- Azzi Y, Bartash R, Scalea J, Loarte-Campos P, Akalin E. COVID-19 and solid organ transplantation: a review article. *Transplantation.* (2021) 105:37–55. doi: 10.1097/TP.0000000000003523
- Thuret G, Courrier E, Poinard S, Gain P, Baud'Huin M, Martinache I, et al. One threat, different answers: the impact of COVID-19 pandemic on cornea donation and donor selection across Europe. *Br J Ophthalmol.* (2020) 106:312–8. doi: 10.1136/bjophthalmol-2020-317938
- Moshirfar M, Odayar VS, McCabe SE, Ronquillo YC. Corneal donation: current guidelines and future direction. *Clin Ophthalmol.* (2021) 15:2963–73. doi: 10.2147/OPHTH.S284617
- European Eye Bank Association. *Ocular Tissue Donation: EEBA Donor Screening Guideline for SARS-CoV-2*. Available online at: <https://www.eeba.eu/news/news-details/ocular-tissue-donation-eeba-donor-screeningguideline-for-sars-cov-2>
- Sawant OB, Singh S, Wright RE, Jones KM, Titus MS, Dennis E, et al. Prevalence of SARS-CoV-2 in human post-mortem ocular tissues. *Ocul Surf.* (2021) 19:322–9. doi: 10.1016/j.jtos.2020.11.002
- Aiello F, Ciotti M, Gallo Afflitto G, Rapanotti MC, Caggiano B, Treglia M, et al. Post-mortem RT-PCR assay for SARS-CoV-2 RNA in COVID-19 patients' corneal epithelium, conjunctival and nasopharyngeal swabs. *J Clin Med.* (2021) 10:4256. doi: 10.3390/jcm10184256
- Mencucci R, Favuzza E, Becatti M, Tani A, Mazzantini C, Vignapiano R, et al. Co-expression of the SARS-CoV-2 entry receptors ACE2 and TMPRSS2 in healthy human conjunctiva. *Exp Eye Res.* (2021) 205:108527. doi: 10.1016/j.exer.2021.108527
- O'Brien SF, Lewin A, Yi QL, Dowling G, Fissette E, Drews SJ. The estimated risk of SARS-CoV-2 infection via cornea transplant in Canada. *Cell Tissue Bank.* (2021) 22:685–95. doi: 10.1007/s10561-021-09964-2

12. dell'Omo R, Filippelli M, Virgili G, Bandello F, Querques G, Lanzetta P, et al. Effect of COVID-19-related lockdown on ophthalmic practice in Italy: a report from 39 institutional centers. *Eur J Ophthalmol.* (2022) 32:695–703. doi: 10.1177/11206721211002442
13. Price MO, Feng MT, Price FW Jr. Endothelial keratoplasty update 2020. *Cornea.* (2021) 40:541–7. doi: 10.1097/ICO.00000000000002565
14. Chilibeck CM, Brookes NH, Gokul A, Kim BZ, Twohill HC, Moffatt SL, et al. Changing trends in corneal transplantation in Aotearoa/New Zealand, 1991 to 2020: effects of population growth, cataract surgery, endothelial keratoplasty, and corneal cross-linking for keratoconus. *Cornea.* (2021). doi: 10.1097/ICO.00000000000002812. [Epub ahead of print].
15. Colby K. Update on corneal transplant in 2021. *JAMA.* (2021) 325:1886–7. doi: 10.1001/jama.2020.17382
16. Das AV, Chaurasia S, Vaddavalli PK, Garg P. Year one of COVID-19 pandemic in India: Effect of lockdown and unlock on trends in keratoplasty at a tertiary eye centre. *Indian J Ophthalmol.* (2021) 69:3658–62. doi: 10.4103/ijo.IJO_1740_21

Conflict of Interest: The authors declare that the research was conducted in the absence of any commercial or financial relationships that could be construed as a potential conflict of interest.

Publisher's Note: All claims expressed in this article are solely those of the authors and do not necessarily represent those of their affiliated organizations, or those of the publisher, the editors and the reviewers. Any product that may be evaluated in this article, or claim that may be made by its manufacturer, is not guaranteed or endorsed by the publisher.

Copyright © 2022 Mencucci, Cennamo, Ponzin, Genzano Besso, Pocobelli, Buzzi, Nucci and Aiello. This is an open-access article distributed under the terms of the Creative Commons Attribution License (CC BY). The use, distribution or reproduction in other forums is permitted, provided the original author(s) and the copyright owner(s) are credited and that the original publication in this journal is cited, in accordance with accepted academic practice. No use, distribution or reproduction is permitted which does not comply with these terms.

Advantages of publishing in Frontiers



OPEN ACCESS

Articles are free to read
for greatest visibility
and readership



FAST PUBLICATION

Around 90 days
from submission
to decision



HIGH QUALITY PEER-REVIEW

Rigorous, collaborative,
and constructive
peer-review



TRANSPARENT PEER-REVIEW

Editors and reviewers
acknowledged by name
on published articles

Frontiers

Avenue du Tribunal-Fédéral 34
1005 Lausanne | Switzerland

Visit us: www.frontiersin.org

Contact us: frontiersin.org/about/contact



REPRODUCIBILITY OF RESEARCH

Support open data
and methods to enhance
research reproducibility



DIGITAL PUBLISHING

Articles designed
for optimal readership
across devices



FOLLOW US

@frontiersin



IMPACT METRICS

Advanced article metrics
track visibility across
digital media



EXTENSIVE PROMOTION

Marketing
and promotion
of impactful research



LOOP RESEARCH NETWORK

Our network
increases your
article's readership